EVOLUTIONARY AND INTEGRATIVE APPROACHES FOR REVEALING ADAPTIVE MECHANISMS IN MARINE ANIMALS ALONG ENVIRONMENTAL GRADIENTS

EDITED BY: Pierre Ulrich Blier, Carlos Rosas and Nelly Tremblay
PUBLISHED IN: Frontiers in Physiology

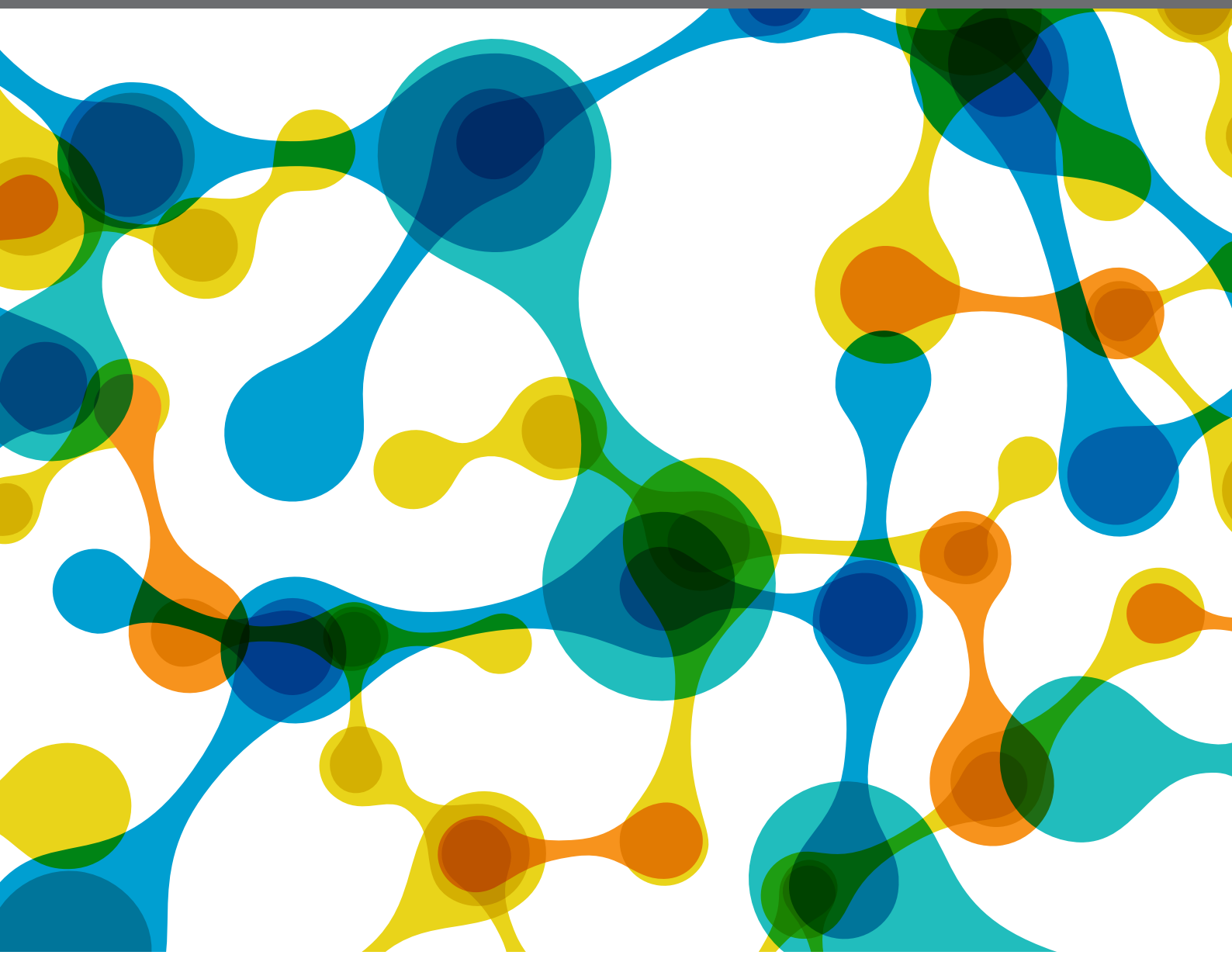

frontiers Research Topics

frontiers

ISSN 1664-8714
ISBN 978-2-88963-981-6
DOI 10.3389/978-2-88963-981-6

About Frontiers

Frontiers is more than just an open-access publisher of scholarly articles: it is a pioneering approach to the world of academia, radically improving the way scholarly research is managed. The grand vision of Frontiers is a world where all people have an equal opportunity to seek, share and generate knowledge. Frontiers provides immediate and permanent online open access to all its publications, but this alone is not enough to realize our grand goals.

Frontiers Journal Series

The Frontiers Journal Series is a multi-tier and interdisciplinary set of open-access, online journals, promising a paradigm shift from the current review, selection and dissemination processes in academic publishing. All Frontiers journals are driven by researchers for researchers; therefore, they constitute a service to the scholarly community. At the same time, the Frontiers Journal Series operates on a revolutionary invention, the tiered publishing system, initially addressing specific communities of scholars, and gradually climbing up to broader public understanding, thus serving the interests of the lay society, too.

Dedication to Quality

Each Frontiers article is a landmark of the highest quality, thanks to genuinely collaborative interactions between authors and review editors, who include some of the world's best academicians. Research must be certified by peers before entering a stream of knowledge that may eventually reach the public - and shape society; therefore, Frontiers only applies the most rigorous and unbiased reviews.
Frontiers revolutionizes research publishing by freely delivering the most outstanding research, evaluated with no bias from both the academic and social point of view. By applying the most advanced information technologies, Frontiers is catapulting scholarly publishing into a new generation.

What are Frontiers Research Topics?

Frontiers Research Topics are very popular trademarks of the Frontiers Journals Series: they are collections of at least ten articles, all centered on a particular subject. With their unique mix of varied contributions from Original Research to Review Articles, Frontiers Research Topics unify the most influential researchers, the latest key findings and historical advances in a hot research area! Find out more on how to host your own Frontiers Research Topic or contribute to one as an author by contacting the Frontiers Editorial Office: researchtopics@frontiersin.org

EVOLUTIONARY AND INTEGRATIVE APPROACHES FOR REVEALING ADAPTIVE MECHANISMS IN MARINE ANIMALS ALONG ENVIRONMENTAL GRADIENTS

Topic Editors:
Pierre Ulrich Blier, Université du Québec à Rimouski, Canada
Carlos Rosas, National Autonomous University of Mexico, Mexico
Nelly Tremblay, Alfred-Wegener-Institut Helmholtz-Zentrum für Polar- und Meeresforschung (AWI), Germany

Citation: Blier, P. U., Rosas, C., Tremblay, N., eds. (2020). Evolutionary and Integrative Approaches for Revealing Adaptive Mechanisms in Marine Animals along Environmental Gradients. Lausanne: Frontiers Media SA.
doi: 10.3389/978-2-88963-981-6

Table of Contents

frontiers in Physiology

EDITORIAL
published: 14 July 2020
doi: 10.3389/fphys.2020.00764

Editorial: Evolutionary and Integrative Approaches for Revealing Adaptive Mechanisms in Marine Animals Along Environmental Gradients

Nelly Tremblay[1], *Pierre U. Blier*[2] *and Carlos Rosas*[3,4]*

[1] Shelf Sea System Ecology, Alfred-Wegener-Institut Helmholtz-Zentrum für Polar- und Meeresforschung, Helgoland, Germany, [2] Département de Biologie, Université du Québec à Rimouski, Rimouski, QC, Canada, [3] Unidad Multidisciplinaria de Docencia e Investigación, Facultad de Ciencias, Universidad Nacional Autónoma de México, Sisal, Mexico, [4] Laboratorio Nacional de Resiliencia Costera, Consejo Nacional de Ciencia y Tecnología, Sisal, Mexico

Keywords: tropical latitudes, hypoxia, warming, ectotherms, osmotic, plasticity

Editorial on the Research Topic

Evolutionary and Integrative Approaches for Revealing Adaptive Mechanisms in Marine Animals along Environmental Gradients

This Research Topic was a result of the 5th Workshop of Ecophysiology: Marine animal resilience in a changing world, held in November 2017 in Sisal (Mexico). The participants highlighted several gaps of knowledge in the mechanisms underlying thermal, oxygen sensing, and osmotic adaptations, particularly in tropical and subtropical marine species. Special attention was thus called to studies contrasting environmental gradients in subtropical and tropical latitudes, including plankton, benthos, and nekton, to better understand their physiological adaptations to multiple stressors.

Plankton species must cross pronounced gradients of temperature, salinity, and oxygen, potentially showing broad ecophysiological plasticity. Harada et al. demonstrated intraspecific variation in thermal tolerance among three populations of the sub-tropical intertidal copepod *Tigriopus californicus* collected over a latitudinal thermal gradient (14 to 18°C) along the coast of California (USA) and acclimated to 20°C. During acute thermal exposure (>34°C for 1 h), the lower latitude population performed better in terms of survival, higher upper thermal limit, and ATP synthesis capacity. There was also a tight correlation between a decline in ATP synthesis capacity and higher upper thermal limits, which suggests a role for mitochondria in setting these limits and indicates that divergence of mitochondrial function is likely a component of adaptation across latitudinal thermal gradients.

Hypoxia tolerance of 10 dominant euphausiid species from Atlantic (sub-tropical), Pacific (temperate, tropical), and Polar regions, with or without exposure to Oxygen Minimum Zones (OMZs) was investigated by Tremblay et al. using the regulation index. This index assesses the regulation ability of aquatic organisms that do not present a clear critical oxygen partial pressure breaking point in their respiration pattern. Species that migrated vertically over long distances in shallow OMZ habitats were qualified as metabolic suppressors, whereas species associated with upwelling events in the neritic area expressed almost perfect oxyconformity. At *in situ* temperatures, polar and deep OMZ species displayed the highest degree of oxyregulation. Most of the studied Euphausiid species have evolved, at all latitudes, various respiratory strategies coupled with oxygen levels and temperatures experienced during their vertical migration, which may help to buffer substantial changes in their respective trophic ecosystems under climate change.

OPEN ACCESS

Edited by:
Kendall D. Clements, The University of Auckland, New Zealand

Reviewed by:
Simon Morley, British Antarctic Survey (BAS), United Kingdom
Anthony John Hickey, The University of Auckland, New Zealand

***Correspondence:**
Carlos Rosas
crv@ciencias.unam.mx

Specialty section:
This article was submitted to Aquatic Physiology, a section of the journal Frontiers in Physiology

Received: *31 March 2020*
Accepted: *11 June 2020*
Published: *14 July 2020*

Citation:
Tremblay N, Blier PU and Rosas C (2020) Editorial: Evolutionary and Integrative Approaches for Revealing Adaptive Mechanisms in Marine Animals Along Environmental Gradients. Front. Physiol. 11:764. doi: 10.3389/fphys.2020.00764

Intertidal and shallow-water benthic communities experience physical environmental variations along with daily and tidal cycles, which exposes animals to high environmental heterogeneity. Brahim et al. investigated heat tolerance plasticity in terms of laboratory acclimation and natural acclimatization of different populations of the tropical rocky-intertidal snail *Echinolittorina malaccana*. Four laboratory treatments (constant cool 22–23°C, warm cycle 25–45°C, constant extra cool 20°C, and extra-warm cycle 25–50°C) yielded similar capacities to acclimate and adjust thermal limits, but the populations differed in the temperature range over which they can make adjustments. This work supports that, irrespective of latitude, habitat heterogeneity drives thermal plasticity selection and should be considered in future studies seeking to assess ectothermic animals' response to environmental warming.

Nitric oxide (NO) could be essential for intertidal organisms, for the adjustment of mitochondrial respiration to local oxygen content. González et al. investigated how NO modulates the hypoxia tolerance of the widely distributed blue mussel *Mytilus edulis* under moderate, severe hypoxia and normoxia (1, 7, and 21 kPa pO_2). Using live imaging techniques on excised gill filaments, the authors showed that NO accumulated under hypoxia, causing blood vessel dilatation after only 30 min of acute exposure. In a parallel measurement on the same tissue, cytochrome c oxidase activity increased in the transgression to moderate hypoxia (7 kPa) to later decrease at severe hypoxia (1 kPa), indicating a potential stabilizing effect of these accumulated NO at 1 kPa. As hypoxia tolerance varies with temperature, this study highlights the importance of laying out the mechanism defining the plasticity of hypoxia tolerance in a changing environment and the adaptability of this trait.

Ectotherms' ability to perform routine activities such as locomotion and fitness-related behaviors should be altered by increasing ocean temperatures. One understudied aspect of invertebrates is the evolution of the functions of contractile proteins in muscle tissue. Muscular mechanics are crucial physiological traits for prey capture and predator avoidance. In an extensive genome analysis of the Pacific white shrimp *Litopenaeus vannamei* myosin gene family, Zhang et al. identified a significant expansion of *Myo2* subfamilies in abdominal muscles, and high expression of *Myo2* during pleonal and pleopod muscle formation and development beginning at the zoea larval stage. This research represents a baseline to study the evolution of crustacean myosin proteins in different thermal habitats and related adaptations to temperature under climate change pressures.

Many invertebrates with direct development and benthic behavior have limited mobility, necessitating physiological and immunological capacities adapted to local or regional environments. Pascual et al. examined the influence of surface temperature, associated with seasonal upwelling, on the physiological and immunological conditions of the tropical species *Octopus maya*. Octopuses from cooler habitats (27°C) in the upwelling zone and transitional zone were in better condition; they expressed higher concentrations of hemocyanin and lower activities of an essential component of the immune system, phenoloxidase. Specimens captured in the warmer zone (>27°C) reflected immunological compensation mechanisms likely associated with metabolic stress that appeared to impair reproduction.

To further explore the connection between reproductive performance and temperature, López-Galindo et al. investigated the transcriptomic profiles of testes from thermally stressed (30°C) and unstressed (24°C) adult male *O. maya* before and after mating. Functional annotation and pathway mapping of the 1,881 differentially expressed transcripts revealed temperature impacts on processes involved in spermatogenesis, gamete generation, germ cell and spermatid development, response to stress, inflammatory response, and apoptosis. In particular, transcripts encoding genes linked to male infertility (sperm motility and spermatogenesis) were overexpressed in the stressed individuals, which was validated by quantitative real-time PCR. These essential genes could be under selective pressures at high temperatures to restore male fertility. The two *O. maya* studies highlight the importance of temperature on the physiological condition, metabolism, immune function, and life cycle that determine the stability and persistence of this endemic population.

In vertebrates, a gradient approach was used by Hunter-Manseau et al. to characterize mitochondrial phenotypic adjustments of the heart tissue of eight ray-finned fishes with thermal niches ranging from −1.9 to 30.1°C. When measured close to their optimal temperature, the enzymes that regulate fatty acid oxidation had higher relative activity in the cold-adapted fish species. These species also exhibited higher cytochrome c oxidase activity, compared to the other enzymes of the Electron Transport System. Thus, at different temperature regimes, selection can act on the mitochondrial organization (i.e., the relative abundance of key enzymes) rather than only tuning mitochondrial content.

Katayama et al. conceptualized the multiple roles of osmoregulating hormones in a comparative review using mudskipper gobies as a model, as these animals bridge the gap between aquatic and terrestrial life. In mudskippers, dehydration triggers angiotensin II secretion when the buccal cavity is dry, but it also produces corticosteroids and neurohypophysial hormones secreted during the escape from predators/conspecifics or in other stressful situations. The result of all these stimuli is a migration toward water bodies. By questioning the origin of the conserved central action of mineralocorticoid signaling in all vertebrates, this review provides a highly relevant benchmark in the context of climate change, to further scrutinize the hormonal regulation of habitat preferences.

Through this Research Topic, it was clear that compensatory processes occur in sub-tropical and tropical organisms faced with environmental stresses. Broad latitudinal comparisons, over multiple time scales of exposure (acute, chronic, or evolutionary), and different organization levels are urgently required to assess better both climate change effects on a global scale and potential evolution and adaptations. More significant strategic collaborations amongst research institutes that share the same coastline are required to achieve these comparisons.

AUTHOR CONTRIBUTIONS

All authors listed have made a substantial, direct and intellectual contribution to the work, and approved it for publication.

FUNDING

NT position was funded by the Alfred-Wegener-Institut Helmholtz-Zentrum fuür Polar- und Meeresforschung (PACES II, WP2T2/3). PB was financially supported for this publication by NSERC (Discovery Grant- RGPIN-2019-05992, Canada). CR was supported by DGAPA-UNAM program through PAPIIT IN204019 project, Direction of Internationalization of UNAM, and Marine Sciences and Limnology Postgraduate of UNAM.

Conflict of Interest: The authors declare that the research was conducted in the absence of any commercial or financial relationships that could be construed as a potential conflict of interest.

frontiers in Physiology

REVIEW
published: 14 August 2018
doi: 10.3389/fphys.2018.01112

The Amphibious Mudskipper: A Unique Model Bridging the Gap of Central Actions of Osmoregulatory Hormones Between Terrestrial and Aquatic Vertebrates

Yukitoshi Katayama[1], Tatsuya Sakamoto[2], Keiko Takanami[2,3] and Yoshio Takei[1]*

[1] Physiology Section, Atmosphere and Ocean Research Institute, The University of Tokyo, Kashiwa, Japan, [2] Ushimado Marine Institute, Faculty of Science, Okayama University, Setouchi, Japan, [3] Mouse Genomics Resource Laboratory, National Institute of Genetics, Mishima, Japan

OPEN ACCESS

Edited by:
Carlos Rosas, Universidad Nacional Autónoma de México, Mexico

Reviewed by:
Juan Fuentes, Centro de Ciências do Mar (CCMAR), Portugal
Steffen Madsen, University of Southern Denmark, Denmark
Hon Jung Liew, Universiti Malaysia Terengganu, Malaysia
Fernando Diaz, Centro de Investigación Científica y de Educación Superior de Ensenada, Mexico

***Correspondence:**
Yukitoshi Katayama
katayama3g@aori.u-tokyo.ac.jp

Specialty section:
This article was submitted to Aquatic Physiology, a section of the journal Frontiers in Physiology

Received: *04 June 2018*
Accepted: *25 July 2018*
Published: *14 August 2018*

Citation:
Katayama Y, Sakamoto T, Takanami K and Takei Y (2018) The Amphibious Mudskipper: A Unique Model Bridging the Gap of Central Actions of Osmoregulatory Hormones Between Terrestrial and Aquatic Vertebrates. Front. Physiol. 9:1112. doi: 10.3389/fphys.2018.01112

Body fluid regulation, or osmoregulation, continues to be a major topic in comparative physiology, and teleost fishes have been the subject of intensive research. Great progress has been made in understanding the osmoregulatory mechanisms including drinking behavior in teleosts and mammals. Mudskipper gobies can bridge the gap from aquatic to terrestrial habitats by their amphibious behavior, but the studies are yet emerging. In this review, we introduce this unique teleost as a model to study osmoregulatory behaviors, particularly amphibious behaviors regulated by the central action of hormones. Regarding drinking behavior of mammals, a thirst sensation is aroused by angiotensin II (Ang II) through direct actions on the forebrain circumventricular structures, which predominantly motivates them to search for water and take it into the mouth for drinking. By contrast, aquatic teleosts can drink water that is constantly present in their mouth only by reflex swallowing, and Ang II induces swallowing by acting on the hindbrain circumventricular organ without inducing thirst. In mudskippers, however, through the loss of buccal water by swallowing, which appears to induce buccal drying on land, Ang II motivates these fishes to move to water for drinking. Thus, mudskippers revealed a unique thirst regulation by sensory detection in the buccal cavity. In addition, the neurohypophysial hormones, isotocin (IT) and vasotocin (VT), promote migration to water via IT receptors in mudskippers. VT is also dipsogenic and the neurons in the forebrain may mediate their thirst. VT regulates social behaviors as well as osmoregulation. The VT-induced migration appears to be a submissive response of subordinate mudskippers to escape from competitive and dehydrating land. Together with implications of VT in aggression, mudskippers may bridge the multiple functions of neurohypophysial hormones. Interestingly, cortisol, an important hormone for seawater adaptation and stress response in teleosts, also stimulates the migration toward water, mediated possibly via the mineralocorticoid receptor. The corticosteroid system that is responsive to external stressors can accelerate emergence of migration to alternative habitats. In this review, we suggest this unique teleost as an important model to deepen insights into the behavioral roles of these hormones in relation to osmoregulation.

Keywords: amphibious behavior, osmoregulation, angiotensin II, neurohypophysial hormones, corticosteroids, thirst, social behavior, mudskipper

EVOLUTION OF BODY FLUID REGULATION FROM FISHES TO TETRAPODS

Ionic concentration, osmolality, and volume of body fluids are important internal parameters that are tightly controlled in vertebrates by the ingestion and excretion of water and ions (Bourque, 2008). As vertebrates expanded their habitats from aquatic to terrestrial environments, terrestrial adaptation requires critical changes in the osmoregulatory and cardiovascular systems to counter both dehydration and gravity (Leow, 2015). To cope with dehydration, they drink water and reduce evaporative water loss from the body surface by a developed body integument consisting of layers of keratinized skin cells. In addition, the kidney of endothermic mammals and birds is equipped with juxtamedullary nephrons that can produce hyperosmotic urine, which is an adaptation to reduce water loss from excretion.

Similar to terrestrial tetrapods, teleost fishes are osmotic and ionic regulators and the ionic composition of their body fluis is similar to those of tetrapods, whose plasma osmolality is approximately one third of seawater regardless of the salinity that they inhabit (Evans, 2008). Their osmoregulatory ability might have allowed them to flourish in a wide range of aquatic environments including freshwater, seawater, and in particular cases allowed survival and success even on land (Takei, 2015). Marine teleosts exposed to severe dehydration drink seawater to cope with this problem (Hirano et al., 1972; Kobayashi et al., 1983; Perrott et al., 1992; Takei, 2015). After drinking, seawater is desalinated in the esophagus, and then water is absorbed together with NaCl in the intestine after isotonic dilution (Parmelee and Renfro, 1983; Nagashima and Ando, 1994; Takei et al., 2016). High amount of HCO_3^- is secreted into intestinal luminal fluid so that Ca^{2+} and Mg^{2+} are removed by precipitation in the form of carbonate aggregates (Wilson et al., 2002; Kurita et al., 2008; Grosell, 2011). The excess monovalent ions such as Na^+ and Cl^- are excreted from the branchial or cutaneous ionocytes (Uchida et al., 1996; Sakamoto et al., 2000; Seo et al., 2015) and divalent ions such as Ca^{2+}, Mg^{2+}, and SO_4^{2-} are excreted from the kidney (Watanabe and Takei, 2011). In freshwater teleosts, uptake of environmental ions through the gill is activated for hyperosmoregulation (Takei et al., 2014). This action is mediated by ion transporters such as Na^+-K^+-ATPase (NKA) and Ca^{2+}-ATPase (Hoenderop et al., 2005; Hwang et al., 2011). In these studies, species differences in osmoregulatory mechanisms and hormonal function have been found (Takei et al., 2014). Further, the osmoregulatory mechanisms are flexible in euryhaline or migratory species such as eels and salmonids, which experience drastic salinity changes during their life cycle and have to switch ion and water regulation to opposite directions via active transport (**Figure 1A**). Studies on these teleosts have highlighted pivotal roles of various hormones in adaptation to fluctuating environmental salinities (McCormick, 2001; Takei and McCormick, 2012).

Ample studies have clarified functions of osmoregulatory and cardiovascular hormones in terrestrial tetrapods and aquatic teleosts (McCormick and Bradshaw, 2006; Bourque, 2008; Mével et al., 2012; Takei et al., 2014; Leow, 2015). In teleosts, however, considerably less research effort is directed at determining their role in behaviors. In addition, it is little known how their functions are conserved or have evolved among diverse taxa through evolutionary time. An exception is drinking behavior induced by angiotensin II (Ang II). In mammals, circulating Ang II is a major factor in the increased thirst and sodium appetite of hypovolemia (Fitzsimons, 1998). These effects play important roles in sustaining the blood volume and blood pressure and would certainly have been evolutionarily advantageous. With regard to thirst, Ang II act on the thirst center to motivate terrestrial mammals to seek for and ingest water. Ingestion of water rapidly satiates thirst sensation by sensory detection of water in the gastrointestinal tract (Zimmerman et al., 2016). Ang II also acts in concert with vasopressin (VP) to decrease the loss of water (Fitzsimons, 1998). In aquatic teleosts, Ang II and neurohypophysial hormones similarly regulate drinking (Takei et al., 1979; Balment and Carrick, 1985; Perrott et al., 1992; Kozaka et al., 2003; Watanabe et al., 2007; Fuentes and Eddy, 2012). However, as we often found differences in the response to osmoregulatory hormones among teleost species (Kobayashi et al., 1983), a comparative approach may benefit deeper understanding on the function of osmoregulatory hormones, which will not be readily available when studying mammals exclusively.

AMPHIBIOUS MUDSKIPPER AS A UNIQUE MODEL FOR STUDYING OSMOREGULATORY BEHAVIOR

Mudskipper fishes including *Periophthalmus modestus* are euryhaline species that can tolerate salinities ranging from 0 to 40 parts per thousand (ppt). They often experience rapid changes in salinity each day with tide in the estuary and so their osmoregulatory mechanisms are highly flexible. Furthermore, they spend the greater time of their lives out of water to feed and to escape from aquatic predators. They have acquired behavioral and physiological adaptations to amphibious lives (Clayton, 1993; Graham, 1997; Sakamoto and Ando, 2002; Sakamoto et al., 2005a). The roles of endocrine systems in their amphibious features have been investigated (**Table 1**). Because of the unique amphibious behavior (i.e., migration between terrestrial and aquatic areas), mudskippers may serve as a valuable experimental model to investigate the central actions of osmoregulatory

Abbreviations: 11β-HSD2, 11β-hydroxysteroid dehydrogenase type 2; Ang II, angiotensin II; AP, area postrema; AT1, angiotensin type 1 receptor; AT2, angiotensin type 2 receptor; BNP, B-type natriuretic peptide; CVOs, circumventricular organs; DOC, 11-deoxycorticosterone; GR, glucocorticoid receptor; GRP, gastrin-releasing peptide; IT, isotocin; ITR, isotocin receptor; MR, mineralocorticoid receptor; NKA, Na^+-K^+-ATPase; NTS, nucleus tractus solitarius; OVLT, organum vasculosum of the lamina terminalis; OXT, oxytocin; PM, magnocellular preoptic nucleus; PP, parvocellular preoptic nucleus; ppt, parts per thousand; PRL, prolactin; PrRP, prolactin-releasing peptide; PVN, paraventricular nuclei of the hypothalamus; SFO, subfornical organ; SON, supraoptic nuclei of the hypothalamus; UES, upper esophageal sphincter; VP, vasopressin; VT, vasotocin; V1a, vasopressin/vasotocin type 1a receptor; V2, vasopressin/vasotocin type 2 receptor.

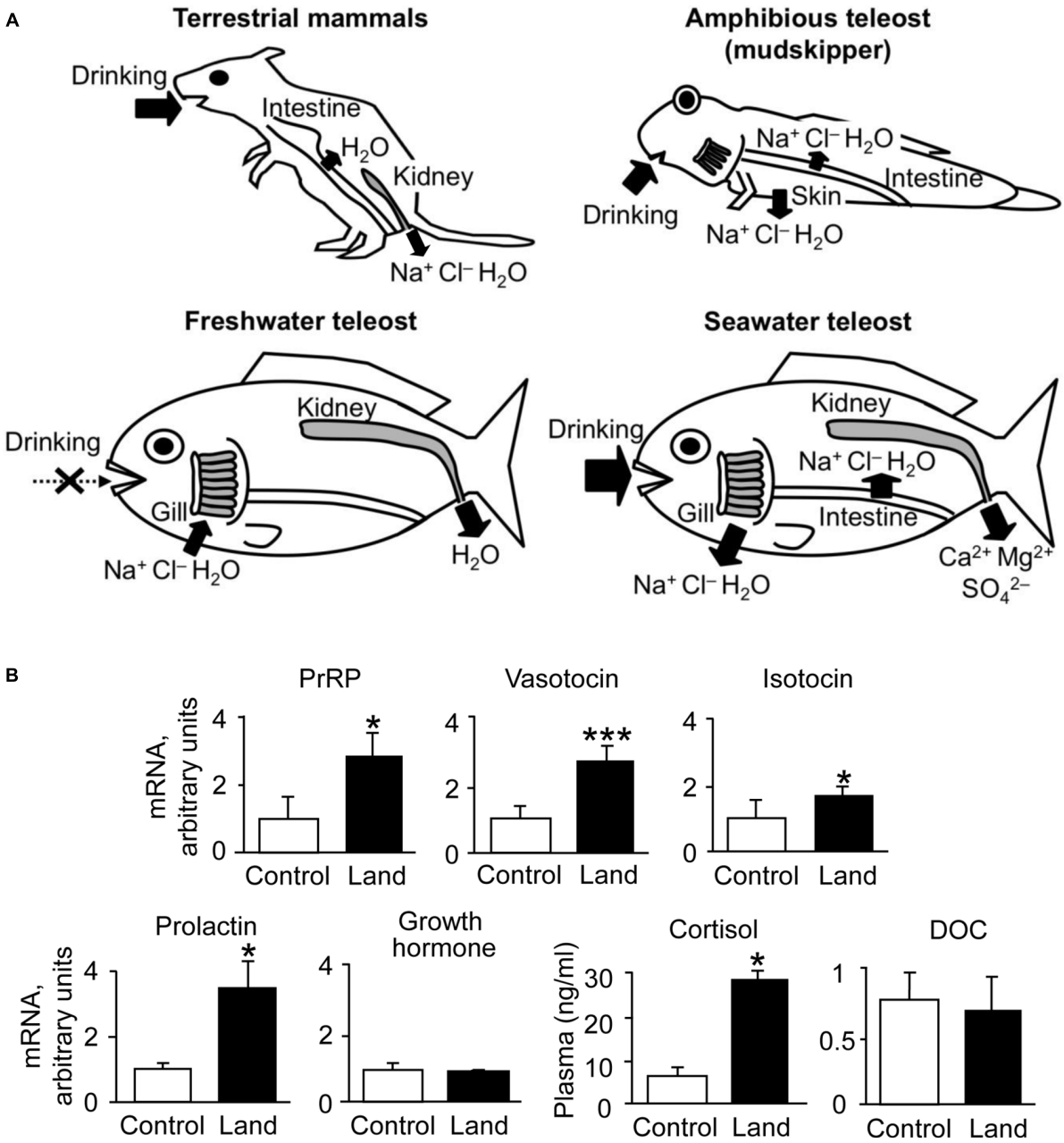

FIGURE 1 | Environmental adaptations in vertebrates. **(A)** Osmoregulatory mechanisms in mammals and teleosts. Arrows show active and passive transport of ions and/or water. The osmoregulatory mechanisms are flexible in euryhaline species such as catadromous eels and anadromous salmonids, which switch ion and water regulation to opposite directions via active transport. In addition to aquatic teleosts, the amphibious and euryhaline mudskipper, which invades land in its lifecycle, is used for the study of osmoregulation. **(B)** Dynamics of osmoregulatory hormones in terrestrial adaptation of mudskippers. Cortisol and DOC are shown as plasma concentrations (Sakamoto et al., 2002, 2011), and the other hormones are shown as the expression of their genes in the brain of mudskippers in controls (in one-third seawater) or on land (n = 4–8) (Sakamoto et al., 2005a, 2015). Data are shown as the means ± SE. *$p < 0.05$, ***$p < 0.001$ with t-test or Mann–Whitney U-test. PrRP, prolactin-releasing peptide; DOC, 11-deoxycorticosterone.

hormones and to provide new insights into the evolution of hormonal actions during transition from aquatic to terrestrial lifestyle.

Which actions of osmoregulatory hormones have been conserved and/or exploited in this teleost? Among the accumulated data, we will focus on three topics in this review. First, we discuss the role of Ang II in drinking behavior. The drinking behavior of mudskippers is composed of migration to water, taking water into the mouth, and swallowing, which may most likely be associated with thirst. The second topic is the interaction between osmoregulation and social behavior, both of which are regulated by the neurohypophysial

TABLE 1 | Hormones involved in the amphibious habits of mudskippers.

Hormone	Dynamics under terrestrial condition	Effect on aquatic preference		Reference
		Treatment		
Vasotocin	+ (mRNA)	+ (IM[b], ICV[c])	via ITR[d]	Sakamoto et al., 2015
Isotocin	+ (mRNA)	+ (IM, ICV)	via ITR	Sakamoto et al., 2015
Prolactin-releasing peptide	+ (mRNA)	ND		Sakamoto et al., 2005a
Prolactin	+ (mRNA)	+ (IM)		Lee and Ip, 1987; Sakamoto et al., 2005a,b
3,5,3′-triiodo-$_L$-thyronine	± (Plasma)	− (Immersion)		Lee and Ip, 1987; Sakamoto et al., 2011
Thyroxine	+ (Plasma)	ND		Lee and Ip, 1987
Cortisol	+ (Plasma)	+ (Immersion, ICV)	via GR[e], MR[f]	Sakamoto et al., 2002, 2011
11-deoxycorticosterone	± (Plasma)	+ (Immersion, ICV)	via MR	Sakamoto et al., 2011
Angiotensin II	ND[a]	+ (IM, ICV)	for drinking	Katayama et al., 2018

[a]ND: Not determined,[b]IM: Intramuscular injection, [c]ICV: Intracerebroventricular injection,[d]ITR: Isotocin receptor, [e]GR: Glucocorticoid receptor, [f]MR: Mineralocorticoid receptor, +: Increase, −: Decrease, ± : No significant change.

hormones, vasotocin (VT) and isotocin (IT). Finally, we introduce the role of corticosteroids in the amphibious behavior. Aldosterone is a major mineralocorticoid in mammals, but only minimally represented in teleosts. In teleosts, cortisol acts as mineralocorticoid as well as glucocorticoid (Takahashi and Sakamoto, 2013). Thus, cortisol action on the amphibious behavior has been investigated. We expect that this review will arouse further interest in the functional evolution of osmoregulatory hormones not only for fish endocrinologists but also for those working on other animals.

Angiotensin II and Thirst-Motivated Migration

Comparative studies using various vertebrates such as teleosts, amphibians, and mammals suggest that adaptation to life on dry land with a full influence of the gravitational force necessitates an elaborate renin-angiotensin system to be evolved (Nishimura, 1978; Leow, 2015). In mammals, the renin-angiotensin cascade is initiated by the release of renin from the juxtaglomerular cells in the renal afferent arteriole. Renin is released by hypovolemia and subsequent decreases in perfusion pressure at the arteriole (Kobayashi and Takei, 1996; Nishimura, 2017). The principal action of the active principle, Ang II, is to restore blood volume by retaining NaCl and water. Ang II stimulates secretion of VP and aldosterone, thereby further contributing to volume retention. Indeed, loss of function of the renin-angiotensin or VP system resulted in a hypotensive phenotype (Doan et al., 2001; Fujiwara and Bichet, 2005). Since inhibitors of the renin-angiotensin system attenuate hypovolemia-induced drinking, plasma Ang II is closely related to extracellular dehydration (Kobayashi and Takei, 1996). Unlike in mammals, plasma Ang II levels increase by hyperosmotic stimulus (cellular dehydration) as well as by hypovolemic stimulus in teleosts (Nishimura, 1978; Tierney et al., 1995; Takei, 2000). Transfer from fresh water to seawater results in a small and transient increase in plasma Ang II concentration in parallel with plasma osmolality (Okawara et al., 1987). Thus, Ang II functions as a fast-acting hormone in response to fluctuation of environmental salinity (Takei et al., 2014). The dipsogenic effect of Ang II has been examined extensively in various vertebrates including teleost and elasmobranch fishes (Kobayashi et al., 1983; Perrott et al., 1992; Anderson et al., 2001; Fuentes and Eddy, 2012). Ang II is the most potent dipsogenic hormone thus far known in many vertebrate species (Fitzsimons, 1998; Takei, 2000; McKinley and Johnson, 2004).

Thirst is defined as a conscious sensation of a need for water and a desire to drink (Fitzsimons, 1979). In terrestrial animals such as mammals, thirst is followed by a search for water, and its motivation or consciousness is generated in the hypothalamic area and the medial thalamic-cortex network (Denton et al., 1999; Gizowski and Bourque, 2018). Thirst is induced by an increase in systemic Ang II concentration (Kobayashi et al., 1979; Fitzsimons, 1998; Takei, 2000; McKinley and Johnson, 2004). In mammals and birds, systemic Ang II binds to the sensory circumventricular organs (CVOs) in the forebrain that lack the blood-brain barrier to induce drinking behaviors (Simpson and Routtenberg, 1973; Kobayashi and Takei, 1996) (**Figure 2A**). Angiotensin type 1 receptors (AT1) are present in high density in the organum vasculosum of the lamina terminalis (OVLT) and the subfornical organ (SFO) which are known as forebrain CVOs for Ang II-induced thirst (Johnson and Buggy, 1978; Fitzsimons, 1998; McKinley, 2003). Although Ang II also binds to type 2 receptors (AT2), AT2 receptors are sparse at these regions (Rowe et al., 1992). AT1 antagonist losartan inhibited Ang II-induced drinking, but AT2 receptor antagonist PD-123177 did not have any inhibitory action (Timmermans et al., 1993; Goodfriend et al., 1996). Thus, Ang II-induced drinking behavior is mediated through AT1 receptors (Fitzsimons, 1998). It is believed that amphibians such as terrestrial toads and arboreal frogs do not normally drink but instead obtain water by absorption through the ventral skin (Jørgensen, 1997; Bentley, 2002). Interestingly, Ang II induces such water-acquiring behavior called "cutaneous drinking", in which the pelvic patch is pressed against a moist surface (Hoff and Hillyard, 1991; Propper et al., 1995; Maejima et al., 2010). The cutaneous drinking behavior seems to be regulated via AT1 in the forebrain where CVOs probably localize (Duvernoy and Risold, 2007; Maejima et al., 2010; Uchiyama, 2015), suggesting conserved neural basis of thirst throughout tetrapods. In aquatic teleost fishes, however, none of the regions in the forebrain appear to be involved in elicitation of drinking,

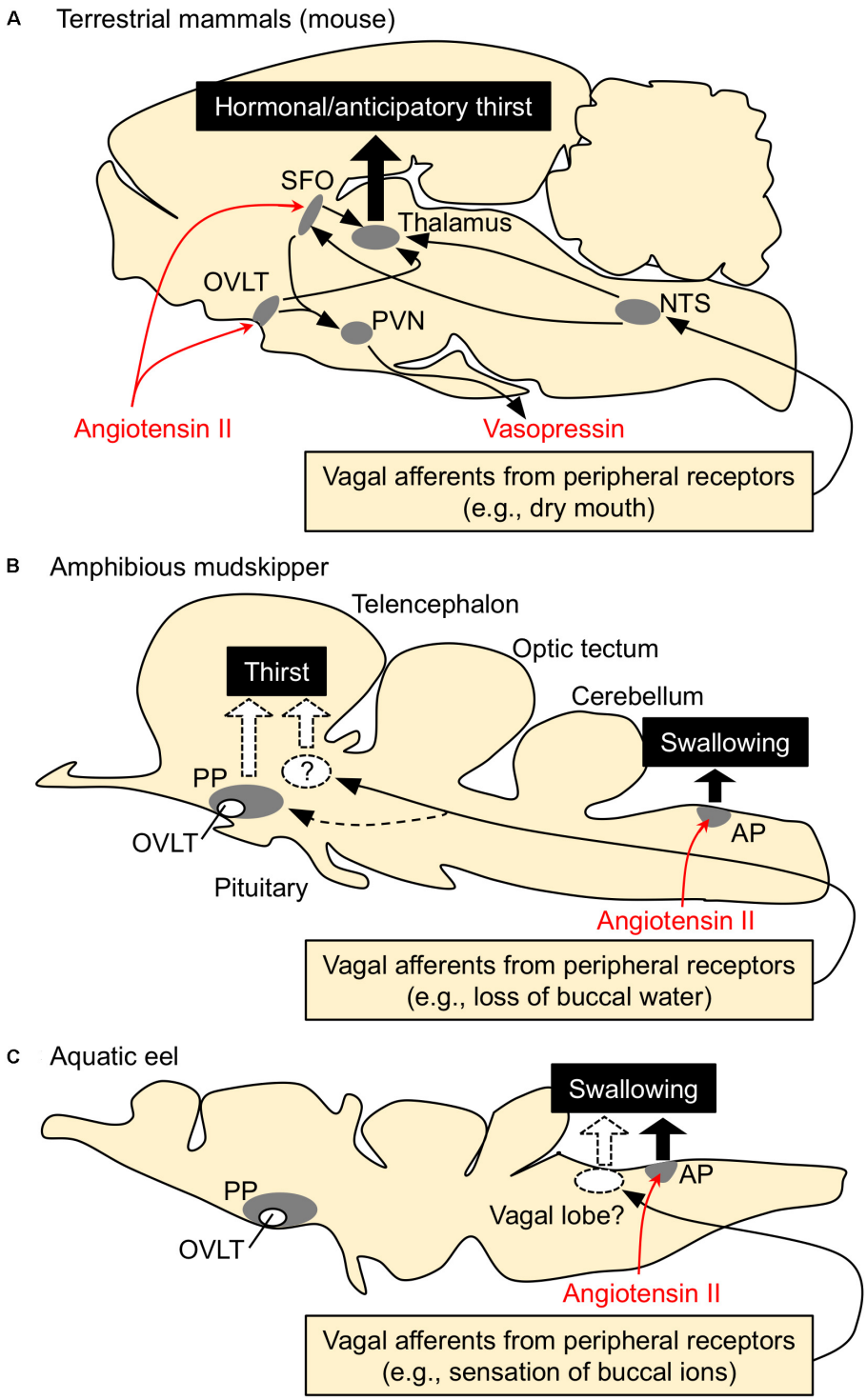

FIGURE 2 | Schematic drawing for the regulatory mechanisms of drinking behavior in terrestrial mammals, amphibious mudskippers, and aquatic eels. Systemic angiotensin II acts on the circumventricular organs (CVOs) that are outside the blood-brain barrier. Among CVOs, the area postrema (AP) and the organum vasculosum of the lamina terminalis (OVLT) exist in mice, mudskippers, and eels, but the subfornical organ (SFO) is identified only in tetrapods. **(A)** Thirst-inducing mechanisms in mice. Systemic angiotensin II is perceived by the neurons in the SFO and OVLT. The signal is transmitted to the thalamus for thirst inducement, and to the paraventricular (PVN) and supraoptic (SON) nuclei for vasopressin secretion. The generation of thirst seems to involve activation of the cortex, which might be mediated by relay neurons in the medial parts of the thalamus. Signals from peripheral receptors (e.g., dry mouth, buccal food) also reach thirst-regulating regions

(*Continued*)

FIGURE 2 | Continued
(e.g., SFO) via visceral afferents that course through spinal or vagal pathways. This thirst is evoked before any changes in blood parameters and thus noted as "anticipatory thirst". NTS, nucleus tractus solitarius. **(B,C)** Mechanisms of drinking in mudskippers and eels. The AP neurons receive systemic angiotensin II and induce swallowing, possibly through the glossopharyngeal-vagal motor complex in the medulla oblongata. In mudskippers **(B)**, sensory detection of loss of buccal water motivates mudskippers to refill water possibly through the vagal afferents, suggesting generation of thirst. Possible thirst center, which regulates migration to water for drinking, has not been identified yet, but vasotocin neurons in the parvocellular preoptic nucleus (PP) might be involved in the neural basis. In eels **(C)**, sensory detection of an increase in Cl^- concentration in buccal water induces swallowing of water as an anticipatory drinking. This local stimulus is sensed by afferent fibers of vagus and glossopharyngeal nerves, while the forebrain and AP are not involved in the anticipatory drinking. Regulation of drinking behavior by the vagal afferents appears to be conserved among vertebrates. In contrast, an involvement of the forebrain in the eel drinking has not been implicated.

since removal of the whole forebrain in eels did not affect the drinking induced by seawater exposure (Hirano et al., 1972) or by injection of Ang II (Takei et al., 1979). These stimuli may act on the hindbrain to initiate swallowing reflex in aquatic teleosts, which complete drinking only by swallowing of buccal water without a search for water (**Figure 2C**). The area postrema (AP) in the hindbrain is proposed to be the primary site of systemic Ang II action, since Evans blue injected into the blood stained this hindbrain CVO (Mukuda et al., 2005) and lesioning of the AP impaired Ang II-induced drinking in eels (Nobata et al., 2013). The AP neurons send cholinergic fibers to the glossopharyngeal-vagal motor complex (Ito et al., 2006), which in turn control the upper esophageal sphincter (UES) muscle (Mukuda and Ando, 2003; Nobata et al., 2013). The UES muscle is the first gate of the alimentary tract and its relaxation leads to initiation of swallowing.

From the comparative point of view, it is intriguing to examine whether amphibious mudskippers have the mechanism inducing thirst as a motivation for drinking. Our recent study showed that peripheral or central administration of Ang II motivates the fish to move to water and to increase the volume of water ingested (Katayama et al., 2018). An OVLT-like structure has been found histologically in the parvocellular preoptic nucleus (PP) of the mudskipper (Hamasaki et al., 2016), but our histochemical study did not support the direct action of Ang II on this region. AT1 receptors have been cloned in teleosts including mudskippers (Nishimura, 2017) although no expression study has demonstrated a calcium signal in the recombinant receptors (Russell et al., 2001). AT1-like mRNA was not detected in the OVLT-like region of mudskippers, while many nuclei in the AP expressed the mRNA (Katayama et al., 2018). AT2 receptors have been cloned in teleosts (Nishimura, 2017), but AT2 mRNA was not detected in the eel brain (Wong and Takei, 2013). Thus, AT1, not AT2, appears to mediate Ang II-induced drinking behavior also in teleosts. In mudskippers, Ang II, through its action on the AP, induced swallowing of buccal water, which is stored on land, and the loss of buccal water motivated mudskippers to move to water (**Figure 2B**; Katayama et al., 2018). Although regulation of the renin-angiotensin system has not been examined when mudskippers are on land, Ang II appears to induce drinking naturally in teleosts since an inhibitor of the renin-angiotensin system (captopril) attenuates spontaneous drinking (Okawara et al., 1987; Perrott et al., 1992; Kobayashi and Takei, 1996). In addition to the osmoregulatory problem, the effect of gravity cannot be nullified in terrestrial environments. Blood pressure of mudskippers is maintained during the transition from submersion to emersion unlike other teleost species, in spite of the influence of gravity (Ishimatsu et al., 1999). Since Ang II contributes to the maintenance of cardiovascular homeostasis in teleosts (Mével et al., 2012; Nishimura, 2017), its relative importance may have been enhanced for cardiovascular regulation as well as for osmoregulation in amphibious mudskippers. In a series of their drinking behaviors, the migration to water stimulated by loss of buccal water is equivalent to the drinking behavior in tetrapods evoked by local stimuli (e.g., dry mouth). Such drinking has been revealed as "anticipatory thirst" in mice because it operates before blood osmolality fluctuates (Berridge, 2004; Zimmerman et al., 2016). In mudskippers, the buccal cavity is filled with water before they exit to land and this behavior appears not to be involved in blood osmolality and hormones. Therefore, the thirst by local sensation may contribute to an anticipatory mechanism to prevent potential dehydration on land.

Although migratory behavior induced by local sensation has not been demonstrated in aquatic fishes, it is well recognized that eels detect an increase in Cl^- concentration in buccal water, which enhances swallowing of water (Hirano, 1974). This local stimulus is sensed by afferent fibers of vagus and/or glossopharyngeal nerves (Mayer-Gostan and Hirano, 1976), whereas the forebrain and AP appear not to be involved in the sensory detection because the lesioning of these regions did not attenuate swallowing induced by seawater exposure in the eel (**Figure 2C**; Hirano et al., 1972; Nobata and Takei, 2011). This "chloride response" could prevent future dehydration in hyperosmotic marine environments, and thus was referred to as an anticipatory drinking (Hirano, 1974). The sensation of ions in the buccal cavity of aquatic fishes may be similar to the sensation of buccal water underlying the thirst of tetrapods and mudskippers. In basal vertebrates such as river lamprey (*Lampetra fluviatilis*), the transfer from seawater to fresh water rapidly decreased drinking rate without a change in plasma osmolality (Rankin, 2002). Thus, the mechanism of anticipatory drinking by local sensation appears to be widely distributed among vertebrates. Mudskippers, which evolved from the aquatic teleosts to invade the terrestrial environment (You et al., 2014; Ord and Cooke, 2016), have developed the thirst-inducing mechanism by local sensation, in addition to the hormonal/anticipatory regulation of swallowing at the medulla oblongata observed in totally aquatic fishes (**Figures 2B,C**). Phylogenetically distant vertebrates (ray-finned fish and tetrapods) appear to have acquired the thirst sensation that elicits a series of drinking behaviors when they are exposed to a desiccating environment (Katayama et al., 2018). From the evolutionary point of view, it is intriguing to examine possible

thirst mechanisms of amphibious lungfish, which belong to the class Sarcopterygii and are recognized as the closest living relatives of tetrapods (Brinkmann et al., 2004). Since ancestral vertebrates should not have experienced terrestrial environments, thirst may have evolved multiple times during the course of terrestrialization in vertebrates.

In mammals, the input signal for anticipatory thirst was shown to be relayed to the SFO neurons that monitor blood factors such as Ang II (**Figure 2A**; Zimmerman et al., 2016). The SFO orchestrates a motivation for drinking by engaging the medial thalamic-cortex network (Gizowski and Bourque, 2018). Given the complex mechanisms of thirst in mammals, the mudskipper with a simpler brain architecture might be a useful model to investigate the mechanisms of anticipatory thirst by local sensation. In addition to the osmoregulatory purpose, the thirst response also prevents the gills from desiccation, and maintains the branchial respiration in mudskippers (Tamura et al., 1976; Sayer, 2005). Thus, maintaining the moistness of the gill could be one of the selection pressures for the development of thirst. Buccal water is also used for sucking of food when mudskippers eat on land (Michel et al., 2015), and thus water in the cavity decreases after feeding. Because the protrusion and retraction of this water mass is essential for intra-oral transport of prey on land, eating appears to be a potent stimulus for thirst development by local sensation. Many mammalian species drink primarily during meals (Fitzsimons and Le Magnen, 1969; Oatley and Toates, 1969; Berridge, 2004). Food consumption rapidly activated SFO neurons in mammals, beginning at the onset of feeding before any changes in blood parameters occurred (Zimmerman et al., 2016). Activation of SFO neurons during eating was unaffected by angiotensin blockers. Thus, sensory detection of buccal food and its consequent activation of SFO neurons through an angiotensin-independent pathway are indicated for prandial thirst in mammals. In teleosts, however, it has not been examined whether prandial drinking functions in anticipatory fashion to prevent food ingestion-dependent alterations in blood composition. More fish studies on anticipatory drinking, as well as on fast-acting Ang II actions, will be required to know the comprehensive mechanisms for "fast" adaptive response to hyperosmotic environments. Given that anticipatory drinking triggered by local sensation is conserved among vertebrates, comparison of drinking behavior in mudskippers with anticipatory thirst in mammals might provide an answer to the question of why the anticipatory response evolved (Krashes, 2016).

Neurohypophysial Hormones for Osmoregulation and Social Behaviors

The neurohypophysial hormones, VP and oxytocin (OXT), regulate fluid homeostasis, which requires a tight control of both NaCl and water in mammals (Johnson and Thunhorst, 1997; McKinley et al., 2004). Particularly, antidiuretic VP is a fast- and short-acting hormone that is indispensable for fluid retention in terrestrial environments. VP neurons in the paraventricular (PVN) and supraoptic (SON) nuclei of the hypothalamus react to increases in plasma osmolality by releasing the antidiuretic hormone (Nielsen et al., 1995; Bourque, 2008; Sands et al., 2011; Watts, 2015). The VP neurons are downstream targets of the angiotensinergic neurons innervating the SFO and OVLT (**Figure 2A**; Ferguson, 2009). Systemic Ang II enhances secretion of VP into the circulation through these neural pathways (Zimmerman et al., 2017). Thus, the Ang II-VP system enhances water retention by the kidney. In contrast, OXT decreases ingestive behaviors, including drinking, salt intake, and feeding (Arletti et al., 1990; Blevins et al., 2003; Stricker and Stricker, 2011; Ryan et al., 2017), and increases renal NaCl excretion after a salt load (Balment et al., 1980; Verbalis et al., 1991; Conrad et al., 1993). In addition to systemic osmoregulation, it has recently been suggested that VP neurons and OXT-receptor-expressing neurons anticipate future osmotic fluctuation by drinking, cues predicting water (e.g., visual cue), feeding, or sleeping (Gizowski et al., 2016; Mandelblat-Cerf et al., 2017; Ryan et al., 2017). For example, the neural activity of VP neurons in the PVN and SON, and thereby VP secretion rapidly fell during drinking before any change in blood parameters occurred (Stricker and Stricker, 2011; Mandelblat-Cerf et al., 2017).

In teleosts, neurohypophysial hormones serve for adaptation to a desiccating seawater environment. Transfer of trout to seawater downregulated transcription of VT (the teleost homolog of VP) in the magnocellular preoptic nucleus (PM) of trout (Hyodo and Urano, 1991). In flounders, however, transfer from seawater to fresh water decreased plasma VT concentration (Bond et al., 2002), whereas transfer from fresh water to seawater increased plasma VT levels and VT mRNAs in the hypothalamus (Balment et al., 2006). Thus, VT responses to environmental osmotic challenges and its physiological functions appear to differ among species. IT (the teleost homolog of OXT), as well as VT, has important functions in teleost osmoregulation. VT and/or IT regulate secretion of extra univalent ions in the gill and opercular epithelium (Guibbolini and Avella, 2003; Martos-Sitcha et al., 2015b). These hormones also regulate water transport via aquaporin-1 paralogs, which contribute to water absorption in the intestine for seawater adaptation (Martos-Sitcha et al., 2015a). IT mRNA levels in the hypothalamus increased after transfer to hypersaline media but not to hyposaline media (Martos-Sitcha et al., 2014). These results suggest that IT and its receptor are important for seawater adaptation. In addition to these osmoregulatory functions, VT and IT neurons localized throughout the hypothalamic regions project not only into the pituitary but also into multiple extra-hypothalamic regions, and are known to mediate social behaviors (Holmqvist and Ekstrom, 1995; Thompson and Walton, 2004; Goodson, 2005; Godwin and Thompson, 2012; Lindeyer et al., 2015). Even in mammals, however, little is known about a possible link between osmoregulation and social behaviors, both of which are controlled by the neurohypophysial hormones.

The amphibious behavior in mudskippers may reflect many functions of neurohypophysial hormones that bridge osmoregulation and social behaviors. Mudskippers moved to water when treated with VT or IT either peripherally or centrally (Sakamoto et al., 2015). Migration to water induced by both VT and IT was inhibited by the OXT receptor blocker (H-9405), which specifically induces IT-receptor blockade in teleosts

(Watanabe et al., 2007). Expression studies of VT type 1a receptor (V1a) and IT receptors of teleosts in mammalian cell lines indicate that V1a is nearly specific to VT, whereas the sensitivity of the IT receptor to IT is 3-10 times higher than that to VT (Mahlmann et al., 1994; Hausmann et al., 1995; Warne, 2001; Yamaguchi et al., 2012). Thus, neurons expressing IT receptors may regulate amphibious behavior for osmoregulation. However, other VT/IT receptors, especially VT type 2 receptor (V2), might be implicated in the aquatic preference. The V2-type receptor, which is localized in the hypothalamus and osmoregulatory organs, is involved in body fluid homeostasis in teleosts (Konno et al., 2010a,b; Lema, 2010; Martos-Sitcha et al., 2014). When VT or IT was intracerebroventricularly injected, the drinking rate of mudskippers was enhanced by VT, but not by IT (Katayama et al., 2018). Considering the affinities of VT/IT to their receptors, the VT-specific regulation of drinking appears to be mediated by VT receptors in the mudskipper brain. In mammals, VP neurons that innervate the OVLT play an important role in the above-mentioned "anticipatory thirst" (Gizowski et al., 2016). In mudskippers, immunoreactive VT fibers were found in the PP including the OVLT-like region (Hamasaki et al., 2016). These findings suggest that VT may transmit the signal to the neural pathway of thirst-motivated behavior (**Figure 2B**; Katayama et al., 2018). In eels, however, peripherally injected VT reduced drinking rate, but IT increased it (Ando et al., 2000; Nobata and Ando, 2013). Thus, the role of neurohypophysial hormones in regulation of drinking has not been established in teleosts. When mudskippers were dehydrated under terrestrial condition, brain mRNA levels of pro-VT markedly increased while a moderate increase was seen in pro-IT mRNA levels (**Figure 1B**). Given the relatively wide distribution of VT-positive fibers throughout the brain, increased VT under terrestrial condition may naturally stimulate drinking and migration to water (Sakamoto et al., 2015). Nuclei involved in the amphibious behavior were not identified, but brain regions where both VT and IT fibers are localized (e.g., the tuberal nuclei of the hypothalamus, medulla oblongata) may include nuclei expressing IT receptors to regulate this behavior.

In addition to the osmoregulatory function, regulation of social behavior by the VT system has been extensively studied in teleosts (Huffman et al., 2015; Yokoi et al., 2015; Loveland and Fernald, 2017; Perrone and Silva, 2018). Central administration of VT in some species indicates that VT neurons mediate aggression, although the directionality (stimulation/inhibition) varies across species (Godwin and Thompson, 2012; Kagawa et al., 2013). In mudskippers, VT specifically regulated general aggressive behavior and/or social communication (i.e., fin display, operculum display, replacement, attacking, chasing, and biting) (**Figure 3A**). In particular, VT-injected males showed significantly higher frequencies of fin display, operculum display and attack than vehicle-injected males. The former two types of behaviors are less aggressive than the latter one, and it is suggested that the VT might modulate social communication as well as aggression in mudskippers. Pro-VT mRNA levels in the whole brain of subordinate, however, were higher than in that of dominant (**Figure 3B**). In several freshwater teleosts, aggressive dominant males have high VT expression in the PM, whereas the submissive subordinate males have high VT expression in the PP (Larson et al., 2006; Greenwood et al., 2008; Kagawa, 2013). Together with prolonged aquatic stay by VT-injected mudskippers, VT in the PP may play a characteristic role in promoting migration into water for submissive subordinates relative to aggressive dominants (Kagawa et al., 2013). VT expression in the PP is involved in the hormonal stress response in the European eel and the rainbow trout (Olivereau and Olivereau, 1990; Gilchriest et al., 2000). However, the migration into water by VT-injected mudskippers cannot be fully explained by a physiological stress response, since there was no difference in plasma cortisol levels (Kagawa et al., 2013). In the mudskipper brain, VT fibers were localized in the preoptic and ventromedial telencephalic areas (Sakamoto et al., 2015). These regions include V1a-expressing neurons in teleosts (Kline et al., 2011; Huffman et al., 2012; Lema et al., 2015). With regard to V1a receptor subtypes, telencephalic V1a1 levels were higher in subordinates compared to dominants, and levels of V1a2 in the telencephalon of dominant males correlated with aggression in killifish (Lema et al., 2015). In cichlid fish, the ventromedial telencephalic area was the site of high density expression for both of these receptors (Loveland and Fernald, 2017). These findings suggest that VT neurons projecting to the ventromedial telencephalic area and/or preoptic area act via V1a2 in the dominant mudskipper to elicit general aggressive behavior, and that the VT neurons act via V1a1 in the subordinate to inhibit general aggressive behavior (**Figure 3C**). As described above, VT neurons projecting to the tuberal nuclei of the hypothalamus and medulla oblongata may act at least in part via IT receptors to stay in the aquatic habitat forced by the dominant fish (**Figure 3C**). Given the suite of processes mediated by neurohypophysial hormones, migration of subordinate mudskippers into water reflects a unique interaction between the hormonal regulations of social and osmoregulatory behaviors from competitive and dehydrating land to aquatic environments in the amphibious teleost. A few studies on teleosts have shown that IT controls the reproductive behavior and/or spawning act (Gonçalves and Oliveira, 2011). Mudskippers spawn in their mudflat burrows filled with water, and secure embryonic development within the hypoxic burrows by transporting mouthfuls of air (Ishimatsu et al., 2007). Thus, the unique link between osmoregulation and reproduction regulated by IT should be possible.

Corticosteroids for Ion Regulation and Stress Response

Corticosteroids function as glucocorticoids and mineralocorticoids in vertebrates. Glucocorticoids regulate metabolism and growth, while mineralocorticoids regulate the body fluid osmolality. In tetrapods, these functions are achieved by two distinct hormones: cortisol/corticosterone (glucocorticoids) and aldosterone (mineralocorticoid). Glucocorticoids and mineralocorticoids activate their receptors – the glucocorticoid receptor (GR) and mineralocorticoid receptor (MR), respectively (**Figure 4A**). In the mammalian brain, the GR and MR are both highly expressed in the hippocampus and in several hypothalamic nuclei such as PVN and arcuate

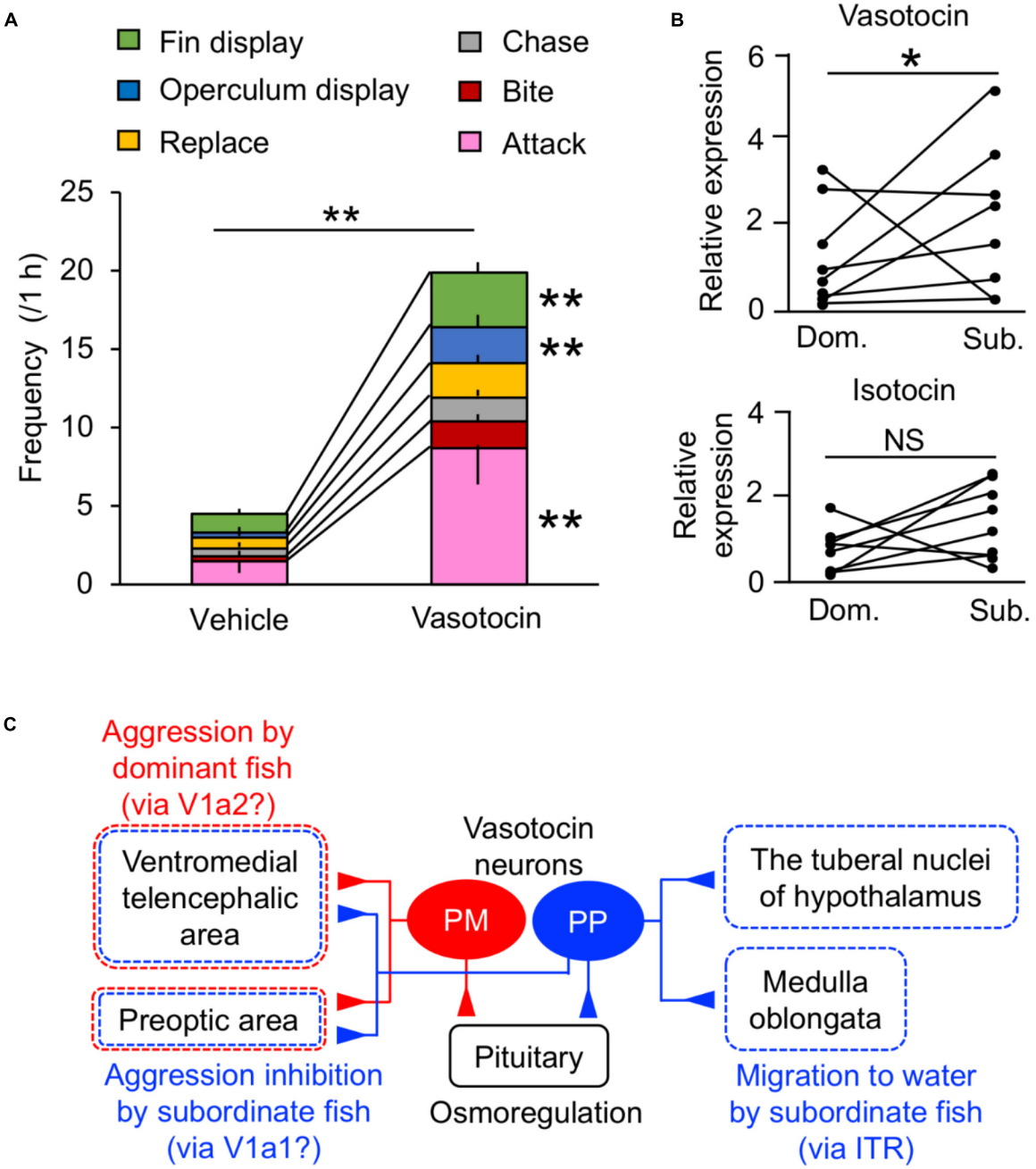

FIGURE 3 | Behavioral actions of vasotocin in mudskippers. **(A)** The frequency of each type of aggressive behavior after injection of vasotocin (500 pg/g-bw) or vehicle in mudskippers ($n = 6$). A size-matched pair of males was used for behavioral observation in a tank with aquatic and terrestrial areas. Data are shown as the means ± SE. $^{**}p < 0.005$ with *t*-test. **(B)** The expression of vasotocin and isotocin mRNAs in dominant (Dom.) and subordinate (Sub.) mudskippers ($n = 7$). Upon introduction in an experimental tank with aquatic and terrestrial areas, a pair of males can be classified as aggressive dominant or submissive subordinate based on the frequency of their aggressive behaviors, which is significantly higher in dominant male. Points of each pair are connected. $^{*}p < 0.05$ with Mann–Whitney *U*-test. NS, not significant. The original data for **(A)** and **(B)** are published in Kagawa et al. (2013). **(C)** A model illustrating the potential influence of vasotocin neurons on the regulation of aggressive behavior. The cell bodies of vasotocin are localized in the magnocellular (PM) and the parvocellular (PP) preoptic nucleus. Vasotocin may act via V1a-type receptors (V1a1/V1a2) in the ventromedial telencephalic area and the preoptic area to regulate general aggressive behavior. PM cells and V1a2 may mediate aggression by dominant males, while PP cells and V1a1 may mediate submissive behaviors by subordinate males. Since stimulation of migration to water by both vasotocin and isotocin is inhibited by the blocker of isotocin receptor (ITR), brain regions where both vasotocin and isotocin fibers are localized, such as the tuberal nuclei of the hypothalamus and the medulla oblongata, may regulate the amphibious behavior via ITR. The main receptors for specific behaviors are given in parentheses. Broken lines show possible brain regions involved in each behavior.

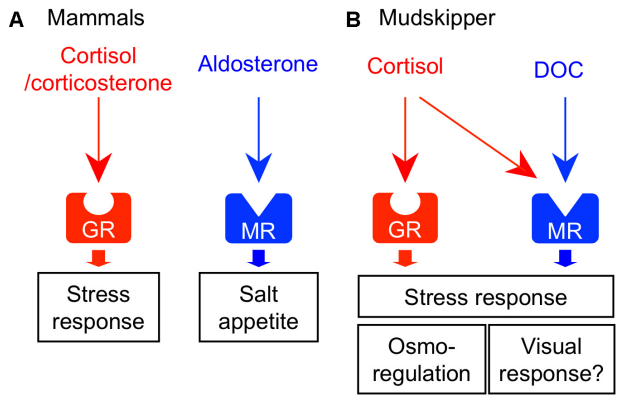

FIGURE 4 | Receptor-ligand interactions of corticosteroids and their central actions. **(A)** Corticosteroid system in mammals. Glucocorticoid (cortisol/corticosterone) and mineralocorticoid (aldosterone) activate their respective receptors – glucocorticoid receptor (GR) and mineralocorticoid receptor (MR). These corticosteroids act on the various brain regions and regulate homeostatic behaviors such as stress response and salt appetite. **(B)** Corticosteroid system in mudskippers. Cortisol-GR system mediates both glucocorticoid and mineralocorticoid functions. 11-deoxycorticosterone (DOC) is the preferred ligand for MR. In mudskippers, both MR and GR regulate the amphibious behavior related to a stress response. The aquatic preferences induced by GR and MR signaling may be related to osmoregulation and visual response, respectively.

nucleus. Co-localization of these receptors has been found in most neurons of the nuclei. These findings suggest that the expression balance of GR/MR within the nucleus is critical for many physiological and short-term behavioral responses, such as regulation of salt intake, mood, appetite, and exploratory behavior (Rozeboom et al., 2007; Kawata et al., 2008; Geerling and Loewy, 2009; Sakamoto et al., 2012). The CVOs such as the SFO and the AP are considered to be involved in the synergistic action of Ang II and mineralocorticoid on salt appetite (Epstein, 1982; Fluharty and Epstein, 1983; Alhadeff and Betley, 2017), since the neurons in those brain areas express both angiotensin receptor (Gehlert et al., 1991; Tsutsumi and Saavedra, 1991; Song et al., 1992) and MR (Coirini et al., 1983).

As mentioned earlier, cortisol functions not only as glucocorticoid but also as mineralocorticoid in teleosts (Mommsen et al., 1999). Two different GR coding genes (GR1 and GR2) and one MR gene have been found in this fish group (Bury et al., 2003; Greenwood et al., 2003). Cortisol interacts with MR as well as with GRs, but cortisol-MR axis appears not to be important for osmoregulation unlike in mammals (Prunet et al., 2006; Stolte et al., 2008) (**Figure 4B**). Indeed, a constitutive MR-knockout medaka can grow and adapt to seawater, as well as to fresh water (Sakamoto et al., 2016). By contrast, inhibition of the GR by RU-486 prevented killifish from seawater adaptation (Shaw et al., 2007). Many studies using euryhaline teleosts indicate that cortisol-GR system plays important roles in both seawater and freshwater adaptation as a slow-acting hormone (McCormick, 2001; Takahashi and Sakamoto, 2013; Takei et al., 2014). In many teleosts, plasma cortisol and GR transcripts in osmoregulatory organs changed after transfer to seawater or fresh water although the directionality varied across species (McCormick, 2001; Takahashi and Sakamoto, 2013). In mudskippers (Sakamoto et al., 2002), plasma cortisol concentrations markedly increased when the teleosts were dehydrated under terrestrial condition (**Figure 1B**). Cortisol stimulated epithelial apoptosis in the mudskipper esophagus so that NaCl was desalinated from ingested seawater. Cortisol also induced cell proliferation to reduce permeability for freshwater adaptation (Takahashi et al., 2006). The dual functions of cortisol in teleosts may stem from the distinct action on multiple GR isoforms with different sensitivities to cortisol for transactivation and transrepression activities (Prunet et al., 2006; Stolte et al., 2008). In the gills of some teleosts, cortisol stimulated the differentiation of ionocytes into seawater type or freshwater type, and elevated the activity and/or transcription of key transporters in ionocytes such as NKA, Na^+-K^+-$2Cl^-$ cotransporter type 1, and cystic fibrosis transmembrane conductance regulator (Deane et al., 2000; McCormick, 2001; Aruna et al., 2012; Takahashi and Sakamoto, 2013). These actions increased ion excretion for seawater adaptation and ion uptake for freshwater adaptation, respectively. Cortisol also elevated the NKA activity and aquaporin expression in the intestine, thereby increasing water absorption across the epithelia to maintain water balance in a dehydrating seawater environment (Veillette et al., 1995; Veillette and Young, 2005; Cutler et al., 2007). These studies suggest that the hypo- and hyper-osmoregulatory action of cortisol-GR system is well conserved among euryhaline teleosts (Takei et al., 2014).

In teleosts, the circulation of aldosterone, present in extremely low levels, is unlikely to have actions on the GRs or MRs (Prunet et al., 2006). However, 11-deoxycorticosterone (DOC) is a circulating corticosteroid that is present in significant concentrations, and can activate MRs but not GRs in teleosts (Sturm et al., 2005; Prunet et al., 2006; Milla et al., 2008; Stolte et al., 2008). In expression studies in mammalian cell lines, transactivation of the teleost MR is 10 times more sensitive to DOC than to cortisol, whereas the teleost GR is specific to cortisol (Sturm et al., 2005; Prunet et al., 2006; Stolte et al., 2008). In agreement with the presence of the ligand for MRs in the plasma, the teleost MR mRNA was found in many tissues (Greenwood et al., 2003; Sturm et al., 2005; Arterbery et al., 2010). The expressions of MR mRNA are relatively modest in osmoregulatory organs involved in ionoregulation (e.g., gill), but considerably higher in the brains of most teleosts examined (e.g., Sakamoto et al., 2016). These recent finding suggested that MR system may carry out some behavioral functions in teleosts. In fact, mudskippers migrated into water when treated with DOC and cortisol (Sakamoto et al., 2011). Cortisol may act as an endogenous ligand for the brain MRs to stimulate the migration to water naturally, since plasma cortisol, rather than DOC, increased in mudskippers under terrestrial condition (**Figure 1B**). However, MRs can be insensitive to cortisol activation *in vivo* because 11β-hydroxysteroid dehydrogenase type 2 (11β-HSD2) catalyzes the conversion of cortisol to the MR-inactive cortisone (Funder et al., 1988). Without the expression of 11β-HSD2, MRs probably function as cortisol receptors. Hence, study on localization of 11β-HSD2 in the teleost brain is further

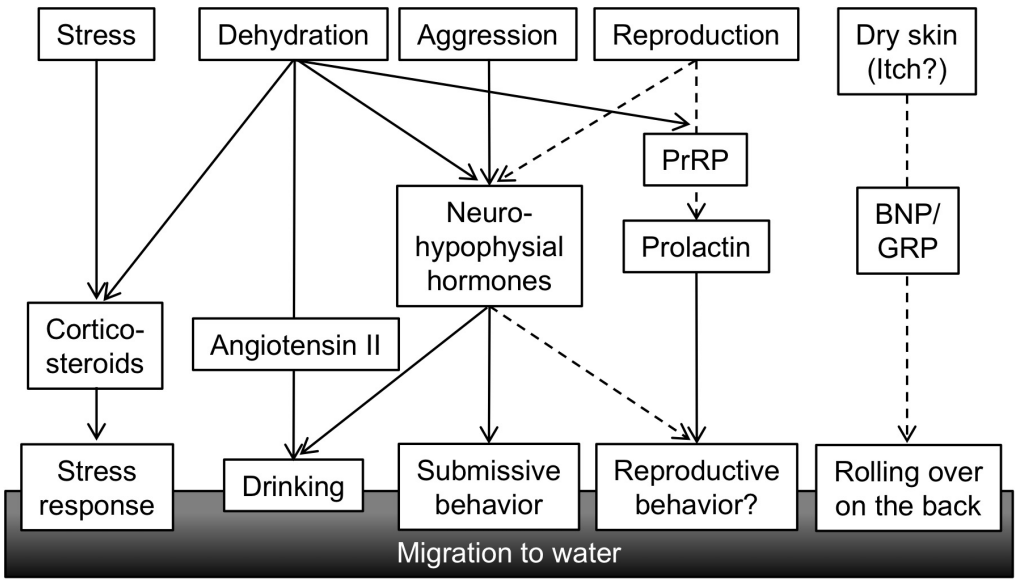

FIGURE 5 | A conceptual diagram of hormones regulating amphibious behavior of mudskippers. Various stimuli related to the amphibious lifestyle of mudskipper activate secretion of hormones, which in turn leads to behavioral and physiological outputs. Solid lines showing functional associations are based on published data, while broken lines are speculation. PrRP, prolactin-releasing peptide; BNP, B-type natriuretic peptide; GRP, gastrin-releasing peptide.

required. The aquatic preference in 10 ppt seawater, possibly stimulated by the brain MR signaling, may reflect the induction of salt appetite as shown by aldosterone in mammals (Alhadeff and Betley, 2017). Thus, it is of interest to examine synergistic effects of Ang II and corticosteroids to evaluate salinity preference of mudskippers using an aquarium test system. In contrast, the GR signaling may also contribute to the aquatic preference because the cortisol-stimulated behavior was not completely inhibited by the specific GR blocker, RU-486. Since the cortisol-GR system is implicated in excretion of extra ions by elevating the NKA activity in teleosts (McCormick, 2001; Takahashi and Sakamoto, 2013), mudskippers may migrate to water for ion excretion through the skin under the pectoral fin (Sakamoto et al., 2000, 2002). The distinct function of MR and GR signaling should be investigated in the osmoregulatory behavior of mudskippers.

In addition to the osmoregulatory function, GRs and MRs appear to regulate stress responses in the teleost brain (Takahashi and Sakamoto, 2013; Myers et al., 2014; Sakamoto et al., 2018). In teleosts, GRs and MRs are localized in key components of the stress axis, such as the forebrain pallial area, the corticotrophin-releasing hormone cells in the preoptic nucleus, and the adrenocorticotropic-hormone cells in the pituitary pars distalis (Stolte et al., 2008; Kikuchi et al., 2015; Sakamoto et al., 2016). The aquatic preference of mudskippers, stimulated by the brain MR/GR signaling, may also be a stress response, since the dehydrated mudskipper under terrestrial condition appears to be stressed (**Figure 4**; Sakamoto et al., 2002). Such a system that is responsive to external stressors can also mediate the start of migration from river to ocean in salmon (Clements and Schreck, 2004; Flores et al., 2012). The expression of GRs and MRs mRNA were observed in most of the PM and PP, known to produce VT and IT (Teitsma et al., 1998), and the cortisol-GR system regulated VT and IT release from the hypothalamus-pituitary complex (Kalamarz-Kubiak et al., 2015). Thus, future studies should focus on the "cross-talk" among these hormones in the brain to clarify the link between osmoregulation and stress response, both of which are primarily regulated by the neurohypophysial hormones and corticosteroids. Furthermore, GR mutant adult zebrafish became immobile with reduced exploratory behavior when placed into an unfamiliar aquarium (Ziv et al., 2013). The mutant did not habituate to this stressor upon repeated exposure. Addition of the antidepressant fluoxetine or visual interactions with a wild type fish restored normal behavior. Thus, GR signaling appears to contribute to mood regulation, as well as to the stress response. In contrast, MR-knockout medaka failed to track moving dots although the swimming motility of the mutant increased (Sakamoto et al., 2016). Thus, MR is required for normal activity of locomotion in response to visual motion stimuli. Vision is more important in terrestrial lifestyle than in aquatic one, and sophisticated vision might have promoted land invasion in vertebrates (MacIver et al., 2017). Mudskippers with their unique vision system (Takiyama et al., 2016) will be a good model to analyze the evolution of corticosteroids-regulated vision response.

CONCLUSION AND PERSPECTIVES

In this review, we summarized the role of Ang II, neurohypophysial hormones, and corticosteroids in the regulation of amphibious behavior in mudskippers. Mudskippers migrate to water for drinking and for escape from dominant conspecifics and stressful situations (**Figure 5**). The analyses of their drinking patterns suggest that the neural basis of

amphibious behavior is connected to a water detection system in the buccal cavity, which is related to induction of thirst. Direct action of systemic Ang II on the OVLT-like structure and the Ang-II/neurohypophysial hormone axis in the forebrain have not yet been investigated in teleosts including mudskippers. In future research, the target site(s) of systemic Ang II other than those along the lamina terminalis might be identified in the mudskipper forebrain. VT also regulates amphibious behavior related to aggression/submission as well as to drinking, suggesting their distinct functions in each site of the brain. Cortisol may bind to the MR in the brain to elicit a preference for aquatic habitation, which reveals a conserved central action of mineralocorticoid signaling throughout vertebrates (Sakamoto et al., 2018).

It remains to be discovered how other behaviors regulated by osmoregulatory hormones have evolved during vertebrate terrestrialization, and these research gaps will need to be addressed in future study (**Figure 5**). As described above in regard to IT function, mudskippers spawn in their mudflat burrows that are filled with water, and they secure embryonic development of their young within the hypoxic burrows by transporting mouthfuls of air (Ishimatsu et al., 2007). These unique reproductive behaviors including both migration and parental care might be regulated by osmoregulatory hormones such as IT and prolactin (PRL). PRL plays a critical role in freshwater adaptation in teleost fishes (Manzon, 2002; Sakamoto and McCormick, 2006). PRL reduces ion and water permeability of osmoregulatory surfaces in fresh water, and increases ion uptake (Hirano, 1986; Manzon, 2002; Sakamoto et al., 2005b; Shu et al., 2016). Further, many of the reproductive functions of PRL appear to be conserved throughout the vertebrates (Whittington and Wilson, 2013). Migration plays an important role in the reproductive cycle of many vertebrates. For example, PRL injection induced migration from land to water in salamanders (Moriya, 1982). In the amphibious behavior of mudskippers, the PRL-releasing peptide/PRL axis induced a preference for aquatic habitation (Sakamoto et al., 2005b). This action resembles the migration to water of salamanders for spawning. PRL transcription and secretion were promoted by PRL-releasing peptide (Sakamoto et al., 2003; Fujimoto et al., 2006). In mudskippers, mRNA levels of PRL-releasing peptide and of PRL are similarly regulated. The mRNA levels in the brain-pituitary axis increased during both terrestrial and freshwater acclimation (Sakamoto et al., 2005a), although the dynamics of PRL mRNA during spawning has not been examined in mudskippers. During the chum salmon maturation process, PRL mRNA levels increased with the onset of anadromy (Onuma et al., 2010), whereas PRL may have no role in the reproductive migration of catadromous eels (Sudo et al., 2013). Thus, the role of PRL in reproductive migration appears to depend on environmental conditions where the teleosts live, and may have become important in the amphibious lifestyles of mudskippers. In teleosts, like in mammals, PRL also regulates reproductive development and brood care behavior as well as migration (Whittington and Wilson, 2013). Mudskippers showing such various reproductive traits can be fascinating models to explore hormonal function in behaviors related to both osmoregulation and reproduction.

Furthermore, in mudskippers, aquatic preference and rolling behavior on wet land are notable for moistening the dorsal skin (Ip et al., 1991). Since natriuretic peptides and gastrin-releasing peptide are currently known as key molecules to transmit itch sensation to the central nervous system in rodents (Sun and Chen, 2007; Mishra and Hoon, 2013; Liu et al., 2014), further analyses of these peptides may elucidate relationships between habitats and itch sensation by dry skin, as well as the unknown evolution of the itch sensation in vertebrates. As mentioned already, the "cross-talk" among these hormones in mudskippers may explain the coordination of amphibious behavior and other physiological regulation throughout vertebrate species.

AUTHOR CONTRIBUTIONS

All authors listed have made a substantial, direct and intellectual contribution to the work, and approved it for publication.

FUNDING

This work was supported in part by JSPS KAKENHI Grant No. JP 16J01114.

ACKNOWLEDGMENTS

We thank Dr. Susumu Hyodo of the University of Tokyo and Dr. Christopher A. Loretz of the State University of New York at Buffalo for critical reading of this manuscript. We also thank Dr. T. Mukuda of Tottori University, Dr. M. Kusakabe of the Shizuoka University, Dr. N. Kagawa of Kindai University, and Drs. H. Sakamoto, N. Tsutsui, Y. Kobayashi, and H. Takahashi of Okayama University for help with this research on the mudskipper.

REFERENCES

Alhadeff, A. L., and Betley, J. N. (2017). Pass the salt: the central control of sodium intake. *Nat. Neurosci.* 20, 130–131. doi: 10.1038/nn.4485

Anderson, W. G., Takei, Y., and Hazon, N. (2001). The dipsogenic effect of the renin–angiotensin system in elasmobranch fish. *Gen. Comp. Endocrinol.* 124, 300–307. doi: 10.1006/gcen.2001.7712

Ando, M., Fujii, Y., Kadota, T., Kozaka, T., Mukuda, T., Takase, I., et al. (2000). Some factors affecting drinking behavior and their interactions in seawater-acclimated eels. *Anguilla japonica*. *Zool. Sci.* 17, 171–178. doi: 10.2108/zsj.17.171

Arletti, R., Benelli, A., and Bertolini, A. (1990). Oxytocin inhibits food and fluid intake in rats. *Physiol. Behav.* 48, 825–830. doi: 10.1016/0031-9384(90)90234-U

Arterbery, A. S., Deitcher, D. L., and Bass, A. H. (2010). Corticosteroid receptor expression in a teleost fish that displays alternative male reproductive tactics. *Gen. Comp. Endocrinol.* 165, 83–90. doi: 10.1016/j.ygcen.2009.06.004

Aruna, A., Nagarajan, G., and Chang, C. F. (2012). Involvement of corticotrophin-releasing hormone and corticosteroid receptors in the brain–pituitary–gill of tilapia during the course of seawater acclimation. *J. Neuroendocrinol.* 24, 818–830. doi: 10.1111/j.1365-2826.2012.02282.x

Balment, R., Brimble, M., and Forsling, M. (1980). Release of oxytocin induced by salt loading and its influence on renal excretion in the male rat. *J. Physiol.* 308, 439–449. doi: 10.1113/jphysiol.1980.sp013481

Balment, R. J., and Carrick, S. (1985). Endogenous renin-angiotensin system and drinking behavior in flounder. *Am. J. Physiol. Regul. Integr. Comp. Physiol.* 248, R157–R160. doi: 10.1152/ajpregu.1985.248.2.R157

Balment, R. J., Lu, W., Weybourne, E., and Warne, J. M. (2006). Arginine vasotocin a key hormone in fish physiology and behaviour: a review with insights from mammalian models. *Gen. Comp. Endocrinol.* 147, 9–16. doi: 10.1016/j.ygcen.2005.12.022

Bentley, P. J. (2002). *Endocrines and Osmoregulation: A Comparative Account in Vertebrates*. Heidelberg: Springer. doi: 10.1007/978-3-662-05014-9

Berridge, K. C. (2004). Motivation concepts in behavioral neuroscience. *Physiol. Behav.* 81, 179–209. doi: 10.1016/j.physbeh.2004.02.004

Blevins, J. E., Eakin, T. J., Murphy, J. A., Schwartz, M. W., and Baskin, D. G. (2003). Oxytocin innervation of caudal brainstem nuclei activated by cholecystokinin. *Brain Res.* 993, 30–41. doi: 10.1016/j.brainres.2003.08.036

Bond, H., Winter, M., Warne, J., McCrohan, C., and Balment, R. (2002). Plasma concentrations of arginine vasotocin and urotensin II are reduced following transfer of the euryhaline flounder (*Platichthys flesus*) from seawater to fresh water. *Gen. Comp. Endocrinol.* 125, 113–120. doi: 10.1006/gcen.2001.7736

Bourque, C. W. (2008). Central mechanisms of osmosensation and systemic osmoregulation. *Nat. Rev. Neurosci.* 9, 519–531. doi: 10.1038/nrn2400

Brinkmann, H., Venkatesh, B., Brenner, S., and Meyer, A. (2004). Nuclear protein-coding genes support lungfish and not the coelacanth as the closest living relatives of land vertebrates. *Proc. Natl. Acad. Sci. U.S.A.* 101, 4900–4905. doi: 10.1073/pnas.0400609101

Bury, N., Sturm, A., Le Rouzic, P., Lethimonier, C., Ducouret, B., Guiguen, Y., et al. (2003). Evidence for two distinct functional glucocorticoid receptors in teleost fish. *J. Mol. Endocrinol.* 31, 141–156. doi: 10.1677/jme.0.0310141

Clayton, D. A. (1993). Mudskippers. *Oceanogr. Mar. Biol. Ann. Rev.* 31, 507–577.

Clements, S., and Schreck, C. B. (2004). Central administration of corticotropin-releasing hormone alters downstream movement in an artificial stream in juvenile chinook salmon (*Oncorhynchus tshawytscha*). *Gen. Comp. Endocrinol.* 137, 1–8. doi: 10.1016/j.ygcen.2004.02.004

Coirini, H., Marusic, E. T., De Nicola, A. F., Rainbow, T. C., and McEwen, B. S. (1983). Identification of mineralocorticoid binding sites in rat brain by competition studies and density gradient centrifugation. *Neuroendocrinology* 37, 354–360. doi: 10.1159/000123575

Conrad, K. P., Gellai, M., North, W. G., and Valtin, H. (1993). Influence of oxytocin on renal hemodynamics and sodium excretion. *Ann. N. Y. Acad. Sci.* 689, 346–362. doi: 10.1111/j.1749-6632.1993.tb55559.x

Cutler, C., Phillips, C., Hazon, N., and Cramb, G. (2007). Cortisol regulates eel (*Anguilla anguilla*) aquaporin 3 (AQP3) mRNA expression levels in gill. *Gen. Comp. Endocrinol.* 152, 310–313. doi: 10.1016/j.ygcen.2007.01.031

Deane, E. E., Kelly, S. P., and Woo, N. Y. (2000). Hypercortisolemia does not affect the branchial osmoregulatory responses of the marine teleost *Sparus sarba*. *Life Sci.* 66, 1435–1444. doi: 10.1016/S0024-3205(00)00454-9

Denton, D., Shade, R., Zamarippa, F., Egan, G., Blair-West, J., McKinley, M., et al. (1999). Neuroimaging of genesis and satiation of thirst and an interoceptor-driven theory of origins of primary consciousness. *Proc. Natl. Acad. Sci. U.S.A.* 96, 5304–5309. doi: 10.1073/pnas.96.9.5304

Doan, T. N., Gletsu, N., Cole, J., and Bernstein, K. E. (2001). Genetic manipulation of the renin-angiotensin system. *Curr. Opin. Nephrol. Hypertens.* 10, 483–491. doi: 10.1097/00041552-200107000-00002

Duvernoy, H. M., and Risold, P. Y. (2007). The circumventricular organs: an atlas of comparative anatomy and vascularization. *Brain Res. Rev.* 56, 119–147. doi: 10.1016/j.brainresrev.2007.06.002

Epstein, A. N. (1982). Mineralocorticoids and cerebral angiotensin may act together to produce sodium appetite. *Peptides* 3, 493–494. doi: 10.1016/0196-9781(82)90113-9

Evans, D. H. (2008). Teleost fish osmoregulation: what have we learned since August Krogh, Homer Smith, and Ancel Keys. *Am. J. Physiol. Regul. Integr. Comp. Physiol.* 295, R704–R713. doi: 10.1152/ajpregu.90337.2008

Ferguson, A. V. (2009). Angiotensinergic regulation of autonomic and neuroendocrine outputs: critical roles for the subfornical organ and paraventricular nucleus. *Neuroendocrinology* 89, 370–376. doi: 10.1159/000211202

Fitzsimons, J. T. (1979). *The Physiology of Thirst and Sodium Appetite*. Cambridge: Cambridge Univ. Press, 1–31.

Fitzsimons, J. T. (1998). Angiotensin, thirst, and sodium appetite. *Physiol. Rev.* 78, 583–686. doi: 10.1152/physrev.1998.78.3.583

Fitzsimons, T., and Le Magnen, J. (1969). Eating as a regulatory control of drinking in the rat. *J. Comp. Physiol. Psychol.* 67, 273–283. doi: 10.1037/h0026772

Flores, A.-M., Shrimpton, J., Patterson, D., Hills, J., Cooke, S., Yada, T., et al. (2012). Physiological and molecular endocrine changes in maturing wild sockeye salmon, *Oncorhynchus nerka*, during ocean and river migration. *J. Comp. Physiol. B* 182, 77–90. doi: 10.1007/s00360-011-0600-4

Fluharty, S. J., and Epstein, A. N. (1983). Sodium appetite elicited by intracerebroventricular infusion of angiotensin II in the rat: II. synergistic interaction with systemic mineralocorticoids. *Behav. Neurosci.* 97, 746–758. doi: 10.1037/0735-7044.97.5.746

Fuentes, J., and Eddy, F. (2012). "Drinking in marine, euryhaline and freshwater," in *Ionic Regulation in Animals: A Tribute to Professor WTW Potts*, eds W. T. W. Potts, N. Hazon, and B. Eddy (Berlin: Springer), 135–149.

Fujimoto, M., Sakamoto, T., Kanetoh, T., Osaka, M., and Moriyama, S. (2006). Prolactin-releasing peptide is essential to maintain the prolactin level and osmotic balance in freshwater teleost fish. *Peptides* 27, 1104–1109. doi: 10.1016/j.peptides.2005.06.034

Fujiwara, T. M., and Bichet, D. G. (2005). Molecular biology of hereditary diabetes insipidus. *J. Am. Soc. Nephrol.* 16, 2836–2846. doi: 10.1681/ASN.2005040371

Funder, J. W., Pearce, P. T., Smith, R., and Smith, A. I. (1988). Mineralocorticoid action: target tissue specificity is enzyme, not receptor, mediated. *Science* 242, 583–585. doi: 10.1126/science.2845584

Geerling, J. C., and Loewy, A. D. (2009). Aldosterone in the brain. *Am. J. Physiol. Renal Physiol.* 297, F559–F576. doi: 10.1152/ajprenal.90399.2008

Gehlert, D. R., Gackenheimer, S. L., and Schober, D. A. (1991). Autoradiographic localization of subtypes of angiotensin II antagonist binding in the rat brain. *Neuroscience* 44, 501–514. doi: 10.1016/0306-4522(91)90073-W

Gilchriest, B., Tipping, D., Hake, L., Levy, A., and Baker, B. (2000). The effects of acute and chronic stresses on vasotocin gene transcripts in the brain of the rainbow trout (*Oncorhynchus mykiss*). *J. Neuroendocrinol.* 12, 795–801. doi: 10.1046/j.1365-2826.2000.00522.x

Gizowski, C., and Bourque, C. W. (2018). The neural basis of homeostatic and anticipatory thirst. *Nat. Rev. Nephrol.* 14, 11–25. doi: 10.1038/nrneph.2017.149

Gizowski, C., Zaelzer, C., and Bourque, C. W. (2016). Clock-driven vasopressin neurotransmission mediates anticipatory thirst prior to sleep. *Nature* 537, 685–688. doi: 10.1038/nature19756

Godwin, J., and Thompson, R. (2012). Nonapeptides and social behavior in fishes. *Horm. Behav.* 61, 230–238. doi: 10.1016/j.yhbeh.2011.12.016

Gonçalves, D. M., and Oliveira, R. F. (2011). "Hormones and sexual behavior of teleost fishes," in *Hormones and Reproduction of Vertebrates: Fishes*, eds D. Norris and K. H. Lopez (New York, NY: Elsevier), 119–147.

Goodfriend, T. L., Elliott, M. E., and Catt, K. J. (1996). Angiotensin receptors and their antagonists. *N. Engl. J. Med.* 334, 1649–1655. doi: 10.1056/NEJM199606203342507

Goodson, J. L. (2005). The vertebrate social behavior network: evolutionary themes and variations. *Horm. Behav.* 48, 11–22. doi: 10.1016/j.yhbeh.2005.02.003

Graham, J. B. (1997). *Air-Breathing Fishes: Evolution, Diversity, and Adaptation*. Cambridge, MA: Academic Press.

Greenwood, A. K., Butler, P. C., White, R. B., DeMarco, U., Pearce, D., and Fernald, R. D. (2003). Multiple corticosteroid receptors in a teleost fish: distinct sequences, expression patterns, and transcriptional activities. *Endocrinology* 144, 4226–4236. doi: 10.1210/en.2003-0566

Greenwood, A. K., Wark, A. R., Fernald, R. D., and Hofmann, H. A. (2008). Expression of arginine vasotocin in distinct preoptic regions is associated with dominant and subordinate behaviour in an African cichlid fish. *Proc. Biol. Sci.* 275, 2393–2402. doi: 10.1098/rspb.2008.0622

Grosell, M. (2011). Intestinal anion exchange in marine teleosts is involved in osmoregulation and contributes to the oceanic inorganic carbon cycle. *Acta Physiol.* 202, 421–434. doi: 10.1111/j.1748-1716.2010.02241.x

Guibbolini, M., and Avella, M. (2003). Neurohypophysial hormone regulation of Cl-secretion: physiological evidence for V1-type receptors in sea bass gill respiratory cells in culture. *J. Endocrinol.* 176, 111–119. doi: 10.1677/joe.0.1760111

Hamasaki, S., Mukuda, T., Kaidoh, T., Yoshida, M., and Uematsu, K. (2016). Impact of dehydration on the forebrain preoptic recess walls in the mudskipper, *Periophthalmus modestus*: a possible locus for the center of thirst. *J. Comp. Physiol. B* 186, 891–905. doi: 10.1007/s00360-016-1005-1

Hausmann, H., Meyerhof, W., Zwiers, H., Lederis, K., and Richter, D. (1995). Teleost isotocin receptor: structure, functional expression, mRNA distribution and phylogeny. *FEBS Lett.* 370, 227–230. doi: 10.1016/0014-5793(95)00832-T

Hirano, T. (1974). Some factors regulating water intake by the eel, *Anguilla japonica*. *J. Exp. Biol.* 61, 737–747.

Hirano, T. (1986). The spectrum of prolactin action in teleosts. *Prog. Clin. Biol. Res.* 205, 53–74.

Hirano, T., Satou, M., and Utida, S. (1972). Central nervous system control of osmoregulation in the eel (*Anguilla japonica*). *Comp. Biochem. Physiol. A Physiol.* 43, 537–544. doi: 10.1016/0300-9629(72)90241-1

Hoenderop, J. G., Nilius, B., and Bindels, R. J. (2005). Calcium absorption across epithelia. *Physiol. Rev.* 85, 373–422. doi: 10.1152/physrev.00003.2004

Hoff, K. V. S., and Hillyard, S. D. (1991). Angiotensin II stimulates cutaneous drinking in the toad *Bufo punctatus*. *Physiol. Zool.* 64, 1165–1172. doi: 10.1086/physzool.64.5.30156238

Holmqvist, B. I., and Ekstrom, P. (1995). Hypophysiotrophic systems in the brain of the atlantic salmon. neuronal innervation of the pituitary and the origin of pituitary dopamine and nonapeptides identified by means of combined carbocyanine tract tracing and immunocytochemistry. *J. Chem. Neuroanat.* 8, 125–145. doi: 10.1016/0891-0618(94)00041-Q

Huffman, L. S., Hinz, F. I., Wojcik, S., Aubin-Horth, N., and Hofmann, H. A. (2015). Arginine vasotocin regulates social ascent in the African cichlid fish *Astatotilapia burtoni*. *Gen. Comp. Endocrinol.* 212, 106–113. doi: 10.1016/j.ygcen.2014.03.004

Huffman, L. S., O'Connell, L. A., Kenkel, C. D., Kline, R. J., Khan, I. A., and Hofmann, H. A. (2012). Distribution of nonapeptide systems in the forebrain of an African cichlid fish, *Astatotilapia burtoni*. *J. Chem. Neuroanat.* 44, 86–97. doi: 10.1016/j.jchemneu.2012.05.002

Hwang, P. P., Lee, T. H., and Lin, L. Y. (2011). Ion regulation in fish gills: recent progress in the cellular and molecular mechanisms. *Am. J. Physiol. Regul. Integr. Comp. Physiol.* 301, R28–R47. doi: 10.1152/ajpregu.00047.2011

Hyodo, S., and Urano, A. (1991). Changes in expression of provasotocin and proisotocin genes during adaptation to hyper- and hypo-osmotic environments in rainbow trout. *J. Comp. Physiol. B* 161, 549–556. doi: 10.1007/BF00260744

Ip, Y. K., Chew, S. F., and Tang, P. C. (1991). Evaporation and the turning behavior of the mudskipper, *Boleophthalmus boddaerti*. *Zoolog. Sci.* 8, 621–623.

Ishimatsu, A., Aguilar, N. M., Ogawa, K., Hishida, Y., Takeda, T., Oikawa, S., et al. (1999). Arterial blood gas levels and cardiovascular function during varying environmental conditions in a mudskipper, *Periophthalmodon schlosseri*. *J. Exp. Biol.* 202, 1753–1762.

Ishimatsu, A., Yoshida, Y., Itoki, N., Takeda, T., Lee, H. J., and Graham, J. B. (2007). Mudskippers brood their eggs in air but submerge them for hatching. *J. Exp. Biol.* 210, 3946–3954. doi: 10.1242/jeb.010686

Ito, S., Mukuda, T., and Ando, M. (2006). Catecholamines inhibit neuronal activity in the glossopharyngeal–vagal motor complex of the Japanese eel: significance for controlling swallowing water. *J. Exp. Zool. A Ecol. Gen. Physiol.* 305, 499–506. doi: 10.1002/jez.a.282

Johnson, A. K., and Buggy, J. (1978). Periventricular preoptic-hypothalamus is vital for thirst and normal water economy. *Am. J. Physiol.* 234, R122–R129. doi: 10.1152/ajpregu.1978.234.3.R122

Johnson, A. K., and Thunhorst, R. L. (1997). The neuroendocrinology of thirst and salt appetite: visceral sensory signals and mechanisms of central integration. *Front. Neuroendocrinol.* 18, 292–353. doi: 10.1006/frne.1997.0153

Jørgensen, C. B. (1997). 200 years of amphibian water economy: from Robert Townson to the present. *Biol. Rev. Camb. Philos. Soc.* 72, 153–237. doi: 10.1017/S0006323196004963

Kagawa, N. (2013). Social rank-dependent expression of arginine vasotocin in distinct preoptic regions in male *Oryzias latipes*. *J. Fish Biol.* 82, 354–363. doi: 10.1111/j.1095-8649.2012.03490.x

Kagawa, N., Nishiyama, Y., Kato, K., Takahashi, H., Kobayashi, Y., Sakamoto, H., et al. (2013). Potential roles of arginine-vasotocin in the regulation of aggressive behavior in the mudskipper (*Periophthalmus modestus*). *Gen. Comp. Endocrinol.* 194, 257–263. doi: 10.1016/j.ygcen.2013.09.023

Kalamarz-Kubiak, H., Kleszczyńska, A., and Kulczykowska, E. (2015). Cortisol stimulates arginine vasotocin and isotocin release from the hypothalamo-pituitary complex of round goby (*Neogobius melanostomus*): probable mechanisms of action. *J. Exp. Zool. A Ecol. Gen. Physiol.* 323, 616–626. doi: 10.1002/jez.1952

Katayama, Y., Sakamoto, T., Saito, K., Tsuchimochi, H., Kaiya, H., Watanabe, T., et al. (2018). Drinking by amphibious fish: convergent evolution of thirst mechanisms during vertebrate terrestrialization. *Sci. Rep.* 8:625. doi: 10.1038/s41598-017-18611-4

Kawata, M., Nishi, M., Matsuda, K., Sakamoto, H., Kaku, N., Masugi-Tokita, M., et al. (2008). Steroid receptor signalling in the brain–lessons learned from molecular imaging. *J. Neuroendocrinol.* 20, 673–676. doi: 10.1111/j.1365-2826.2008.01727.x

Kikuchi, Y., Hosono, K., Yamashita, J., Kawabata, Y., and Okubo, K. (2015). Glucocorticoid receptor exhibits sexually dimorphic expression in the medaka brain. *Gen. Comp. Endocrinol.* 223, 47–53. doi: 10.1016/j.ygcen.2015.09.031

Kline, R. J., O'Connell, L. A., Hofmann, H. A., Holt, G. J., and Khan, I. A. (2011). The distribution of an AVT V1a receptor in the brain of a sex changing fish, *Epinephelus adscensionis*. *J. Chem. Neuroanat.* 42, 72–88. doi: 10.1016/j.jchemneu.2011.06.005

Kobayashi, H., and Takei, Y. (1996). *The Renin-Angiotensin System: Comparative Aspects*. Berlin: Springer Science & Business Media. doi: 10.1007/978-3-642-61164-3

Kobayashi, H., Uemura, H., Takei, Y., Itatsu, N., Ozawa, M., and Ichinohe, K. (1983). Drinking induced by angiotensin II in fishes. *Gen. Comp. Endocrinol.* 49, 295–306. doi: 10.1016/0016-6480(83)90147-8

Kobayashi, H., Uemura, H., Wada, M., and Takei, Y. (1979). Ecological adaptation of angiotensin-induced thirst mechanism in tetrapods. *Gen. Comp. Endocrinol.* 38, 93–104. doi: 10.1016/0016-6480(79)90093-5

Konno, N., Hyodo, S., Yamaguchi, Y., Matsuda, K., and Uchiyama, M. (2010a). Vasotocin/V2-type receptor/aquaporin axis exists in African lungfish kidney but is functional only in terrestrial condition. *Endocrinology* 151, 1089–1096. doi: 10.1210/en.2009-1070en.2009-1070

Konno, N., Kurosawa, M., Kaiya, H., Miyazato, M., Matsuda, K., and Uchiyama, M. (2010b). Molecular cloning and characterization of V2-type receptor in two ray-finned fish, gray bichir, *Polypterus senegalus* and medaka, *Oryzias latipes*. *Peptides* 31, 1273–1279. doi: 10.1016/j.peptides.2010.04.014

Kozaka, T., Fujii, Y., and Ando, M. (2003). Central effects of various ligands on drinking behavior in eels acclimated to seawater. *J. Exp. Biol.* 206, 687–692. doi: 10.1242/jeb.00146

Krashes, M. J. (2016). Physiology: forecast for water balance. *Nature* 537, 626–627. doi: 10.1038/537626a

Kurita, Y., Nakada, T., Kato, A., Doi, H., Mistry, A. C., Chang, M. H., et al. (2008). Identification of intestinal bicarbonate transporters involved in formation of carbonate precipitates to stimulate water absorption in marine teleost fish. *Am. J. Physiol. Regul. Integr. Comp. Physiol.* 294, R1402–R1412. doi: 10.1152/ajpregu.00759.2007

Larson, E. T., O'Malley, D. M., and Melloni, R. H. Jr. (2006). Aggression and vasotocin are associated with dominant-subordinate relationships in zebrafish. *Behav. Brain Res.* 167, 94–102. doi: 10.1016/j.bbr.2005.08.020

Lee, C. G. L., and Ip, Y. K. (1987). Environmental effect on plasma thyroxine (T4), 3, 5, 3′-triido-L-thyronine (T3), prolactin and cyclic adenosine 3′, 5′-monophosphate (cAMP) content in the mudskippers *Periophthalmus chrysospilos* and *Boleophthalmus boddaerti*. *Comp. Biochem. Physiol. A Physiol.* 87, 1009–1014. doi: 10.1016/0300-9629(87)90028-4

Lema, S. C. (2010). Identification of multiple vasotocin receptor cDNAs in teleost fish: sequences, phylogenetic analysis, sites of expression, and regulation in

the hypothalamus and gill in response to hyperosmotic challenge. *Mol. Cell. Endocrinol.* 321, 215–230. doi: 10.1016/j.mce.2010.02.015

Lema, S. C., Sanders, K. E., and Walti, K. A. (2015). Arginine vasotocin, isotocin and nonapeptide receptor gene expression link to social status and aggression in sex-dependent patterns. *J. Neuroendocrinol.* 27, 142–157. doi: 10.1111/jne.12239

Leow, M. K. S. (2015). Environmental origins of hypertension: phylogeny, ontogeny and epigenetics. *Hypertens. Res.* 38, 299–307. doi: 10.1038/hr.2015.7

Lindeyer, C. M., Langen, E. M., Swaney, W. T., and Reader, S. M. (2015). Nonapeptide influences on social behaviour: effects of vasotocin and isotocin on shoaling and interaction in zebrafish. *Behaviour* 152, 897–915. doi: 10.1163/1568539X-00003261

Liu, X. Y., Wan, L., Huo, F.-Q., Barry, D. M., Li, H., Zhao, Z.-Q., et al. (2014). B-type natriuretic peptide is neither itch-specific nor functions upstream of the GRP-GRPR signaling pathway. *Mol. Pain* 10:4. doi: 10.1186/1744-8069-10-4

Loveland, J. L., and Fernald, R. D. (2017). Differential activation of vasotocin neurons in contexts that elicit aggression and courtship. *Behav. Brain Res.* 317, 188–203. doi: 10.1016/j.bbr.2016.09.008

MacIver, M. A., Schmitz, L., Mugan, U., Murphey, T. D., and Mobley, C. D. (2017). Massive increase in visual range preceded the origin of terrestrial vertebrates. *Proc. Natl. Acad. Sci. U.S.A.* 114, E2375–E2384. doi: 10.1073/pnas.1615563114

Maejima, S., Konno, N., Matsuda, K., and Uchiyama, M. (2010). Central angiotensin II stimulates cutaneous water intake behavior via an angiotensin II type-1 receptor pathway in the Japanese tree frog *Hyla japonica*. *Horm. Behav.* 58, 457–464. doi: 10.1016/j.yhbeh.2010.05.007

Mahlmann, S., Meyerhof, W., Hausmann, H., Heierhorst, J., Schonrock, C., Zwiers, H., et al. (1994). Structure, function, and phylogeny of [Arg8]vasotocin receptors from teleost fish and toad. *Proc. Natl. Acad. Sci. U.S.A.* 91, 1342–1345. doi: 10.1073/pnas.91.4.1342

Mandelblat-Cerf, Y., Kim, A., Burgess, C. R., Subramanian, S., Tannous, B. A., Lowell, B. B., et al. (2017). Bidirectional anticipation of future osmotic challenges by vasopressin neurons. *Neuron* 93, 57–65. doi: 10.1016/j.neuron.2016.11.021

Manzon, L. A. (2002). The role of prolactin in fish osmoregulation: a review. *Gen. Comp. Endocrinol.* 125, 291–310. doi: 10.1006/gcen.2001.7746

Martos-Sitcha, J. A., Campinho, M. A., Mancera, J. M., Martinez-Rodriguez, G., and Fuentes, J. (2015a). Vasotocin and isotocin regulate aquaporin 1 function in the sea bream. *J. Exp. Biol.* 218, 684–693. doi: 10.1242/jeb.114546

Martos-Sitcha, J. A., MartinezRodriguez, G., Mancera, J. M., and Fuentes, J. (2015b). AVT and IT regulate ion transport across the opercular epithelium of killifish (*Fundulus heteroclitus*) and gilthead sea bream (*Sparus aurata*). *Comp. Biochem. Physiol. A Mol. Integr. Physiol.* 182, 93–101. doi: 10.1016/j.cbpa.2014.12.027

Martos-Sitcha, J. A., Fuentes, J., Mancera, J. M., and Martinez-Rodriguez, G. (2014). Variations in the expression of vasotocin and isotocin receptor genes in the gilthead sea bream *Sparus aurata* during different osmotic challenges. *Gen. Comp. Endocrinol.* 197, 5–17. doi: 10.1016/j.ygcen.2013.11.026

Mayer-Gostan, N., and Hirano, T. (1976). The effects of transecting the IXth and Xth cranial nerves on hydromineral balance in the eel Anguilla anguilla. *J. Exp. Biol.* 64, 461–475.

McCormick, S. D. (2001). Endocrine control of osmoregulation in teleost fish. *Am. Zool.* 41, 781–794. doi: 10.1093/icb/41.4.781

McCormick, S. D., and Bradshaw, D. (2006). Hormonal control of salt and water balance in vertebrates. *Gen. Comp. Endocrinol.* 147, 3–8. doi: 10.1016/j.ygcen.2005.12.009

McKinley, M., Cairns, M., Denton, D., Egan, G., Mathai, M., Uschakov, A., et al. (2004). Physiological and pathophysiological influences on thirst. *Physiol. Behav.* 81, 795–803. doi: 10.1016/j.physbeh.2004.04.055

McKinley, M. J. (2003). *The Sensory Circumventricular Organs of the Mammalian Brain: Subfornical Organ, OVLT and Area Postrema*. Berlin: Springer Science & Business Media. doi: 10.1007/978-3-642-55532-9

McKinley, M. J., and Johnson, A. K. (2004). The physiological regulation of thirst and fluid intake. *News Physiol. Sci.* 19, 1–6. doi: 10.1152/nips.01470.2003

Mével, L., Lancien, F., Mimassi, N., and Conlon, J. M. (2012). Brain neuropeptides in central ventilatory and cardiovascular regulation in trout. *Front. Endocrinol.* 3:124. doi: 10.3389/fendo.2012.00124

Michel, K. B., Heiss, E., Aerts, P., and Van Wassenbergh, S. (2015). A fish that uses its hydrodynamic tongue to feed on land. *Proc. R. Soc. B Biol. Sci.* 282:20150057. doi: 10.1098/rspb.2015.0057

Milla, S., Terrien, X., Sturm, A., Ibrahim, F., Giton, F., Fiet, J., et al. (2008). Plasma 11-deoxycorticosterone (DOC) and mineralocorticoid receptor testicular expression during rainbow trout *Oncorhynchus mykiss* spermiation: implication with 17alpha, 20beta-dihydroxyprogesterone on the milt fluidity? Reprod. *Biol. Endocrinol.* 6:19. doi: 10.1186/1477-7827-6-19

Mishra, S. K., and Hoon, M. A. (2013). The cells and circuitry for itch responses in mice. *Science* 340, 968–971. doi: 10.1126/science.1233765

Mommsen, T. P., Vijayan, M. M., and Moon, T. W. (1999). Cortisol in teleosts: dynamics, mechanisms of action, and metabolic regulation. *Rev. Fish Biol. Fish.* 9, 211–268. doi: 10.1023/A:1008924418720

Moriya, T. (1982). Prolactin induces increase in the specific gravity of salamander, *Hynobius retardatus*, that raises adaptability to water. *J. Exp. Zool.* 223, 83–88. doi: 10.1002/jez.1402230114

Mukuda, T., and Ando, M. (2003). Medullary motor neurones associated with drinking behaviour of Japanese eels. *J. Fish Biol.* 62, 1–12. doi: 10.1046/j.1095-8649.2003.00002.x

Mukuda, T., Matsunaga, Y., Kawamoto, K., Yamaguchi, K. I., and Ando, M. (2005). "Blood-contacting neurons" in the brain of the Japanese eel *Anguilla japonica*. *J. Exp. Zool. A Comp. Exp. Biol.* 303, 366–376. doi: 10.1002/jez.a.134

Myers, B., McKlveen, J. M., and Herman, J. P. (2014). Glucocorticoid actions on synapses, circuits, and behavior: implications for the energetics of stress. *Front. Neuroendocrinol.* 35:180–196. doi: 10.1016/j.yfrne.2013.12.003

Nagashima, K., and Ando, M. (1994). Characterization of esophageal desalination in the seawater eel, *Anguilla japonica*. *J. Comp. Physiol. B Biochem. Syst. Environ. Physiol.* 164, 47–54. doi: 10.1007/BF00714570

Nielsen, S., Chou, C. L., Marples, D., Christensen, E. I., Kishore, B. K., and Knepper, M. A. (1995). Vasopressin increases water permeability of kidney collecting duct by inducing translocation of aquaporin-CD water channels to plasma membrane. *Proc. Natl. Acad. Sci. U.S.A.* 92, 1013–1017. doi: 10.1073/pnas.92.4.1013

Nishimura, H. (1978). Physiological evolution of the renin-angiotensin system. *Jpn. Heart J.* 19, 806–822. doi: 10.1536/ihj.19.806

Nishimura, H. (2017). Renin-angiotensin system in vertebrates: phylogenetic view of structure and function. *Anat. Sci. Int.* 92, 215–247. doi: 10.1007/s12565-016-0372-8

Nobata, S., and Ando, M. (2013). "Regulation of drinking," in *Eel Physiology*, eds F. Trischitta, Y. Takei, and P. Sébert (Boca Raton, FL: CRC Press), 225–248. doi: 10.1201/b15365-9

Nobata, S., Ando, M., and Takei, Y. (2013). Hormonal control of drinking behavior in teleost fishes; insights from studies using eels. *Gen. Comp. Endocrinol.* 192, 214–221. doi: 10.1016/j.ygcen.2013.05.009

Nobata, S., and Takei, Y. (2011). The area postrema in hindbrain is a central player for regulation of drinking behavior in Japanese eels. *Am. J. Physiol. Regul. Integr. Comp. Physiol.* 300, R1569–R1577. doi: 10.1152/ajpregu.00056.2011

Oatley, K., and Toates, F. (1969). The passage of food through the gut of rats and its uptake of fluid. *Psychono. Sci.* 16, 225–226. doi: 10.3758/BF03332656

Okawara, Y., Karakida, T., Aihara, M., Yamaguchi, K. I., and Kobayashi, H. (1987). Involvement of angiotensin II in water intake in the Japanese eel, *Anguilla japonica*: endocrinology. *Zool. Sci.* 4, 523–528.

Olivereau, M., and Olivereau, J. (1990). Effect of pharmacological adrenalectomy on corticotropin-releasing factor-like and arginine vasotocin immunoreactivities in the brain and pituitary of the eel: immunocytochemical study. *Gen. Comp. Endocrinol.* 80, 199–215. doi: 10.1016/0016-6480(90)90165-I

Onuma, T. A., Ban, M., Makino, K., Katsumata, H., Hu, W., Ando, H., et al. (2010). Changes in gene expression for GH/PRL/SL family hormones in the pituitaries of homing chum salmon during ocean migration through upstream migration. *Gen. Comp. Endocrinol.* 166, 537–548. doi: 10.1016/j.ygcen.2010.01.015

Ord, T. J., and Cooke, G. M. (2016). Repeated evolution of amphibious behavior in fish and its implications for the colonisation of novel environments. *Evolution* 70, 1747–1759. doi: 10.1111/evo.12971

Parmelee, J. T., and Renfro, J. L. (1983). Esophageal desalination of seawater in flounder: role of active sodium transport. *Am. J. Physiol. Regul. Integr. Comp. Physiol.* 245, R888–R893. doi: 10.1152/ajpregu.1983.245.6.R888

Perrone, R., and Silva, A. C. (2018). Status-dependent vasotocin modulation of dominance and subordination in the weakly electric fish *Gymnotus omarorum*. *Front. Behav. Neurosci.* 12:1. doi: 10.3389/fnbeh.2018.00001

Perrott, M., Grierson, C., Hazon, N., and Balment, R. (1992). Drinking behaviour in sea water and fresh water teleosts, the role of the renin-angiotensin system. *Fish Physiol. Biochem.* 10, 161–168. doi: 10.1007/BF00004527

Propper, C. R., Hillyard, S. D., and Johnson, W. E. (1995). Central angiotensin II induces thirst-related responses in an amphibian. *Horm. Behav.* 29, 74–84. doi: 10.1006/hbeh.1995.1006

Prunet, P., Sturm, A., and Milla, S. (2006). Multiple corticosteroid receptors in fish: from old ideas to new concepts. *Gen. Comp. Endocrinol.* 147, 17–23. doi: 10.1016/j.ygcen.2006.01.015

Rankin, J. (2002). Drinking in hagfishes and lampreys. *Symp. Soc. Exp. Biol.* 2002, 1–17.

Rowe, B. P., Saylor, D. L., and Speth, R. C. (1992). Analysis of angiotensin II receptor subtypes in individual rat brain nuclei. *Neuroendocrinology* 55, 563–573. doi: 10.1159/000126177

Rozeboom, A. M., Akil, H., and Seasholtz, A. F. (2007). Mineralocorticoid receptor overexpression in forebrain decreases anxiety-like behavior and alters the stress response in mice. *Proc. Natl. Acad. Sci. U.S.A.* 104, 4688–4693. doi: 10.1073/pnas.0606067104

Russell, M. J., Klemmer, A. M., and Olson, K. R. (2001). Angiotensin signaling and receptor types in teleost fish. *Comp. Biochem. Physiol. A Mol. Integr. Physiol.* 128, 41–51. doi: 10.1016/S1095-6433(00)00296-8

Ryan, P. J., Ross, S. I., Campos, C. A., Derkach, V. A., and Palmiter, R. D. (2017). Oxytocin-receptor-expressing neurons in the parabrachial nucleus regulate fluid intake. *Nat. Neurosci.* 20, 1722–1733. doi: 10.1038/s41593-017-0014-z

Sakamoto, H., Takahashi, H., Matsuda, K., Nishi, M., Takanami, K., Ogoshi, M., et al. (2012). Rapid signaling of steroid hormones in the vertebrate nervous system. *Front. Biosci.* 17:996–1019. doi: 10.2741/3970

Sakamoto, T., Agustsson, T., Moriyama, S., Itoh, T., Takahashi, A., Kawauchi, H., et al. (2003). Intra-arterial injection of prolactin-releasing peptide elevates prolactin gene expression and plasma prolactin levels in rainbow trout. *J. Comp. Physiol. B* 173, 333–337. doi: 10.1007/s00360-003-0340-1

Sakamoto, T., Amano, M., Hyodo, S., Moriyama, S., Takahashi, A., Kawauchi, H., et al. (2005a). Expression of prolactin-releasing peptide and prolactin in the euryhaline mudskippers (*Periophthalmus modestus*): prolactin-releasing peptide as a primary regulator of prolactin. *J. Mol. Endocrinol.* 34, 825–834.

Sakamoto, T., Oda, A., Narita, K., Takahashi, H., Oda, T., Fujiwara, J., et al. (2005b). Prolactin: fishy tales of its primary regulator and function. *Ann. N. Y. Acad. Sci.* 1040, 184–188.

Sakamoto, T., and Ando, M. (2002). Calcium ion triggers rapid morphological oscillation of chloride cells in the mudskipper, *Periophthalmus modestus*. *J. Comp. Physiol. B* 172, 435–439. doi: 10.1007/s00360-002-0272-1

Sakamoto, T., Hyodo, S., and Takagi, W. (2018). A possible principal function of corticosteroid signaling that is conserved in vertebrate evolution: lessons from receptor-knockout small fish. *J. Steroid Biochem. Mol. Biol.* doi: 10.1016/j.jsbmb.2018.02.011 [Epub ahead of print].

Sakamoto, T., and McCormick, S. D. (2006). Prolactin and growth hormone in fish osmoregulation. *Gen. Comp. Endocrinol.* 147, 24–30. doi: 10.1016/j.ygcen.2005.10.008

Sakamoto, T., Mori, C., Minami, S., Takahashi, H., Abe, T., Ojima, D., et al. (2011). Corticosteroids stimulate the amphibious behavior in mudskipper: potential role of mineralocorticoid receptors in teleost fish. *Physiol. Behav.* 104, 923–928. doi: 10.1016/j.physbeh.2011.06.002

Sakamoto, T., Nishiyama, Y., Ikeda, A., Takahashi, H., Hyodo, S., Kagawa, N., et al. (2015). Neurohypophysial hormones regulate amphibious behaviour in the mudskipper goby. *PLoS One* 10:e0134605. doi: 10.1371/journal.pone.0134605

Sakamoto, T., Yasunaga, H., Yokota, S., and Ando, M. (2002). Differential display of skin mRNAs regulated under varying environmental conditions in a mudskipper. *J. Comp. Physiol. B* 172, 447–453. doi: 10.1007/s00360-002-0274-z

Sakamoto, T., Yokota, S., and Ando, M. (2000). Rapid morphological oscillation of mitochondrion-rich cell in estuarine mudskipper following salinity changes. *J. Exp. Zool.* 286, 666–669. doi: 10.1002/(SICI)1097-010X(20000501)286:6<666::AID-JEZ14>3.0.CO;2-G

Sakamoto, T., Yoshiki, M., Takahashi, H., Yoshida, M., Ogino, Y., Ikeuchi, T., et al. (2016). Principal function of mineralocorticoid signaling suggested by constitutive knockout of the mineralocorticoid receptor in medaka fish. *Sci. Rep.* 6:37991. doi: 10.1038/srep37991

Sands, J. M., Blount, M. A., and Klein, J. D. (2011). Regulation of renal urea transport by vasopressin. *Trans. Am. Clin. Climatol. Assoc.* 122, 82–92.

Sayer, M. D. J. (2005). Adaptations of amphibious fish for surviving life out of water. *Fish Fish.* 6, 186–211. doi: 10.1111/j.1467-2979.2005.00193.x

Seo, M. Y., Kuroki, M., Okamura, A., Tsukamoto, K., Watanabe, S., and Kaneko, T. (2015). Occurrence of larval and adult types of ion-secreting ionocytes in Japanese eel *Anguilla japonica*. *Ichthyol. Res.* 62, 487–494. doi: 10.1007/s10228-015-0463-x

Shaw, J. R., Gabor, K., Hand, E., Lankowski, A., Durant, L., Thibodeau, R., et al. (2007). Role of glucocorticoid receptor in acclimation of killifish (*Fundulus heteroclitus*) to seawater and effects of arsenic. *Am. J. Physio. Regul. Integr. Comp. Physiol.* 292, R1052–R1060. doi: 10.1152/ajpregu.00328.2006

Shu, Y., Lou, Q., Dai, Z., Dai, X., He, J., Hu, W., et al. (2016). The basal function of teleost prolactin as a key regulator on ion uptake identified with zebrafish knockout models. *Sci. Rep.* 6:18597. doi: 10.1038/srep18597

Simpson, J. B., and Routtenberg, A. (1973). Subfornical organ: site of drinking elicitation by angiotensin II. *Science* 181, 1172–1175. doi: 10.1126/science.181.4105.1172

Song, K., Allen, A. M., Paxinos, G., and Mendelsohn, F. A. (1992). Mapping of angiotensin II receptor subtype heterogeneity in rat brain. *J. Comp. Neurol.* 316, 467–484. doi: 10.1002/cne.903160407

Stolte, E. H., de Mazon, A. F., Leon-Koosterziel, K. M., Jesiak, M., Bury, N. R., Sturm, A., et al. (2008). Corticosteroid receptors involved in stress regulation in common carp, *Cyprinus carpio*. *J. Endocrinol.* 198, 403–417. doi: 10.1677/JOE-08-0100

Stricker, E. M., and Stricker, M. L. (2011). Pre-systemic controls of fluid intake and vasopressin secretion. *Physiol. Behav.* 103, 86–88. doi: 10.1016/j.physbeh.2010.11.019

Sturm, A., Bury, N., Dengreville, L., Fagart, J., Flouriot, G., Rafestin-Oblin, M., et al. (2005). 11-deoxycorticosterone is a potent agonist of the rainbow trout (*Oncorhynchus mykiss*) mineralocorticoid receptor. *Endocrinology* 146, 47–55. doi: 10.1210/en.2004-0128

Sudo, R., Suetake, H., Suzuki, Y., Aoyama, J., and Tsukamoto, K. (2013). Profiles of mRNA expression for prolactin, growth hormone, and somatolactin in Japanese eels, *Anguilla japonica*: the effect of salinity, silvering and seasonal change. *Comp. Biochem. Physiol. A Mol. Integr. Physiol.* 164, 10–16. doi: 10.1016/j.cbpa.2012.09.019

Sun, Y. G., and Chen, Z. F. (2007). A gastrin-releasing peptide receptor mediates the itch sensation in the spinal cord. *Nature* 448, 700–703. doi: 10.1038/nature06029

Takahashi, H., and Sakamoto, T. (2013). The role of 'mineralocorticoids' in teleost fish: relative importance of glucocorticoid signaling in the osmoregulation and 'central' actions of mineralocorticoid receptor. *Gen. Comp. Endocrinol.* 181, 223–228. doi: 10.1016/j.ygcen.2012.11.016

Takahashi, H., Takahashi, A., and Sakamoto, T. (2006). In vivo effects of thyroid hormone, corticosteroids and prolactin on cell proliferation and apoptosis in the anterior intestine of the euryhaline mudskipper (*Periophthalmus modestus*). *Life Sci.* 79, 1873–1880. doi: 10.1016/j.lfs.2006.06.021

Takei, Y. (2000). Comparative physiology of body fluid regulation in vertebrates with special reference to thirst regulation. *Jpn. J. Physiol.* 50, 171–186. doi: 10.2170/jjphysiol.50.171

Takei, Y. (2015). From aquatic to terrestrial life: evolution of the mechanisms for water acquisition. *Zool. Sci.* 32, 1–7. doi: 10.2108/zs140142

Takei, Y., Hirano, T., and Kobayashi, H. (1979). Angiotensin and water intake in the Japanese eel, *Anguilla japonica*. *Gen. Comp. Endocrinol.* 38, 466–475. doi: 10.1016/0016-6480(79)90155-2

Takei, Y., Hiroi, J., Takahashi, H., and Sakamoto, T. (2014). Diverse mechanisms for body fluid regulation in teleost fishes. *Am. J. Physio. Regul. Integr. Comp. Physiol.* 307, R778–R792. doi: 10.1152/ajpregu.00104.2014

Takei, Y., and McCormick, S. D. (2012). "Hormonal control of fish euryhalinity," in *Fish physiology*, eds S. D. McCormick, A. P. Farrell, and C. J. Brauner (New York, NY: Elsevier), 69–123.

Takei, Y., Wong, M. K. S., Pipil, S., Ozaki, H., Suzuki, Y., Iwasaki, W., et al. (2016). Molecular mechanisms underlying active desalination and low water

permeability in the esophagus of eels acclimated to seawater. *Am. J. Physiol. Regul. Integr. Comp. Physiol.* 312, R231–R244. doi: 10.1152/ajpregu.00465.2016

Takiyama, T., Hamasaki, S., and Yoshida, M. (2016). Comparison of the visual capabilities of an amphibious and an aquatic goby that inhabit tidal mudflats. *Brain Behav. Evol.* 87, 39–50. doi: 10.1159/000443923

Tamura, S. O., Morii, H., and Yuzuriha, M. (1976). Respiration of the amphibious fishes *Periophthalmus cantonensis* and *Boleophthalmus chinensis* in water and on land. *J. Exp. Biol.* 65, 97–107.

Teitsma, C. A., Anglade, I., Toutirais, G., Muñoz-Cueto, J. A., Saligaut, D., Ducouret, B., et al. (1998). Immunohistochemical localization of glucocorticoid receptors in the forebrain of the rainbow trout (*Oncorhynchus mykiss*). *J. Comp. Neurol.* 401, 395–410. doi: 10.1002/(SICI)1096-9861(19981123)401:3<395::AID-CNE7>3.0.CO;2-P

Thompson, R. R., and Walton, J. C. (2004). Peptide effects on social behavior: effects of vasotocin and isotocin on social approach behavior in male goldfish (*Carassius auratus*). *Behav. Neurosci.* 118, 620–626. doi: 10.1037/0735-7044.118.3.620

Tierney, M., Luke, G., Cramb, G., and Hazon, N. (1995). The role of the renin-angiotensin system in the control of blood pressure and drinking in the European eel, Anguilla anguilla. *Gen. Comp. Endocrinol.* 100, 39–48. doi: 10.1006/gcen.1995.1130

Timmermans, P. B., Wong, P. C., Chiu, A. T., Herblin, W. F., Benfield, P., Carini, D., et al. (1993). Angiotensin II receptors and angiotensin II receptor antagonists. *Pharmacol. Rev.* 45, 205–251.

Tsutsumi, K., and Saavedra, J. M. (1991). Quantitative autoradiography reveals different angiotensin II receptor subtypes in selected rat brain nuclei. *J. Neurochem.* 56, 348–351. doi: 10.1111/j.1471-4159.1991.tb02602.x

Uchida, K., Kaneko, T., Yamauchi, K., and Hirano, T. (1996). Morphometrical analysis chloride cell activity in the gill filaments and lamellae and changes in Na+, K+-ATPase activity during seawater adaptation in chum salmon fry. *J. Exp. Zool. A Ecol. Genet. Physiol.* 276, 193–200. doi: 10.1002/(SICI)1097-010X(19961015)276:3<193::AID-JEZ3>3.0.CO;2-I

Uchiyama, M. (2015). "Angiotensin II and water balance in amphibians," in *Sodium and Water Homeostasis*, eds K. A. Hyndman and T. L. Pannabecker (Berlin: Springer), 73–90. doi: 10.1007/978-1-4939-3213-9_4

Veillette, P. A., Sundell, K., and Specker, J. L. (1995). Cortisol mediates the increase in intestinal fluid absorption in Atlantic salmon during parr-smolt transformation. *Gen. Comp. Endocrinol.* 97, 250–258. doi: 10.1006/gcen.1995.1024

Veillette, P. A., and Young, G. (2005). Tissue culture of sockeye salmon intestine: functional response of Na+-K+-ATPase to cortisol. *Am. J. Physiol. Regul. Integr. Comp. Physiol.* 288, R1598–R1605. doi: 10.1152/ajpregu.00741.2004

Verbalis, J. G., Mangione, M. P., and Stricker, E. M. (1991). Oxytocin produces natriuresis in rats at physiological plasma concentrations. *Endocrinology* 128, 1317–1322. doi: 10.1210/endo-128-3-1317

Warne, J. M. (2001). Cloning and characterization of an arginine vasotocin receptor from the euryhaline flounder *Platichthys flesus*. *Gen. Comp. Endocrinol.* 122, 312–319. doi: 10.1006/gcen.2001.7644

Watanabe, T., and Takei, Y. (2011). Molecular physiology and functional morphology of SO42– excretion by the kidney of seawater-adapted eels. *J. Exp. Biol.* 214, 1783–1790. doi: 10.1242/jeb.051789

Watanabe, Y., Sakihara, T., Mukuda, T., and Ando, M. (2007). Antagonistic effects of vasotocin and isotocin on the upper esophageal sphincter muscle of the eel acclimated to seawater. *J. Comp. Physiol. B* 177, 867–873. doi: 10.1007/s00360-007-0184-1

Watts, A. G. (2015). 60 years of neuroendocrinology: the structure of the neuroendocrine hypothalamus: the neuroanatomical legacy of Geoffrey Harris. *J. Endocrinol.* 226, T25–T39. doi: 10.1530/JOE-15-0157

Whittington, C. M., and Wilson, A. B. (2013). The role of prolactin in fish reproduction. *Gen. Comp. Endocrinol.* 191, 123–136. doi: 10.1016/j.ygcen.2013.05.027

Wilson, R. W., Wilson, J. M., and Grosell, M. (2002). Intestinal bicarbonate secretion by marine teleost fish—why and how? *Biochim. Biophys. Acta* 1566, 182–193. doi: 10.1016/S0005-2736(02)00600-4

Wong, M. K. S., and Takei, Y. (2013). Angiotensin AT2 receptor activates the cyclic-AMP signaling pathway in eel. *Mol. Cell. Endocrinol.* 365, 292–302. doi: 10.1016/j.mce.2012.11.009

Yamaguchi, Y., Kaiya, H., Konno, N., Iwata, E., Miyazato, M., Uchiyama, M., et al. (2012). The fifth neurohypophysial hormone receptor is structurally related to the V2-type receptor but functionally similar to V1-type receptors. *Gen. Comp. Endocrinol.* 178, 519–528. doi: 10.1016/j.ygcen.2012.07.008

Yokoi, S., Okuyama, T., Kamei, Y., Naruse, K., Taniguchi, Y., Ansai, S., et al. (2015). An essential role of the arginine vasotocin system in mate-guarding behaviors in triadic relationships of medaka fish (*Oryzias latipes*). *PLoS genet.* 11:e1005009. doi: 10.1371/journal.pgen.1005009

You, X., Bian, C., Zan, Q., Xu, X., Liu, X., Chen, J., et al. (2014). Mudskipper genomes provide insights into the terrestrial adaptation of amphibious fishes. *Nat. Commun.* 5:5594. doi: 10.1038/ncomms6594

Zimmerman, C. A., Leib, D. E., and Knight, Z. A. (2017). Neural circuits underlying thirst and fluid homeostasis. *Nat. Rev. Neurosci.* 18, 459–469. doi: 10.1038/nrn.2017.71

Zimmerman, C. A., Lin, Y.-C., Leib, D. E., Guo, L., Huey, E. L., Daly, G. E., et al. (2016). Thirst neurons anticipate the homeostatic consequences of eating and drinking. *Nature* 537, 680–684. doi: 10.1038/nature18950

Ziv, L., Muto, A., Schoonheim, P. J., Meijsing, S. H., Strasser, D., Ingraham, H. A., et al. (2013). An affective disorder in zebrafish with mutation of the glucocorticoid receptor. *Mol. Psychiatry* 18, 681–691. doi: 10.1038/mp.2012.64

Conflict of Interest Statement: The authors declare that the research was conducted in the absence of any commercial or financial relationships that could be construed as a potential conflict of interest.

frontiers in Physiology

ORIGINAL RESEARCH
published: 14 January 2019
doi: 10.3389/fphys.2018.01909

Non-reversible and Reversible Heat Tolerance Plasticity in Tropical Intertidal Animals: Responding to Habitat Temperature Heterogeneity

*Amalina Brahim, Nurshahida Mustapha and David J. Marshall**

Environmental and Life Sciences, Faculty of Science, Universiti Brunei Darussalam, Bandar Seri Begawan, Brunei

The theory for thermal plasticity of tropical ectotherms has centered on terrestrial and open-water marine animals which experience reduced variation in diurnal and seasonal temperatures, conditions constraining plasticity selection. Tropical marine intertidal animals, however, experience complex habitat thermal heterogeneity, circumstances encouraging thermal plasticity selection. Using the tropical rocky-intertidal gastropod, *Echinolittorina malaccana*, we investigated heat tolerance plasticity in terms of laboratory acclimation and natural acclimatization of populations from thermally-dissimilar nearby shorelines. Laboratory treatments yielded similar capacities of snails from either population to acclimate their lethal thermal limit (LT_{50} variation was ~2°C). However, the populations differed in the temperature range over which acclimatory adjustments could be made; LT_{50} plasticity occurred over a higher temperature range in the warm-shore snails compared to the cool-shore snails, giving an overall acclimation capacity for the populations combined of 2.9°C. In addition to confirming significant heat tolerance plasticity in tropical intertidal animals, these findings reveal two plasticity forms, reversible (laboratory acclimation) and non-reversible (population or shoreline specific) plasticity. The plasticity forms should account for different spatiotemporal scales of the environmental temperature variation; reversible plasticity for daily and tidal variations in microhabitat temperature and non-reversible plasticity for lifelong, shoreline temperature conditions. Non-reversible heat tolerance plasticity, likely established after larvae settle on the shore, should be energetically beneficial in preventing heat shock protein overexpression, but also should facilitate widespread colonization of coasts that support thermally-diverse shorelines. This first demonstration of different plasticity forms in benthic intertidal animals supports the hypothesis that habitat heterogeneity (irrespective of latitude) drives thermal plasticity selection. It further suggests that studies not making reference to different spatial scales of thermal heterogeneity, nor seeking how these may drive different thermal plasticity forms, risk misinterpreting ectothermic responses to environmental warming.

Keywords: developmental plasticity, *Echinolittorina malaccana*, habitat heterogeneity, heat resistance, thermal acclimation

OPEN ACCESS

Edited by:
Carlos Rosas, National Autonomous University of Mexico, Mexico

Reviewed by:
Mikko Juhani Nikinmaa, University of Turku, Finland
Fernando Diaz, Ensenada Center for Scientific Research and Higher Education (CICESE), Mexico

***Correspondence:**
David J. Marshall
davidmarshall11@gmail.com

Specialty section:
This article was submitted to Aquatic Physiology, a section of the journal Frontiers in Physiology

Received: *06 September 2018*
Accepted: *18 December 2018*
Published: *14 January 2019*

Citation:
Brahim A, Mustapha N and Marshall DJ (2019) Non-reversible and Reversible Heat Tolerance Plasticity in Tropical Intertidal Animals: Responding to Habitat Temperature Heterogeneity. Front. Physiol. 9:1909. doi: 10.3389/fphys.2018.01909

INTRODUCTION

Thermal plasticity enables ectothermic animals to modify their lifetime responses to environmental temperature. In the context of climate warming, a complex theory for this plasticity has emerged, which considers its energetic benefits, environmental drivers and evolutionary constraints (see the *beneficial acclimation hypothesis*, and hypotheses for thermal variability, predictability and latitudinal effects; Leroi et al., 1994; Kingsolver and Huey, 1998; Wilson and Franklin, 2002; Angilletta et al., 2006; Deere and Chown, 2006; Gunderson and Stillman, 2015). This theory has, however, been developed with taxonomic and ecological biases toward terrestrial insects, lizards, amphibians, and marine fishes (Huey et al., 1999; Mitchell et al., 2011; Overgaard et al., 2011; Kingsolver et al., 2013; Phillips et al., 2015), to the exclusion largely of animals inhabiting marine intertidal zones (but see Stillman, 2003; Somero, 2010). Marine intertidal circumstances are important as the theory may not always apply to them, despite its assumed generality. For example, studies investigating environmental temperature variation as the primary driver of thermal plasticity selection, commonly consider latitudinal and seasonal effects (Angilletta, 2009). These studies frequently conclude that temperate species, which typically experience greater thermal variation possess a greater capacity for thermal acclimation than tropically-distributed species, which experience relatively limited thermal variation (Gunderson and Stillman, 2015; Rohr et al., 2018). Although this may be true for most tropical animals and habitats, tropical marine intertidal habitats often promote extreme and variable temperature conditions, likely to drive thermal plasticity selection (Helmuth et al., 2006a,b; Marshall et al., 2010, 2018; Denny et al., 2011; Gedan et al., 2011).

Thermal heterogeneity in benthic tropical intertidal ecosystems derives from multiple within- and between-shore effects (**Figure 1**). Within-shore temperature regimes depend primarily on the vertical position on the shore (low- to high-shore), which determines the degree of tidal inundation by relatively cool, thermally-stable seawater and concomitantly the period of exposure to warm, thermally-variable air. At any shore height, the microclimate at scales of below 1 m varies in relation to topography, slope, texture and color of the rocky substratum (Helmuth and Hofmann, 2001; Marshall et al., 2010; Denny et al., 2011; Gedan et al., 2011; Dong et al., 2017). Nearby shorelines which experience similar ambient air temperatures can, however, differ greatly in heat-loading in relation to aspect (north, south, east or west facing), slope, and level of protection from the prevailing winds and swells (**Figure 1**; Helmuth et al., 2006a,b).

From a temporal perspective, tropical rocky-shore thermal heterogeneity is encompassed within daily and tidal timeframes (**Figure 1**), rather than a seasonal timeframe as in temperate regions (Helmuth and Hofmann, 2001; Marshall et al., 2010; Denny et al., 2011; Gedan et al., 2011). Whereas conspecific individuals on the same shoreline often experience different thermal regimes in relation to different vertical or microhabitat distributions (see above), behavioral idiosyncrasies of some species result in the same individual undergoing rapid regime change within the narrow timeframe of a tidal cycle. This is exemplified by high-shore snails whose settling positions when the tide recedes are preferentially determined by desiccation risk avoidance rather than by thermal cues causing snails to rapidly stop crawling when rock surfaces become hot and dry (Monaco et al., 2017). New resting sites can be retained for weeks and can be much hotter (25 to >45°C in full sun-exposed individuals) or much cooler (25–35°C in individuals settling the shade) than the original sites occupied before tidal wetting and activity (Marshall et al., 2013). The exceptional habitat heterogeneity and dynamic variability of the thermal regimes experienced by many tropical intertidal animals should drive plasticity selection.

Because high-shore animals are particularly threatened by acute overheating (Williams and Morritt, 1995; Harley, 2008; Garrabou et al., 2009), heat tolerance plasticity should be under significant selection pressure, especially where behavioral thermoregulatory capabilities are limited. Although reversible plasticity is better known with respect to seasonality, this plasticity should also benefit intertidal animals facing variations in daily maximum temperatures. Superimposed on microhabitat thermal regimes are shoreline-specific thermal conditions, resulting in hotter microhabitats on hotter shores and *vice versa*, throughout an individual's lifetime. Between-shore temperature differences present circumstances likely to drive non-reversible (or developmental) plasticity selection (Hoffmann et al., 2003; Angilletta, 2009; Seebacher et al., 2012, 2014; Beaman et al., 2016). Despite the important contributions of Somero and Stillman to ecological and evolutionary perspectives for intertidal thermal plasticity (Stillman, 2003; Somero, 2010), no previous studies have investigated different plasticity forms in benthic intertidal animals. Most of the research considering non-reversible thermal plasticity (developmental and transgenerational) concerns insects and fishes, and refers more commonly to performance than tolerance traits (Angilletta et al., 2006; Angilletta, 2009; Donelson et al., 2011, 2012; Beaman et al., 2016; Sørensen et al., 2016).

Gastropods represent a dominant ecological component of rocky intertidal zones, and nearly exclusively inhabit the uppermost shore level. Consequently, they have evolved complex behavioral and physiological mechanisms to endure energy gain constraints and resist extreme heat and desiccation exposures (Marshall and McQuaid, 2011; Marshall et al., 2011, 2013, 2015; Marshall and Chua, 2012; Verberk et al., 2016; Ng et al., 2017). The ubiquitous tropical high-shore gastropod, *Echinolittorina malaccana*, is emerging as a model species for exploring molecular heat stress innovations (Dong et al., 2011, 2017; Liao et al., 2017; Somero et al., 2017; Han et al., 2019). Contrary to the general theory predicting a trade-off between thermal acclimation capacity and basal heat tolerance, this thermophilic snail has been shown to exhibit substantial heat tolerance plasticity (Gunderson and Stillman, 2015; Marshall et al., 2018).

The present study aimed to determine whether the heat tolerance plasticity of *E. malaccana* snails could be described in terms of reversibility and non-reversibility. Reversible plasticity of the lethal temperature (LT_{50}) was investigated from laboratory acclimation experiments. Non-reversible plasticity was assessed by comparing the thermal bands for lethal temperature

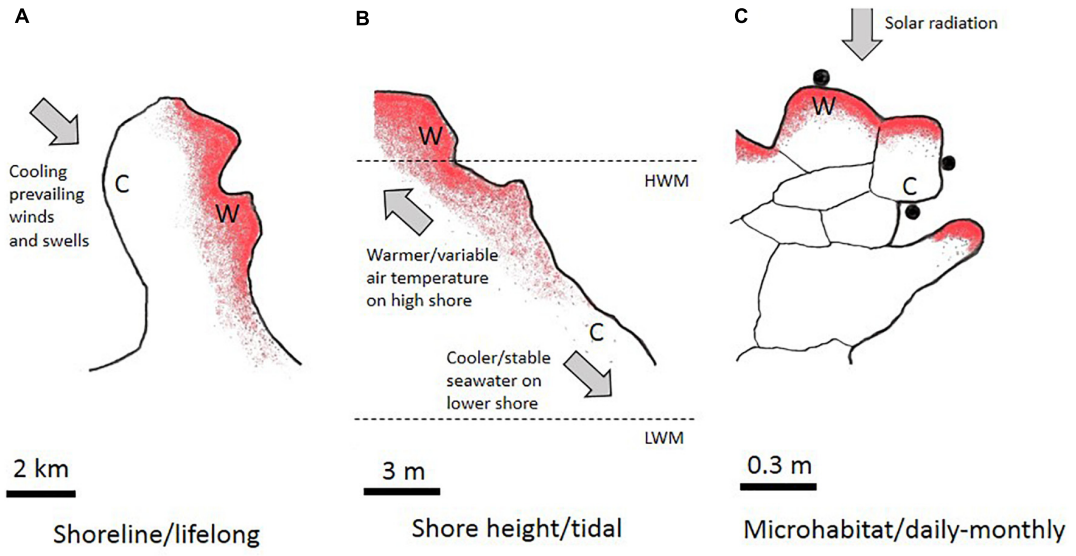

FIGURE 1 | Concept for spatiotemporal scaling of rocky-shore thermal heterogeneity. **(A)** Aerial view of a coastal headland (2 km scale) showing the heat-load distribution (more intense red shading represents greater heat-load). One side of the headland (C) is exposed to prevailing winds and swells whereas the other side (W) is sheltered. Organisms experience either cooler or warmer shoreline conditions throughout their lifetimes. **(B)** Vertical profile of a rocky-shore (3 m scale), showing greater heat-loading in the higher shore (W) due to the variable air temperature. Relatively stable, cooler conditions (C) are experienced in the lower-shore. HWM, high water mark; LWM, low water mark. **(C)** Microhabitats of resting snails (0.3 m scale) showing the effect of solar heating on heat loads. Snails (solid circles) may retain these positions for months in the supratidal or may be redistributed after splashing during spring high-water or high monsoon swell conditions. Snails are primarily heated from the rock surface (see Marshall and Chua, 2012).

acclimation of snail populations from warmer or cooler shorelines. Because reversible laboratory acclimation is expected to eliminate the effects of recent field temperature exposures, non-reversible acclimatization was assumed in cases where the thermal acclimation bands varied between the populations.

MATERIALS AND METHODS

Snail Habitats and Thermal Regimes

Echinolittorina malaccana (Philippi 1847) occurs abundantly on rocky-shores throughout the Indo-Pacific (Reid, 2007). The local shores of Brunei Darussalam sustain two morphologically-distinct ecotypes, occupying different vertical zones. A brown ecotype inhabits the upper intertidal zone (roughly 1–2.5 m Chart Datum) and experiences tidal wetting, whereas a pale blue ecotype inhabits the supratidal zone (2.5- above 5 m Chart Datum) and is only wetted during high seas and monsoon swells. After periods of wetting and feeding, snails stop moving as the tide recedes, glue their shells to the rock surface, and withdraw into the shell (Marshall et al., 2011; Monaco et al., 2017). Because avoidance of desiccation while moving over hot dry rocks supersedes behavioral selection of thermally suitable resting (aestivating) sites, individuals often settle under direct sunlight (Marshall and Chua, 2012; Marshall et al., 2013; Monaco et al., 2017). Isolated resting snails undergo temperature-insensitive metabolic rate depression to overcome the energetic problem of high temperature exposure (Marshall and McQuaid, 2011; Marshall et al., 2011).

This study considered the intertidal brown ecotype. We determined the thermal regimes experienced at their upper distribution on a cool and a warm shoreline at Pantai Tungku, Brunei Darussalam (4.974°N, 114.867°E), between 21 June and 22 July 2018 (30 days during the warmest time of the year; **Supplementary Figure S1**). Pantai Tungku comprises a man-built promontory with artificial seawalls having diametrically-opposed orientations and carrying very different heat-loads. Study sites were established on the seawalls around 2 km apart, along the contour of the coast; the cool shoreline (CS) comprised a north-west-facing seawall exposed to prevailing monsoon winds and swells (#1, **Supplementary Figure S1**), whereas the warm shoreline comprised a north-east-facing sheltered seawall (#2, **Supplementary Figure S1**). To assess the potential range of temperature conditions experienced in snail microhabitats on either shoreline, temperature-loggers (see details in Monaco et al., 2017) were deployed on rocks under direct solar exposure (a 45° angled surface), or in total shade under the rocks. Loggers were set to record temperatures every 30 min.

Snail Collection and Laboratory Treatments

Snails (7–9 mm) were collected from both shorelines within the proximity of the temperature loggers, while awash and feeding. In the laboratory they were rinsed in freshly-collected seawater to rehydrate the snails before starting the acclimation treatments. Prior to field-fresh thermal tolerance determinations, snails were exposed to blown air (30°C for 20 min; Memmert UFE 500, Schwabach, Germany) to inactivate them, dry shells and induce

withdrawal into the shell (Marshall et al., 2018). Field-fresh tolerance experiments were carried out within 12 h of collection of the snails.

Four (4) primary laboratory temperature acclimation treatments were conducted on both warm-shore (WS, warm-acclimatized) and cool-shore (CS, cool-acclimatized) snails. The first set of experiments involved using a programmable Memmert Peltier-cooled (IPP400) incubator to cool-acclimate (CA) one group of randomly selected snails in air at 22–23°C, which approximates the coolest thermal regimes naturally experienced by tropical populations of *E. malacccana* (Marshall et al., 2010; Monaco et al., 2017; **Figure 2** and **Supplementary Figure S2**). A second group was warm-acclimated (WA) to a daily 25–45°C thermal cycle, holding the temperature at 45°C for 4 h (midday) and at 25°C for 12 h (night-time), to mimic hot daily field conditions (**Figure 2** and **Supplementary Figure S2**). Notably, whereas sun-exposure associates with high daily temperature fluctuations, cool-shaded conditions are relatively stable. These acclimations proceeded for 10 d, with snails, unfed and resting, immersed each day in flowing seawater for 5 min, to simulate tidal wetting, maintain full hydration and prevent deep aestivation (Marshall and McQuaid, 2011). Another set of experiments, which tested whether complete acclimation occurred during the above thermal treatments, involved 10 d more severe cooling [near-constant 20°C; extra-cool acclimation (ECA)] and warming (25–50°C cycle, 2 h at 50°C; extra-warm acclimation, EWA; **Supplementary Figure S2**). We further tested whether full acclimation occurred within a 10 d period, by assessing the effect of WA for 20 d.

Heat Ramping and LT_{50} Determination

We assayed the effect of acute heating on mortality using the median lethal temperature (LT_{50}; Marshall and McQuaid, 2011; Marshall et al., 2011, 2015, 2018). Acute overheating, rather than chronic temperature conditions that involve energetics, is the most likely cause of thermal stress related mortality in high-shore animals (Williams and Morritt, 1995; Marshall and McQuaid, 2011; Marshall et al., 2011). The critical thermal maximum (CT_{max}), the temperature at which neuromuscular co-ordination fails, which is commonly used in ectotherm experiments, is unsuitable for determining gastropod lethality. This is because inactivity in high-shore littorinid snails relates to desiccation-risk-avoidance, and snails with shells glued to rock surfaces withstand temperatures well above those limiting foot physiological performance (Marshall and McQuaid, 2011; Marshall et al., 2013, 2015; Monaco et al., 2017). Much controversy surrounds the effects of ramping on acute heat tolerance determination (Terblanche et al., 2011). We selected a ramp rate of 0.25°C.min^{-1} or slightly slower, appropriate to the heating experienced in the field (**Figure 2**; Marshall et al., 2011). Prior to determining heat tolerance of acclimated snails, individuals were rehydrated and their shells dried as in the case of the field-fresh snails.

To determine heat tolerance, acclimated snails were placed in dry 50 ml glass tubes in a programmable bath (Grant TXF200, Cambridge, United Kingdom) and equilibrated at 30°C for 10 min, before being heated at 0.25°C.min^{-1}. To maintain water bath temperature stability during the LT_{50} experiment, the heating rate was slowed to 0.12°C.min^{-1} between 50 and 60°C. Naturally, the apparent lethal temperature will be affected by time at different temperatures. Temperatures inside the test tubes were recorded every minute using calibrated K-type thermocouples connected to a TC-08 interface and Picolog software (Pico Technology, Cambridge, United Kingdom). Lethality (LT_{50}) was determined for groups of 10 snails that were randomly removed from the water bath at 1°C intervals between 55 and 60°C, and allowed to recover at 28°C in wetted Petri dishes. Snails that emerged from their shells, extended their foot, and remained attached to the surface after 12 h were scored as alive. Alive but unattached snails, which are ecologically non-functional and vulnerable, were scored dead. All experiments were repeated either three or six times based on logistic constraints, with numbers of individuals limited for conservation purposes. One thousand nine hundred individual snails were used in the experiments. The study was approved by the Faculty of Science Ethics Committee, Universiti Brunei Darussalam. The effect of acclimation on LT_{50} was statistically compared between paired treatments using Generalized Linear Models (GLZM) for a binomial distribution, with a logit-link function (Statistica v12, StatSoft, New York, United States). Actual values of LT_{50} were computed from three parameter logistic regressions, which were plotted using Sigmaplot v14 (Systat Software, Inc., New York, United States).

RESULTS

Field Temperature Conditions

The daily temperature conditions and thermal frequencies for four habitats, the coolest in the shade and the hottest in the sun, are shown for each shoreline in **Figure 2**. There was little difference between the habitats in average temperature for this period (28.5–30.1°C; **Table 1**). Likewise, absolute and mean daily minimum temperatures were largely invariable among the habitats (21.7–23.7 and 24.2–26.0°C, respectively).

TABLE 1 | Field temperatures in the four habitats, logged every 30 min for 30 days using DS1923-F Hygrochron I-buttons (see **Figure 2**).

	Average	Max	Min	$\bar{X}$ daily max	$\bar{X}$ daily min	$\bar{X}$ daily ΔT
Cool shore (CS) (sun)	28.95	41.69	23.13	34.91	24.98	9.93
Cool shore (shade)	28.49	34.31	23.69	30.61	26.03	4.58
Warm shore (WS) (sun)	32.06	53.25	21.69	45.79	24.16	21.63
Warm shore (shade)	30.07	39.50	22.69	35.42	25.59	9.82

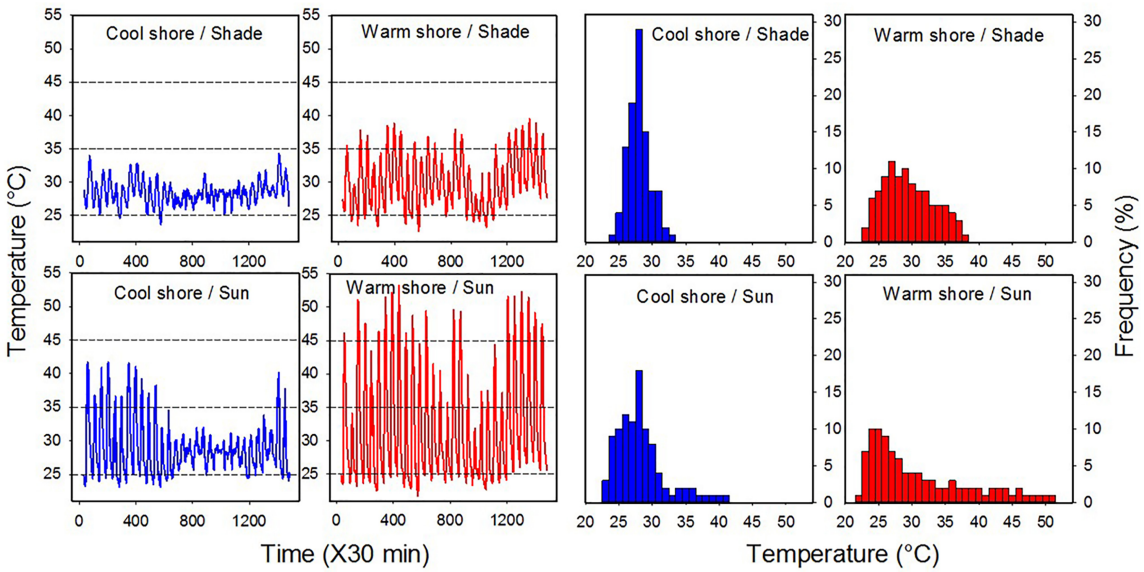

FIGURE 2 | Daily field temperature regimes and thermal frequencies for the four habitats (cool shore, CS, sun and shaded, and warm shore, WS, sun and shaded). All data were logged using DS1923-F5# Hygrochron I-buttons over 30 days. Temperatures were recorded between 21 June and 22 July 2018 at the sites where snails were collected (see **Supplementary Figure S1**).

However, the maxima differed greatly (34.3–53.3 and 30.6–45.8°C, respectively), being markedly elevated in the sun-exposed habitats. Notably, in the three cooler habitats, daily temperatures did not rise above 45°C, the temperature around which a heat shock response (HSR) is induced (Marshall et al., 2011; Han et al., 2019), whereas peak temperatures in the warmest habitat surpassed 45°C on 18 (of the 30) days (**Figure 2**). Daily temperature variation (ΔT) was greatest in the warmest habitat (sun-exposed, WS; 21.6°C) and lowest in the coolest habitat (shade, CS; 4.6°C; **Table 1**); the warmest habitat exhibited the highest maximum and the lowest minimum temperatures (**Figure 2** and **Table 1**). The stark difference in temperatures between the shores is highlighted by similar measures (means, maxs, mins, and ΔT) for the sun-exposed, CS and the shaded, WS habitats (**Figure 2** and **Table 1**). Although several factors influence long-term temperature variations in these tropical habitats, including seasonal and El Nino effects, our recordings for a narrow timeframe are representative of relative daily thermal regime differences between the habitats and shores.

Heat Tolerance Plasticity

Substantial heat tolerance plasticity was observed in *E. malaccana* snails. The overall magnitude of their LT_{50} adjustment was 2.9°C, when accounting for all laboratory-acclimated and field-acclimatized conditions (mean LT_{50} ranged from 56.1 to 59.0; **Figures 3**, **4** and **Table 2**). Whereas snails from either shore exhibited similar magnitudes in reversible acclimation (∼2°C), the thermal bands over which acclimatory adjustments were made differed between the shores. The acclimation band for WS snails was shifted to a hotter temperature range compared to that for CS snails (**Figure 4**).

Cool acclimation (CA) significantly lowered the mean LT_{50} of CS snails below that of WS snails ($p < 0.001$; **Table 2**). Because further cooling (ECA) of CS snails did not reduce the LT_{50} further, we consider the mean hard lower limit to heat

TABLE 2 | Statistical information comparing effects of field acclimatization (shoreline) and laboratory acclimation temperature conditions on the LT_{50} of *Echinolittorina malaccana*.

Shoreline	Acclimation	LT_{50}	95% CI (n)	Wald stat.	*P*<
Cool (CS)	Cool (CA)	56.4	56.2–56.7 (5)		
Warm (WS)	Cool	57.1	57.0–57.3 (5)	30.91	**0.001**
Cool	Warm (WA)	58.1	58.0–58.5 (5)		
Warm	Warm	58.2	58.1–58.5 (5)	2.33	0.127
Cool	Extra cool (ECA)	56.1	55.9–56.7 (3)		
Warm	Extra cool	57.5	57.3–57.7 (3)	31.36	**0.001**
Cool	Extra warm (EWA)	58.3	58.1–58.6 (3)		
Warm	Extra warm	59.0	58.6–59.5 (3)	16.72	**0.001**
Cool	Cool				
Cool	Extra cool			1.83	0.177
Cool	Warm				
Cool	Extra warm			3.39	0.065
Warm	Cool				
Warm	Extra cool			10.15	**0.001**
Warm	Warm				
Warm	Extra warm			22.01	**0.001**
Cool	Field	57.0	56.1–57.8 (3)		
Warm	Field	57.7	57.4–57.9 (3)	23.19	**0.001**

*LT_{50}s were computed from logistic regressions (SigmaPlot Ver. 14; **Figure 3**) and differences between pairs of conditions were assessed from logit-linked binomial regressions (Generalized Linear Model, Statistica Ver. 13.3). Significant differences are indicated in bold.*

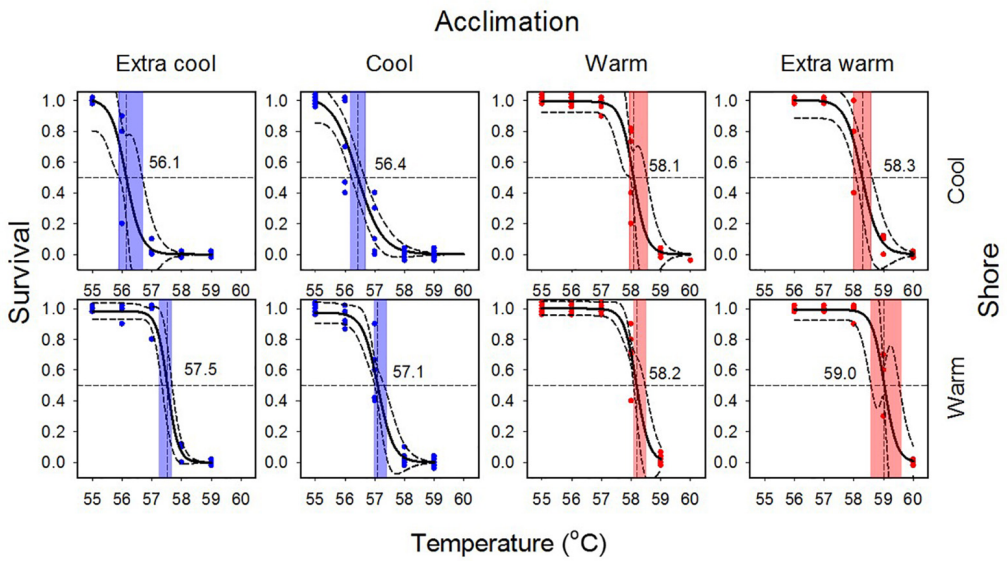

FIGURE 3 | Survival curves for laboratory-acclimated *Echinolittorina malaccana* snails from the cool (CS) and the warm shore (WS). Solid black logistic regressions are based on the combined data for each trial. Dashed lines associated with regressions represent 95% CIs. Colored symbols refer to individual trials for cool and warm acclimation (CA and WA, 5 trials) and extra cool and extra warm acclimation (ECA and EWA, 3 trials) using 50 snails per trial. Vertical lines indicate LT_{50} values and their associated colored bands, their 95% CIs.

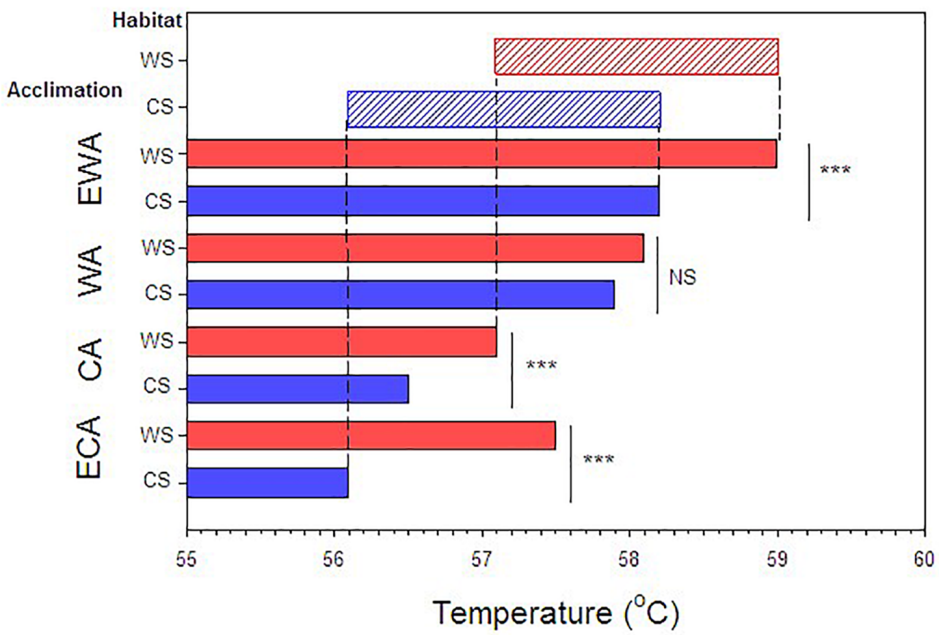

FIGURE 4 | Compilation of results showing the LT_{50} values for the various acclimation and acclimatization (habitat) conditions. Red bars indicate warm shore acclimatization (WS) and blue bars, cool shore acclimatization (CS). ECA, CA, WA, EWA refer to extra-cool, cool, warm and extra-warm acclimation, respectively. Asterisk indicates $P < 0.01$ and NS, non-significant difference. Lightly shaded upper bars indicate acclimation capacities and ranges for warm shore (red) and cool shore (blue) acclimatized snails.

tolerance of this snail population to be 56.1°C ($p = 0.177$; **Table 2**). Similarly, the hard lower limit for WS snails is apparently 57.1°C (**Figure 4** and **Table 2**). Warm acclimation (WA) markedly raised the mean LT_{50} of CS snails (58.1°C), but no further increase in heat tolerance was observed for this population with further warming (EWA, extra-warm acclimation; $p = 0.065$; **Table 2**), suggesting that their hard upper heat tolerance boundary is reached under WA (**Figure 4**). There was also no significant

difference between the two shoreline populations under WA (p = 0.127; **Table 2**). However, WA apparently did not result in complete thermal acclimation of the WS snails, as their heat tolerance rose following extra-warm temperature acclimation (EWA, LT_{50} = 59.0°C; $p < 0.001$, **Table 2**).

Mean field-fresh LT_{50} was greater in WS snails (57.7°C) compared to CS snails (57.0°C; $p < 0.001$; **Table 2**), reflecting the different recent thermal histories experienced on the different shorelines. There was no difference in LT_{50} between the 10 d and 20 d WA treatment for warm shore snails, indicating that 10 d is sufficiently long to produce complete compensation (p = 0.295). When the cool and warm habitat data were combined (CS and WS), and compared with the data for WS snails, the combined data set showed significantly lower LT_{50} values for ECA, CA, and EWA ($p < 0.007$; **Table 3**), but not for the WA laboratory treatments (p = 0.369; **Table 3**). While it was not investigated in the present study, individual variation can be as important an endpoint as the mean value in any study investigating temperature responses.

DISCUSSION

Ectotherms vary widely in ability to adjust physiological performances and tolerances in response to lifetime changes in environmental temperature (Angilletta, 2009). Contrary to the prediction of mainstream theory that thermal acclimation is relatively constrained in tropical and high-intertidal animals (Stillman and Somero, 2000; Stillman, 2002; Somero, 2005, 2010; Gunderson and Stillman, 2015; Rohr et al., 2018), we found substantial plasticity in the lethal thermal limit (LT_{50}) of *Echinolittorina* snails (see also, Marshall et al., 2018). However, we additionally, show that heat tolerance plasticity of these snails comprises both a reversible and a non-reversible component. Reversible plasticity was induced by laboratory acclimation and non-reversible plasticity was shown by differences in the thermal bands for lethal temperature (LT_{50}) acclimation between populations from thermally-different shorelines (see **Figure 4**). Snails from the warmer shore were found to shift the band for thermal acclimation to a higher range of temperatures compared to the CS snails. These different forms of plasticity align with different spatiotemporal scales of the environmental temperature variation. Reversible plasticity facilitates thermal tolerance adjustments in response to daily or tidal habitat temperature variation, whereas non-reversibility canalizes or fixes the thermal tolerance to shoreline-specific temperature conditions throughout the individual's lifetime.

TABLE 3 | Statistical information comparing effects of warm-shore (WS) and combined-shore (warm and cool) on the LT_{50} of *Echinolittorina malaccana* for the various acclimation treatments.

Shoreline	Acclimation	LT_{50}	95% CI (n)	Wald stat.	$P<$
Warm	Cool				
Combined	Cool	56.7	56.5–56.9 (10)	11.85	**0.001**
Warm	Warm				
Combined	Warm	58.1	58.0–58.4 (10)	0.81	0.369
Warm	Extra cool				
Combined	Extra cool	56.9	56.4–57.3 (6)	18.71	**0.001**
Warm	Extra warm				
Combined	Extra warm	58.7	58.4–58.9 (6)	7.34	**0.007**

*LT_{50} values for WS are given in **Table 2**. Significant differences are indicated in bold.*

Reversible and Non-reversible Plasticity

Reversible plasticity enables individual organisms to adjust performances and tolerances in response to cycling temperatures for timeframes from seasons to days. In comparative studies, laboratory acclimation is typically performed to eliminate the effect of recent field temperatures on the physiological performance of individuals. Our observed persistence of phenotypic differences after laboratory acclimation in populations from thermally-different shorelines (**Figure 3** and **Table 2**) suggests an effect of heritable differences between the populations or non-reversible plasticity. Because the snail larvae settling on either shoreline were randomly drawn from the same planktotrophic pool, comprising individuals derived from multiple different parents, we disregard local adaptation or other inherited effects as the cause of the observed population difference (Schmidt and Rand, 1999; Williams and Reid, 2004; Kelly et al., 2011; Foo and Byrne, 2016). Non-reversible plasticity has been described as transgenerational, such as non-genetic heat-hardening transferred to the embryo from the parent, or as developmental, such as post-embryonic heat-hardening (Angilletta, 2009; Donelson et al., 2011, 2012; Reusch, 2014). Using the same argument as above for random shoreline recruitment of larvae, the shoreline (population) differences in thermal plasticity can also not be explained by a transgenerational response to heat exposure (Williams and Reid, 2004). Our findings therefore suggest that non-reversible heat tolerance is most likely founded after larval snails have settled on the shore; thus, shoreline differences are best described as developmental plasticity (Angilletta, 2009). Because the crawling snails occupy meter-size habitats, cross-shore migrations can be discounted. Notably, the apparent developmental plasticity should be reinforced by the shoreline-specific temperature conditions during the lifetime of each snail, from the crawling juvenile to the adult (Angilletta, 2009; see Slotsbo et al., 2016 on reversibility of developmental plasticity).

Environmental Temperature and Molecular Underpinnings of Plasticity

Molecular processes underlying thermal plasticity are cued by different components of the thermal regime (mean, maxima, and minima) for different durations of thermal cycling (daily or seasonal). Whereas seasonal acclimatization, regulated by isozyme expression (Hochachka and Somero, 2002), is typically cued by mean temperature change (Angilletta, 2009), acute daily heating of rocky-shores elicits thermal plasticity through a HSR, triggered by peak (maximum) temperatures (Hofmann and Somero, 1996; Feder and Hofmann, 1999; Tomanek and Somero, 1999; Somero et al., 2017). Although HSRs are

complex, involving upregulation of multiple heat shock proteins (Hsps), much information can be gleaned from individual gene *thermal expression profiles* (relative levels and thermal ranges of expression) and *thermal thresholds* (Tomanek and Somero, 1999; Wang et al., 2017; Han et al., 2019). Previous studies on *E. malaccana* showed that *hsp70* expression profiles differ among geographically-separated populations (Wang et al., 2017; Han et al., 2019), such that reduced expression correlates with populations from cooler locations and *vice versa* (Wang et al., 2017; Han et al., 2019). The same mechanism in a spatially scaled-down form could underlie the heat tolerance differences observed between our cool and warm shore populations. Whereas these findings imply plasticity of *hsp* expression profiles, studies for diverse populations of *E. malacanna* suggest that the HSR thermal threshold for this species may otherwise be fixed at around 45°C (Marshall et al., 2011; Han et al., 2019; see also Hoffmann et al., 2003). Interestingly, whereas our cool and warm shore snails adjusted heat tolerance to the same level when acclimated to a daily maximum of 45°C, only the WS snails that commonly experience temperatures above 45°C responded positively to the extra-warm acclimation treatment (EWA; for which the daily thermal peak was 50°C; **Figure 3** and **Table 2**).

Whereas daily maximum temperatures varied greatly across the snail habitats, mean field temperatures (which typically drive seasonal acclimatization) were largely similar across habitats (sunned and shaded) and shorelines (cooler and warmer; **Table 1**). Clearly, mean temperatures contribute insignificantly to heat tolerance plasticity selection in tropical *Echinolittorina* snails. Likewise, minimum field temperatures were largely invariable across the habitats and shores, which excludes these temperatures as potential determinants of the lower boundary for heat tolerance plasticity. The limit to this boundary, assessed during CA for both shores, possibly relates to the loss of heat-hardening, a mechanism which should be beneficial by eliminating costs associated with the upregulating and functioning of Hsps (Angilletta, 2009).

Benefits of Dual Heat Tolerance Plasticity

Plastic responses involving Hsps incur significant energetic and fitness costs, a topic extensively critiqued in the framework of the *beneficial acclimation hypothesis* (Leroi et al., 1994; Huey et al., 1999; Wilson and Franklin, 2002; Woods and Harrison, 2002; Deere and Chown, 2006). In their high-shore habitat, *Echinolittorina* snails face severe energy intake restrictions due to limited food availability and limited time in which to feed. Consequently, they have evolved multifaceted behavioral and physiological mechanisms to conserve energy resources (Marshall et al., 2011, 2013; Marshall and Chua, 2012). Among the most impressive energy-conserving mechanism is deep temperature-independent metabolic rate depression (10% of resting metabolism; Marshall et al., 2011; Verberk et al., 2016). In view of their energetic constraints, advantage should be gained by minimizing the use of costly physiological processes, including HSRs.

Non-reversible plasticity should be energetically beneficial by ensuring that the range for reversible heat tolerance plasticity matches the habitat temperatures of a particular shore. Such matching should prevent snails on warmer shores from experiencing excessive HSR induction and *hsp* overexpression (Feder and Hofmann, 1999; Sørensen et al., 2003). Non-reversible heat tolerance plasticity should enable reversible acclimatization to occur in similar ways and at similar costs on thermally-different shores under the same regional change in ambient air temperature. Furthermore, this plasticity should yield species-level benefits by enabling colonization of a broader range of shores (warmer and cooler shores) along a coastline. Importantly, these findings accounting for non-reversibility supersede an earlier suggestion that *E. malaccana* is unlikely to benefit from reversible plasticity (Marshall et al., 2018).

Taxonomic Generalization and Habitat Heterogeneity

Our understanding of thermal acclimation of rocky-intertidal animals in the context of contemporary theory (Angilletta, 2009) is encompassed by the influential work of Somero and Stillman (see Stillman, 2002; Somero, 2005, 2010). This work suggesting a reduced acclimation capacity in higher-shore species compared to their lower-shore congeners, arises from generalization of data for porcelain crabs (Stillman, 2002; Somero, 2005, 2010). These crabs, however, behaviourally thermoregulate by sheltering in the shade under rocks during air emersion, limiting their exposure to the full spectrum of the shoreline's thermal heterogeneity. The substantial heat tolerance plasticity observed in high-shore *Echinolittorina* snails contradicts this theory, and we suggest that the difference between the crab and snail responses relates to the snails using a broader spectrum of the shoreline thermal heterogeneity. They experience relatively great habitat temperature variation through the behavior of settling when air-exposed in thermally-divergent microhabitats, including those under direct solar heating (Marshall et al., 2010, 2013). This habitat temperature variation persists despite the phenomenal variety of morphological and behavioral thermoregulatory attributes of littorinid snails (Miller and Denny, 2011; Marshall and Chua, 2012; Marshall et al., 2013; Ng et al., 2017), primarily because the most effective thermoregulatory behavior, shade-seeking, can be undermined by desiccation risk avoidance behavior (Monaco et al., 2017).

An arising question is whether capacity for non-reversible plasticity (the shoreline effect) is restricted to high-shore species or whether it is independent of vertical distribution on the shore. Because lower-shore habitats are strongly stabilized by the seawater temperature, and because the seawater temperature is largely invariable across nearby shorelines, the shoreline effect should be lessened in the lower-shore. In addition to suggesting that seawater temperature stability is likely to restrict thermal acclimation selection in lower-shore tropical species, we propose as a testable hypothesis that non-reversible plasticity should also be more constrained in lower-shore compared to higher-shore species.

Methodological Implications

Acclimation capacity (the degree of change in a trait following cool or warm laboratory acclimation) is becoming a key

measure of the vulnerability of ectothermic animals to future warming (Gunderson and Stillman, 2015; Rohr et al., 2018). An earlier study revealed that laboratory experiments alone (without field-referencing) may underestimate this vulnerability in animals living in near-completely acclimatized states, which are unable to improve heat hardening with further warming (Marshall et al., 2018). The present study adds to this caveat by showing that inaccuracies in determining heat-tolerance acclimation capacity can potentially arise from not accounting for shoreline-specific temperature differences. Whereas the capacity for reversible acclimation was similar for each shoreline (∼2°C), this became greater when the data for the shores were combined (∼2.9°C; **Table 3** and **Figure 4**). This highlights the importance, when assessing acclimation capacities, of prior knowledge of the habitat thermal heterogeneity of experimental animals.

Emerging from this study is a second methodological issue relating to diel cycling of the laboratory acclimation temperature. This is not only important considering that such cycling occurs naturally, but also in terms of initiating an acclimatory HSR. If the primary heat-hardening response requires that exposure temperature surpasses an HSR induction threshold, then acclimation temperatures that are stable or fluctuate below this threshold will conceivably not yield an acclimatory response, leading to erroneous conclusions. This further highlights the need to determine the HSR threshold temperature prior to developing acclimation protocols in marine intertidal animal studies.

CONCLUSION

Our study adds an important dimension to the existing theory proposing that thermal tolerance plasticity is relatively constrained in tropical ectotherms. In particular, it reveals that this plasticity can be complex in thermally-heterogeneous tropical marine intertidal ecosystems. Whereas the contribution of marine intertidal circumstances to a body of theory for thermal plasticity developed largely from terrestrial and subtidal animals might be questionable, our findings nonetheless caution against the indiscriminate use of this theory when interpreting intertidal data. We further show that without critical consideration of the thermal heterogeneity at the scale of the organism and how this heterogeneity may drive different forms of thermal tolerance plasticity, investigations risk generating misleading conclusions.

AUTHOR CONTRIBUTIONS

AB and DM developed the hypothesis and prepared the manuscript. AB and NM carried out the experimental laboratory work. DM undertook the field recordings. NM reviewed the manuscript.

FUNDING

DM was supported by a Universiti Brunei Darussalam grant (UBD/RSCH/1.4/FICBF(b)/2018/016).

SUPPLEMENTARY MATERIAL

The Supplementary Material for this article can be found online at: https://www.frontiersin.org/articles/10.3389/fphys.2018.01909/full#supplementary-material

REFERENCES

Angilletta, M. J. (2009). *Thermal Adaptation: a Theoretical and Empirical Synthesis*. Oxford: Oxford University Press. doi: 10.1093/acprof:oso/9780198570875.001.1

Angilletta, M. J., Bennett, A. F., Guderley, H., Navas, C. A., Seebacher, F., and Wilson, R. S. (2006). Coadaptation: a unifying principle in evolutionary thermal biology. *Physiol. Biochem. Zool.* 79, 282–294. doi: 10.1086/499990

Beaman, J. E., White, C. R., and Seebacher, F. (2016). Evolution of plasticity: mechanistic link between development and reversible acclimation. *Trends. Ecol. Evol.* 31, 237–249. doi: 10.1016/j.tree.2016.01.004

Deere, J. A., and Chown, S. L. (2006). Testing the beneficial acclimation hypothesis and its alternatives for locomotor performance. *Am. Nat.* 168, 630–644. doi: 10.1086/508026

Denny, M. W., Dowd, W. W., Bilir, L., and Mach, K. J. (2011). Spreading the risk: small-scale body temperature variation among intertidal organisms and its implications for species persistence. *J. Exp. Mar. Biol. Ecol.* 400, 175–190. doi: 10.1016/j.jembe.2011.02.006

Donelson, J. M., Munday, P. L., McCormick, M. I., and Nilsson, G. E. (2011). Acclimation to predicted ocean warming through developmental plasticity in a tropical reef fish. *Glob. Change Biol.* 17, 1712–1719. doi: 10.1371/journal.pone.0097223

Donelson, J. M., Munday, P. L., McCormick, M. I., and Pitcher, C. R. (2012). Rapid transgenerational acclimation of a tropical reef fish to climate change. *Nat. Clim. Change* 2, 30. doi: 10.1038/nclimate1323

Dong, Y. W., Li, X., Choi, F. M. P., Williams, G. A., Somero, G. N., and Helmuth, B. (2017). Untangling the roles of microclimate, behaviour and physiological polymorphism in governing vulnerability of intertidal snails to heat stress. *Proc. R. Soc. Lond. B. Biol. Sci.* 284:20162367. doi: 10.1098/rspb.2016.2367

Dong, Y. W., Yu, S. S., Wang, Q. L., and Dong, S. L. (2011). Physiological responses in a variable environment: relationships between metabolism, HSP and thermotolerance in an intertidal-subtidal species. *PLoS One* 6:e26446. doi: 10.1371/journal.pone.0026446

Feder, M. E., and Hofmann, G. E. (1999). Heat-shock proteins, molecular chaperones, and the stress response. *Annu. Rev. Physiol.* 61, 243–282. doi: 10.1146/annurev.physiol.61.1.243

Foo, S. A., and Byrne, M. (2016). "Acclimatization and adaptive capacity of marine species in a changing ocean," in *Advances in Marine Biology*, Vol. 74, ed. E. C. Barbara (Cambridge, MA: Academic Press), 69–116. doi: 10.1016/bs.amb.2016.06.001

Garrabou, J., Coma, R., Bensoussan, N., Bally, M., Chevaldonné, P., Cigliano, M., et al. (2009). Mass mortality in Northwestern Mediterranean rocky benthic communities: effects of the 2003 heat wave. *Glob. Change Biol.* 15, 1090–1103. doi: 10.1111/j.1365-2486.2008.01823.x

Gedan, K. B., Bernhardt, J., Bertness, M. D., and Leslie, H. M. (2011). Substrate size mediates thermal stress in the rocky intertidal. *Ecology* 92, 576–582. doi: 10.1890/10-0717.1

Gunderson, A. R., and Stillman, J. H. (2015). Plasticity in thermal tolerance has limited potential to buffer ectotherms from global warming. *Proc. R. Soc. Lond. B. Biol. Sci.* 282:20150401. doi: 10.1098/rspb.2015.0401

Han, G. D., Cartwright, S. R., Ganmanee, M., Chan, B. K., Adzis, K. A., Hutchinson, N., et al. (2019). High thermal stress responses of *Echinolittorina* snails at their range edge predict population vulnerability to future warming. *Sci. Total. Environ.* 647, 763–771. doi: 10.1016/j.scitotenv.2018.08.005

Harley, C. D. (2008). Tidal dynamics, topographic orientation, and temperature-mediated mass mortalities on rocky shores. *Mar. Ecol. Prog. Ser.* 371, 37–46. doi: 10.3354/meps07711

Helmuth, B., Broitman, B. R., Blanchette, C. A., Gilman, S., Halpin, P., Harley, C. D., et al. (2006a). Mosaic patterns of thermal stress in the rocky intertidal zone: implications for climate change. *Ecol. Monogr.* 76, 461–479. doi: 10.1890/0012-9615(2006)076[0461:MPOTSI]2.0.CO;2

Helmuth, B., and Hofmann, G. E. (2001). Microhabitats, thermal heterogeneity, and patterns of physiological stress in the rocky intertidal zone. *Biol. Bull.* 201, 374–384. doi: 10.2307/1543615

Helmuth, B., Mieszkowska, N., Moore, P., and Hawkins, S. J. (2006b). Living in the edge of two changing worlds: forecasting the responses of rocky intertidal ecosystems to climate change. *Annu. Rev. Ecol. Evol. Syst.* 37, 373–404. doi: 10.1146/annurev.ecolsys.37.091305.110149

Hochachka, P. W., and Somero, G. N. (2002). *Biochemical Adaptation: Mechanism and Process in Physiological Evolution*. New York, NY: Oxford University Press.

Hoffmann, A. A., Sørensen, J. G., and Loeschcke, V. (2003). Adaptation of *Drosophila* to temperature extremes: bringing together quantitative and molecular approaches. *J. Therm. Biol.* 28, 175–216. doi: 10.1016/S0306-4565(02)00057-8

Hofmann, G. E., and Somero, G. N. (1996). Interspecific variation in thermal denaturation of proteins in the congeneric mussels *Mytilus trossulus* and *M. galloprovincialis*: evidence from the heat shock response and protein ubiquitination. *Mar. Biol.* 126, 65–75. doi: 10.1007/BF00571378

Huey, R. B., Berrigan, D., Gilchrist, G. W., and Herron, J. C. (1999). Testing the adaptive significance of acclimation: a strong inference approach. *Am. Zool.* 39, 323–336. doi: 10.1093/icb/39.2.323

Kelly, M. W., Sanford, E., and Grosberg, R. K. (2011). Limited potential for adaptation to climate change in a broadly distributed marine crustacean. *Proc. Biol. Sci.* 279, 349–356. doi: 10.1098/rspb.2011.0542

Kingsolver, J. G., Diamond, S. E., and Buckley, L. B. (2013). Heat stress and the fitness consequences of climate change for terrestrial ectotherms. *Funct. Ecol.* 27, 1415–1423. doi: 10.1098/rspb.2013.1149

Kingsolver, J. G., and Huey, R. B. (1998). Evolutionary analyses of morphological and physiological plasticity in thermally variable environments. *Am. Zool.* 38, 545–560. doi: 10.1093/icb/38.3.545

Leroi, A. M., Bennett, A. F., and Lenski, R. E. (1994). Temperature acclimation and competitive fitness: an experimental test of the beneficial acclimation assumption. *Proc. Natl. Acad. Sci. U.S.A.* 91, 1917–1921. doi: 10.1073/pnas.91.5.1917

Liao, M. L., Zhang, S., Zhang, G. Y., Chu, Y. M., Somero, G. N., and Dong, Y. W. (2017). Heat-resistant cytosolic malate dehydrogenases (cMDHs) of thermophilic intertidal snails (genus *Echinolittorina*): protein underpinnings of tolerance to body temperatures reaching 55°C. *J. Exp. Biol.* 220, 2066–2075. doi: 10.1242/jeb.156935

Marshall, D. J., Baharuddin, N., and McQuaid, C. D. (2013). Behaviour moderates climate warming vulnerability in high-rocky-shore snails: interactions of habitat use, energy consumption and environmental temperature. *Mar. Biol.* 160, 2525–2530. doi: 10.1007/s00227-013-2245-1

Marshall, D. J., Baharuddin, N., Rezende, E., and Helmuth, B. (2015). Thermal tolerance and climate warming sensitivity in tropical snails. *Ecol. Evol.* 5, 5905–5919. doi: 10.1002/ece3.1785

Marshall, D. J., Brahim, A., Mustapha, N., Dong, Y. W., and Sinclair, B. J. (2018). Substantial heat-tolerance acclimatory capacity in tropical thermophilic snails, but to what benefit? *J. Exp. Biol* 221:jeb187476. doi: 10.1242/jeb.187476

Marshall, D. J., and Chua, T. (2012). Boundary layer convective heating and thermoregulatory behaviour during aerial exposure in the rocky eulittoral fringe snail *Echinolittorina malaccana*. *J. Exp. Mar. Biol. Ecol.* 430, 25–31. doi: 10.1016/j.jembe.2012.06.011

Marshall, D. J., Dong, Y. W., Williams, G. A., and McQuaid, C. D. (2011). Thermal adaptation in the intertidal snail *Echinolittorina malaccana* contradicts current theory by revealing the crucial roles of resting metabolism. *J. Exp. Biol.* 214, 3649–3657. doi: 10.1242/jeb.059899

Marshall, D. J., and McQuaid, C. D. (2011). Warming reduces metabolic rate in marine snails: adaptation to fluctuating high temperatures challenges the metabolic theory of ecology. *Proc. R. Soc. Lond. B Biol. Sci.* 278, 281–288. doi: 10.1098/rspb.2010.1414

Marshall, D. J., McQuaid, C. D., and Williams, G. A. (2010). Non-climatic thermal adaptation: implications for species' responses to climate warming. *Biol. Lett.* 6, 669–673. doi: 10.1098/rsbl.2010.0233

Miller, L. P., and Denny, M. W. (2011). Importance of behavior and morphological traits for controlling body temperature in littorinid snails. *Biol. Bull.* 220, 209–223. doi: 10.1086/BBLv220n3p209

Mitchell, K. A., Sgrò, C. M., and Hoffmann, A. A. (2011). Phenotypic plasticity in upper thermal limits is weakly related to *Drosophila* species distributions. *Funct. Ecol.* 25, 661–670. doi: 10.1111/j.1365-2435.2010.01821.x

Monaco, C. J., McQuaid, C. D., and Marshall, D. J. (2017). Decoupling of behavioural and physiological thermal performance curves in ectothermic animals: a critical adaptive trait. *Oecologia* 185, 583–593. doi: 10.1007/s00442-017-3974-5

Ng, T. P. T., Lau, S. L. Y., Seuront, L., Davies, M. S., Stafford, R., Marshall, D. J., et al. (2017). Linking behaviour and climate change in intertidal ectotherms: insights from littorinid snails. *J. Exp. Mar. Biol. Ecol.* 492, 121–131. doi: 10.1016/j.jembe.2017.01.023

Overgaard, J., Kristenses, T. N., Mitchell, K. A., and Hoffmann, A. A. (2011). Thermal tolerance in widespread and tropical *Drosophila* species: Does phenotypic plasticity increase with latitude? *Am. Nat.* 178, S80–S96. doi: 10.1086/661780

Phillips, B. L., Munoz, M. M., Hatcher, A., Macdonald, S. L., Llewelyn, J., Lucy, V., et al. (2015). Heat hardening in a tropical lizard: geographic variation explained by the predictability and variance in environmental temperatures. *Funct. Ecol.* 30, 1161–1168. doi: 10.1111/1365-2435.12609

Reid, D. (2007). The genus *Echinolittorina* (Habe, 1956) (Gastropoda: Littorinidae) in the Indo-West Pacific Ocean. *Zootaxa* 1420, 1–161. doi: 10.11646/zootaxa.1420.1.1

Reusch, T. B. H. (2014). Climate change in the oceans: evolutionary versus phenotypically plastic responses of marine animals and plants. *Evol. Appl.* 7, 104–122. doi: 10.1111/eva.12109

Rohr, J. R., Civitello, D. J., Cohen, J. M., Roznik, E. A., Sinervo, B., and Dell, A. I. (2018). The complex drivers of thermal acclimation and breadth in ectotherms. *Ecol. Lett.* 21, 1425–1439. doi: 10.1111/ele.13107

Schmidt, P. S., and Rand, D. M. (1999). Intertidal microhabitat and selection at Mpi: interlocus contrasts in the northern acorn barnacle, Semibalanus balanoides. *Evolution* 53, 135–146. doi: 10.1111/j.1558-5646.1999.tb05339.x

Seebacher, F., Beaman, J., and Little, A. G. (2014). Regulation of thermal acclimation varies between generations of the short-lived mosquitofish that developed in different environmental conditions. *Funct. Ecol.* 28, 137–148. doi: 10.1111/1365-2435.12156

Seebacher, F., Holmes, S., Roosen, N. J., Nouvian, M., Wilson, R. S., and Ward, A. J. (2012). Capacity for thermal acclimation differs between populations and phylogenetic lineages within a species. *Funct. Ecol.* 26, 1418–1428. doi: 10.1111/j.1365-2435.2012.02052.x

Slotsbo, S., Schou, M. F., Kristensen, T. N., Loeschcke, V., and Sørensen, J. G. (2016). Reversibility of developmental heat and cold plasticity is asymmetric and has long-lasting consequences for adult thermal tolerance. *J. Exp. Biol.* 219, 2726–2732. doi: 10.1242/jeb.143750

Somero, G. N. (2005). Linking biogeography to physiology: evolutionary and acclimatory adjustments of thermal limits. *Front. Zool.* 2:1. doi: 10.1186/1742-9994-2-1

Somero, G. N. (2010). The physiology of climate change: how potentials for acclimatization and genetic adaptation will determine "winners" and "losers". *J. Exp. Biol.* 213, 912–920. doi: 10.1242/jeb.037473

Somero, G. N., Lockwood, B. L., and Tomanek, L. (2017). *Biochemical Adaptation: Response to Environmental Challenges from Life's Origins to the Anthropocene*. Sunderland, MA: Sinauer Associates, Inc.

Sørensen, J. G., Kristensen, T. N., and Loeschcke, V. (2003). The evolutionary and ecological role of heat shock proteins. *Ecol. Lett.* 6, 1025–1037. doi: 10.1046/j.1461-0248.2003.00528.x

Sørensen, J. G., Kristensen, T. N., and Overgaard, J. (2016). Evolutionary and ecological patterns of thermal acclimation capacity in *Drosophila*: is it

important for keeping up with climate change? *Curr. Opin. Insect. Sci.* 17, 98–104. doi: 10.1016/j.cois.2016.08.003

Stillman, J. H. (2002). Causes and consequences of thermal tolerance limits in rocky intertidal porcelain crabs, genus *Petrolisthes*. *Integr. Comp. Biol.* 42, 790–796. doi: 10.1093/icb/42.4.790

Stillman, J. H. (2003). Acclimation capacity underlies susceptibility to climate change. *Science* 301:65. doi: 10.1126/science.1083073

Stillman, J. H., and Somero, G. N. (2000). A comparative analysis of the upper thermal tolerance limits of eastern Pacific porcelain crabs, genus *Petrolisthes*: influences of latitude, vertical zonation, acclimation, and phylogeny. *Physiol. Biochem. Zool.* 73, 200–208. doi: 10.1086/316738

Terblanche, J. S., Hoffmann, A. A., Mitchell, K. A., Rako, L., le Roux, P. C., and Chown, S. L. (2011). Ecologically relevant measures of tolerance to potentially lethal temperatures. *J. Exp. Biol.* 214, 3713–3725. doi: 10.1242/jeb.061283

Tomanek, L., and Somero, G. N. (1999). Evolutionary and acclimation-induced variation in the heat-shock responses of congeneric marine snails (genus *Tegula*) from different thermal habitats: implications for limits of thermotolerance and biogeography. *J. Exp. Biol.* 202, 2925–2936.

Verberk, W. C., Bartolini, F., Marshall, D. J., Pörtner, H. O., Terblanche, J. S., White, C. R., et al. (2016). Can respiratory physiology predict thermal niches? *Ann. N. Y. Acad. Sci.* 1365, 73–88. doi: 10.1111/nyas.12876

Wang, W., Ding, M. W., Li, X. X., Wang, J., and Dong, Y. W. (2017). Divergent thermal sensitivities among different life stages of the pulmonate limpet *Siphonaria japonica*. *Mar. Biol.* 164:125. doi: 10.1007/s00227-017-3157-2

Williams, G. A., and Morritt, D. (1995). Habitat partitioning and thermal tolerance in a tropical limpet, *Cellana grata*. *Mar. Ecol. Prog. Ser.* 124, 89–103. doi: 10.3354/meps124089

Williams, S. T., and Reid, D. G. (2004). Speciation and diversity on tropical rocky shores: a global phylogeny of snails of the genus *Echinolittorina*. *Evolution* 58, 2227–2251. doi: 10.1111/j.0014-3820.2004.tb01600.x

Wilson, R. S., and Franklin, C. E. (2002). Testing the beneficial acclimation hypothesis. *Trends Ecol. Evol.* 17, 66–70. doi: 10.1016/S0169-5347(01)02384-9

Woods, H. A., and Harrison, J. F. (2002). Interpreting rejections of the beneficial acclimation hypothesis: When is physiological plasticity adaptive? *Evolution* 56, 1863–1866.

Conflict of Interest Statement: The authors declare that the research was conducted in the absence of any commercial or financial relationships that could be construed as a potential conflict of interest.

frontiers in Physiology

ORIGINAL RESEARCH
published: 15 January 2019
doi: 10.3389/fphys.2018.01920

Transcriptomic Analysis Reveals Insights on Male Infertility in *Octopus maya* Under Chronic Thermal Stress

*Laura López-Galindo[1], Oscar E. Juárez[1], Ernesto Larios-Soriano[2], Giulia Del Vecchio[3], Claudia Ventura-López[1], Asunción Lago-Lestón[4] and Clara Galindo-Sánchez[1]**

[1] Laboratorio de Genómica Funcional, Departamento de Biotecnología Marina, Centro de Investigación Científica y de Educación Superior de Ensenada, Ensenada, Mexico, [2] Laboratorio de Fisiología Integrativa de Organismos Marinos, Departamento de Biotecnología Marina, Centro de Investigación Científica y de Educación Superior de Ensenada, Ensenada, Mexico, [3] Facultad de Ciencias, Universidad Nacional Autónoma de México, Mexico City, Mexico, [4] Departamento de Innovación Biomédica, Centro de Investigación Científica y de Educación Superior de Ensenada, Ensenada, Mexico*

OPEN ACCESS

Edited by:
Nelly Tremblay, Alfred-Wegener-Institut Helmholtz-Zentrum für Polar- und Meeresforschung, Helmholtz-Gemeinschaft Deutscher Forschungszentren (HZ), Germany

Reviewed by:
Gianluca Polese, University of Naples Federico II, Italy
Oleg Simakov, Universität Wien, Austria

***Correspondence:**
Clara Galindo-Sánchez
cgalindo@cicese.mx

Specialty section:
This article was submitted to Aquatic Physiology, a section of the journal Frontiers in Physiology

Received: *02 October 2018*
Accepted: *20 December 2018*
Published: *15 January 2019*

Citation:
López-Galindo L, Juárez OE, Larios-Soriano E, Del Vecchio G, Ventura-López C, Lago-Lestón A and Galindo-Sánchez C (2019) Transcriptomic Analysis Reveals Insights on Male Infertility in Octopus maya Under Chronic Thermal Stress. Front. Physiol. 9:1920. doi: 10.3389/fphys.2018.01920

Octopus maya endemic to the Yucatan Peninsula, Mexico, is an ectotherm organism particularly temperature-sensitive. Studies in *O. maya* females show that temperatures above 27°C reduce the number of eggs per spawn, fertilization rate and the viability of embryos. High temperatures also reduce the male reproductive performance and success. However, the molecular mechanisms are still unknown. The transcriptomic profiles of testes from thermally stressed (30°C) and not stressed (24°C) adult male octopuses were compared, before and after mating to understand the molecular bases involved in the low reproductive performance at high temperature. The testis paired-end cDNA libraries were sequenced using the Illumina MiSeq platform. Then, the transcriptome was assembled *de novo* using Trinity software. A total of 53,214,611 high-quality paired reads were used to reconstruct 85,249 transcripts and 77,661 unigenes with an N50 of 889 bp length. Later, 13,154 transcripts were annotated implementing Blastx searches in the UniProt database. Differential expression analysis revealed 1,881 transcripts with significant difference among treatments. Functional annotation and pathway mapping of differential expressed transcripts revealed significant enrichment for biological processes involved in spermatogenesis, gamete generation, germ cell development, spermatid development and differentiation, response to stress, inflammatory response and apoptosis. Remarkably, the transcripts encoding genes such as ZMYND15, KLHL10, TDRD1, TSSK2 and DNAJB13, which are linked to male infertility in other species, were differentially expressed among the treatments. The expression levels of these key genes, involved in sperm motility and spermatogenesis were validated by quantitative real-time PCR. The results suggest that the reduction in male fertility at high temperature can be related to alterations in spermatozoa development and motility.

Keywords: male infertility, chronic thermal stress, RNA-Seq, reproduction, inflammation

INTRODUCTION

Octopus maya endemic to the Yucatan Peninsula (YP) is an ectotherm organism particularly temperature-sensitive mainly due to the characteristics of its habitat (Noyola et al., 2013a,b; Regil et al., 2015). It is one of the most important commercial fisheries in the YP and the American continent (Gamboa-Álvarez et al., 2015). The YP is divided into two distinct zones. The eastern zone located in front of the Yucatan state presents a summer upwelling that brings a mass of cold water from the Caribbean (16–22°C) that enters the YP and acts as an external temperature control for the shelf with temperatures fluctuating between 23 and 27.5°C (Noyola et al., 2013b). Meanwhile, the western zone located in front of Campeche has no influences of deep cold waters, and as a consequence, the surficial temperatures can rise above 30°C in summer (Noyola et al., 2013b; Regil et al., 2015). Gamboa-Álvarez et al. (2015) observed that temperature modules two essential aspects in the YP such as the fishing seasons which presents higher octopus abundances with low biomass in the western zone. In the eastern zone, lower abundances and higher biomass had been recorded. In the other hand, low temperatures in the different zones of the YP favor the spawning (Avila-Poveda et al., 2015; Gamboa-Álvarez et al., 2015; Regil et al., 2015).

Temperature plays a crucial role in different life aspects of *O. maya*. In females, it has been observed that temperatures above 27°C inhibit the spawning and drastically reduce the eggs production, the fertilization rate, the embryonic development time, the number of hatchlings and hatchling survival (Juárez et al., 2015, 2016). In embryos, high temperatures increase the metabolic rates affecting the embryo development (smaller embryos) and hatching rate. Embryos have a thermal threshold at 26°C and temperatures around 30°C inhibit growth, reduce the metabolic rate and embryos present a high yolk proportion (Caamal-Monsreal et al., 2016; Sanchez-García et al., 2017). Recently, in males of *O. tankahkeei*, through histological analysis in the testis of octopus exposed to 32°C for 2 h, Long et al. (2015) observed ultrastructural changes and damaged mitochondria in spermatocytes and spermatids.

The testis is the male gonad, responsible for the production of male gametes via spermatogenesis and androgenic hormones (Waiho et al., 2017). The spermatogenesis is a dynamic, synchronized and highly regulated process that involves the division and differentiation of spermatogonial germ cells into mature spermatozoa, which take place in the seminiferous tubules (Shaha et al., 2010; Akmal et al., 2016). The normal process begins with a spermatogenic phase regulated by mitotic divisions, followed by two meiotic divisions to produce secondary spermatocytes and ends with spermiogenesis, a remarkably morphological transformation process. The spermiogenesis involves: (a) nucleus condensation, where DNA is compacted by protamines; (b) formation of acrosome that contains hydrolytic enzymes crucial for oocyte penetration during fertilization; (c) flagellum formation, which involves the development of microtubules arising from the centrioles of the round spermatid; and (d) cytoplasm reorganization, where a large part of the cytoplasm is phagocytosed by the Sertoli cells, that constitutes a hematotesticular barrier (Sheng et al., 2014).

The morphology and ultrastructure of testis and germ cells in *O. maya* and their histological changes during sexual maturation has been described in detail by Avila-Poveda et al. (2009, 2016). In a previous work of our team, the effect of thermal stress over the physiology and the reproductive performance and success of male *O. maya* exposed to preferred (24°C) and stress (28 and 30°C) temperatures was assessed. Our research findings indicated that chronic thermal stress inhibited the growth rate: organisms exposed to 30°C had a specific growth rate six times lower than those exposed to 24°C and gained weight nine times lower. A significant reduction in oxygen consumption was identified with increasing temperatures. High temperatures induced the immune response in *O. maya* males by increasing the circulating hemocytes in the hemolymph. At the reproductive level, a significant increment in the production of spermatophores with increasing temperatures was observed. Although, despite this reproductive strategy, the reproductive success was affected, with no parental contribution from octopus exposed to 30°C. The histological analysis of the testis showed damage from moderate to severe in octopus exposed to 28 and 30°C, seriously affecting the cellular testis organization (López-Galindo et al., 2019).

Nevertheless, the molecular mechanisms that regulate reproduction process in *O. maya* males and the response to environmental factors as temperature are poorly understood. The transcriptome analysis through RNA-Seq methodology could reveal transcripts that are being actively expressed in testis of *O. maya* under chronic thermal stress and facilitate the discovery of novel genes involved in this response and the reproductive processes with high sensitivity and accuracy as has been successfully identified in other invertebrate species as the Pacific oyster *Crassostrea gigas* (Lim et al., 2016; Kim et al., 2017), green lip abalone *Haliotis laevigata* (Shiel et al., 2014), snail *Echinolittorina malaccana* (Wang et al., 2014), king scallop *Pecten maximus* (Artigaud et al., 2015), Chinese mitten crab *Eriocheir sinensis* (Li and Qian, 2017), orange mud crab *Scylla olivacea* (Waiho et al., 2017), and squid *Loligo bleekeri* (Yoshida et al., 2014). To date, in cephalopods transcriptome information related to reproduction is still insufficient. In this regard, this study aims to provide insights into the molecular mechanisms that regulate the reproductive processes such as spermatogenesis and spermiogenesis in testis of *O. maya* under chronic thermal stress. Here, we present a comprehensive analysis of the transcriptome data obtained from testis tissue of *O. maya* males exposed to optimal, intermediate and stressful temperature before and after mating using Illumina Miseq. This is the first report of how octopus male fertility is affected at the molecular level and which mechanisms are triggered to cope with chronic thermal stress. Our results indicated that despite the adaptative mechanisms present in *O. maya* to tolerate temperatures close to 30°C, apparently a prolonged exposure to them causes infertility related to alterations in sperm development and motility.

MATERIALS AND METHODS

Ethics Statement

We established protocols that were approved by the Experimental Animal Ethics Committee of the Faculty of Chemistry at Universidad Nacional Autónoma de México (Permit No. Oficio/FQ/CICUAL/099/15). Octopuses were anesthetized with 3% ethanol to induce narcotization to enable humane killing in consideration of animal's welfare during manipulations (Mather and Anderson, 2007; Estefanell et al., 2011; Andrews et al., 2013; Gleadall, 2013).

Experimental Design and Sampling

Octopus maya males were captured off the coast of Sisal Yucatan, from June to September of 2015, we obtained a total of 63 testis samples. Thirty-six testis were sampled from males before the copula (PRE) that were maintained in 80 L individual tanks and exposed at three experimental temperatures during 30 days ($n = 12$ per treatment): (a) preferred temperature (24°C; 24PRE); (b) intermediate temperature (28°C; 28PRE); and (c) stress temperature (30°C; 30PRE). Meanwhile, twenty-seven testis were sampled from males after the copula (POS), exposed to chronic thermal stress and mated with females maintained at 24°C ($n = 9$ per temperature). Testis samples were removed surgically and immediately preserved in Nap buffer (Camacho-Sanchez et al., 2013), and stored at −80°C until required. Furthers details are shown in López-Galindo et al. (2019).

RNA Isolation, Library Preparation, and Sequencing

Total RNA was obtained from 30 mg of testis tissue homogenized in Fastprep-24 Instrument (MP Biomedicals, Solon, OH, United States) with a speed of 5.0 m/s for 20 s. Then, total RNA was extracted using the RNEasy Plus mini kit (Qiagen, Hilden, Germany) following the manufacturer's protocol. Total RNA samples were then digested with RQ1 RNase-Free DNase (Promega, Madison, WI, United States) to remove potential genomic DNA contamination using the manufacturer's protocol with an additional precipitation and purification steps as follows: each treated sample was precipitated with 1:10 volumes of 3 M sodium acetate and three volumes of absolute Ethanol at −80°C for 1 h; centrifuged at 13,000 rpm for 10 min at 4°C. The RNA pellets were washed with 200 μl of cold 70% Ethanol; centrifuged at 7,500 rpm for 10 min at 4°C and dried at room temperature for 10 min. The RNA pellets were resuspended in RNase free-DNase water. The quality of the RNA was assessed by 1% agarose gel electrophoresis and quantified using a Nanodrop 2000 spectrophotometer (Thermo Scientific, Wilmington, DE, United States). For transcriptomic analysis, only the organisms exposed to 24 and 30°C were sequenced. To construct the libraries, we prepared three different pools with equal amounts of RNA from four individuals per experimental condition (24PRE and 30PRE, 24POST and 30POST).

The quality of the 12 RNA pools (three pools 24PRE, three pools 24POST, three pools 30PRE, and three pools 30POST) were analyzed with an Agilent 2100 Bioanalyzer system (Agilent Technologies, Santa Clara, CA, United States). cDNA libraries were prepared using the TruSeq®RNA Sample Prep kit V2 (Illumina, San Diego, CA, United States) following manufacturer's protocol. Amplified libraries were purified with AMPure XP magnetic beads (Beckman Coulter, Brea, CA, United States). The fragment sizes were verified and quantified with the 2100 Bioanalyzer system. The 12 paired-end libraries were normalized at 4 nM and then pooled equally. They were sequenced using the MiSeq Reagent Kit v3, with a read length of 2 bp × 75 bp on Illumina MiSeq sequencing system (San Diego, CA, United States). PhiX control was used at 1% for cluster generation.

De novo Transcriptome Assembly

The FastQC software was used to assess the quality of the raw reads[1]. Then, Illumina adapters, indexes and low-quality reads were removed with Trimmomatic version 0.36 (Andrews et al., 2013; Bolger et al., 2014). Clean reads with a Phred33 score > 30 and length > 36 bp were used in subsequent analysis. The testis reference transcriptome was assembled *de novo* (including all the libraries) using Trinity version 2.4.0 (Grabherr et al., 2011) with default settings except for the no_bowtie option. The raw reads from each library are available in the Sequence Read Archive database (SRA) with Accession No. SRR7880397 to SRR7880408 and the assembled contigs are available in TSA database with Accession No. GGXQ00000000 in BioProject: PRJNA492175 at the National Center for Biotechnology Information (NCBI, United States[2]).

Functional Annotation

Homology searches were carried out against UniProt release 2018_02 database, and Non-redundant protein (Nr) databases release 2017_09 using Blastx (version NCBI-blast-2.7.1+) software with a cut-off E-value of 1e-05 (Camacho et al., 2009). Gene ontologies were further analyzed using Blast2GO software (version 4.1.9) (Conesa and Götz, 2008) with default parameters to identify the best-represented biological processes detected in the reference transcriptome, based on the number of sequences included in each gene ontology (GO) category. The Kyoto encyclopedia of genes and genomes (KEGG) database was used to identify the transcripts involved in different metabolic pathways (Kanehisa and Goto, 2000).

Differential Expression Analysis

The reads from each library were aligned back to the reference transcriptome with Bowtie2 version 2.3.4.1 (Langmead and Salzberg, 2012). The estimation of transcripts abundance and normalization [fragments per kilobase million (FPKM)] was carried out with RSEM version 1.3.0 (Li and Dewey, 2011). The matrix built with the FPKM of all libraries was analyzed to obtain the differential expressed transcripts (DETs) among treatments with DeSeq2 (False discovery rate, FDR < 0.05, fold change > 2) (Love et al., 2014). TransDecoder v5.5.0 (Haas et al., 2013) was used to predict the longest open reading

[1] http://www.bioinformatics.babraham.ac.uk/projects/fastqc/

[2] http://www.ncbi.nlm.nih.gov/

frame (ORF) for each differentially expressed transcript, using default parameters. Four experimental conditions were defined to understand the relationship between the reproductive condition and the thermal stress. Each treatment was compared (24POST, 30PRE, and 30POST) against the control treatment (24PRE). The DETs were arranged in clusters according to their expression pattern and represented in a heatmap in R software. The complete differential expression analysis was performed using the Perl and R scripts included in the Trinity package[3]. Shared and exclusive transcripts among treatments were analyzed via Venn diagrams using VennDiagram package in R software.

Gene Ontology (GO) Enrichment Analysis

The GO enrichment analysis for each transcript was performed to identify the possible biological processes in which these transcripts participate. An enrichment analysis (Fisher's exact test) was realized in Blast2GO to identify the best-represented categories in the biological process terms (p-value < 0.001).

Quantitative Relative Expression by Real-Time PCR

Thirteen DETs were selected for real-time PCR analysis in a CFX-96 system (Bio-Rad, United States) to validate the transcriptomics results. These transcripts were selected according to two criterions: (a) their significant high expression and (b) their importance in processes involved in the stress response and the reproductive processes.

We used the same RNA samples that were used for sequencing, and additionally, the samples obtained from males exposed to intermediate temperature (28°C), PRE and POST mating conditions were included. cDNA was synthesized using ImProm-II™ Reverse Transcription System (PROMEGA) with 1.0 μg of total purified RNA in a total reaction volume of 20 μL (50 ng/μl) following the manufacturer's protocol. The obtained cDNA′s were stored at −20°C until use for PCR reactions. Gene-specific primers were designed using Primer3web software v.4.1.0 (Koressaar and Remm, 2007; Untergasser et al., 2012) based on RNA-Seq transcripts sequences. The primers sequences for each selected transcript are shown in **Supplementary Table 1**. The efficiency of the target and reference transcripts were calculated from a standard curve with an initial dilution factor of 1:5 and six subsequent serial dilutions with a factor of 1:2 of a cDNA pool including all experimental conditions. In our study, genes commonly used in the literature as housekeepings in other organisms (for example tubulins, elongation factors, actins, Glycerol-3-phosphate dehydrogenase) were significantly differentially expressed among the experimental conditions. For this reason, the housekeeping transcripts used in this study were chosen from the annotated transcript database of the assembled reference transcriptome. The selection was based on the lack of differential expression among treatments (FDR value = 1).

A total of 10 potential reference transcripts were evaluated for expression stability with the Genorm, Normfinder and Bestkeeper software, which results indicated that TUFM and TUBGCP were the most stable transcripts and were used as housekeeping transcripts for the relative expression analysis.

The qPCR reactions were carried out by triplicate with homemade Evagreen Mix 2x (Evagreen 20,000x in water, Biotium and AccuStart Taq DNA polymerase, Quanta, Beverly, MA, United States). The reaction consisted in 5 μL of Evagreen Mix 2x, 0.2 μM of forward and reverse primers, 3 μL of cDNA template (dilution 1:5 or equivalent to 30 ng of total RNA) and 1.6 μL of sterile, free nuclease water, for a final volume of 10 μL. The thermal cycling conditions were 94°C for 3 min, followed by 40 cycles at 94°C 30 s, annealing temperature for 30 s (**Supplementary Table 1**) and 72°C for 30 s. A melt curve analysis was included at the end (95°C for 10 s, 65°C to 95°C for 5 s, with increments of 0.5°C) to corroborate PCR products specificity. The amplicons length were confirmed in agarose gel electrophoresis at 1.5%. Relative expression (RE) of target transcripts was estimated using the ΔΔ Cq method, as proposed by Hellemans et al. (2007). For statistical analysis, all RE values were transformed to logarithm (log10), and a two-way ANOVA model was used to establish the effects of temperature and mating condition, with a statistical significance of $P < 0.05$. A *post hoc* analysis of means was done using Fisher's LSD test. All statistical analyses were performed using STATISTICA 6.1 (StatSoft, Tulsa, OK, United States).

RESULTS

Transcriptome Sequencing, Trimming, and Assembly

The sequencing of all the testis libraries generated 53,214,611 paired-end raw reads with a length of 75 bp. After discarding Illumina adaptors and reads with low quality, a total of 48,101,426 reads with a Phred score over 30, were *de novo* assembled to generate the reference transcriptome using Trinity. **Table 1** summarizes the number of sequenced reads and the trimming statistics per sample.

TABLE 1 | RNA-Seq reads obtained on Illumina MiSeq system.

Sequencing statistics	Number of raw reads before trimming	Number of raw reads after trimming	Raw reads after trimming (%)
24PRE-1	4,261,482	3,715,125	87.18
24PRE-2	3,801,367	3,514,073	92.44
24PRE-3	3,783,317	3,509,953	92.77
24POST-1	4,144,156	3,634,299	87.70
24POST-2	4,529,867	3,997,421	88.25
24POST-3	3,908,012	3,596,089	92.02
30PRE-1	5,792,353	5,164,041	89.15
30PRE-2	4,160,642	3,705,038	89.05
30PRE-3	4,933,884	4,580,123	92.83
30POST-1	4,648,617	4,135,854	88.97
30POST-2	4,822,915	4,452,090	92.31
30POST-3	4,427,999	4,097,320	92.53
Total	53,214,611	48,101,426	90.39

[3]https://github.com/trinityrnaseq/trinityrnaseq/wiki/Post-Transcriptome-Assembly-Downstream-Analyses

The *de novo* assembled testis transcriptome consisted in 53,848,027 bases. The contigs length ranged from 201 nt to 12,758 nt with an average length of 631 nt, N50 = 889 nt (based on all transcript contigs) and GC content of 38%. A total of 85,249 transcripts (including all isoforms) and 77,661 genes were reconstructed (**Table 2**). The *de novo* testis transcriptome of *O. maya* was deposited at the NCBI.

From the reference testis transcriptome, a total of 915 transcripts were exclusively expressed in the control treatment (24PRE), 923 in 24POST, 1,492 in 30PRE and 2,002 in 30POST (**Figure 1A**).

Functional Annotation of *O. maya* Testis Transcriptome

The transcripts were annotated by comparing with Nr, UniProt and KEGG databases. In total, 16,804 (19.7%) and 31,555 (37.0%) transcripts had at least one significant homolog against proteins of the UniProt and Nr databases, respectively (e-value cut-off: 1e-5). Most of the sequences with homology against those databases had an e-value among 1e-05 to 1e-45. The 51% of the homologous sequences obtained from UniProt presented a similarity distribution among 60 to 80%, while the 76% of the homologous found in the Nr had a similarity distribution among 80–100%. **Figures 2A,B** show the e-value and the similarity distribution for the blastx hits against UniProt and Nr databases. From the blast hits obtained with the UniProt database, the higher number of matches corresponded with sequences of *Homo sapiens* (37%) followed by sequences of *Mus musculus* (24%), *Rattus norvegicus* (7%), and *Bos taurus* (7%) (**Figure 2D**). In the case of the hits matched with the Nr database, the highest number of matches corresponded to sequences of *Octopus bimaculoides* (96%) (**Figure 2C**). This high identity percentage suggests that the *O. maya* gene fragments were correctly assembled and annotated.

We applied the Blast2GO algorithm to classify the transcripts in functional categories: biological process, molecular function, and cellular component. The results showed that only 13,154 transcripts (15.4%, UniProt database) and 11,151 (13.1%, Nr database) of 85,249 transcripts had at least one GO term assignation and could be annotated (**Table 2**).

The GO assignments carried out at level three revealed that most of the sequences were categorized in cellular components (10,856; 82.5%), followed by biological processes (10,663; 81.1%) and molecular functions (10,535; 80.1%). The biological processes identified were cellular metabolic process (6,764 transcripts; GO:0044237), response to stress (1,184 transcripts; GO:0006950), cell cycle (1,279 transcripts; GO:0007049), microtubule-based process (530 transcripts; GO:0007017), response to abiotic stimulus (445 transcripts; GO:0009628), cell motility (444 transcripts; GO:0048870), chromosome segregation (174 transcripts; GO:0007059), immune response (316 transcripts; GO:0006955), sperm part (64 transcripts; GO:0097223), and meiotic cell cycle (90 transcripts; GO:0051321). The main cellular components identified were intracellular (9,594 transcripts; GO:0005622), membrane-bounded organelle (6,855 transcripts; GO:0043227), endomembrane system (2,026 transcripts; GO:0012505), and protein complex (1,640 transcripts; GO:0043234). The main molecular functions identified were protein binding (5,139 transcripts; GO:0005515), hydrolase and transferase activity (2,448 and 2,257 transcripts, respectively; GO:0016787 and GO:0016740; **Figure 3**).

A total of 3,317 transcripts (25.2%) matched with homologous proteins in the KEGG database associated with 130 distinct KEGG pathways. Among the top five categories, nucleotide, cofactors, and vitamins metabolism are the largest represented classes, and the top-hits pathways in these categories were purine and thiamine metabolism with 705 transcripts.

TABLE 2 | *De novo* assembly and annotation statistics.

Trinity assembly statistics	All contig transcripts
Total assembled bases	53,848,027
Total number of transcripts	85,249
Total number of genes	77,661
GC content (%)	38
Contig N10	2,949
Contig N20	2,118
Contig N30	1,604
Contig N40	1,204
Contig N50 (based on all transcript contigs)	889
Contig N50 (based on longest contig isoform)	783
Median contig length (nt)	381
Average transcript length (nt)	631
Total transcripts with ORF	14,331
Maximum length (bp)	12,758
Minimum length (bp)	201
Number of transcripts over 1 kb	14,331
Annotation statistics	
Annotated transcripts by UniProt	13,154 (15.4%)
Contigs with cellular component terms	10,856 (82.5%)
Contigs with biological process terms	10,663 (81.1%)
Contigs with molecular function terms	10,535 (80.1%)
Annotated transcripts by Nr	11,151 (13.1%)
Annotated transcripts by KEGG	5,461 (6.4%)

Differentially Expressed Transcripts (DETs)

The heatmap of DETs detected in each library is shown in **Figure 4**. The expression patterns revealed that 24PRE and 24POST had a similar expression pattern, which evidences that copula did not affect gene expression under optimal thermal condition. In 30PRE treatment, it was observed some transcripts (273) with significantly higher expression in comparison to the control treatment (24PRE). At this point, we found that thermal increment modifies the expression patterns in the testis. In the case of 30POST, we observed the major number of transcripts with higher expression in comparison to the control treatment. The 30POST condition showed an expression profile entirely different for the control, where a significant number of transcripts were upregulated meanwhile under normal

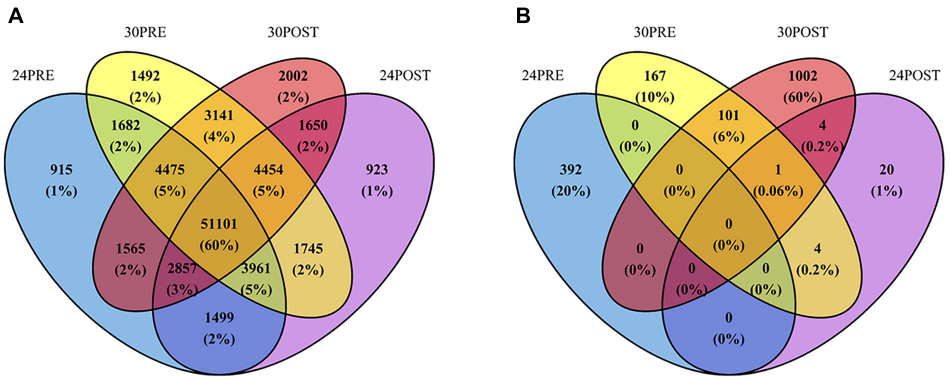

FIGURE 1 | (A) Venn diagram of the number of transcripts expressed in the reference testis transcriptome of *Octopus maya* in each treatment. **(B)** Venn diagram of DETs with significant higher expression in each treatment. Treatments: 24PRE – control treatment exposed to 24°C; 24POST – mated and exposed to 24°C; 30PRE – exposed to 30°C; 30POST – mated and exposed to 30°C.

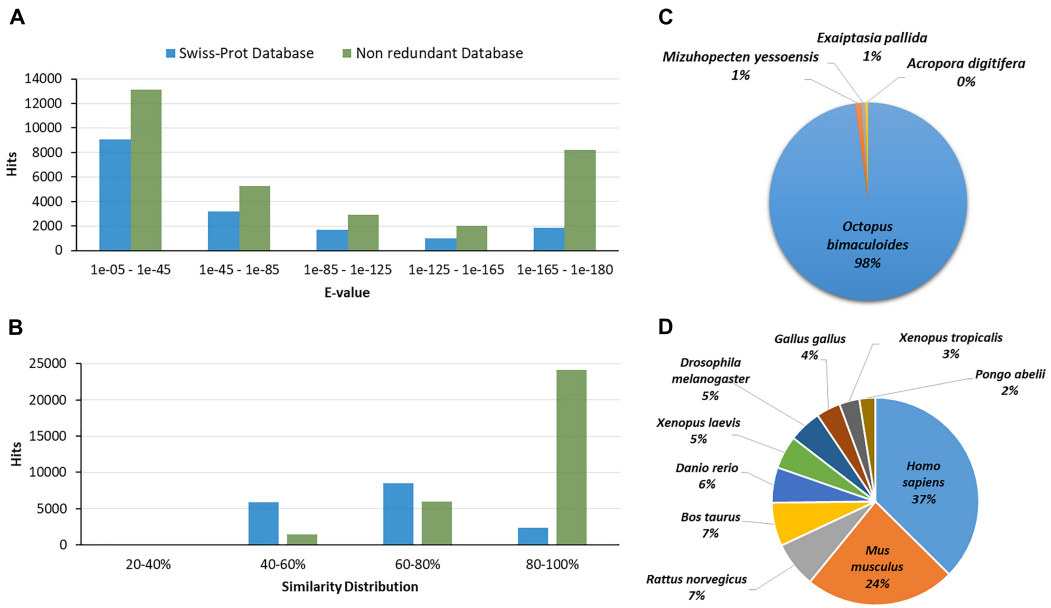

FIGURE 2 | (A) E-value distribution of the Blastx hits against the UniProt and Non-redundant (Nr) database for each transcript. **(B)** Similarity distribution of the Blastx hits against the UniProt and Nr database. **(C)** Species distribution of the top blast hits of the transcripts in the Nr database in the testis transcriptomic analysis of *O. maya* males. **(D)** Species distribution of the top blast hits of the transcripts in the UniProt database in the testis transcriptomic analysis of *O. maya* males.

conditions these same transcripts are downregulated. This pattern evidences that the combined effect of high temperatures and the reproductive activity has a significant effect over the molecular mechanisms that regulate gene expression in the testis of *O. maya* males.

The differential expression analysis showed 1,881 significantly differentially expressed transcripts using 24PRE as the control treatment. A total of 1,410 transcripts (1,114 coding transcripts and 296 non-coding, **Supplementary Table 4**) were significantly more abundant (29 transcripts in 24POST, 167 transcripts in 30PRE and 1,002 transcripts in 30POST; $P < 0.05$, FC > 2) in all treatments vs. the control. **Figure 1B** shows the Venn diagram of the transcripts with significantly higher expression in the treatments that had homologs with the UniProt database. A total of 471 (378 coding transcripts and 93 non-coding, **Supplementary Table 4**) transcripts were significantly more abundant in the control vs. all the treatments (16 transcripts vs. 24POST, 160 transcripts vs. 30PRE and 295 transcripts vs. 30POST; FDR < 0.05, FC > 2). We also found differentially expressed transcripts that did not match the protein databases, a total of 13 in 24POST, 176 in 30PRE and 977 in 30POST. Even, some of these transcripts have higher expression than those putative transcripts with homologs in the peptide databases. The longest ORF region of the DETs validated in qPCR are shown in **Table 3**.

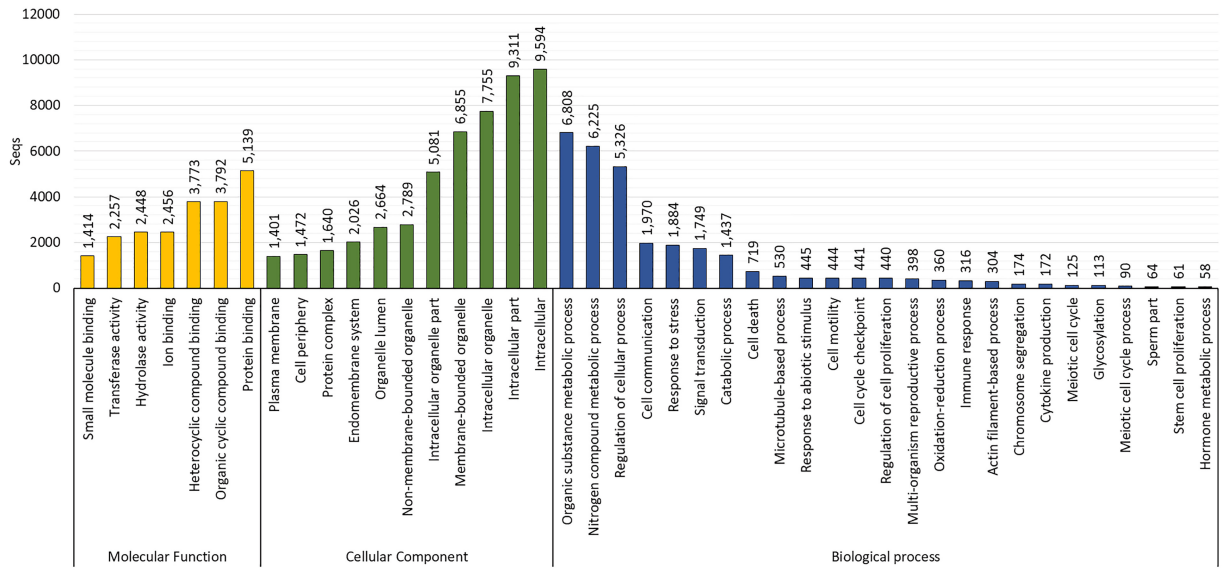

FIGURE 3 | Gene ontology (GO) distribution by category at level 3 in the reference testis transcriptome of *O. maya* males.

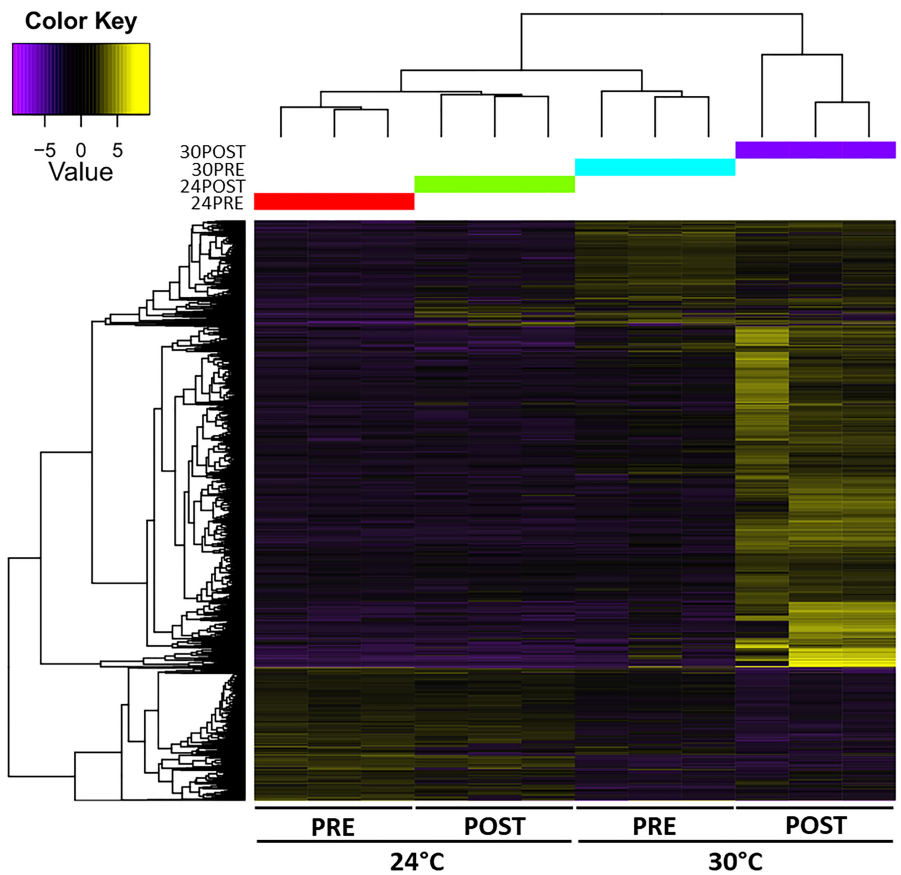

FIGURE 4 | Heatmap of the abundance of differentially expressed transcripts (rows, FDR < 0.05, Fold change > 2) in the *O. maya* testis transcriptome in each treatment (columns). The dendrogram shows that temperature modulated the expression patterns. Treatments: 24PRE – control treatment exposed to 24°C; 24POST – mated and exposed to 24°C; 30PRE – exposed to 30°C; 30POST – mated and exposed to 30°C.

TABLE 3 | Longest ORF regions of the differential expressed transcripts used in qPCR.

Contig ID	Transcript encoding	Start	End
TRINITY_DN7707_c0_g1_i1	CASP7	359	1126
TRINITY_DN16555_c1_g1_i2	CHD5	3	4217
TRINITY_DN3007_c0_g1_i1	DNAJB13	101	1051
TRINITY_DN26602_c0_g1_i1	GPX4	280	1437
TRINITY_DN33756_c0_g1_i1	HSPA9	3	2150
TRINITY_DN2386_c0_g1_i1	HTT	1	3105
TRINITY_DN16585_c0_g1_i1	KLHL10	479	2116
TRINITY_DN13245_c0_g1_i1	MIF	65	409
TRINITY_DN11092_c0_g1_i1	NFKB2	98	2449
TRINITY_DN7210_c0_g1_i1	RABL2A	342	881
TRINITY_DN9963_c0_g1_i1	TDRD1	311	2029
TRINITY_DN17275_c0_g1_i1	TSSK2	849	1205
TRINITY_DN17130_c0_g1_i2	ZMYND15	297	1823
TRINITY_DN35138_c0_g1_i1	TUFM	3	1382
TRINITY_DN14290_c0_g1_i1	TUBGCP	312	2627

GO Enrichment Analysis

Biological processes with significant enrichment ($P < 0.05$) were detected in each thermal and reproductive condition by using the transcripts with higher expression in each treatment. In 24POST, 16 of the 29 upregulated DETs significantly enriched 146 biological process categories (**Figure 5**), while nine of the 16 downregulated DETs significantly enriched a unique biological process category. In 30PRE, 96 of the 273 upregulated DETs significantly enriched 396 biological processes (**Figure 6**), while 76 of the 160 downregulated DETs significantly enriched21 biological processes. In 30POST, 531 of the 1,108 upregulated DETs enriched 390 biological processes significantly (**Figure 7**), while 129 of the 295 downregulated DETs significantly enriched 67 biological process categories. The transcripts that best represented the enriched biological processes involved in stress response and reproductive process are shown in **Supplementary Tables 2, 3**.

Stress Response

Transcripts Involved in Response to Thermal (TS) and Oxidative Stress (OS)

All the differentially expressed transcripts involved in the thermal stress response were highly expressed at 30°C (**Figure 8A**). In the 30PRE condition, the transcript encoding SH3RF1 gene (TS) showed higher expression in comparison to 30POST. The transcripts encoding genes such as CRIP1, ITGA9, SLC8A3, FLNA, DDXN1, and PDCD6 (ST) were conspicuous in 30POST condition. The transcripts encoding ABR, SETMAR, UBC6, BABAM1, and C3 genes (TS) were induced in both conditions.

The transcripts involved in the oxidative stress response as CSK and SOD2 were highly abundant in both treatments (30PRE and 30POST), while the transcripts encoding PKM, STK24, GPX4, and SOD2 genes were highly expressed specifically in 30POST treatment (**Figure 8A**).

Transcripts Involved in Cytokine Production, Inflammatory Process, Apoptosis, and Necroptosis

The transcripts that best-represented these categories were exclusively induced at 30°C and specific changes were observed between PRE and POST condition (**Figure 8A**). The transcripts involved in the cytokine production as PPMB1, CSK, and PGBD3 showed higher expression in both 30PRE and 30POST conditions, meanwhile C3, and BCL only in 30POST condition. The transcripts up-regulated in inflammatory processes as MIF, MAPKAPK2, and CHIA presented higher expression in 30POST and NFKB2 only in 30PRE condition. The transcripts encoding HSPA9, TRAF2 and TNIP2, showed higher expression in 30POST condition, and SH3GLB1 and TFDP1 in 30PRE. The transcript encoding RIPK1 (necroptotic process) presented higher expression in 30PRE condition. The transcripts encoding CASP7 gene was highly abundant in the condition 30POST.

Reproductive Processes

Transcripts Involved in Spermatogenesis, Spermiogenesis, and Gamete Generation Processes

The transcripts that best-represented these biological processes were exclusively induced at 30°C and specific changes were observed between PRE and POST condition (**Figure 8B**). The transcripts involved in the spermatogenesis process as ZAN and TDRD1 showed higher expression at 30°C under PRE and POST conditions meanwhile PSME4 showed higher expression in 24POST and 30PRE treatments. SPATA5 showed unique higher expression in 24°C after copula. The up-regulated transcripts PGM3, HTT, ASPM, CHD5, ITGB1 and MMP19, showed the highest expression in 30POST treatment. The transcripts involved in spermiogenesis as RABL2, KLHL10, and TSSK2 showed higher expression in 30°C PRE and POST conditions meanwhile ZMYND15 showed higher expression in 24POST and 30PRE treatments. The up-regulated DNAJB13 transcript showed the highest expression in 30POST. The KDM1B transcript (gamete

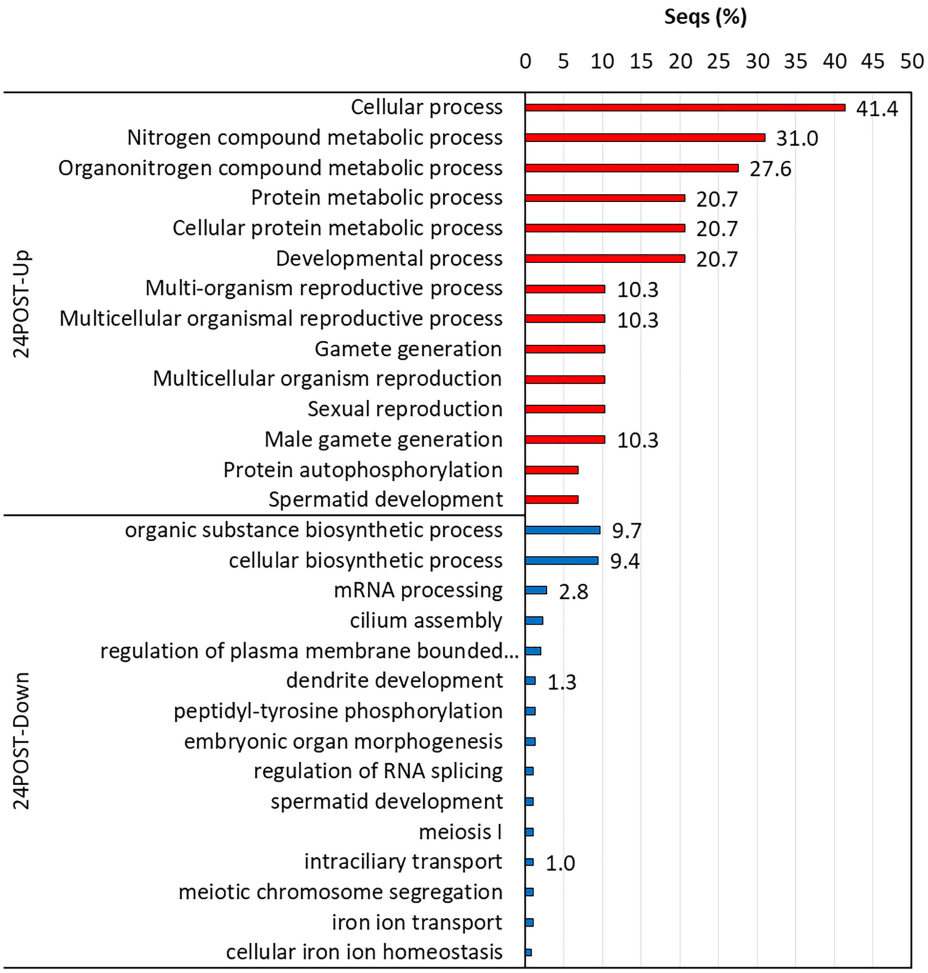

FIGURE 5 | Enriched GO terms of biological processes (Fisher exact test, FDR < 0.05) in 24POST treatment vs. the control treatment (24PRE). Up (red) and down-regulated (blue) transcripts are shown.

generation process) was highly expressed in 30POST treatment.

qPCR Validation

The Pearson correlation coefficient was measured in the RNA-Seq and qPCR data. The correlation coefficient for GPX (r = 0.91), HSPA9 (r = 0.90), CASP7 (r = 0.99), NFKB2 (r = 0.95), and MIF (r = 0.94) revealed that relative expression measured by qPCR is consistent with the RNA-Seq data (**Supplementary Figure 1**). The expression patterns of the up-regulated transcripts involved in the reproductive process were confirmed by qRT-PCR (**Supplementary Figure 2**). The results revealed high correlation values for KLHL10 (r = 0.99), HTT (r = 0.99), TDRD1 (r = 0.80), and RABL2A (r = 0.83).

Different transcripts presented in oxidative stress response (GPX4), inflammatory processes (MIF, NFKB2) apoptosis (CASP7, HSPA9) were selected for relative expression analysis by qPCR to validate the differential expression results described above. Consistent with the RNA-Seq data, transcripts encoding the genes GPX4, CASP7, HSPA9, and MIF showed a higher expression in 30POST condition. Meanwhile, transcript NFKB2 presented the highest expression at 30°C compared to 24°C PRE condition. Additionally, when the intermediate temperature was included in the expression analysis, ANOVA results for stress response-related transcripts (**Figure 9**) indicated that temperature has a significant effect on the expression levels of GPX4 (P = 0.0029), CASP7 (P = 0.0005), HSPA9 (P = 0.0026), and NFKB2 (P = 0.0006). On the other hand, differences between mating condition were detected only for GPX4 (P = 0.0003) and CASP7 (P = 0.0085), with the interaction between temperature and condition being also significant for both transcripts (P < 0.05). This result was mainly caused by the expression in PRE 28°C, which was significantly higher than that at 24 and 30°C in the same reproductive condition. Meanwhile, in POST condition, the expression was significantly higher at 30°C respectively to that observed at 24 and 28°C. No significant differences between mating conditions were observed for HSPA9 (P = 0.96) and NFKB2 (P = 0.99), nor for the interaction between factors (P > 0.05). Finally, the relative expression of MIF did not show significant differences between temperature

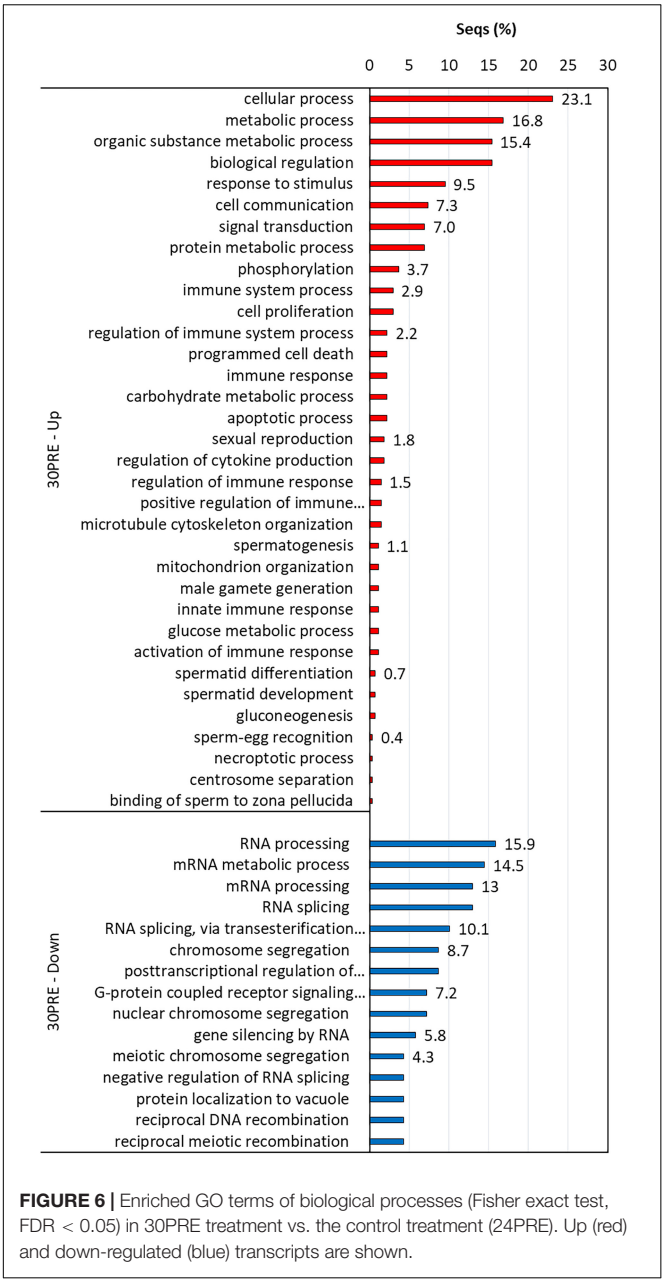

FIGURE 6 | Enriched GO terms of biological processes (Fisher exact test, FDR < 0.05) in 30PRE treatment vs. the control treatment (24PRE). Up (red) and down-regulated (blue) transcripts are shown.

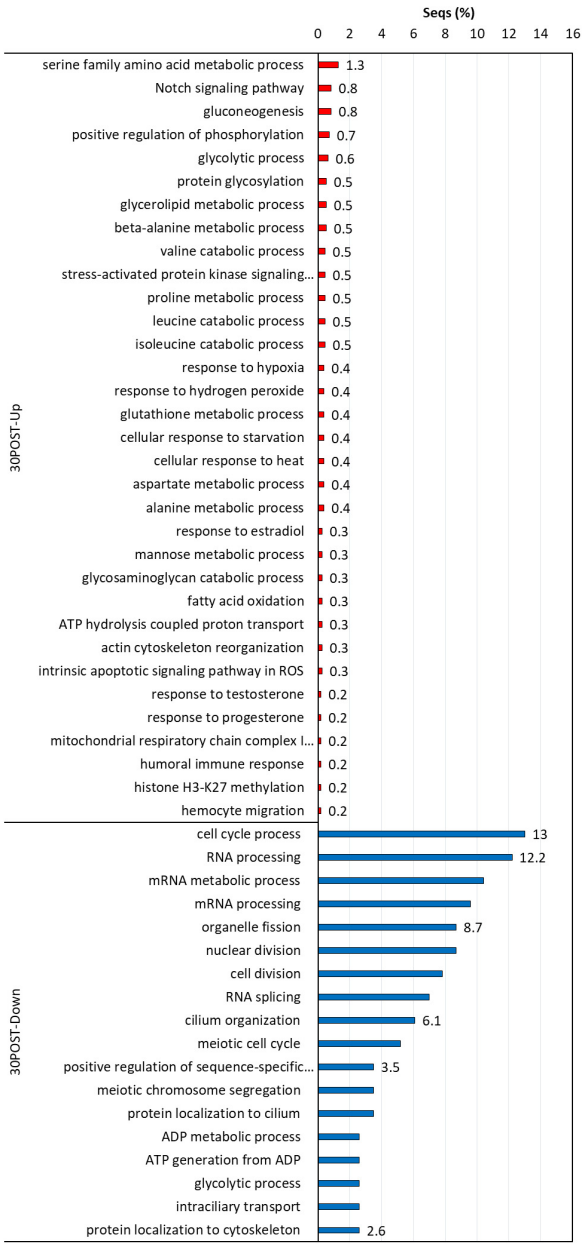

FIGURE 7 | Enriched GO terms of biological processes (Fisher exact test, FDR < 0.05) in 30POST treatment vs. the control treatment (24PRE). Up (red) and down-regulated (blue) transcripts are shown.

($P = 0.067$), condition ($P = 0.44$) or the interaction between them (0.537), although its expression appeared to be increased with temperature in both conditions.

The expression pattern of the eight highly expressed transcripts involved in the reproductive process (KLHL10, TSSK2, DNAJB13, RABL2A, CHD5, ZMYND15, TDRD1, and HTT) were confirmed by qRT-PCR (**Figure 10**). For HTT, the highest expression was observed in 30POST, whereas for TDRD1 and KLHL10 both PRE and POST condition showed the highest expression. In the case of RABL2A, 30PRE condition showed higher expression than 24PRE. All these results were consistent with differential expression analysis of the transcriptome.

In order to determine the role of temperature and mating condition in *O. maya* in the expression pattern of the selected transcripts, the 28°C temperature was included in the analysis. This temperature allowed to find that there was a significant effect of temperature in the expression of KLHL10 ($P < 0.01$), RABL2A ($P = 0.009$), CHD5 ($P = 0.025$), TDRD1 ($P < 0.01$), ZMYND15 ($P = 0.036$), and HTT ($P = 0.002$). However, different patterns were observed regarding the reproductive condition and the interaction between the factors. For KLHL10 and RABL2, no effect of mating condition ($P > 0.05$) or the

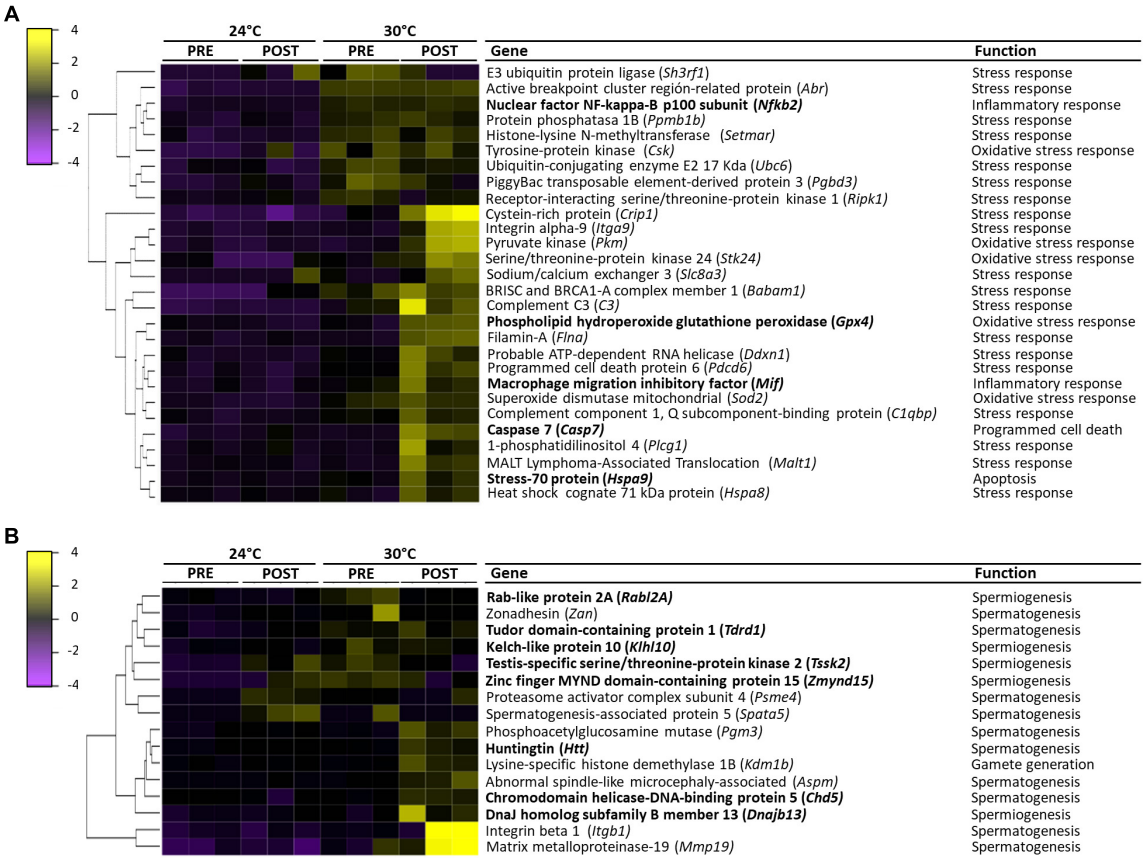

FIGURE 8 | Heatmap representing the expression values of differentially expressed transcripts (FDR < 0.05, Fold change > 2) between 24PRE, 24POST, 30PRE, and 30POST treatments and their main function. **(A)** Transcripts involved in the stress response. **(B)** Transcripts involved in reproductive process. Sample names are represented in columns and significant transcripts are represented in rows. Transcripts are clustered together based on expression similarity. Low to high expression is represented by a change of color from purple to yellow, respectively.

interaction between factors ($P > 0.05$) was observed, indicating that expression between temperatures has similar patterns in PRE and POST mating, being significantly higher in average at 30°C for both transcripts. On the other hand, for CHD5 no significant differences between PRE and POST condition were observed ($P = 0.136$), but the significance of the interaction between temperature and mating conditions ($P = 0.0352$) was caused by the significantly lower expression at 28°C in POST condition. For TDRD1 the expression in PRE condition was significantly higher on average respect to POST ($P = 0.001$), but no significant interaction was observed ($P = 0.944$) indicating that for PRE and POST condition the expression of TDRD1 has a similar pattern between temperatures with the lowest expression observed at 24°C.

DISCUSSION

Octopus maya as an ectotherm organism is strongly influenced by temperature (Regil et al., 2015). Temperature plays an important role in different life aspects as embryo development, growth patterns, morphology, physiology, and reproduction. As an endemic species of the YP, is influenced by the thermal characteristics of the platform, where temperatures can vary since 21 to 30°C along the year (Noyola et al., 2013a,b). In this study, male octopuses were exposed at three temperatures 24°C (Optimal), 28°C (intermediate) and 30°C (Stress) during 30 days, and then, a group of males for each experimental temperature were mated with females acclimated at 24°C. An RNA-Seq analysis of the testis transcriptome at contrasting temperatures (24 and 30°C) was realized to evaluate the transcriptomic responses to chronic thermal stress and the mechanisms involved in the regulation of reproductive processes. In recent years, the high-throughput sequencing techniques have allowed obtaining genetic and genomic information of both model and non-model organisms, the latter in which there are no (or very limited) genomic resources (Ekblom and Galindo, 2011). This technique allows evaluating the expression profiles of a large number of genes, robustly. In our RNA-Seq analysis, we used pooled samples to minimize the effects of biological variation in treatments. We obtained the *de novo* transcriptome of *O. maya* testis constituted by 85,249 transcripts reconstructed. The main species that matched our blast hits against UniProt and Nr Databases were *Homo sapiens* and *O. bimaculoides*, respectively.

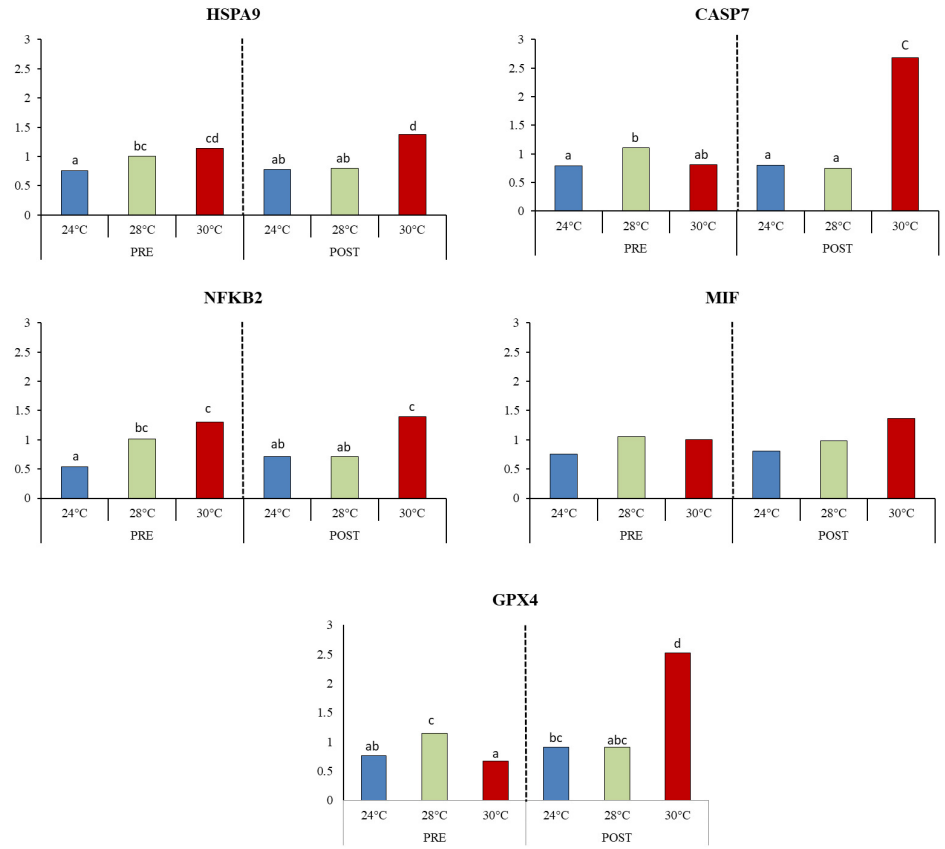

FIGURE 9 | Relative expression of transcripts associated with thermal stress response. Mean values (back-transformed from logarithms) are shown in bars and letters are used to denote differences between means ($P < 0.05$).

This match is completely attributable to the big number of known proteins of model organisms like *Homo sapiens* in the UniProt database and in the case of *O. bimaculoides,* the recent release of its genome (Albertin et al., 2015), and the close phylogenetic relationship between *O. maya* and *O. bimaculoides* (Juárez et al., 2012). The GO functional annotation showed 13,154 (15.4%) and 11,151 (13.1%) transcripts with homologies in the UniProt and Nr databases, with similar proportion to that found in other cephalopods as *Octopus vulgaris* (Zhang et al., 2012; Castellanos-Martínez et al., 2014), *Euprymna tasmanica* (Salazar et al., 2015), and *Sepia officinalis* (Cornet et al., 2014). The fact that the 84.6 and 86.9% (UniProt and Nr databases) of the transcripts did not match any known proteins suggests that there may be a high number of potentially uncharacterized transcripts in *O. maya* that remain to be properly characterized. In this study, 1,166 transcripts without homology were differentially expressed among treatments with high expression values; more studies have to be done to characterize these uncharacterized transcripts. This lack of molecular data emphasizes the importance of cephalopods studies to elucidate the molecular mechanisms involved in their physiology, development, growth, and reproduction.

In general, in the reference testis transcriptome, we identified putative transcripts involved in the biological process as metabolism, stress response, cell cycle, microtubule-based process, sperm part, and chromosome segregation. These results indicated that some important traits inherent to the organisms as metabolic activity, cellular response, and cellular processes occurred in *O. maya* testis during chronic thermal stress and mating activity.

Transcripts Related to Thermal Stress Response in *O. maya* Testis Transcriptome

One of the goals in the present study was to assess the presence of transcripts involved in stress response, apoptosis, and inflammatory processes in the *O. maya* testis transcriptome to confirm that thermal stress affects the molecular mechanisms that regulate the reproductive performance and success of this species. There are different heat stress response mechanisms as DNA reparation, heat shock response, antioxidant defense, cell cycle checkpoints, and apoptosis (Pérez-Crespo et al., 2008). The apoptosis process in the testis is characterized by the apparition of acidophilic bodies. These acidophilic bodies under normal conditions of spermatogenesis, maintain the equilibrium between cellular proliferation and apoptotic degeneration (Lin et al., 1997). Apoptosis process has been well-understood in

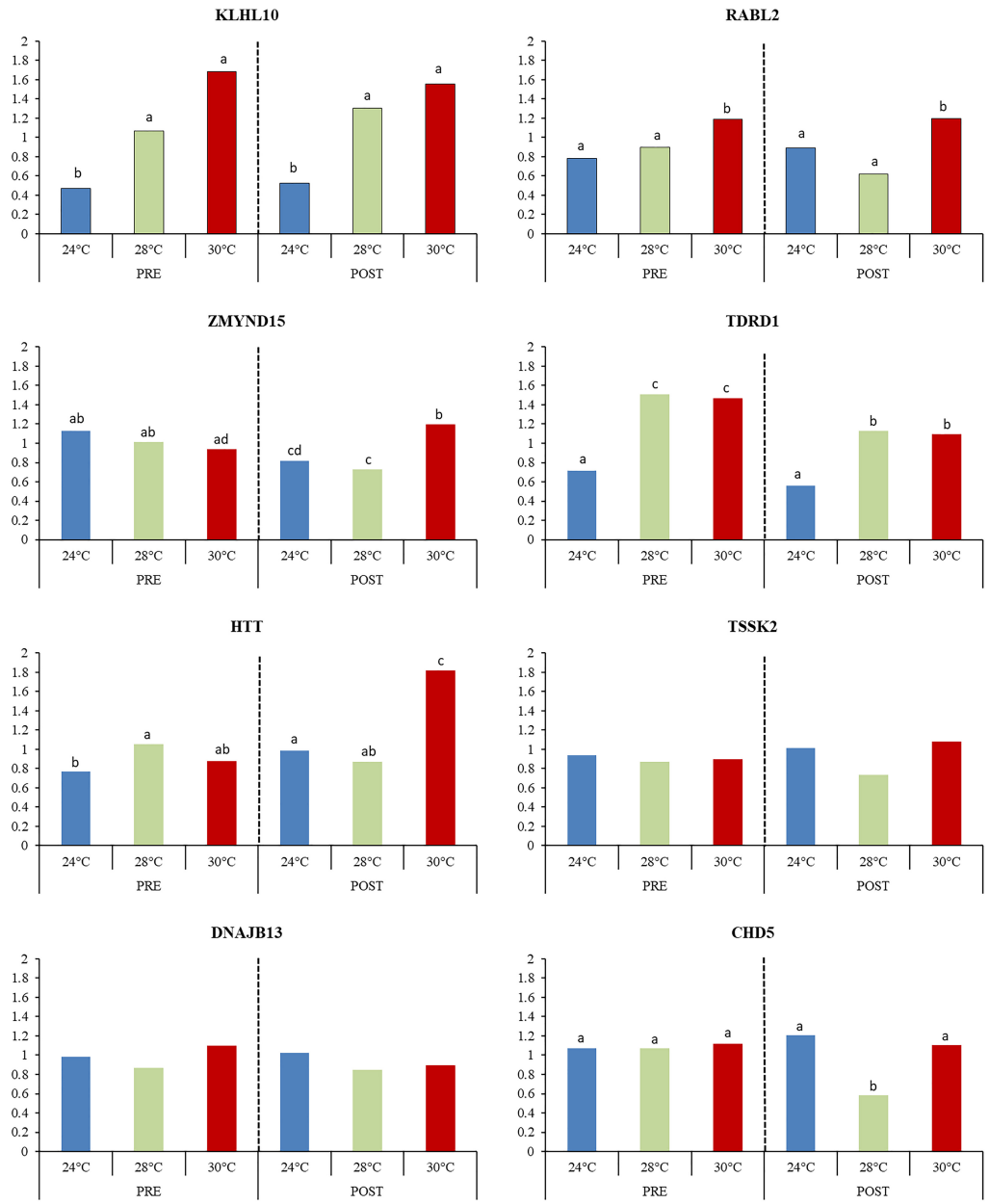

FIGURE 10 | Relative expression of transcripts associated with male reproductive process. Mean values (back-transformed from logarithms) are shown in bars and letters are used to denote differences between means ($P < 0.05$).

humans with infertility issues, where an increment in the process such as maturity arrest and hypospermatogenesis has been observed (William et al., 1997). In this study, we identified necroptotic processes in male octopus exposed to 30°C; this is coincident with the severe testicular damage observed at 30°C, an increment four times higher than that of those exposed to 24°C, and dilation of germ cells strata (López-Galindo et al., 2019). The necrosis is a process of programmed cell death caused by external factors which trigger an immune response characterized by the inflammatory process (Shaha et al., 2010). In this sense, the gene ontology analysis of the *O. maya* testis transcriptome revealed the presence of transcripts involved in regulation of cytokine production (PPMB1, C3, CSK, PGBD3, BCL3) which are cell signaling proteins that regulate the inflammation and infection in the body (Castellanos-Martínez et al., 2014); inflammatory process which is important for a rapid and efficient elimination of damaged tissue (NFKB2, MIF, MAPKAPK2, CHIA2) (Ottaviani et al., 2010); apoptosis which is a process characterized by dying cells, cytoplasmatic shrinkage, active membrane blebbing, chromatin condensation, and typically, fragmentation into membrane-enclosed vesicles or apoptotic bodies (HSPA9, SH3GLB1, TFDP1, TRAF2, TNIP2);

and necroptotic process where necrosis is characterized by cytoplasmic and organelle swelling, and plasma membrane rupture (RIPK1) (Peterson et al., 2015). The necroptosis has been recently investigated. This form of necrosis is dependent of the kinases RIP1 and RIP3, and a pseudokinase MLKL (Peterson et al., 2015). The differential expression of these transcripts can explain the presence of fourfold acidophilic bodies at 30°C, compared to the other treatments, in addition to basophilic material, and vacuolated basal compartments (López-Galindo et al., 2019).

The heat shock proteins (HSP's) are a group of functionally related proteins present in all living organisms. Among other important roles, the HSP's are involved in protein folding and unfolding, and their expression is induced by increasing temperature as well as other stresses (Wang et al., 2014). The upregulation of HSP genes constitutes the core part of the cellular heat shock response (Wang et al., 2014). We identified six members of three HSP families: HSP20 (HSPB6), HSP40 (DNAJB13), and HSP70 family (HSPA9, HSPA12A, HSP70B2, and HSPA8) involved in heat stress response. HSP's as the stress-70 protein, mitochondrial (HSPA9) were highly expressed on conditions of high temperature. The family of the HSP 70 is one of the most highly conserved of the HSP's. They function as molecular chaperones that act as a first defense line and mediate the refold of stress-denatured proteins, prevent the aggregation of denatured proteins and limit the cellular damage (Guzman and Conaco, 2016). HSP's protect the cell from de deleterious effects of heat and module the stress response (Castellanos-Martínez et al., 2014). The analysis of relative expression by qPCR revealed that HSPA9 transcript had a high-level expression in organisms exposed to 28 and 30°C in the PRE condition, while in the POST condition this transcript had a high relative expression at 30°C in comparison to 24 and 28°C. Since this protein plays a role in cell proliferation, stress response and maintenance of the mitochondria, HSPA9 could be playing an important role in the preservation of mitochondria during thermal stress, which is of vital importance.

The caspase-7 (CASP7) is an executioner caspase that degrades cellular components. The caspase proteins constituted the core of apoptotic machinery (Castellanos-Martínez et al., 2014). Caspases have been described in vertebrates. However, there is limited information in invertebrates such as the abalone *Haliotis diversicolor* and the mussel *M. galloprovincialis*, but there are just a few studies in cephalopods such as the common octopus *O. vulgaris* (Romero et al., 2011; Castellanos-Martínez et al., 2014). In our study, CASP7 was induced under both thermal stress and mating, presenting its higher relative expression in 30POST treatment. This expression pattern could indicate that apoptotic mechanisms have been executed in the testis of *O. maya* males under chronic thermal stress and corroborate the findings of severe tisular damage at high temperatures observed by López-Galindo et al. (2019).

The nuclear factor NF-kappa-B p100 subunit (NFKB2) is an inducible transcription factor that plays a central role in the inflammatory response and immune function, which is activated quickly by a wide group of agents and cell stress (Srikanth et al., 2017; Sun, 2017). It seems that NF-Kb is an innate immune system pathway evolutionarily conserved and present in mollusks (Castellanos-Martínez et al., 2014). NFKB2 presented significant higher relative expression under chronic thermal stress at 28 and 30°C (Srikanth et al., 2017; Sun, 2017). This response confirms the inflammatory processes observed in the testis in both temperatures by López-Galindo et al. (2019). In Holstein's calves, NFKB2 has been identified as an important transcription factor that modulates the heat stress response (Srikanth et al., 2017).

The macrophage migration inhibitory factor (MIF) is a multifunctional protein which acts as a pro-inflammatory cytokine, a pituitary hormone, immunoregulator, and mitogen (Anahara et al., 2008). MIF transcript did not show significant differences in relative expression levels between treatments, which could be related to the multifunctional role of this protein (Anahara et al., 2008). However, a positive relationship to temperature was observed.

The Phospholipid hydroperoxide glutathione peroxidase (GPX4) protects cells against membrane lipid peroxidation and cell death (Imai et al., 2009). GPX4 transcript showed a significant relative expression in organisms of 28PRE and its highest expression was observed in organisms of 30POST treatment.

The heat stress is a determinant factor that affects the physiology and reproductive performance of the organisms. Pérez-Crespo et al. (2008) mentioned that heat stress affects the sperm viability, sperm motility, reduced the fertilization capacity and survival, temporarily delays embryonic growth and promotes degeneration, causes abnormalities in the chromatin condensation, damage to DNA, RNA, and protein synthesis and denatures proteins. In this study, it was possible to corroborate that thermal stress induces the expression of transcripts involved in the stress response to compensate the damage caused by chronic thermal stress, however, when the effect of mating is added, this expression is increased. Unfortunately, despite these compensatory mechanisms, testicular damage caused by chronic thermal stress at 30°C is severe and directly affects the reproductive success of *O. maya* males. It is important to realize more studies that allow us to elucidate if severe testicular damage could have a gradual return to normal conditions of spermatogenesis.

Critical DETs Involved in Spermatogenesis and Spermiogenesis Process in *O. maya* Testis Transcriptome

Spermatogenesis is a dynamic and synchronized maturation process from germ cells to mature spermatozoa that take place in the seminiferous tubules in the testis (Shaha et al., 2010). Stringent temporal and spatial expression of genes during both transcriptional and translational processes during protein synthesis is of fundamental importance to ensure the highly ordered processes of spermatogenesis (He et al., 2012). The goal of spermatogenesis is to produce a genetically male gamete that can fertilize an ovum ultimately produce offspring, and this process involves series of intricate, cellular, proliferative, and developmental phases such as mitotic proliferation (proliferation and differentiation of spermatogonia), meiotic

phase (differentiation of spermatocytes), and spermiogenesis (differentiation oh haploid germ cells from round spermatids to elongated spermatids and spermatozoa) (Yan et al., 2010; Dang et al., 2012; He et al., 2012). Protein phosphorylation is the most common post-translational protein modification in eukaryotes that controls the spermatogenesis process (Zhang et al., 2010). A protein kinase family, the testis-specific serine/threonine kinases (TSSK's) may play a role in male spermatogenesis because they are expressed mainly or specifically in the testis. Five members of the TSSK family has been identified in mouse (TSSK1, TSSK2, TSSK3, TSSK3, TSSK4, and TSSK5) (Zhang et al., 2010). Previous research revealed that TSSK2 phosphorylates several flagellar proteins in the central apparatus of the sperm axoneme, such as SPAG16 and testis-specific kinase substrate (Xu et al., 2008; Zhang et al., 2010). The TSSK2 are implied in the formation of microtubule structures during spermatogenesis and is crucial for spermatid production (Zhang et al., 2010). In this study, TSSK2 transcript was identified at 30°C in both PRE and POST conditions. The higher expression was identified in 30PRE condition. Insufficient expression of TSSK2 could interrupt spermiogenesis and results in failure of elongated spermatids, triggering male infertility. This results coincides with the lack of spermatids in the testis of octopus thermally stress and could explain the lack of parental contribution as observed by López-Galindo et al. (2019).

Spermiogenesis involves three subsequent significant events: formation of the acrosome, flagellum formation, and cytoplasm reorganization. Yan et al. (2010) mentioned that meiosis is unique to germ cells, and spermatogenesis is unique to male germ cell development, and this particularity demands unique genes and gene products to execute their functions. The spermatogenesis process implies the use of ∼10% of the entire protein-encoding genes meanwhile spermiogenesis alone involves 500 testis-specific genes (Yan et al., 2010). There are a series of transcription factors that are important to regulate the gene expression. In the present study, we identified the transcriptional repressor ZMYND15 with significant level expression in the 30PRE treatment. ZMYND15 interacts with histone deacetylases and plays an essential role in the regulation of spatial-temporal expression of many haploid genes.

Moreover, is specifically expressed in spermatids during spermiogenesis process and is essential for normal spatiotemporal haploid gene expression. Male infertility and azoospermia have been linked to the inactivation of this gene in mice (Yan et al., 2010). In our study, ZMYND15 transcript presents low levels of relative expression in 30POST in comparison to the control. The expression pattern of this gene in invertebrates, mollusks or even cephalopods has not been described. This is the first report about the existence of this gene in cephalopods and its potential role in *O. maya* male infertility.

Another haploid gene required for male fertility during spermiogenesis is KLHL10. This gene is involved in protein ubiquitination. In mice is critical for the maturation process of spermatozoa, and is one of the essential proteins for post-meiotic spermatozoa (Yatsenko et al., 2010). KLHL10 is a member of a large BTB (Brica-brac, Tramtrack, and Broad-Complex)-kelch protein superfamily, characterized by an amino-terminal BTB/POZ domain and kelch repeats at the carboxyl terminus. This protein is specifically expressed in the testis and has similar expression pattern than CUL3. Wang et al. (2006) suggested that KLHL10 interacts with CUL3 to form a CUL3-based ubiquitin E3 ligase that functions specifically in the testis to mediate protein ubiquitination during spermiogenesis. This is the first time that KLHL10 is identified in mollusks and specifically cephalopods as *O. maya*. The RNA-Seq and qPCR analysis showed that KLHL10 presented the higher expression at 30°C in both PRE and POST condition. An increase in the expression values was observed directly proportional to the temperature. As was observed in human and mice, we can hypothesize that the increment in the expression of this transcript at 30°C affected the male fertility in *O. maya*. Disrupted spermatogenesis, degeneration of late spermatids and reduction in late spermatid number which was reported by López-Galindo et al. (2019) where they observed disruption in the germ cell strata of the seminiferous tubules and did not find a parental contribution from thermally-stressed fathers.

During the spermiogenesis process, haploid germ cells are transformed into highly polarized cells with the potential for motility and fertilization (Lo et al., 2012). The sperm tail, like motile cilia and flagella of other species, contains an axoneme at its core composed of a 9+2 microtubule arrangement. The axoneme develops from a single centriole at the base of the sperm head and functions to metabolize ATP and generate microtubule sliding and motility (Maxwell, 1974; Lo et al., 2012). Defects in sperm axoneme function result in asthenospermia (Abnormal sperm motility) (Lo et al., 2012). Lo et al. (2012) identified the RABL2 gene as critically involved in sperm tail function and male fertility in mice. In this study, RABL2 transcript, agree to RNA-Seq and qPCR analysis showed the highest expression in the 30PRE treatment. An expression increment from 24 to 30°C was observed. We hypothesize that the overexpression of this transcript starts with the response at 28°C, intending to repair the damage caused to the sperm tail. However, we can attribute that the reduced parental contribution and its lack at 30°C are directly related to the injury in sperm motility of *O. maya* males (López-Galindo et al., 2019).

Another gene involved in the sperm tail function is DNAJB13, which is a type II HSP40/DnaJ protein (Li and Liu, 2014). This gene is also known as testis spermatogenesis apoptosis-related protein expressed abundantly in mouse testis (Li and Liu, 2014). DNAJB13 was characterized in mature mouse testis and epididymal spermatozoa by Guan et al. (2010). Li and Liu (2014) confirmed the expression of DNAJB13 in the cytoplasm of spermatids and the flagella of mature spermatozoa, indicating its function in sperm motility. In our study, DNAJB13 transcript was also highly expressed at 30°C post copula.

According to the transcripts identified in response to thermal stress and spermatogenesis and spermiogenesis, it can be corroborated that the temperature significantly affects these processes carried out in the *O. maya* testis. These transcripts presented a high expression perhaps with the objective of compensating the damage caused by the rise in temperature. However, at the tissue level, these mechanisms are insufficient

triggering inflammatory processes and tissue necrosis in the testis of thermally-stressed octopuses.

The increase in the expression of transcripts involved in spermatogenesis processes may explain the increase in the number of spermatophores observed in octopuses exposed to 28 and 30°C (López-Galindo et al., 2019). This expression patterns could demonstrate an effort at the reproductive level to compensate for the deleterious damage attributed to temperature.

The transcripts TSSK2, KLHL10, ZMYND15, RABL2A, and DNAJB13 indicated that there is a harmful effect on the production of viable sperm cells, the structural conformation of sperm, training, and motility. This was reinforced by histological analyzes, which show the moderate to severe damage to the testis and the lost of different cell types (spermatogonia, spermatocytes, spermatids, and mature spermatozoa) in *O. maya* males exposed to temperatures above 28°C. Chronic thermal stress generated infertility in *O. maya* which was corroborated through analysis of parental assignment, where no parental contribution of thermally-stressed parents was found.

CONCLUSION

Under optimal temperature conditions, mating at the physiological, reproductive, and transcriptomic level does not represent a stressor for *O. maya* males. Under mating conditions, there is a significant expression of transcripts involved in the fundamental processes carried out in the testis such as spermatogenesis, gamete generation, and spermiogenesis. Under thermal stress, at the three levels mentioned above, there are severe alterations. The histology of the testis shows that temperature causes severe damage in the testis, affecting the morphology of the different cell types and the seminiferous tubules. These effects coupled with the transcriptomic analysis showed that there is a range of transcripts that are significantly expressed in response to thermal stress (response to stimuli, immune system, programmed cell death, apoptosis, regulation of cytokine production, necroptotic processes). At the reproductive level transcripts involved in spermatogenesis and spermiogenesis are significantly upregulated. When evaluating the combined effect of temperature and reproduction, at the transcriptomic level, there is a significant upregulation concerning optimal conditions. This pattern of expression reveals that under this condition, mating implies a stressor for the individual. In addition to the spermatogenesis processes in this condition, a large number of transcripts involved in energy production processes (catabolic and metabolic processes of amino acids, gluconeogenesis, glycolytic processes, fatty acid oxidation) were observed. This could indicate that in the testis of *O. maya* males a high amount of energy is produced for three essential aspects: to compensate the severe damage generated to the testis, to provide energy to be able to carry out the mating and try to produce more sperm. However, this strategy seems to be insufficient, since males of this species cannot produce offspring in spite of carrying out mating.

In the other hand, as observed in *O. maya* females and embryos, the problems presented a thermal threshold at 28°C, from which the physiological process, the reproductive performance and success, and the molecular mechanisms involved in the stress response and reproductive traits are severely affected. This study provides relevant information on the adaptive mechanisms presented in *O. maya* males against the effects of temperature. This is of vital importance, due to the predictions about the rise of sea temperatures between 2.5 and 3°C in the western zone of the Yucatan Peninsula causing a significant reduction of the population in this area, and/or migration to the eastern zone of the peninsula.

AUTHOR CONTRIBUTIONS

LL-G and CG-S conceived the project. LL-G performed the experiments and sample collection. LL-G and EL-S contributed to sample processing. LL-G and OJ conducted the bioinformatics analysis. LL-G, GDV, and CV-L conducted the qPCR validation and data analysis. CG-S, OJ, EL-S, and AL-L revised the manuscript.

FUNDING

This work was supported by the projects SEP-CONACYT-CB-2014-01/241690 and CICESE: 682123.

ACKNOWLEDGMENTS

We thank Dr. Carlos Rosas and Claudia Caamal for the experimental facilities in the Multidisciplinary Teaching and Research Unit at UNAM in Sisal, Yucatan. We also thank to Dr. Edna Sánchez Castrejón for the given facilities in the Laboratory of Functional Genomics in CICESE.

SUPPLEMENTARY MATERIAL

The Supplementary Material for this article can be found online at: https://www.frontiersin.org/articles/10.3389/fphys.2018.01920/full#supplementary-material

REFERENCES

Akmal, M., Aulanni'am, A., Widodo, M. A., Sumitro, S. B., and Purnomo, B. B. (2016). The important role of protamine in spermatogenesis and quality of sperm: a mini review. *Asian Pac. J. Reprod.* 5, 357–360. doi: 10.1016/j.apjr.2016.07.013

Albertin, C. B., Simakov, O., Mitros, T., Wang, Z. Y., Pungor, J. R., Edsinger-Gonzales, E., et al. (2015). The octopus genome and the evolution of cephalopod neural and morphological novelties. *Nature* 524, 220–224. doi: 10.1038/nature14668

Anahara, R., Toyama, Y., and Mori, C. (2008). Review of the histological effects of the anti-androgen, flutamide, on mouse

testis. *Reprod. Toxicol.* 25, 139–143. doi: 10.1016/j.reprotox.2007.12.003

Andrews, P. L. R., Darmaillacq, A. S., Dennison, N., Gleadall, I. G., Hawkins, P., Messenger, J. B., et al. (2013). The identification and management of pain, suffering and distress in cephalopods, including anaesthesia, analgesia and humane killing. *J. Exp. Mar. Bio. Ecol.* 447, 460–464. doi: 10.1016/j.jembe.2013.02.010

Artigaud, S., Richard, J., Thorne, M. A. S., Lavaud, R., Flye-Sainte-Marie, J., Jean, F., et al. (2015). Deciphering the molecular adaptation of the king scallop (*Pecten maximus*) to heat stress using transcriptomics and proteomics. *BMC Genomics* 16:988. doi: 10.1186/s12864-015-2132-x

Avila-Poveda, O. H., Colin-Flores, R. F., and Rosas, C. (2009). Gonad development during the early life of *Octopus maya* (mollusca: cephalopoda). *Biol. Bull.* 216, 94–102. doi: 10.1086/BBLv216n1p94

Avila-Poveda, O. H., Koueta, N., Benítez-Villalobos, F., Santos-Valencia, J., and Rosas, C. (2016). Reproductive traits of *Octopus maya* (Cephalopoda: Octopoda) with implications for fisheries management. *Molluscan Res.* 36, 29–44. doi: 10.1080/13235818.2015.1072912

Avila-Poveda, O. H., Montes-Pérez, R. C., Koueta, N., Benítez-Villalobos, F., Ramírez-Pérez, J. S., Jimenez-Gutierrez, L. R., et al. (2015). Seasonal changes of progesterone and testosterone concentrations throughout gonad maturation stages of the Mexican octopus, *Octopus maya* (Octopodidae: Octopus). *Molluscan Res.* 35, 161–172. doi: 10.1080/13235818.2015.1045055

Bolger, A. M., Lohse, M., and Usadel, B. (2014). Trimmomatic: a flexible trimmer for Illumina sequence data. *Bioinformatics* 30, 2114–2120. doi: 10.1093/bioinformatics/btu170

Caamal-Monsreal, C., Uriarte, I., Farias, A., Díaz, F., Sánchez, A., Re, D., et al. (2016). Effects of temperature on embryo development and metabolism of *O. maya*. *Aquaculture* 451, 156–162. doi: 10.1016/j.aquaculture.2015.09.011

Camacho, C., Coulouris, G., Avagyan, V., Ma, N., Papadopoulos, J., Bealer, K., et al. (2009). BLAST+: architecture and applications. *BMC Bioinformatics* 10:421. doi: 10.1186/1471-2105-10-421

Camacho-Sanchez, M., Burraco, P., Gomez-Mestre, I., and Leonard, J. A. (2013). Preservation of RNA and DNA from mammal samples under field conditions. *Mol. Ecol. Resour.* 13, 663–673. doi: 10.1111/1755-0998.12108

Castellanos-Martínez, S., Arteta, D., Catarino, S., and Gestal, C. (2014). De novo transcriptome sequencing of the *Octopus vulgaris* hemocytes using illumina RNA-Seq technology: response to the infection by the gastrointestinal parasite *Aggregata octopiana*. *PLoS One* 9:e107873. doi: 10.1371/journal.pone.0107873

Conesa, A., and Götz, S. (2008). Blast2GO: a comprehensive suite for functional analysis in plant genomics. *Int. J. Plant Genomics* 2008:619832. doi: 10.1155/2008/619832

Cornet, V., Henry, J., Corre, E., Le Corguille, G., Zanuttini, B., and Zatylny-Gaudin, C. (2014). Dual role of the cuttlefish salivary proteome in defense and predation. *J. Proteomics* 108, 209–222. doi: 10.1016/j.jprot.2014.05.019

Dang, R., Zhu, J. Q., Tan, F. Q., Wang, W., Zhou, H., and Yang, W. X. (2012). Molecular characterization of a KIF3B-like kinesin gene in the testis of *Octopus tankahkeei* (cephalopoda, octopus). *Mol. Biol. Rep.* 39, 5589–5598. doi: 10.1007/s11033-011-1363-4

Ekblom, R., and Galindo, J. (2011). Applications of next generation sequencing in molecular ecology of non-model organisms. *Heredity* 107, 1–15. doi: 10.1038/hdy.2010.152

Estefanell, J., Socorro, J., Afonso, J. M., Roo, J., Fernandez-Palacios, H., and Izquierdo, M. S. (2011). Evaluation of two anaesthetic agents and the passive integrated transponder tagging system in *Octopus vulgaris* (Cuvier 1797). *Aquac. Res.* 42, 399–406. doi: 10.1111/j.1365-2109.2010.02634.x

Gamboa-Álvarez, M. Á, López-Rocha, J. A., and Poot-López, G. R. (2015). Spatial analysis of the abundance and catchability of the red octopus *Octopus maya* (Voss and Solís-Ramírez, 1966) on the continental shelf of the Yucatan Peninsula, Mexico. *J. Shellfish Res.* 34, 481–492. doi: 10.2983/035.034.0232

Gleadall, I. G. (2013). The effects of prospective anaesthetic substances on cephalopods: summary of original data and a brief review of studies over the last two decades. *J. Exp. Mar. Biol. Ecol.* 447, 23–30. doi: 10.1016/j.jembe.2013.02.008

Grabherr, M. G., Haas, B. J., Yassour, M., Levin, J. Z., Thompson, D. A., Amit, I., et al. (2011). Full-length transcriptome assembly from RNA-Seq data without a reference genome. *Nat. Biotechnol.* 29, 644–652. doi: 10.1038/nbt.1883

Guan, J., Ekwurtzel, E., Kvist, U., Hultenby, K., and Yuan, L. (2010). DNAJB13 is a radial spoke protein of mouse "9+2" axoneme. *Reprod. Domest. Anim.* 45, 992–996. doi: 10.1111/j.1439-0531.2009.01473.x

Guzman, C., and Conaco, C. (2016). Gene expression dynamics accompanying the sponge thermal stress response. *PLoS One* 11:e0165368. doi: 10.1371/journal.pone.0165368

Haas, B. J., Papanicolaou, A., Yassour, M., Grabherr, M., Blood, P. D., Bowden, J., et al. (2013). De novo transcript sequence reconstruction from RNA-seq using the Trinity platform for reference generation and analysis. *Nat. Protoc.* 8, 1494–1506. doi: 10.1038/nprot.2013.084

He, L., Wang, Q., Jin, X., Wang, Y., Chen, L., Liu, L., et al. (2012). Transcriptome profiling of testis during sexual maturation stages in *Eriocheir sinensis* using Illumina sequencing. *PLoS One* 7:e33735. doi: 10.1371/journal.pone.0033735

Hellemans, J., Mortier, G., De Paepe, A., Speleman, F., and Vandesompele, J. (2007). qBase relative quantification framework and software for management and automated analysis of real-time quantitative PCR data. *Genome Biol.* 8:R19. doi: 10.1186/gb-2007-8-2-r19

Imai, H., Hakkaku, N., Iwamoto, R., Suzuki, J., Suzuki, T., Tajima, Y., et al. (2009). Depletion of selenoprotein GPx4 in spermatocytes causes male infertility in mice. *J. Biol. Chem.* 284, 32522–32532. doi: 10.1074/jbc.M109.016139

Juárez, O. E., Galindo-Sánchez, C. E., Díaz, F., Re, D., Sánchez-García, A. M., Camaal-Monsreal, C., et al. (2015). Is temperature conditioning *Octopus maya* fitness? *J. Exp. Mar. Bio. Ecol.* 467, 71–76. doi: 10.1016/j.jembe.2015.02.020

Juárez, O. E., Hau, V., Caamal-Monsreal, C., Galindo-Sánchez, C. E., Díaz, F., Re, D., et al. (2016). Effect of maternal temperature stress before spawning over the energetic balance of *Octopus maya* juveniles exposed to a gradual temperature change. *J. Exp. Mar. Biol. Ecol.* 474, 39–45. doi: 10.1016/j.jembe.2015.10.002

Juárez, O. E., Rosas, C., and Arena-Ortiz, M. L. (2012). Phylogenetic relationships of *Octopus maya* revealed by mtDNA sequences relaciones. *Ciencias Mar.* 38, 563–575. doi: 10.7773/cm.v38i3.1962

Kanehisa, M., and Goto, S. (2000). KEGG: kyoto encyclopedia of genes and genomes. *Nucleic Acids Res.* 28, 27–30. doi: 10.1093/nar/27.1.29

Kim, B. M., Kim, K., Choi, I. Y., and Rhee, J. S. (2017). Transcriptome response of the Pacific oyster, *Crassostrea gigas* susceptible to thermal stress: a comparison with the response of tolerant oyster. *Mol. Cell. Toxicol.* 13, 105–113. doi: 10.1007/s13273-017-0011-z

Koressaar, T., and Remm, M. (2007). Enhancements and modifications of primer design program Primer3. *Bioinformatics* 23, 1289–1291. doi: 10.1093/bioinformatics/btm091

Langmead, B., and Salzberg, S. L. (2012). Fast gapped-read alignment with Bowtie 2. *Nat. Methods* 9, 357–359. doi: 10.1038/nmeth.1923

Li, B., and Dewey, C. N. (2011). RSEM: accurate transcript quantification from RNA-Seq data with or without a reference genome. *BMC Bioinformatics* 12:323. doi: 10.1186/1471-2105-12-323

Li, G. L., and Qian, H. (2017). Transcriptome using illumina sequencing reveals the traits of spermatogenesis and developing testes in *Eriocheir sinensis*. *PLoS One* 12:e0172478. doi: 10.1371/journal.pone.0172478

Li, W., and Liu, G. (2014). DNAJB13, a type II HSP40 family member, localizes to the spermatids and spermatozoa during mouse spermatogenesis. *BMC Dev. Biol.* 14:38. doi: 10.1186/s12861-014-0038-5

Lim, H. J., Kim, B. M., Hwang, I. J., Lee, J. S., Choi, I. Y., Kim, Y. J., et al. (2016). Thermal stress induces a distinct transcriptome profile in the Pacific oyster *Crassostrea gigas*. *Comp. Biochem. Physiol. Part D Genomics Proteomics* 19, 62–70. doi: 10.1016/j.cbd.2016.06.006

Lin, W. W., Lamb, D. J., Wheeler, T. M., Lipshultz, L. I., and Kim, E. D. (1997). In situ end-labeling of human testicular tissue demonstrates increased apoptosis in conditions of abnormal spermatogenesis. *Fertil. Steril.* 68, 1065–1069. doi: 10.1016/S0015-0282(97)00372-5

Lo, J. C. Y., Jamsai, D., O'Connor, A. E., Borg, C., Clark, B. J., Whisstock, J. C., et al. (2012). RAB-Like 2 has an essential role in male fertility, sperm intra-flagellar transport, and tail assembly. *PLoS Genet.* 8:e1002969. doi: 10.1371/journal.pgen.1002969

Long, L. L., Han, Y. L., Sheng, Z., Du, C., Wang, Y. F., and Zhu, J. Q. (2015). Expression analysis of HSP70 in the testis of *Octopus tankahkeei* under thermal stress. *Comp. Biochem. Physiol. Part A Mol. Integr. Physiol.* 187, 150–159. doi: 10.1016/j.cbpa.2015.05.022

López-Galindo, L., Galindo-Sánchez, C., Olivares, A., Avila-Poveda, O. H., Díaz, F., Juárez, O. E., et al. (2019). Reproductive performance of *Octopus maya* males conditioned by thermal stress. *Ecol. Indic.* 96, 437–447. doi: 10.1016/j.ecolind.2018.09.036

Love, M. I., Huber, W., and Anders, S. (2014). Moderated estimation of fold change and dispersion for RNA-Seq data with DESeq2. *Genome Biol.* 15, 1–21. doi: 10.1186/s13059-014-0550-8

Mather, J. A., and Anderson, R. C. (2007). Ethics and invertebrates: a cephalopod perspective. *Dis. Aquat. Organ.* 75, 119–129. doi: 10.3354/dao075119

Maxwell, W. L. (1974). Spermiogenesis of *Eledone cirrhosa* Lamarck (Cephalopoda, Octopoda). *Proc. R. Soc. London Biol. Sci.* 186, 181–190. doi: 10.1098/rspb.1974.0045

Noyola, J., Caamal-Monsreal, C., Díaz, F., Re, D., Sánchez, A., and Rosas, C. (2013a). Thermopreference, tolerance and metabolic rate of early stages juvenile *Octopus maya* acclimated to different temperatures. *J. Therm. Biol.* 38, 14–19. doi: 10.1016/j.jtherbio.2012.09.001

Noyola, J., Mascaró, M., Caamal-Monsreal, C., Noreña-Barroso, E., Díaz, F., Re, D., et al. (2013b). Effect of temperature on energetic balance and fatty acid composition of early juveniles of *Octopus maya*. *J. Exp. Mar. Bio. Ecol.* 445, 156–165. doi: 10.1016/j.jembe.2013.04.008

Ottaviani, E., Franchini, A., and Malagoli, D. (2010). Inflammatory response in molluscs: cross-taxa and evolutionary considerations. *Curr. Pharm. Des.* 16, 4160–4165. doi: 10.2174/138161210794519084

Pérez-Crespo, M., Pintado, B., and Gutiérrez-Adán, A. (2008). Scrotal heat stress effects on sperm viability, sperm DNA integrity, and the offspring sex ratio in mice. *Mol. Reprod. Dev.* 75, 40–47. doi: 10.1002/mrd

Peterson, J. S., Timmons, A. K., Mondragon, A. A., and McCall, K. (2015). *The End of the Beginning: Cell Death in the Germline*, 1st Edn. New York, NY: Elsevier Inc.

Regil, N. J., Mascaro, M., Díaz, F., Denisse Re, A., Sánchez-Zamora, A., Caamal-Monsreal, C., et al. (2015). Thermal biology of prey (*Melongena corona bispinosa*, *Strombus pugilis*, *Callinectes similis*, *Libinia dubia*) and predators (*Ocyurus chrysurus*, *Centropomus undecimalis*) of *Octopus maya* from the Yucatan Peninsula. *J. Therm. Biol.* 53, 151–161. doi: 10.1016/j.jtherbio.2015.11.001

Romero, A., Estévez-Calvar, N., Dios, S., Figueras, A., and Novoa, B. (2011). New insights into the apoptotic process in mollusks: characterization of caspase genes in *Mytilus galloprovincialis*. *PLoS One* 6:e17003. doi: 10.1371/journal.pone.0017003

Salazar, K. A., Joffe, N. R., Dinguirard, N., Houde, P., and Castillo, M. G. (2015). Transcriptome analysis of the white body of the squid *Euprymna tasmanica* with emphasis on immune and hematopoietic gene discovery. *PLoS One* 10:e0119949. doi: 10.1371/journal.pone.0119949

Sanchez-García, A., Rodríguez-Fuentes, G., Díaz, F., Galindo-Sánchez, C. E., Ortega, K., Mascaró, M., et al. (2017). Thermal sensitivity of *O. maya* embryos as a tool for monitoring the effects of environmental warming in the Southern of Gulf of Mexico. *Ecol. Indic.* 72, 574–585. doi: 10.1016/j.ecolind.2016.08.043

Shaha, C., Tripathi, R., and Prasad Mishra, D. (2010). Male germ cell apoptosis: regulation and biology. *Philos. Trans. R. Soc. B Biol. Sci.* 365, 1501–1515. doi: 10.1098/rstb.2009.0124

Sheng, K., Liang, X., Huang, S., and Xu, W. (2014). The role of histone ubiquitination during spermatogenesis. *Biomed. Res. Int.* 2014:870695. doi: 10.1155/2014/870695

Shiel, B. P., Hall, N. E., Cooke, I. R., Robinson, N. A., and Strugnell, J. M. (2014). De novo characterisation of the greenlip abalone transcriptome (*Haliotis laevigata*) with a focus on the heat shock protein 70 (HSP70) family. *Mar. Biotechnol.* 17, 23–32. doi: 10.1007/s10126-014-9591-y

Srikanth, K., Lee, E., Kwan, A., Lim, Y., Lee, J., Jang, G., et al. (2017). Transcriptome analysis and identification of significantly differentially expressed genes in Holstein calves subjected to severe thermal stress. *Int. J. Biometeorol.* 61, 1993–2008. doi: 10.1007/s00484-017-1392-3

Sun, S. C. (2017). The non-canonical NF-κB pathway in immunity and inflammation. *Nat. Rev. Immunol.* 17, 545–558. doi: 10.1038/nri.2017.52

Untergasser, A., Cutcutache, I., Koressaar, T., Ye, J., Faircloth, B. C., Remm, M., et al. (2012). Primer3-new capabilities and interfaces. *Nucleic Acids Res.* 40, 1–12. doi: 10.1093/nar/gks596

Waiho, K., Fazhan, H., Shahreza, M. S., Moh, J. H. Z., Noorbaiduri, S., Wong, L. L., et al. (2017). Transcriptome analysis and differential gene expression on the testis of orange mud crab, *Scylla olivacea*, during sexual maturation. *PLoS One* 12:e0171095. doi: 10.1371/journal.pone.0171095

Wang, S., Zheng, H., Esaki, Y., Kelly, F., and Yan, W. (2006). Cullin3 is a KLHL10-interacting protein preferentially expressed during late spermiogenesis. *Biol. Reprod.* 74, 102–108. doi: 10.1095/biolreprod.105.045484

Wang, W., Hui, J. H. L., Chan, T. F., and Chu, K. H. (2014). De novo transcriptome sequencing of the snail *Echinolittorina malaccana*: identification of genes responsive to thermal stress and development of genetic markers for population studies. *Mar. Biotechnol.* 16, 547–559. doi: 10.1007/s10126-014-9573-0

Xu, B., Hao, Z., Jha, K. N., Zhang, Z., Urekar, C., Digilio, L., et al. (2008). Targeted deletion of Tssk1 and 2 causes male infertility due to haploinsufficiency. *Dev. Biol.* 319, 211–222. doi: 10.1016/j.ydbio.2008.03.047

Yan, W., Si, Y., Slaymaker, S., Li, J., Zheng, H., Young, D. L., et al. (2010). Zmynd15 encodes a histone deacetylase-dependent transcriptional repressor essential for spermiogenesis and male fertility. *J. Biol. Chem.* 285, 31418–31426. doi: 10.1074/jbc.M110.116418

Yatsenko, A. N., Iwamori, N., Iwamori, T., and Matzuk, M. M. (2010). The power of mouse genetics to study spermatogenesis. *J. Androl.* 31, 34–44. doi: 10.2164/jandrol.109.008227

Yoshida, M. A., Yamada, L., Ochi, H., Iwata, Y., Tamura-Nakano, M., Sawada, H., et al. (2014). Integrative omics analysis reveals differentially distributed proteins in dimorphic euspermatozoa of the squid, *Loligo bleekeri*. *Biochem. Biophys. Res. Commun.* 450, 1218–1224. doi: 10.1016/j.bbrc.2014.04.076

Zhang, H., Su, D., Yang, Y., Zhang, W., Liu, Y., Bai, G., et al. (2010). Some single-nucleotide polymorphisms of the TSSK2 gene may be associated with human spermatogenesis impairment. *J. Androl.* 31, 388–392. doi: 10.2164/jandrol.109.008466

Zhang, X., Mao, Y., Huang, Z., Qu, M., Chen, J., Ding, S., et al. (2012). Transcriptome analysis of the *Octopus vulgaris* central nervous system. *PLoS One* 7:e40320. doi: 10.1371/journal.pone.0040320

Conflict of Interest Statement: The authors declare that the research was conducted in the absence of any commercial or financial relationships that could be construed as a potential conflict of interest.

frontiers in Physiology

ORIGINAL RESEARCH
published: 05 March 2019
doi: 10.3389/fphys.2018.01709

Hypoxically Induced Nitric Oxide: Potential Role as a Vasodilator in *Mytilus edulis* Gills

Paula Mariela González[1,2], *Iara Rocchetta*[3], *Doris Abele*[4]* and *Georgina A. Rivera-Ingraham*[4,5]

[1] Facultad de Farmacia y Bioquímica, Universidad de Buenos Aires, Fisicoquímica, Buenos Aires, Argentina, [2] Instituto de Bioquímica y Medicina Molecular (IBIMOL), CONICET-Universidad de Buenos Aires, Buenos Aires, Argentina, [3] Laboratorio de Ecotoxicología Acuática, INIBIOMA, CONICET-COMAHUE, Neuquén, Argentina, [4] Department of Biosciences, Alfred Wegener Institute Helmholtz Centre for Polar and Marine Research, Bremerhaven, Germany, [5] Laboratoire Environnement de Petit Saut, Hydreco-Guyane, Kourou, French Guiana

OPEN ACCESS

Edited by:
Carlos Rosas,
National Autonomous University of Mexico, Mexico

Reviewed by:
Mikko Juhani Nikinmaa,
University of Turku, Finland
Tania Zenteno-Savin,
Centro de Investigación Biológica del Noreste (CIBNOR), Mexico

***Correspondence:**
Doris Abele
doris.abele@awi.de

Specialty section:
This article was submitted to Aquatic Physiology, a section of the journal Frontiers in Physiology

Received: 24 September 2018
Accepted: 14 November 2018
Published: 05 March 2019

Citation:
González PM, Rocchetta I, Abele D and Rivera-Ingraham GA (2019) Hypoxically Induced Nitric Oxide: Potential Role as a Vasodilator in Mytilus edulis Gills. Front. Physiol. 9:1709. doi: 10.3389/fphys.2018.01709

Intertidal *Mytilus edulis* experience rapid transgression to hypoxia when they close their valves during low tide. This induces a physiological stress response aiming to stabilize tissue perfusion against declining oxygen partial pressure in shell water. We hypothesized that nitric oxide (NO) accumulation supports blood vessel opening in hypoxia and used live imaging techniques to measure NO and superoxide anion ($O_2^{\bullet-}$) formation in hypoxia-exposed gill filaments. Thirty minutes of moderate (7 kPa pO_2) and severe hypoxia (1 kPa pO_2) caused 1.6- and 2.4-fold increase, respectively, of NO accumulation in the endothelial muscle cells of the hemolymphatic vessels of the gill filaments. This led to a dilatation of blood vessel diameter by 43% (7 kPa) and 56% (1 kPa), which facilitates blood flow. Experiments in which we applied the chemical NO-donor Spermine NONOate (concentrations ranging from 1 to 6 mM) under normoxic conditions corroborate the dilatational effect of NO on the blood vessel. The formation of $O_2^{\bullet-}$ within the filament epithelial cells increased 1.5 (7 kPa) and 2-fold (1 kPa) upon treatment. Biochemical analysis of mitochondrial electron transport complexes in hypoxia-exposed gill tissue indicates decreased activity of complexes I and III in both hypoxic conditions; whereas complex IV (cytochrome-c oxidase) activity increased at 7 kPa and decreased at 1 kPa compared to normoxic exposure conditions. This corresponds to the pattern of pO_2-dependent gill respiration rates recorded in *ex-vivo* experiments. Severe hypoxia (1 kPa) appears to have a stabilizing effect on NO accumulation in gill cells, since less O_2 is available for NO oxidation to nitrite/nitrate. Hypoxia thus supports the NO dependent inhibition of complex IV activity, a mechanism that could fine tune mitochondrial respiration to the local O_2 availability in a tissue. Our study highlights a basal function of NO in improving perfusion of hypoxic invertebrate tissues, which could be a key mechanism of tolerance toward environmental O_2 variations.

Keywords: blood vessel opening, blue mussels, hypoxia, mitochondria, nitric oxide

INTRODUCTION

Mytilus edulis, the blue mussel, is a bank forming species that colonizes intertidal and subtidal habitats. It belongs to the group of outstandingly hypoxia and anoxia tolerant marine invertebrates, endowed with specialized "anaerobic mitochondria" that can alternate between the use of oxygen (O_2) and of endogenous fumarate as electron acceptor for anaerobic ATP production (Tielens et al., 2002). The extent of hypoxia and of anoxia tolerance, however, varies with individual environmental adaptation. In intertidal environments blue mussels experience a reduction of shell water O_2 partial pressure (pO_2) to hypoxic or even anoxic levels during low tides caused by intermittent valve closure that prevents desiccation (Bayne et al., 1976; for review see Abele et al., 2017). Transplant experiments with subtidal and intertidal mussels between both habitats demonstrated hypoxic tolerance to be higher in intertidal than subtidal mussels, but also to be enhanced within weeks after transplantation and adaptation to the intertidal (Altieri, 2006). Hence hypoxia tolerance in blue mussels has an acquired and adaptive component modulating the evolutionary trait. Depending on length and intensity, anoxic exposure can cause cellular stress, including oxidative stress when cells are re-oxidized during valve opening (Rivera-Ingraham et al., 2013b).

Gills are the main organs of respiration in bivalves and, contrary to other diffusive surfaces such as mantle, can functionally stabilize the rates of whole animal respiration against fluctuant environmental O_2 concentrations. Enhanced ciliary (ventilation) and heart beat rates (perfusion) (Bayne, 1971), combined with a widening of the inter-lamellar blood vessel, caused by contraction of the muscles in the inter-lamellar connections (Aiello and Guideri, 1965, named "intracellular junctions" in **Figure 1**), are central mechanisms by which *Mytilus* can stabilize respiration rates against declining O_2 availability. Using freshly excised gills, we demonstrated a distinct pattern of increasing respiration rate below ∼9.5 kPa (critical pO_2 1) (pc1) in support of faster ciliary beating at lower pO_2, before onset of oxyconformity at ∼6.5 kPa (pc2) (i.e., 35–40% of the normoxic level, Rivera-Ingraham et al., 2013b). It is an open question how this complex response pattern of O_2 turnover in mussel gill mitochondria is regulated. Cytochrome c oxidase (CytOx) is generally accepted to be the rate limiting factor of mitochondrial O_2 turnover, but its affinity for O_2 would need to change dramatically in the O_2 range above 7 kPa to achieve the activity pattern observed in our previous study. Alternatively, another O_2 related molecule could be functioning as a mediator between pO_2 levels and CytOx - O_2 affinity.

Nitric oxide (NO) is a reactive nitrogen species (RNS) that plays an important role as cellular mediator, specifically with respect to its interaction with O_2 at the CytOx reactive center (Taylor and Moncada, 2010). Intracellular formation of NO is almost exclusively catalyzed by NO synthases, a group of heme-based monooxygenases present in different tissues of marine and freshwater molluscs, including the central nervous system (Moroz et al., 1996), molluscan hemocytes cells (Conte and Ottaviani, 1995; Tafalla et al., 2003; Palumbo, 2005); and bivalve digestive glands (González et al., 2008; González and Puntarulo, 2011). More recent investigations into microbial biofilms on internal surfaces, external structures (shells), and in gut contents of marine and freshwater molluscs highlight nitrification/ denitrification processes of associated facultative anaerobic bacteria to be another potential source of NO and nitrous oxide (N_2O) in marine invertebrates (Heisterkamp et al., 2010; Svenningsen et al., 2012; Stief, 2013). Especially under near anaerobic conditions N_2O and NO form as products of nitrite (NO_2^-) reduction, similar to denitrification processes in anoxic sediment layers (Anderson and Levine, 1986; Stief, 2013). Whether NO produced by microbial denitrification in molluscan shell water, or the NO produced inside the cells by NO synthase activity can have an effect on gills or hemocyte cells and respiratory activities, is so far unexplored.

At least for mammalian cells the interactions between NO and respiration rates are sufficiently clear. Mammalian CytOx has a higher affinity for NO than for O_2 and catalyzes its oxidation to NO_2^- at normoxic cellular pO_2 (note that "normoxic cellular pO_2" is much lower than 21 kPa aerial partial pressure in bivalve tissues, and even lower in mammalian cells). At high pO_2, this oxidation occurs in a manner that is non-competitive to O_2, which means that NO oxidation and respiration, two O_2 consuming processes, proceed simultaneously. As O_2 diminishes in hypoxia, the CytOx reactive center becomes reduced, which causes NO binding at the catalytic site for the O_2 reduction (the heme a_3 in its ferrous state). This abrogates NO oxidation to NO_2^- and stabilizes intracellular NO levels, which will further reduce and eventually fully inhibit CytOx catalytic activity (for a detailed description of the biochemical mechanism underlying the interaction between NO and CytOx see Taylor and Moncada (2010) and references cited therein. Thus, NO can have a mediator function in mammalian cells, diminishing CytOx catalytic activity in an O_2 dependent manner at the onset of hypoxia. The physiological effect of the curtailed O_2 consumption is a better diffusive distribution of O_2 across hypoxia sensitive mammalian tissues, in which the peripheral cells would have better access than the cells in central tissue regions (Poderoso et al., 1996).

Bivalves have open circulatory systems and O_2 distribution occurs over the hemolymph that, in most bivalves including Mytilides, is void of O_2 binding respiratory proteins. Big hemolymphatic vessels run through the gill branches and filaments and also connect the heart with the major tissues, foot, mantle/gonads, and digestive tract for O_2 supply. Heart beat is controlled by the inspired pO_2 (and not the pCO_2) detected by peripheral O_2 sensors within the inhalant siphon (Abele et al., 2017).

A suitable model to mechanistically study O_2 transport and the biochemical and functional responses of cells and their mitochondria to diminishing O_2 levels *in vitro* is the intact gill, immediately after its removal from the living mussel. In our previous papers we used live imaging techniques in combination with fluorescent dyes to measure the response of the gills to O_2 deprivation and reoxygenation in terms of reactive species formation and oxidative damage accumulation (Rivera-Ingraham et al., 2013b). We also investigated the

compartmentalization of the different reactive O_2 species (ROS) to better understand their diverse functions in the gills. It resulted that DAF-2DA fluorescence (NO) and dichlorofluorescein diacetate (DCF) staining (ROS and RNS) are compartmentalized in the endothelial muscle cells around the hemolymphatic sinus of the filaments, and additionally stain hemocyte cells within the vessel lumen (especially DCFH, see Rivera-Ingraham et al., 2016). Contrary the $O_2^{\bullet-}$ sensitive dye dihydroethidium (DHE) stained the palisade cells of the gills and here the outer ciliated and mitochondria rich areas fluoresced most strongly. Especially the distinctive staining of the longitudinal endothelial muscle cells around the blood vessel by the NO sensitive fluorophore DAF-2D suggested that NO could be a messenger molecule involved in the hypoxic adjustment of the hemolymphatic vessel lumen to regulate blood pressure under hypoxic conditions. Hence in the present paper we investigated the hypoxic NO accumulation in endothelial muscle cells and, in parallel, determined blood vessel diameter in the filaments.

To better understand potential effects of NO accumulation on cellular and mitochondrial processes in the gills, we compared the effects of natural and hypoxic NO accumulation to experimental addition of the NO donor (SpermineNONOate, SpNONOate) on gill respiration, mitochondrial membrane potential and ROS formation. Inhibitory effects of hypoxia and of externally added NO on mitochondrial respiratory chain components (electron transport system, ETS, complexes I and III and CytOx) were tested directly *in vitro* using gill homogenates. The overall aim of our study was to understand whether NO accumulation in hypoxic gills can lead to modifications of mitochondrial respiratory complex activities and gill perfusion (vessel diameter) in a hypoxia tolerant and partially oxyconforming marine bivalve.

MATERIALS AND METHODS

Animal Collection and Maintenance

M. edulis were collected at the Island of Sylt in the North Sea, Germany (55° 01′ 323 N and 008° 26′ 430 E) during autumn 2016 after the reproductive season (spring and summer). With a mean shell length of 39.5 ± 0.3 mm all mussels were beyond the period of strongest growth for North Sea populations, and were considered to represent young adults (Sukhotin et al., 2006). No distinctions were made regarding gender. The animals were transferred to the laboratory (Alfred-Wegener-Institute Helmholtz-Zentrum für Polar- und Meeresforschung, AWI), cleaned from epibiontic growth, and kept completely submerged in two aquaria with fully aerated (>99 % air saturation) natural seawater of 32.3 ‰ at 10°C. Mussels were allowed to acclimate to the aquarium conditions for 3 weeks prior to the experiments and were fed live phytoplankton using PhytoMaxx Live Plankton Concentrate (NYOS Aquatics GmbH, Korntal-Muenchingen, Germany) (500 x 10^6 cell·mL^{-1}) once a week. During feeding water circulation in the aquaria was stopped for 4 h. Mussels were fasted for 48 h before experimentation to avoid possible interference of nutrition-induced increase in metabolic rates. Water quality was monitored weekly for ammonium and nitrate levels using Nanocolor® Tube Tests (Macherey-Nagel GmbH & Co. KG, Düren, Germany). Water in the aquaria was changed when ammonium values exceeded 0.4 mg·L^{-1} or when nitrate values exceeded 0.2 mg·L^{-1}.

Experimentation With Live Tissues

Respiration rates and live imaging of physiological parameters were carried out *ex-vivo*, using freshly excised mussel gill pieces or isolated filaments. Mussels for these experiments were obtained directly from the acclimation aquaria and sacrificed on ice. The entire gill was removed and kept in 15 mM Na-HEPES and 0.5 mM glucose (NH-FSW) for experimentation.

Experimental exposure *ex-vivo* included different pO_2 levels: normoxia (21 kPa pO_2), moderate (7 kPa pO_2, coinciding with the critical pO_2 for *M. edulis* excised gills (Rivera-Ingraham et al., 2013b), and severe hypoxia of 1 kPa pO_2 to mimic conditions in shell water of naturally hypoxia-exposed or shell-closed mussels. To test for the effect of NO on the same functions, freshly excised gill tissue was exposed to different concentrations of the NO donor SpNONOate (Sigma S-150) under normoxic conditions in an open chamber (i.e., pO_2 conditions were maintained constant between 18 and 20 kPa throughout these experiments) used for the live imaging experiments. Measurements of respiration rates were conducted in a closed system (see section Respirometry of excised gill pieces exposed to Spermine NONOate) in which the gill pieces were maintained with SpNONOate while pO_2 decreased in the chamber, so that the results could be evaluated for different ranges of mild and severe hypoxic exposure.

SpNONOate was chosen as NO donor because of its long half-life of 230 min between 22° and 25°C (Sinha, 2011). Previous measurements in our laboratory demonstrated a slight pO_2 dependence of NO formation/accumulation by SpNONOate in that a 6 mM SpNONOate generated approximately 50 nM · min^{-1} at 16 kPa (Julia Strahl, pers. comm).

Respirometry of Excised Gill Pieces Exposed to Spermine NONOate

The wells of a 96-well Nunclon plastic microtiter plate (NunclonTM Nalge Nunc, Denmark) served as respiration chambers. Wells with a volume of 0.33 mL and a diameter of 8 mm were equipped with O_2 sensor spots. A 4-channel fiber-optical O_2 meter (Oxy-4) and noninvasive O_2 sensors (SP-PSt3-NAU-D5-YOP, Precision Sensing GmBH, Regensburg, Germany) were used after daily calibration following the manufacturer's description. Spots were glued to the bottom of the wells using silicon paste. Animals were dissected, and freshly excised gills were divided into two approximately equal sections. Since the amount of tissue in a respiration chamber can have an effect on the O_2 consumption measurements (Van Winkle, 1968), approximately the same amount of tissue (10–15 mg fresh weight, FW) was used for each animal. Following the measurement, the exact FW of each gill piece was determined after blotting it dry on tissue paper. Two gill pieces per animal were placed individually in respiration wells: one containing sterile NH-FSW, and the other one containing NH-FSW supplemented with either 1, 3, or 6 mM SpNONOate. Wells were filled completely with normoxic medium and sealed (to avoid the formation of air bubbles) as

described in Rivera-Ingraham et al. (2013b). All measurements started in fully oxygenated medium and respiration was recorded as function of declining pO_2 over time. Measurements were conducted at room temperature (20°C). Data were recorded at 5 s intervals until complete anoxia was reached in a well-chamber, or until gills stopped breathing. Measuring time was always less than 5 h.

Respiration data over the whole range of pO_2 from normoxia to anoxia were divided into three pO_2 range sections: (i) normoxia from 21-15 kPa, (ii) range around the critical pO_2 previously determined for the same *M. edulis* population (Acevedo et al., 1993; Rivera-Ingraham et al., 2013b): 8.5–5 kPa and including our experimental treatment of moderate hypoxia, and (iii) severe hypoxia 4-0 kPa representative of the experimental treatment at 1 kPa. Data for each pO_2 interval were fitted by linear regression and the corresponding slope was used to calculate gill respiration rate as nmol $O_2 \cdot min^{-1} \cdot mg^{-1}$ FW. For each individual, gill respiration rate was calculated for treatments with and without the presence of SpNONOate in the respiration medium and for the respective pO_2 ranges. Results are given as respiration rates for each range and the percentage of inhibition by SpNONOate for each individual.

Fluorometric Analyses of Nitric Oxide and Superoxide Anion Formation, and Mitochondrial Membrane Potential

Live imaging of NO and $O_2^{\bullet -}$ formation, as well as the changes of the mitochondrial membrane potential ($\Delta\psi_m$) in live gill filaments under different treatment conditions was conducted using a Leica TCS SP5II confocal microscope (Leica Microsystems CMS GmbH, Wetzlar, Germany) equipped with a multiphoton laser (MaiTai-DeepSee, Spectra-Physics, Newport Corp.). A 40X optical objective was used with a resolution of 500 × 500 pixels. Quantification of fluorescence intensity was done with Leica LAS AF-TCS-SPS Lite software (Leica Microsystems CMS GmbH 2011, Version 2.6.0).

Freshly excised demibranch pieces of mussel gills were loaded with the corresponding fluorophore at room temperature (20°C) under normoxic (loading) conditions and for the time indicated in **Table 1**. Loading and measuring medium was in all cases NH-FSW. Chemical reaction mechanisms, concentrations of fluorophores, incubation times, as well as the conditions of visualization are summarized in **Table 1**.

After loading of the fluorophore, gill filaments were placed and fixed in the confocal chamber containing 2 mL of NH-FSH with a pO_2 at normoxic conditions. The confocal chamber (Bachofer, with a diameter of 5 cm) was perfused with NH-FSW medium at 1.77 mL · min^{-1} for 30 min of experimental treatment (see **Figure 1** for experimental setup). The pO_2 in the incubation medium was controlled in the reservoir. Room temperature was maintained between 18 and 20°C throughout the measurement.

For each gill sample, an area comprising one or two filaments (area of analysis, AA) was chosen far from the dissection border and showing no sign of manipulation damage of the gill structures. Only this area was analyzed throughout the experiment (lasting 30 min). All image adjustments, including fluorescence gain and selection of the AA were accomplished within a maximum of 3 min of pre-incubation in the chamber before starting the measurement (normoxic conditions, serving as control and expressed as 0 min in figures). The system was then either maintained under normoxic conditions, changed to moderate (7 kPa pO_2), or severe hypoxia (1 kPa pO_2), or treated with either 3 or 6 mM SpNONOate at normoxic conditions. For the hypoxically incubated gill, the medium in the flow-through system was replaced by hypoxic medium immediately after the initial confocal measurement under control conditions.

TABLE 1 | Analysis conditions for each of the dyes used during the study.

Dye	Mechanism of function	N per treatment	Final Concentration (μM)	Incubation time (min)	Excitation		Emission		Calculation
					λ_1 (nm)	λ_2 (nm)	PMT1 (nm)	PMT2 (nm)	
DAF-2DA (in DMSO)	DAF-2 is formed by intracellular hydrolyzation of its ester bonds by esterases. It remains essentially non-fluorescent until it reacts with nitrosonium cation (forming the fluorescent DAF-2T) and such fluorescence increases in a NO-dependent manner.	7	20	30	488	–	505–525	–	Average intensity
MitoSOX (in DMSO)	Dye targeting mitochondria where it is readily oxidized by $O_2^{\bullet -}$ the oxidized product becomes fluorescent upon binding to nucleic acids.	8	5	30	514	–	560–600	–	Average intensity
JC-10 (in DMSO)	Green fluorescent probe which exists as a monomer at low $\Delta\psi$m. With high $\Delta\psi$m values JC-10 aggregates shows a red fluorescence.	6	10	30	488	488	500–550	560–600	Ratio PMT1/PMT2

PMT, Photomultiplier tube.

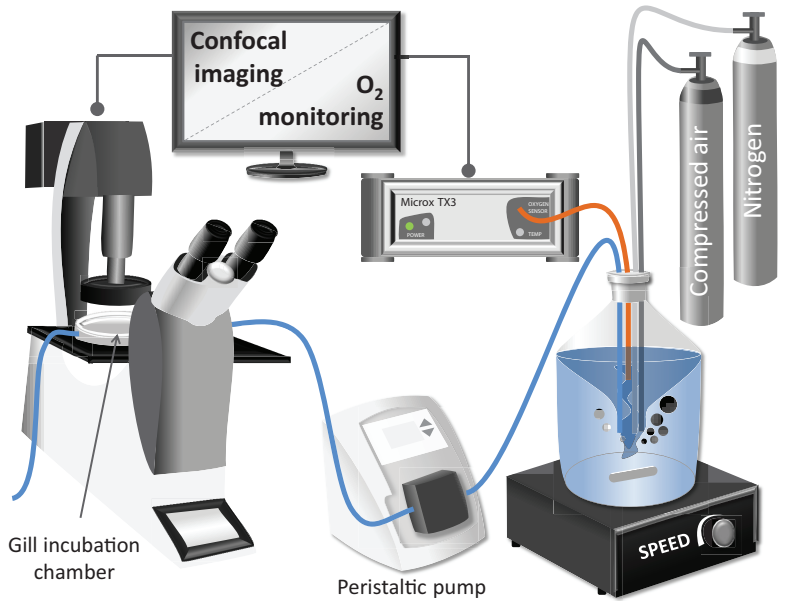

FIGURE 1 | Schematic representation of the experimental setup used for the confocal analysis of excised mussel gills.

To minimize photobleaching, for each AA one single image was taken at each time point (0, 10, 20, and 30 min, 4 images in total per AA). Only one AA was selected per gill piece and only one gill piece was used per mussel. A minimum of 4 mussels were used per fluorophore. The pO_2 of the hypoxic medium was constantly monitored directly in the reservoir and pO_2 was also measured in the perfusion chamber at the beginning and at the end of the experiment using a calibrated O_2 meter Microx TX3 (Presens GmbH, program Oxy View TX3-V6.02) equipped with a needle type O_2 micro-sensor NTH-PSt 1. For normoxic exposures, the Bachofer chamber was maintained open. For hypoxic conditions the chamber was closed with a coverslip and perfused with hypoxic medium.

Nitric oxide formation in gill filaments was visualized using DAF-2DA (Sigma D225). For each of the pictures taken, a total of 10 regions of interest (ROIs) were defined on epithelial cells, perpendicularly to the longitudinal axis of the gill filament (**Figure 2A**). For each of these ROIs the average fluorescence intensity was calculated (EPI-DAF2T). Additionally, another 10 ROIs were defined on the endothelial cells, in this case parallel to the longitudinal axis of the filament and the average fluorescence intensity was equally calculated (END-DAF2T). Since absolute DAF-2DA loading differs between gills, EPI-DAF2T values were used to obtain a ratio (END-DAF2T: EPI-DAF2T) (called fluorescence ratio from now on) for each picture to allow comparisons between gill pieces.

The formation of $O_2^{\bullet-}$ was assessed by incubating a minimum of 4 gills pieces per time point (one gill piece per mussel) with the fluorescent dye MitoSOX (Invitrogen M36008). For each image, 10 ROIs were defined perpendicularly to the longitudinal axis of the gill filament (**Figure 2B**). The region of the blood vessel lumen was not considered in this analysis to avoid interference from the high fluorescence emitted by hemocyte cells. Given that the maximum MitoSOX fluorescence was in all cases located in the outer region of epithelial cells (Rivera-Ingraham et al., 2016), each of these ROIs was subdivided in two equally sized regions at higher image resolution (outer and inner regions and in all cases excluding the vessel lumen as in Rivera-Ingraham et al., 2016). Two values were then calculated**:** (i) the average fluorescence intensity of the ROI inner region ($MSOX_{IR}$) and (ii) the average fluorescence intensity of the ROI outer region ($MSOX_{OR}$). Then, the MitoSOX fluorescence for each sample was calculated as $MSOX_{OR}$-$MSOX_{IR}$.

The fluorescence probe JC-10 (Enzo Life Sciences ENZ-52305) was used to observe the differences in the $\Delta\psi m$ in both epithelial and endothelial gill cells. In each image fluorescence analysis was done using square ROIs (approximate diameter of 1.5 µm) (**Figure 2C**): (i) 10 ROIs were evenly distributed in the region of the epithelial cells of the filament and (ii) 10 in the endothelial cells. Mean intensity values were recorded for each square for both the green (JC10ENDgreen and JC10EPIgreen for endothelial and epithelial cells, respectively; **Figure 2C1**) and the red channels (JC10ENDred and JC10EPIred for endothelial and epithelial cells, respectively; **Figure 2C2**). The ratio of red fluorescence over green fluorescence was then calculated separately for both endothelia and epithelial cells as a measure of changes in $\Delta\psi m$ using Leica LAS AF Lite software (Leica, Microsystems CMS GmbH 2011).

Measurements of Blood Vessel Diameters

Using the same 4-8 bivalves as for DAF-2DA measurements, blood vessel diameter was measured in freshly excised gills under normoxic (control) and treatment conditions. Treatments were conducted in the perfusion chamber of the confocal

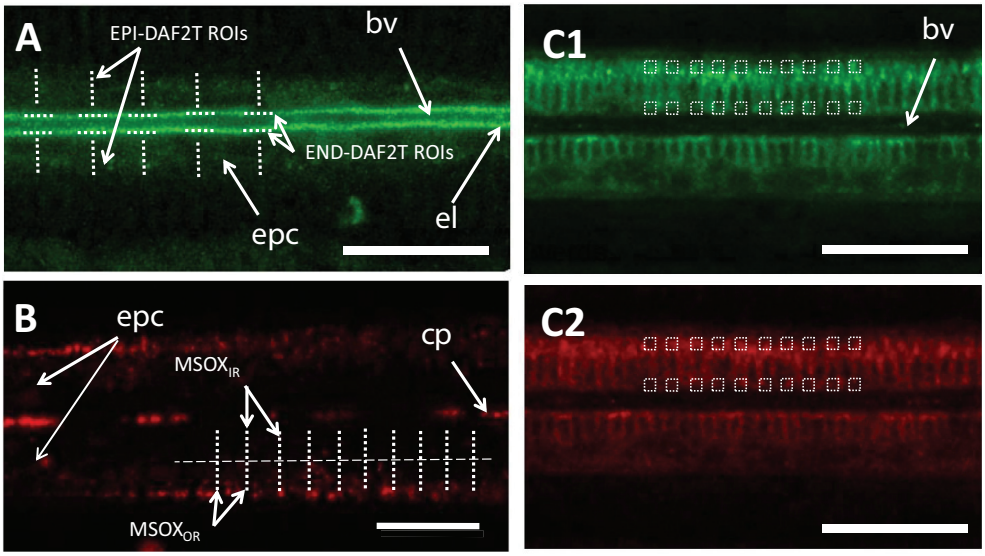

FIGURE 2 | Schematic representation of the number and type of regions of interest used for the image analyses of confocal experiments using: **(A)** DAF-2DA, **(B)** MitoSOX, and **(C)** JC-10 in the **(C1)** green and **(C2)** red spectrum ranges. Scale bars: 20 μm. bv, blood vessel; cp, circulating particles; epc, epithelial cells; el, endothelial lining surrounding the blood vessel. Dotted lines indicate regions of interest.

microscope, using the same set-up described in the next section: Mitochondrial respiratory complex assays in gill homogenates. During the incubations, the gills were maintained at room temperature (18°C) and were exposed under the respective gaseous atmosphere in NH-FSH for each time point (0, 10, 20, and 30 min). A 40X optical objective was used for imaging and 13 vertical sections (Z-stack images) were taken at 1.4 μm steps. For each time point, the image from the Z-stack showing the widest blood vessel diameter was selected for quantification. In order to measure the overall width of the blood vessel for each image, 10 width measurements were conducted of the inner vessel lumen just up to the limits of the surrounding endothelial cells. Images were taken and analyzed along the gill filament. Given that the blood vessel diameter is not consistent along the filament, the largest diameter determined in each image was used for quantification, using the software routines to measure distances on imaged structures.

Mitochondrial Respiratory Complex Assays in Gill Homogenates

Measurements of respiratory complex activities were conducted on frozen gill pieces that were homogenized and incubated under experimental pO_2 conditions or in the presence of SpNONOate for 3 h before the activity measurement. Mitochondrial respiratory complex I, III, and IV assays were performed in the incubated homogenates *in-vitro* no later than 48 h after freezing the gills.

Each frozen gill was cut into equal pieces that were weighed to the nearest 0.1 mg. One piece of each individual gill was used for one out of five experimental pO_2 and NO treatments (normoxia: 21 kPa, hypoxia: 7 kPa, severe hypoxia: 1 kPa, normoxia + 3 mM SpNONOate and normoxia + 6 mM SpNONOate) to enable direct comparability between treatments for each individual. Each gill piece was homogenized in a medium containing 20 mM Tris (hydroxymethyl) aminomethane supplemented with 1 mM EDTA, 0.1% Tween 20, and SpNONOate (for NO treatments only) at 7.4 pH. Adjustment of treatment conditions (pO_2 and addition of NO donor) were established by equilibrating the homogenization buffer with air (for normoxic conditions) or a mixture of air and nitrogen (N_2) (for hypoxia). To control buffer-pO_2, the respirometer described in the respirometry description was used. For hypoxic exposures, homogenization and subsequent incubation were carried out in a hypoxic atmosphere (achieved by the same air and N_2 mixture used for equilibrating the homogenization buffer). Once the desired pO_2 was reached, the required volume (i.e., 1/6: w/v) was transferred under hypoxic atmosphere (for the hypoxic treatments) to a 1.5 mL tube containing the sample. Final homogenate volumes ranged between 62 and 230 μL. Homogenization was done at 4°C using a Precellys Homogenizer 24 (2 cycles × 15 s 5,000 rotations and 15 s break) equipped with a cryolysis advanced temperature controller (Bertin Technologies, Montigny-le-Bretonneux, France). The preparation of the microplate was also carried out under normoxic/hypoxic atmosphere, as required. The final activity measurement was conducted at normoxic conditions and at room temperature (20°C) in a TriStar microplate reader (Berthold Technologies, Bad Wildbad, Germany).

Activity of the ETS was measured according to Châtelain (2008) at $\lambda = 485$ nm with $\varepsilon = 15.9\ mM^{-1} \cdot cm^{-1}$. Each well of a 96 well microplate contained: 117 μL of the measuring buffer (100 mM imidazole at 8.0 pH), 20 μL of 0.1 M sodium azide, 49 μL of 7.9 mM iodonitrotetrazolium chloride (INT, Sigma I-8377) to which 4 μL of the homogenized sample were

added. All solute ions were equilibrated at the three experimental pO_2 conditions (21, 7, 1 kPa). A blank signal was allowed to stabilize for a maximum time of 10 min (pre-run), and the reaction was triggered by injection of 10 μL of 8 mM NADH into each well. The final reaction volume per well was 200 μL. The increase in absorbance was recorded at intervals of 30 s for an entire duration of 10 min (main run). Plates were shaken between measurements to avoid precipitation of INT using the ellipsoidal shaker function of the instrument at medium velocity in backward and forward mode. The ETS activity in the extract was calculated by subtracting the slope of the pre-run from the slope of the main run (abs · min^{-1}). Results are expressed as U · g FW^{-1}.

CytOx activity was measured after Moyes et al. (1997) at λ = 550 nm with ε = 19.1 · mM^{-1} · cm^{-1}. The measurement of CytOx is based on the oxidation of reduced cytochrome c by CytOx. A 5 min pre-run was conducted using 170 μL of the measuring buffer (20 mM Tris HCl with 0.5% Tween 20, 8.0 pH) and 20 μL of the homogenate. The reaction was started by the addition of 10 μL of reduced cytochrome c (200 μL in total per well). The reduced cytochrome c solution was prepared by dissolving 100 mg of cytochrome c in 4 mL of in N_2-bubbled reduction buffer (20 mM Tris HCl, 8.0 pH) and adding a small amount of sodium dithionite under a N_2 atmosphere. The reduced cytochrome c was passed over a Sephadex G-25 column using 10 mL of anoxic reduction buffer. Absorbance decrease reflecting the oxidation of cytochrome c was measured over 5 min (main run) at 15 s measuring interval. The samples were shaken between each measurement and activity was calculated by subtracting the slope of the pre-run from the slope of the main run (abs · min^{-1}). CytOx activity is expressed as U · g FW^{-1}.

Statistical Analyses

All data was tested for normality (Kolmogorov-Smirnov test) and homocedasticity (Levene test). A one-way ANOVA was carried out if the requirements for parametric analysis were met, followed by a Student-Newman-Keuls *post-hoc* test. For the rest of cases, a Kruskal-Wallis test was conducted, followed by U-Mann Whitney pairwise comparisons. The level of significance was $p < 0.05$ if not otherwise indicated.

RESULTS

Respiration Experiments

Respiration rates of *M. edulis* gill pieces significantly decreased in a pO_2-dependent (oxyconforming) manner (**Figure 3A**) (*K*

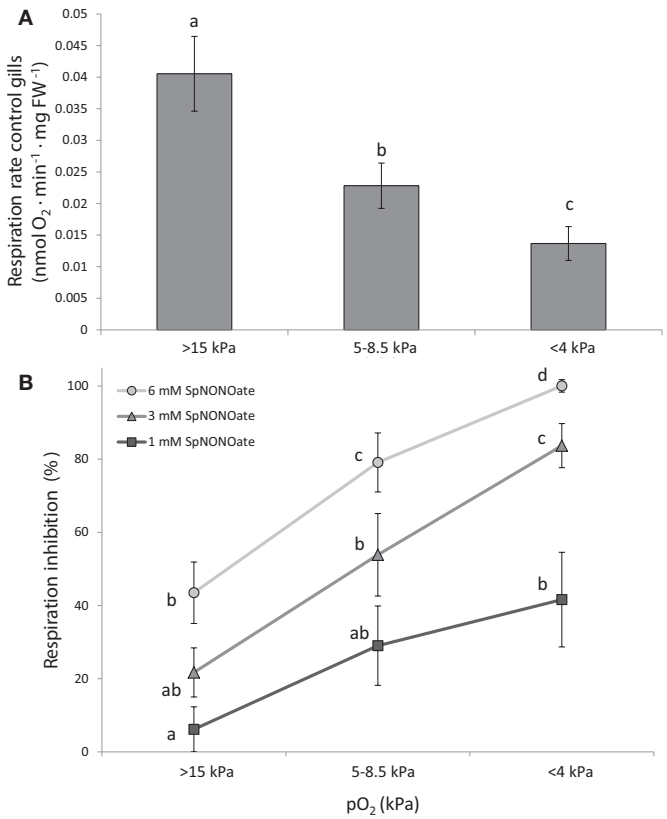

FIGURE 3 | Respiration rates of *Mytilus edulis* excised gills at different O_2 partial pressures under: **(A)** control conditions and **(B)** different concentrations of Spermine NONOate. Results in **(B)** are expressed as the percentage of inhibition that Spermine NONOate induces in gill respiration compared to the values obtained in undisturbed gill tissues of the same individual. Letters indicate significant differences between mean values based on Kruskal-Wallis test followed by U Mann-Whitney pairwise comparisons.

= 16.285; $p < 0.001$, $n = 24$) with moderate (5–8.5 kPa) and acute (<4 kPa) hypoxia causing a 1.8- and 3-fold reduction over normoxic conditions, respectively. Addition of SpNONOate reduced respiration rates in a concentration dependent manner (**Figure 3B**, $n = 8$). At each SpNONOate concentrations, the inhibitory effect increased at lower pO_2 to the point that gills exposed to the highest NO donor amounts (6 mM) showed complete respiratory shut down below 4 kPa.

Response of Isolated Gills to Hypoxia and Experimental Nitric Oxide Exposure (*ex vivo*)

Nitric oxide formation (DAF-2T fluorescence) was mainly detectable in the endothelial cells surrounding the blood vessel and less intense in the epithelial cells in the periphery of the gills (**Figure 4A1**). Given that fluorescence intensities in different animal gills varied strongly in epithelial cells, a ratio was calculated between fluorescence in endothelial and epithelial cells as explained in the section describing the fluorimetric nitric oxide analysis. The DAF-2T fluorescence increased more pronouncedly in endothelial than epithelial cells in a time and pO_2 dependent manner ($K = 50.983$; $p < 0.001$, $n = 4$–9; **Figures 4A2,B**). The effect of hypoxia on NO formation was much greater (roughly 2 times more fluorescence) at 1 than at 7 kPa pO_2. Compared to normoxic control conditions (**Figure 4C1**), treatment with SpNONOate caused DAF-2T fluorescence intensity to increase significantly at 30 min of exposure to the NO donor (**Figures 4C2,D**) ($K = 20.877$; $p < 0.05$, $n = 3$–5). No difference in DAF-fluorescence was observed between the effects of 3 mM and 6 mM SpNONOate in endothelial cells around the blood vessel (**Figure 4D**).

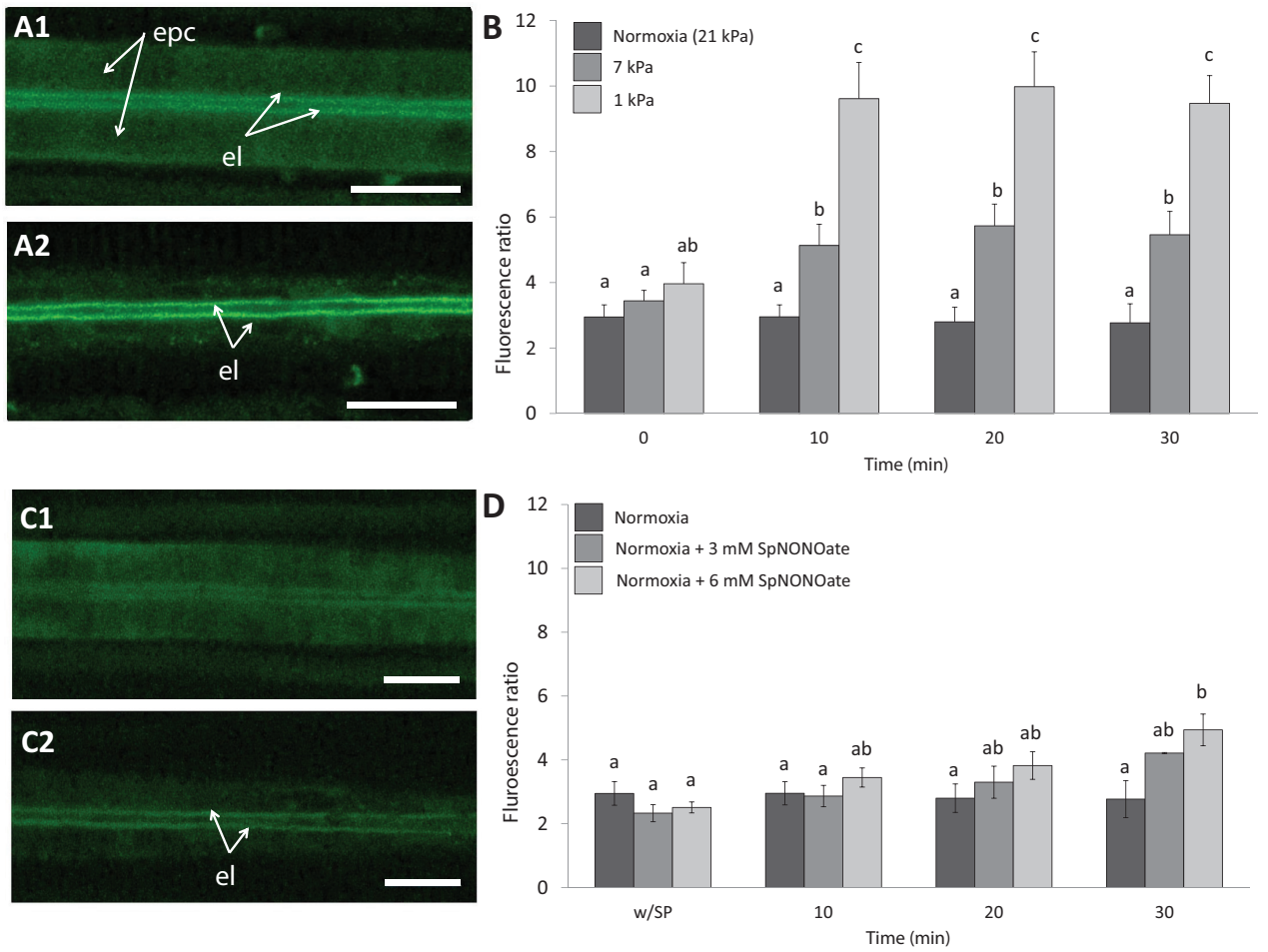

FIGURE 4 | Nitric oxide formation as shown by DAF-2T fluorescence in *Mytilus edulis* gill tissues over time when exposed to different: **(A,B)** Degrees of hypoxia or **(C,D)** Concentrations of Spermine NONOate. **(A)** Representative images of the gills of the same individual with DAF, **(A1)** taken under control (normoxic) conditions and **(A2)** under severe hypoxia 1 kPa for 30 min. **(C)** Representative images of the gills of the same individual under **(C1)** normoxia and **(C2)** incubated with 6 mM Spermine NONOate for 30 min. Quantitative data are shown in **(B,D)** and values were expressed as the average fluorescence intensity of END-DAF2T: EPI-DAF2T. Letters indicate significant differences between mean values based on Kruskal-Wallis test followed by U Mann-Whitney pairwise comparisons. Scale bars: 20 μm; epc, epithelial cells; el, endothelial lining surrounding the blood vessel.

Hypoxic exposure of gills caused a pO_2 and time-dependent increase of $O_2^{\bullet-}$ formation in the mitochondria (MitoSOX fluorescence) within the epithelial cells of the outer gill region (**Figures 5A1,2**). In fact, MitoSOX fluorescence increased stepwise with hypoxic intensity (1 kPa > 7 kPa) with the tiered effect reaching statistical significance after 20 (1 kPa) and 30 min (7 kPa) (**Figure 5B**) ($K = 33.532$; $p < 0.001$, $n = 4$–6). Fluorescence intensity after application of SpNONOate under normoxia increased mainly in the mitochondria at the basis of the cilia themselves and thus in the outer periphery of the filaments (**Figure 5C**). The effect was significant for both the 3 mM ($F = 3.352$; $p = 0.05$, $n = 3$–5) and 6 mM ($F = 5.762$; $p = 0.009$, $n = 3$–5) SpNONOate treatments (**Figure 5D**). Furthermore, we observed that circulating particles/hemocyte cells in the hemolympahtic blood vessel emitted intense MitoSOX fluorescence under all experimental conditions including normoxia (**Figure 5C**).

The $\Delta\psi m$ of cilia-associated (outer) mitochondria (JC-10 fluorescence ratio) remained unaffected over time of exposure to hypoxia or NO donor (21 kPa: $F = 0.155$; $p = 0.925$, $n = 5$; 7 kPa: $F = 0.324$, $n = 5$; $p = 0.808$; 1 kPa: $F = 1.152$; $p = 0.357$, $n = 6$; 3 mM SpNONOate: $F = 0.520$; $p = 0.674$, $n = 5$; 6 mM SpNONOate: $F = 0.018$; $p = 0.996$, $n = 6$) (**Table 2**). Likewise, no change of $\Delta\psi m$ was observed in the mitochondria around the blood vessel (endothelial mitochondria) (21 kPa: $F = 0.134$; $p = 0.938$; 7 kPa: $F = 0.761$; $p = 0.531$; 1 kPa: $F = 0.300$; $p = 0.825$, $n = 4$–6; 3 mM SpNONOate: $F = 0.013$; $p = 0.998$, $n = 5$; 6 mM SpNONOate: $F = 0.018$; $p = 0.997$, $n = 6$) (**Table 2**).

Blood vessels under undisturbed conditions (normoxia) had an average width of 0.99 ± 0.01 µm ($N = 29$). In each piece of gill we analyzed, exposure to hypoxia caused an increase of

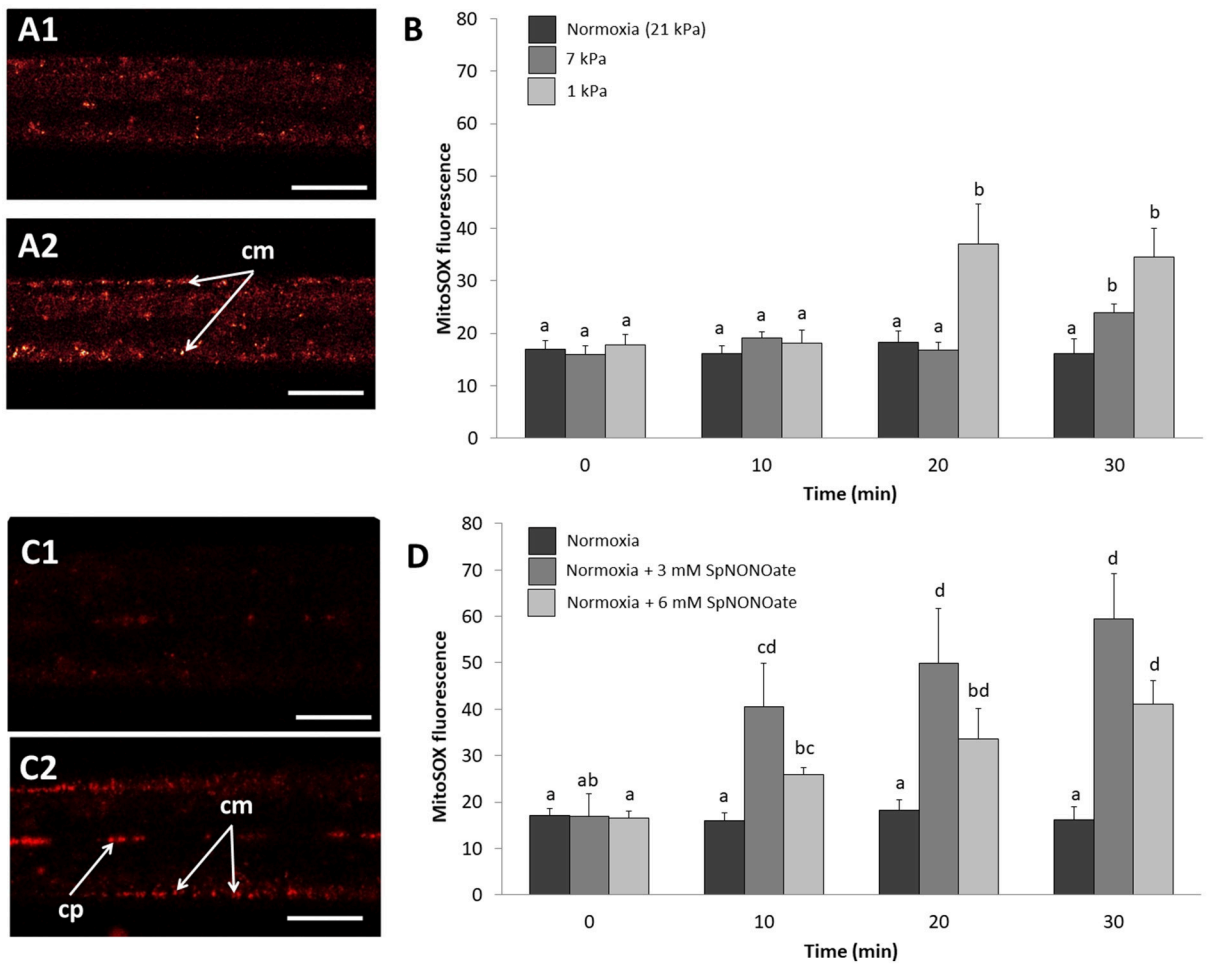

FIGURE 5 | Mitochondrial superoxide anion formation imaged by MitoSOX fluorescence in *Mytilus edulis* gill tissues over time when exposed to different: **(A,B)** degrees of hypoxia or **(C,D)** concentrations of Spermine NONOate. **(A)** Representative images of the gills of the same individual with MitoSOX, **(A1)** taken under control (normoxic) conditions and **(A2)** under hypoxia 1 kPa for 30 min. **(C)** Representative images of the gills of the same individual under **(C1)** normoxia and **(C2)** incubated with 6 mM Spermine NONOate for 30 min. Quantitative data are shown in **(B,D)** and values are expressed as $MitoSOX_{OR}$ – $MitoSOX_{IR}$ (see Materials and Methods sections for details). Letters indicate significant differences between mean values based on Kruskal-Wallis test followed by U Mann-Whitney pairwise comparisons **(B)** or a one-way ANOVA followed by a Student-Newman-Keuls *post hoc* multiple comparison test **(D)**. Scale bars: 20 µm; cm, ciliary-associated mitochondria; cp, circulating particles.

TABLE 2 | JC-10 ratio values (indicative of mitochondrial membrane potential) for inner (endothelial) and outer mitochondria (cilia-associated).

Exposure time	0 min		10 min		20 min		30 min	
Treatment	Outer	Inner	Outer	Inner	Outer	Inner	Outer	Inner
Normoxia (21 kPa)	0.70 ± 0.08	0.63 ± 0.07	0.62 ± 0.10	0.57 ± 0.09	0.69 ± 0.07	0.63 ± 0.08	0.68 ± 0.10	0.62 ± 0.09
7 kPa	0.99 ± 0.04	0.87 ± 0.03	0.98 ± 0.05	0.85 ± 0.04	1.05 ± 0.05	0.93 ± 0.04	1.01 ± 0.05	0.86 ± 0.04
1 kPa	0.82 ± 0.04	0.77 ± 0.04	0.77 ± 0.04	0.75 ± 0.03	0.76 ± 0.05	0.75 ± 0.04	0.70 ± 0.04	0.73 ± 0.03
Normoxia + 3 mM SpNONOate	0.86 ± 0.07	0.67 ± 0.09	0.83 ± 0.08	0.68 ± 0.07	0.77 ± 0.09	0.67 ± 0.08	0.70 ± 0.10	0.66 ± 0.08
Normoxia + 6 mM SpNONOate	0.7 ± 0.1	0.6 ± 0.1	0.7 ± 0.1	0.6 ± 0.1	0.6 ± 0.1	0.6 ± 0.1	0.7 ± 0.1	0.6 ± 0.1

Values are expressed as average ± SE.

the blood vessel diameter (**Figures 6A1,2**) and the effect differed significantly depending on the level of hypoxic intensities the gills experienced ($F = 56.673$; $p < 0.001$, $n = 4$–7; **Figure 6B**). The opening occurred rapidly and a 1.4- and 1.6-fold increase in blood vessel diameter was recorded when tissues were exposed to 7 and 1 kPa for 30 min, respectively (**Figure 6B**). The difference amounts to roughly a doubling (7 kPa) and tripling (1 kPa) of vessel cross sectional width compared to normoxia. Exposing gills to SpNONOate (**Figure 6C**) resulted in a significant increase of blood vessel diameter ($F = 37.153$; $p < 0.001$, $n = 5$) between controls and both concentrations applied: 1.4- and 1.5-fold increase for 30 min exposure to 3 and 6 mM SpNONOate, respectively. Values corresponding to 30 min exposure to 3 mM SpNONOate did not differ significantly from those registered for 7 kPa pO_2 ($F = 0.921$; $p = 0.365$; **Figure 6D**).

Respiratory Complex Activities

In vitro CytOx activity assayed in homogenates of frozen gill tissues (**Figure 7**: dark bars) increased significantly between the normoxic incubations ($n = 12$) and homogenates incubated at moderate hypoxia (7 kPa pO_2, $K = 42.499$; $p < 0.001$, $n = 12$). The percentage increase when calculated for individual comparisons amounted to 125% of the activity in normoxia. Incubation of the same homogenates at severe O_2 deficiency of 1 kPa pO_2 reduced CytOx activity by 16% ($n = 11$ comparisons between normoxia and 1 kPa pO2, $F = 8.338$, $p = 0.009$). Addition of SpNONOate reduced CytOx activity on average by over 70% at 3 mM ($n = 9$, $F = 101.502$, $p < 0.001$) and by 35% at 6 mM ($n = 9$, $F = 10.695$, $p = 0.004$) compared to the normoxic controls without NO donor (**Table S1**).

Compared to normoxic conditions ($n = 12$), activity of both ETS complexes I and III in homogenates decreased at both hypoxic conditions ($n = 12$) and if assayed in the presence of SpNONOate ($n = 10$) (**Figure 7**, $K = 41.993$; $p < 0.001$). A decrease of 27 and 22% in ETS activity was recorded under moderate ($F = 102.987$, $p < 0.001$) and acute hypoxia ($F = 73.929$, $p < 0.001$), respectively. The addition of SpNONOate in normoxic medium caused a partial inhibition of the ETS activity by 51 and 34% for 3 mM ($K = 13.635$, $p < 0.001$) and 6 mM ($F = 189.277$, $p < 0.001$), respectively, based on mean values (**Table S2**).

DISCUSSION

The respiratory response of *M. edulis* to declining environmental O_2 tension has been the focus of a great number of studies over the past 50 years, as researchers became fascinated with the enormous physiological flexibility of this successful colonizer of marine coastal habitats (Zandee et al., 1980) but also worried about the increasing impact of climate global change, mussel fisheries, neobiota, and hypoxia on the marine coastal environments (Eriksson et al., 2010).

Nitric Oxide: A Local Vasodilator in *M. edulis* Endothelial Gill Cells

In the present paper we documented widening of the hemolymphatic vessel in isolated gill filaments exposed to hypoxia in a microscopic chamber. Increasing NO (DAF-2T) fluorescence in the endothelial muscle cells below 7 kPa is a strong indication that NO functions as a hypoxic messenger and local vasodilator in these gills pieces. The effect is rapid and sets on after 10 min of filament exposure; and both effects, NO accumulation and relaxation of the muscular endothelium that causes opening of the blood vessel increase in parallel as pO_2 declines to 1 kPa. A 50% increase of the blood vessel lumen under hypoxia appears as a rather strong effect detected with our approach. By contrast, experimental exposure of gill pieces to addition of NO donor had less pronounced effects on both parameters, presumably because the addition occurred in normoxic medium in which NO is rapidly oxidized to NO_2^-. Still, also in this experiment, 50% increase of the blood vessel lumen was observed after 20 and 30 min in NO donor treated samples, but not in control gills maintained in the chamber for the same duration under normoxic conditions. This experiment supports the notion that NO acts as mediator of blood vessel relaxation in *Mytilus*. The experiment with SpNONOate followed a different dynamic because the NO donor was added to the outside medium and NO accumulated only in the endothelial cells of the blood vessel. NO diffuses freely through membranes and can reach the endothelium from the outside within seconds, especially as heme-containing blood pigments are absent in *Mytilus*. Alternatively, NO with a vasodilatory effect could also be released from the strongly DAF-2T fluorescing hemocyte cells moving within the blood vessel (Rivera-Ingraham et al., 2016), which play a role in bivalve immune response (Philipp et al.,

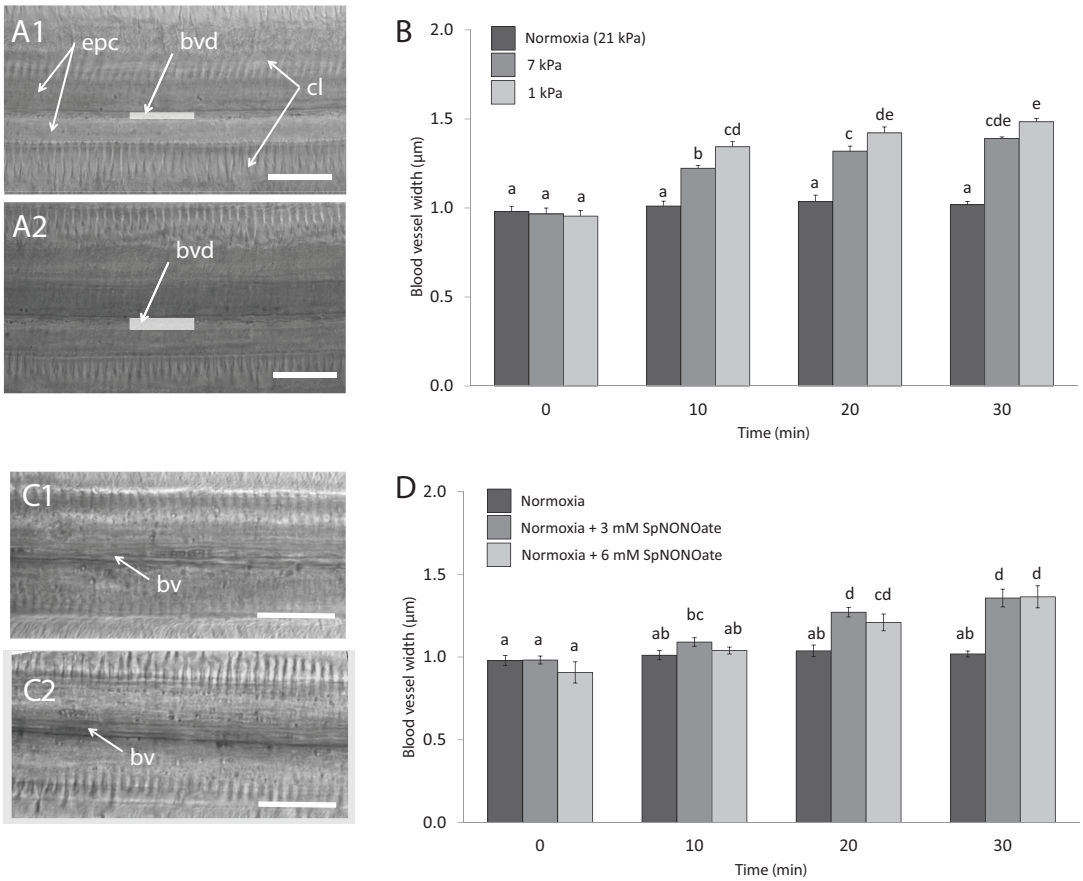

FIGURE 6 | Blood vessel diameter in gill filaments exposed to different: **(A,B)** degrees of hypoxia and **(C,D)** concentrations of Spermine NONOate. **(A)** Representative transmission images of the gills of the same individual **(A1)** taken under control (normoxic) conditions and **(A2)** under hypoxia 1 kPa for 30 min. **(C)** Representative images of the gills of the same individual under **(C1)** normoxia and **(C2)** incubated with 3 mM Spermine NONOate for 30 min. Letters indicate significant differences between mean values based on one-way ANOVA followed by a Student-Newman-Keuls *post-hoc* multiple comparison test. Scale bars: 20 µm; bv: blood vessel, bvd: blood vessel diameter, indicated with a gray bar, cl: gill cilia, epc: epithelial cells.

2012). NO emitted within the blood vessel could also function as blood-borne vasodilator, triggered under hypoxic conditions or during parasite invasion (Kaiser et al., 1989, 1991).

At any rate this is—to our knowledge—the first explicit report of a vasodilatory effect of NO in endothelial cells of mussel gills. Biological functions of NO have been reported for terrestrial and aquatic non-model invertebrates (summarized in Palumbo, 2005), but its involvement in regulating blood pressure is so far documented only in cephalopods by Schipp and Gebauer (1999). Our study underlines NO induced vasodilation to be an evolutionarily old mechanism of endothelial cells (Jacklet, 1997). Indeed it is logical to reduce vessel resistance when heart beat increases in a hypoxic mussel (Bayne, 1971).

Effects of Hypoxia and Nitric Oxide Donor on Gill Respiration, Mitochondria, and Respiratory Chain Components

Experimental addition of NO donor to freshly excised gill pieces inhibited gill respiration in a concentration and pO_2 dependent manner. Indeed, addition of 6 mM SpNONOate completely abolished respiration under near anoxic conditions. The pO_2 dependency of the inhibition effect is a clear indication of NO oxidation in the normoxic medium. Even at 21 kPa pO_2, 6 mM SpNONOate decreased respiration by 44% compared to NO free controls directly at the start of experimentation. Data on NO concentrations in bivalve shell water or hemolymph are not available so far, but NO concentrations that cause blood vessel relaxation in mammals are in the low nM range (Demoncheaux et al., 2002), suggesting that sufficient amount of NO was generated in our SpNONOate experiments to achieve a vasodilatory effect. This is a hint that NO accumulating in shell water and hemolymph as O_2 diminishes during shell closure might also have a physiological effect on gill performance and potentially reduces metabolic rate also in other tissues.

The NO donor treatment of cell free gill homogenates during 3 h strongly inhibited both CytOx (complex IV) and ETS (complex I and III) activities in a concentration independent manner, which suggests inhibition of respiratory complexes to be saturated at 3 mM SpNONOate. These assays in which

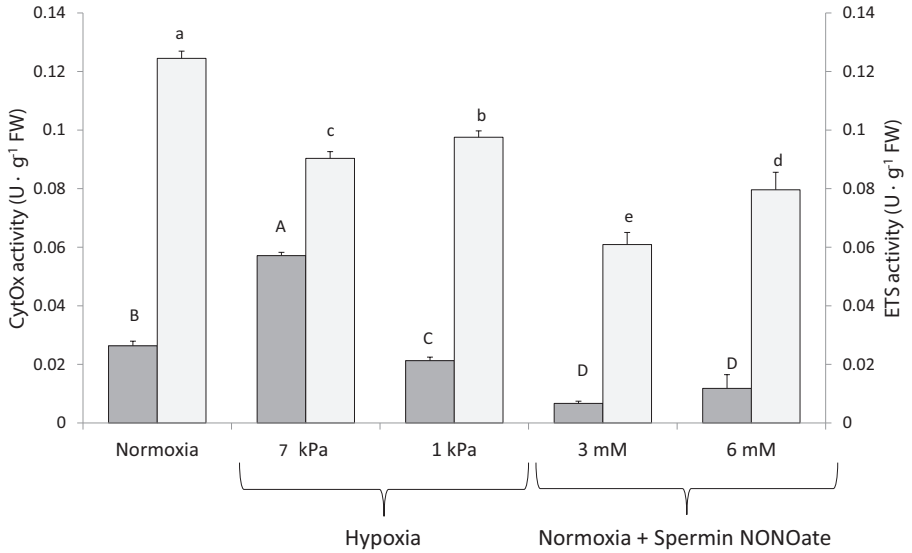

FIGURE 7 | Cytochrome c oxidase (■) and electron transport system (□) activities recorded in excised gill tissues under different degrees of hypoxia and Spermine NONOate concentration. Different letters (capital and lowercase letters for cytochrome c oxidase and electron transport system, respectively) indicate significant differences between mean values based on U Mann-Whitney pairwise comparisons.

we apparently applied excess amounts of NO donor were intended to clarify chemical susceptibility of *M. edulis* respiratory complexes to NO inhibition. This being confirmed, it seems likely that the strong effect of NO donor administration on respiration of freshly excised intact gill pieces is due to the inhibition of the mitochondrial electron transport complexes. The multisite inhibitory effect is known from experiments with rat heart submitochondrial particles (SMPs) that were exposed to slightly higher concentrations of NO (0.1 and 0.3 μM, Poderoso et al., 1996). The authors found substantial inhibition of NADH-cytochrome c reductase (complex I), as well as complex III (ubiquinone-cytochrome b reductase) with the strongest inhibition of complex IV (CytOx, 50% inhibition with 0.1 μM NO). Higher effective concentrations of NO (0.3–0.6 μM) caused significant H_2O_2 release from SMPs supplied with succinate as respiratory electron donor, indicating $O_2^{\bullet-}$ production, which in aqueous media rapidly dismutates to H_2O_2. In intact tissues, $O_2^{\bullet-}$ produced by NO inhibited mitochondria would rapidly form peroxynitrite ($ONOO^-$) and cause oxidative and cellular damage at NO concentrations that, according to these authors, are about one order of magnitude higher than the concentrations affording inhibition of CytOx (Poderoso et al., 1996).

Hypoxia had a strong effect on respiration rates and the activities of respiratory chain complexes I, III, and IV. It is interesting to note that CytOx activity measured in the homogenates incubated at mildly hypoxic pO_2 (7 kPa) was higher than in homogenates from the same gill assayed after normoxic incubation (21 kPa). This would have appeared as an artifact, if not replicated with 12 individual gill experiments, and if the activity maximum at 7 kPa pO_2 had not been observed in the range of the elevated respiration pattern shown for *M. edulis* gills in our previous study (Rivera-Ingraham et al., 2013b). As all gills originated from the same batch of control mussels taken directly from the holding tank, physiological differences in the extracts incubated at different pO_2 levels can be excluded. It appears that in the 21 kPa O_2 treatment something may have inhibited CytOx activity, such as a potential production of ROS in the air equilibrated homogenates. Indeed, mitochondrial ROS formation has been shown to increase linearly with O_2 concentration (Turrens et al., 1982) and studies in invertebrates have shown that ROS formation is higher under normoxia than under reduced O_2 conditions (e.g., Rivera-Ingraham et al., 2013a). As plenty of O_2 was present in the normoxic homogenate based assay that was not reduced by CytOx activity, it may very well have caused $O_2^{\bullet-}$ formation from autoxidation of ETS compounds as shown for hyperoxically perfused rat lung endothelia (Brueckl et al., 2006) or from other cellular compounds easily prone to oxidation once exposed to air. Hence the results obtained with the cell free homogenates must not be over interpreted in terms of their physiological implications for the intact tissue.

It was also interesting to see that $O_2^{\bullet-}$ formed in the mitochondria of the intact gill filaments exposed to hypoxia and near anoxia, and that $O_2^{\bullet-}$ production was even more strongly induced by NO donor treatment in peripheral than in endothelial mitochondria (**Figure 5C2**). Thus, $O_2^{\bullet-}$ production appears to be induced as mitochondrial electron transport slows near anoxia and can also be triggered by NO as a mitochondrial ETS inhibitor in *M. edulis*. The effect of the NO donor was not only stronger but also quicker, and could potentially mimic an oxidative burst reaction triggered by NO. It is characteristic of marine invertebrate mitochondria that their lower membrane potential and flexibly adjustable proton leak supports mitochondrial integrity and stabilizes inner $\Delta\psi m$ against environmental factor

fluctuations including hypoxia (Abele et al., 2007). Stable $\Delta\psi m$ in epithelial and endothelial gill mitochondria, recorded with the membrane potential sensitive fluorophore JC10 in our short-term hypoxia and SpNONOate exposure experiments, underline this mitochondrial tolerance. It might have been different if experimental exposure of gill pieces had persisted over longer time than 30 min. In meiofauna flatworms we observed an increase of $\Delta\psi m$ with life imaging following 1.5 h in anoxia (Rivera-Ingraham et al., 2013a). A potential mechanism to stabilize $\Delta\psi m$ is the alternative oxidase (AOX) that enables branching electron transport and maintenance of $\Delta\psi_m$ when CytOx becomes inhibited by cyanide, hydrogen sulfide (Parrino et al., 2000), or NO (further reading in Abele et al., 2017). Recently AOX sequences have been reported from several molluscan species, among them *Mytilus californianus* and *M. galloprovincialis* (McDonald et al., 2009). This is a very powerful and efficient mechanism in hypoxia tolerant aquatic invertebrates, and it seems likely that AOX may have stabilized $\Delta\psi m$ against short term hypoxic exposure in *M. edulis* gills.

CONCLUSION AND FUTURE PERSPECTIVES

With this study we highlighted for the first time that NO, formed in the endothelial muscle cells around the hemolymphatic vessel of *M. edulis* gill filaments, can function as a local vasodilator under hypoxic conditions. Externally applied NO has a concentration dependent effect on gill respiration and blood vessel diameter and might affect the physiological performance of the gills and other tissues if it accumulates to significant amounts in the nM range under hypoxic conditions. Indeed, shell water NO and potentially NO_2^- levels [see (van Faassen et al., 2009) for effects of NO_2^- on cellular signaling and mitochondrial respiration under hypoxic conditions] could have a mediating effect inducing metabolic shut down in hypoxia-exposed or stress exposed mussels that keep the shell closed for prolonged periods. A controlled metabolic shut down and a tiered reduction of ETS activities, including CytOx, may prevent significant ROS formation during hypoxic and anoxic transgression. All this may show an ancient mechanism for controlling respiratory electron transport under conditions of variable environmental oxygenation, typical for coastal marine environments to date. The interaction between animals and their microbial biofilms is a fascinating future topic that could also be of relevance with respect to hypoxic adaptation of marine benthic macrofauna.

AUTHOR CONTRIBUTIONS

All co-authors planned the experiments together and designed the workplan. PG and GR-I carried out the main body of experimental work in the laboratory of DA. GR-I, PG, and DA analyzed the data and produced the figures and tables. All authors contributed to the discussion and the writing of the manuscript.

ACKNOWLEDGMENTS

We are especially grateful to Stefanie Meyer (AWI) for her help in the laboratory and the AWI Department Functional Ecology for supporting this research. Thanks also go to two referees who helped to improve the original version of the manuscript. This study was supported by a funding for international research stays for argentine researchers from the National Council for Science and Technology (CONICET, Res D N°2834). PG is a career investigator from CONICET.

SUPPLEMENTARY MATERIAL

The Supplementary Material for this article can be found online at: https://www.frontiersin.org/articles/10.3389/fphys.2018.01709/full#supplementary-material

REFERENCES

Abele, D., Brey, T., and Philipp, E. E. R. (2017). "Ecophysiology of extant marine *Bivalvia*," in *Treatise Online XX*, ed. J. Carter (Lawrence, KS), 1–47.

Abele, E., Philipp, E., Gonzalez, P. M., and Puntarulo, S. (2007). Marine invertebrate mitochondria and oxidative stress. *Front. Biosci.* 12, 933–946. doi: 10.2741/2115

Acevedo, S., Arias, N., Crego, P., Diehl, P., Flores, V., Funes, F., et al. (1993). *Analisis del Contenido Intestinal de Diplodon chilensis*. Trabajo especial. Catedra de Invertebrados A. Biblioteca Parasitologia C.R.U.B. Universidad del Comahue, Bariloche.

Aiello, E., and Guideri, G. (1965). Distribution and function of the branchial nerve in the mussel. *Biol. Bull.* 129, 431–438. doi: 10.2307/1539722

Altieri, A. H. (2006). Inducible variation in hypoxia tolerance across the intertidal–subtidal distribution of the blue mussel *Mytilus edulis*. *Marine Ecol. Progr. Ser.* 325, 295–300. doi: 10.3354/meps325295

Anderson, I. C., and Levine, J. S. (1986). Relative rates of nitric oxide and nitrous oxide production by nitrifiers, denitrifiers, and nitrate respirers. *Appl. Environ. Microbiol.* 51, 938–945.

Bayne, B., Bayne, C., Carefoot, T., and Thompson, R. (1976). The physiological ecology of *Mytilus californianus* Conrad. *Oecologia* 22, 229–250. doi: 10.1007/BF00344794

Bayne, B. L. (1971). Ventilation, the heart beat and oxygen uptake by *Mytilus edulis* L. in declining oxygen tension. *Compar. Biochem. Physiol. A Physiol.* 40, 1065–1085. doi: 10.1016/0300-9629(71)90295-7

Brueckl, C., Kaestle, S., Kerem, A., Habazettl, H., Krombach, F., Kuppe, H., et al. (2006). Hyperoxia-induced reactive oxygen species formation in pulmonary capillary endothelial cells in situ. *Am. J. Respir. Cell Mol. Biol.* 34, 453–463. doi: 10.1165/rcmb.2005-0223OC

Châtelain, E. H. (2008). *Effet de la Variabilité de l'ADN mitochondrial et du Régime Termique sur le Métabolisme et la Gestion du Stress Oxydant Durant le Vieillissement chez Drosophila simulans*. Maitraise en gestion de la faune et de ses habitats, Université du Québec à Rimouski.

Conte, A., and Ottaviani, E. (1995). Nitric oxide synthase activity in molluscan hemocytes. *FEBS Lett.* 365, 120–124. doi: 10.1016/0014-5793(95)00439-G

Demoncheaux, E. A., Higenbottam, T. W., Foster, P. J., Borland, C. D., Smith, A. P., Marriott, H. M., et al. (2002). Circulating nitrite anions are a directly acting vasodilator and are donors for nitric oxide. *Clin. Sci.* 102, 77–83. doi: 10.1042/cs10 20077

Eriksson, B. K., van der Heide, T., van de Koppel, J., Piersma, T., van der Veer, H. W., and Olff, H. (2010). Major changes in the ecology of the Wadden Sea: human impacts, ecosystem engineering and sediment dynamics. *Ecosystems* 13, 752–764. doi: 10.1007/s10021-010-9352-3

González, P. M., Abele, D., and Puntarulo, S. (2008). Iron and radical content in *Mya arenaria*: possible sources of NO generation. *Aquat. Toxicol.* 89, 122–128. doi: 10.1016/j.aquatox.2008.06.008

González, P. M., and Puntarulo, S. (2011). Iron and nitrosative metabolism in the Antarctic mollusc *Laternula elliptica*. *Compar. Biochem. Physiol. C Toxicol. Pharmacol.* 153, 243–250. doi: 10.1016/j.cbpc.2010.11.003

Heisterkamp, I. M., Schramm, A., De Beer, D., and Stief, P. (2010). Nitrous oxide production associated with coastal marine invertebrates. *Mar. Ecol. Progr. Ser.* 415, 1–9. doi: 10.3354/meps08727

Jacklet, J. W. (1997). Nitric oxide signaling in invertebrates. *Invertebr. Neurosci.* 3, 1–14. doi: 10.1007/BF02481710

Kaiser, L., Spickard, R. C., Sparks Jr, H. V., and Williams, J. F. (1989). Dirofilaria immitis: alteration of endothelium-dependent relaxation in the *in vivo* canine femoral artery. *Exper. Parasitol.* 69, 9–15. doi: 10.1016/0014-4894(89)90165-3

Kaiser, L., Tithof, P. K., Lamb, V. L., and Williams, J. F. (1991). Depression of endothelium-dependent relaxation in aorta from rats with *Brugia pahangi* lymphatic filariasis. *Circulat. Res.* 68, 1703–1712. doi: 10.1161/01.RES.68.6.1703

McDonald, A. E., Vanlerberghe, G. C., and Staples, J. F. (2009). Alternative oxidase in animals: unique characteristics and taxonomic distribution. *J. Exper. Biol.* 212, 2627–2634. doi: 10.1242/jeb.032151

Moroz, L. L., Chen, D., Gillette, M. U., and Gillette, R. (1996). Nitric oxide synthase activity in the molluscan CNS. *J. Neurochem.* 66, 873–876. doi: 10.1046/j.1471-4159.1996.66020873.x

Moyes, C. D., Mathieu-Costello, O. A., Tsuchiya, N., Filburn, C., and Hansford, R. G. (1997). Mitochondrial biogenesis during cellular differentiation. *Am. J. Physiol.* 272(4 Pt 1), C1345–C1351. doi: 10.1152/ajpcell.1997.272.4.C1345

Palumbo, A. (2005). Nitric oxide in marine invertebrates: a comparative perspective. *Comp. Biochem. Physiol. A Mol. Integr. Physiol.* 142, 241–248. doi: 10.1016/j.cbpb.2005.05.043

Parrino, V., Kraus, D. W., and Doeller, J. E. (2000). ATP production from the oxidation of sulfide in gill mitochondria of the ribbed mussel. *Geukensia demissa*. *J. Exper. Biol.* 203, 2209–2218.

Philipp, E. E. R., Lipinski, S., Rast, J., and Rosenstiel, P. (2012). "Immune defense of marine invertebrates: the role of reactive oxygen and nitrogen species oxidative stress in aquatic ecosystems," in *Oxidative Stress in Aquatic Ecosystems*, eds D. Abele, J. P. Vázquez-Medina, and T. Zenteno-Savín. doi: 10.1002/9781444345988.ch17

Poderoso, J. J., Carreras, M. C., Lisdero, C., Riobó, N., Schöpfer, F., and Boveris, A. (1996). Nitric oxide inhibits electron transfer and increases superoxide radical production in rat heart mitochondria and submitochondrial particles. *Archiv. Biochem. Biophys.* 328, 85–92. doi: 10.1006/abbi.1996.0146

Rivera-Ingraham, G. A., Bickmeyer, U., and Abele, D. (2013a). The physiological response of the marine platyhelminth *Macrostomum lignano* to different environmental oxygen concentrations. *J. Exp. Biol.* 216, 2741–2751. doi: 10.1242/jeb.081984

Rivera-Ingraham, G. A., Rocchetta, I., Bickmeyer, U., Meyer, S., and Abele, D. (2016). Spatial compartmentalization of free radical formation and mitochondrial heterogeneity in bivalve gills revealed by live-imaging techniques. *Front. Zool.* 13:4. doi: 10.1186/s12983-016-0137-1

Rivera-Ingraham, G. A., Rocchetta, I., Meyer, S., and Abele, D. (2013b). Oxygen radical formation in anoxic transgression and hypoxia-reoxygenation: foe or phantom? Experiments with an anoxia tolerant bivalve. *Mar. Environ. Res.* 92, 110–119. doi: 10.1016/j.marenvres.2013.09.007

Schipp, R., and Gebauer, M. (1999). Nitric oxide: a vasodilatatory mediator in the cephalic aorta of *Sepia officinalis* (L.) (Cephalopoda). *Invertebr. Neurosci.* 4, 9–15. doi: 10.1007/s101580050002

Sinha, S. (2011). *Studying the Role of Nitric Oxide in Initiating Angiogenesis and Its Patterning*. Ph.D. thesis, Anna University.

Stief, P. (2013). Stimulation of microbial nitrogen cycling in aquatic ecosystems by benthic macrofauna: mechanisms and environmental implications. *Biogeosciences* 10:7829. doi: 10.5194/bg-10-7829-2013

Sukhotin, A., Abele, D., and Pörtner, H.-O. (2006). Ageing and metabolism of *Mytilus edulis*: populations from various climate regimes. *J. Shellfish Res.* 25, 893–899. doi: 10.2983/0730-8000(2006)25[893:AAMOME]2.0.CO;2

Svenningsen, N. B., Heisterkamp, I. M., Sigby-Clausen, M., Larsen, L. H., Nielsen, L. P., Stief, P., et al. (2012). Shell biofilm nitrification and gut denitrification contribute to emission of nitrous oxide by the invasive freshwater mussel *Dreissena polymorpha* (zebra mussel). *Appli. Environ. Microbiol.* 78, 4505–4509. doi: 10.1128/AEM.00401-12

Tafalla, C., Gómez-León, J., Novoa, B., and Figueras, A. (2003). Nitric oxide production by carpet shell clam (*Ruditapes decussatus*) hemocytes. *Develop. Compar. Immunol.* 27, 197–205. doi: 10.1016/S0145-305X(02)00098-8

Taylor, C. T., and Moncada, S. (2010). Nitric oxide, cytochrome C oxidase, and the cellular response to hypoxia. *Arterioscler. Thrombosis Vasc. Biol.* 30, 643–647. doi: 10.1161/ATVBAHA.108.181628

Tielens, A. G., Rotte, C., van Hellemond, J. J., and Martin, W. (2002). Mitochondria as we don't know them. *Trends Biochem. Sci.* 27, 564–572. doi: 10.1016/S0968-0004(02)02193-X

Turrens, J. F., Freeman, B. A., Levitt, J. G., and Crapo, J. D. (1982). The effect of hyperoxia on superoxide production by lung submitochondrial particles. *Archiv. Biochem. Biophys.* 217, 401–410. doi: 10.1016/0003-9861(82)90518-5.

van Faassen, E. E., Bahrami, S., Feelisch, M., Hogg, N., Kelm, M., Kim-Shapiro, D. B., et al. (2009). Nitrite as regulator of hypoxic signaling in mammalian physiology. *Medic. Res. Rev.* 29, 683–741. doi: 10.1002/med.20151

Van Winkle, W. J. (1968). The effects of season, temperature and salinity on the oxygen consumption of bivalve gill tissue. *Compar. Biochem. Physiol.* 26, 69–80. doi: 10.1016/0010-406X(68)90313-7

Zandee, D., Kluytmans, J., Zurburg, W., and Pieters, H. (1980). Seasonal variations in biochemical composition of *Mytilus edulis* with reference to energy metabolism and gametogenesis. *Netherl. J. Sea Res.* 14, 1–29. doi: 10.1016/0077-7579(80)90011-3

Conflict of Interest Statement: The authors declare that the research was conducted in the absence of any commercial or financial relationships that could be construed as a potential conflict of interest.

frontiers in Physiology

ORIGINAL RESEARCH
published: 15 March 2019
doi: 10.3389/fphys.2019.00213

Variation in Thermal Tolerance and Its Relationship to Mitochondrial Function Across Populations of *Tigriopus californicus*

Alice E. Harada, Timothy M. Healy and Ronald S. Burton*

Marine Biology Research Division, Scripps Institution of Oceanography, University of California, San Diego, La Jolla, CA, United States

Variation in thermal tolerance plays a key role in determining the biogeographic distribution of organisms. Consequently, identifying the mechanistic basis for thermal tolerance is necessary for understanding not only current species range limits but also the capacity for range limits to shift in response to climate change. Although variation in mitochondrial function likely contributes to variation in thermal tolerance, the extent to which mitochondrial function underlies local thermal adaptation is not fully understood. In the current study, we examine variation in thermal tolerance and mitochondrial function among three populations of the intertidal copepod *Tigriopus californicus* found across a latitudinal thermal gradient along the coast of California, USA. We tested (1) acute thermal tolerance using survivorship and knockdown assays, (2) chronic thermal tolerance using survivorship of nauplii and developmental rate, and (3) mitochondrial performance at a range of temperatures using ATP synthesis fueled by complexes I, II, and I&II, as well as respiration of permeabilized fibers. We find evidence for latitudinal thermal adaptation: the southernmost San Diego population outperforms the northernmost Santa Cruz in measures of survivorship, knockdown temperature, and ATP synthesis rates during acute thermal exposures. However, under a chronic thermal regime, survivorship and developmental rate are more similar in the southernmost and northernmost population than in the mid-range population (Abalone Cove). Though this pattern is unexpected, it aligns well with population-specific rates of ATP synthesis at these chronic temperatures. Combined with the tight correlation of ATP synthesis decline and knockdown temperature, these data suggest a role for mitochondria in setting thermal range limits and indicate that divergence in mitochondrial function is likely a component of adaptation across latitudinal thermal gradients.

Keywords: local adaptation, ATP synthesis, intertidal, timescale, ectotherm, copepod, latitudinal gradient

OPEN ACCESS

Edited by:
Pierre Blier,
University of Québec in Rimouski, Canada

Reviewed by:
Marco Passamonti,
University of Bologna, Italy
Nicolas Pichaud,
Université de Moncton, Canada
Eric Pante,
Centre National de la Recherche Scientifique (CNRS), France

****Correspondence:***
Alice E. Harada
aharada@ucsd.edu

Specialty section:
This article was submitted to Aquatic Physiology, a section of the journal Frontiers in Physiology

Received: *18 September 2018*
Accepted: *19 February 2019*
Published: *15 March 2019*

Citation:
Harada AE, Healy TM and Burton RS (2019) Variation in Thermal Tolerance and Its Relationship to Mitochondrial Function Across Populations of Tigriopus californicus. Front. Physiol. 10:213. doi: 10.3389/fphys.2019.00213

INTRODUCTION

Environmental temperature is one of the most influential abiotic factors in shaping the performance and survival of organisms (Hochachka and Somero, 2002). Upper and lower thermal limits of populations and species typically increase from the poles to the equator (Sunday et al., 2011), and in general, maximum habitat temperatures at equatorward range

limits closely match maximum tolerated temperatures (Sunday et al., 2012). Temperatures that limit organismal performance also often align with habitat temperatures that occur over prolonged periods (i.e., seasons) (Johnston and Dunn, 1987; Pörtner, 2010). Together, these observations suggest that variation in temperature and upper thermal tolerance play key roles in determining the biogeographic distribution of organisms (Pörtner, 2010; Sunday et al., 2011, 2012; Deutsch et al., 2015). Thus, identifying the mechanistic basis for differences in upper thermal limits among species and populations is necessary to understand not only current species range limits but also the capacity for range limits to shift as a result of local genetic adaptation and phenotypic plasticity in response to natural or anthropogenic climate change (Pörtner et al., 2006; Pritchard and Di Rienzo, 2010; Sunday et al., 2012; Seebacher et al., 2015; Bay et al., 2017; Healy et al., 2018).

Mitochondria play a role in a diversity of cellular functions (e.g., calcium signaling, cell growth and differentiation, cell cycle control, and cell death), and their central role in energy metabolism suggests that mitochondria may be intimately associated with thermal performance and tolerance in ectotherms. For instance, the loss of mitochondrial ATP synthesis capacity in fish hearts is thought to occur at temperatures immediately below tolerance limits during acute exposures to high temperatures (Iftikar and Hickey, 2013; Christen et al., 2018; O'Brien et al., 2018). In contrast, in some species, the loss of whole organism tolerance occurs at temperatures below those resulting in decreased mitochondrial oxidative capacity (e.g., see Dahlhoff et al., 1991;

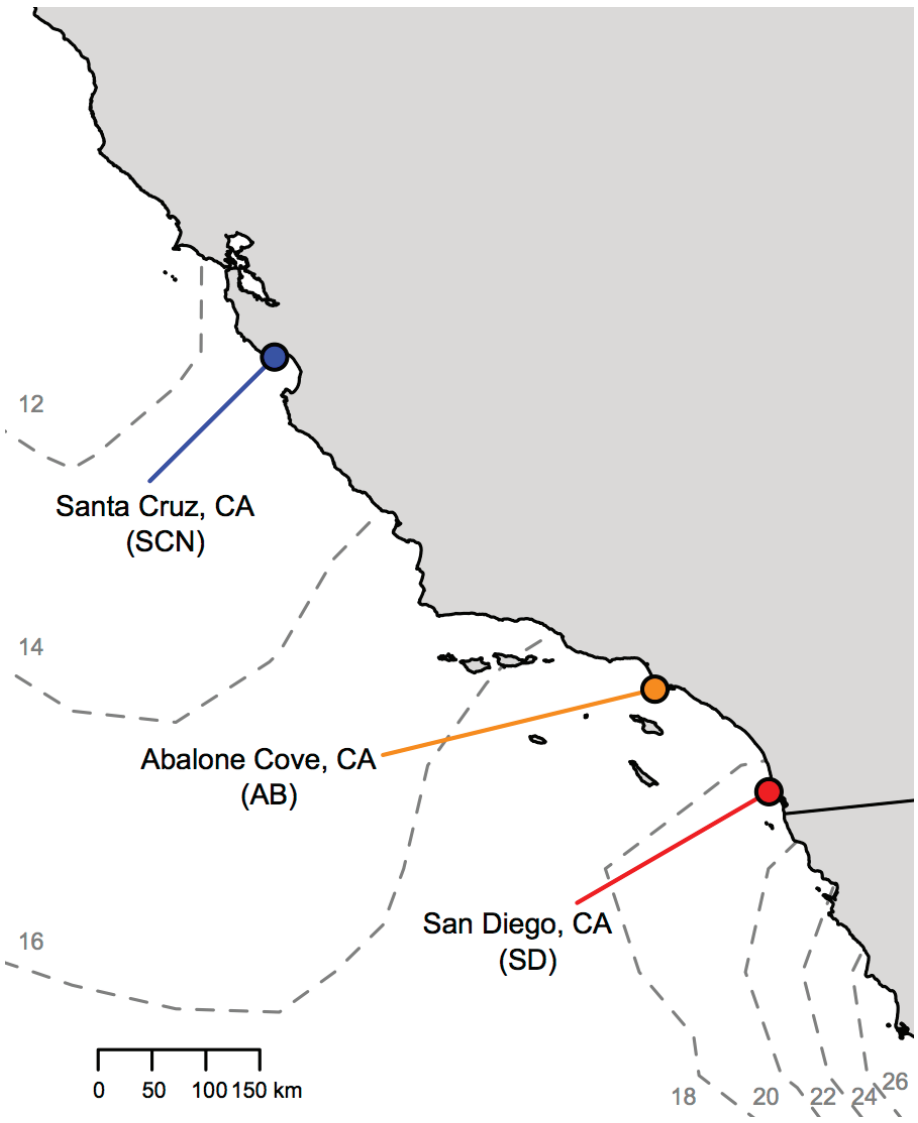

FIGURE 1 | Locations of *T. californicus* collection sites along the coast of California (gray = land; white = Pacific Ocean). Sites are indicated by colored circles [red = San Diego (SD); orange = Abalone Cove (AB); blue = Santa Cruz (SCN)]. Dashed gray lines outline contours of average sea surface temperatures from the first week of July 2017 with temperature in degrees Celsius indicated by small gray numbers (obtained from: http://www.cpc.ncep.noaa.gov/products/GIS/GIS_DATA/sst_oiv2/index.php).

Dahlhoff and Somero, 1993). In any case, relative changes in mitochondrial oxidative phosphorylation and proton leak at sublethal temperatures may underlie thermal limits for whole-organism aerobic capacity and variation in aerobic capacity across temperatures (e.g., Pörtner, 2001). In addition, mitochondrial functions are known to respond to temperature both as a result of phenotypic plasticity and local genetic adaptation through changes in mitochondrial amount (Egginton and Johnston, 1984; Orczewska et al., 2010; Dhillon and Schulte, 2011; O'Brien, 2011), oxidative capacity (Guderley, 2004; Kraffe et al., 2007; Grim et al., 2010; Seebacher et al., 2010; Chung and Schulte, 2015; Chung et al., 2017a), oxygen affinity (Chung et al., 2017b), membrane composition (Hazel, 1995; Kraffe et al., 2007; Grim et al., 2010; Chung et al., 2018a), and enzyme activities and amounts (St-Pierre et al., 1998; Guderley, 2004; McClelland et al., 2006; LeMoine et al., 2008; Orczewska et al., 2010), which clearly suggest that modulation of mitochondrial functions is an important component of cellular responses to temperature change. Thus, although variation in mitochondrial functions likely contributes to the mechanistic basis for variation in thermal tolerance, neither the role of mitochondrial mechanisms across different timescales of thermal exposure (i.e., acute versus chronic) nor the extent to which variation in mitochondrial functions underlies local thermal adaptation across environmental temperature gradients is fully understood.

In the current study, we examine variation in thermal tolerance and mitochondrial function among three populations of the intertidal copepod *Tigriopus californicus* found across a latitudinal thermal gradient along the coast of California, USA (**Figure 1**). *T. californicus* inhabits high-intertidal splash pools on the west coast of North America from Baja California, Mexico, to Alaska, USA, and is an ideal candidate species to study local genetic adaptation of both thermal tolerance and mitochondrial functions. Gene flow among populations of *T. californicus* is remarkably low even over short distances (Burton, 1998; Willett and Ladner, 2009; Peterson et al., 2013), and consequently, there are high levels of genetic divergence among populations both in genes encoded in the mitochondrial genome and in genes in the nuclear genome that encode products that function in the mitochondria (e.g., 9.5–26.5% sequence divergence in the mitochondrial genome among populations with Fst ≈ 0.98 across a large number of populations; Edmands, 2001; Peterson et al., 2013; Pereira et al., 2016; Barreto et al., 2018). Furthermore, there is substantial evidence for local adaptation of upper thermal tolerance among populations of *T. californicus,* with more southern populations generally able to tolerate higher temperatures than more northern populations (Willett, 2010; Kelly et al., 2012; Tangwancharoen and Burton, 2014; Hong and Shurin, 2015; Pereira et al., 2017; Leong et al., 2018; Willett and Son, 2018).

Differences in mitochondrial genotype and function have been linked to variation in thermal performance in species of *Drosophila* (Pichaud et al., 2012; Hoekstra et al., 2013); however, previously published studies in *T. californicus* have not directly addressed this potential mechanistic relationship. It has been observed that disruption of mitochondrial functions in inter-population F_2 hybrids of *T. californicus* does not result in decreased thermal tolerance (Willett, 2012; Pereira et al., 2014), despite lower mitochondrial ATP synthesis capacities at 20°C (Ellison and Burton, 2008). However, ATP synthesis capacity has not been measured during exposures to high temperatures in *T. californicus,* and thus it is possible that mitochondrial dysfunction may play a role in determining variation in upper thermal tolerance in this species in general. To investigate the mechanistic relationships between upper thermal tolerance and mitochondrial function in *T. californicus* and how these relationships may contribute to latitudinal thermal adaptation across timescales (i.e., acute versus chronic or within-generation versus across-generations), here we assess (1) intraspecific variation in upper thermal tolerance and performance among populations using survivorship of heat stresses from 34 to 37°C, knockdown temperatures, developmental survivorship, and developmental rate at 20 and 25°C, (2) inter-population variation in mitochondrial ATP synthesis capacity and thermal sensitivity of ATP synthesis rates during acute thermal exposure, and (3) variation in mitochondrial oxidative and leak respiration rates among populations at both intermediate and high temperatures.

MATERIALS AND METHODS

Copepod Collection and Culture

Tigriopus californicus were collected from high rocky tide pools at three locations in California, USA (**Figure 1**): "SD" from Ocean Beach, San Diego County (32° 45′ N, 117° 15′ W); "AB" from Abalone Cove, Los Angeles County (33° 44′ N, 118° 22′ W); and "SCN" from Santa Cruz County (36° 56′ N, 122° 02′ W). These populations are found across a latitudinal gradient in temperature along ~775 km of the coast of California with about a 6°C difference in sea surface temperature (**Figure 1**) and ~4°C difference in mean annual air temperatures (e.g., Pereira et al., 2017) from SD to SCN.

Copepods were kept in multiple 400-ml beakers containing 250-ml filtered seawater (0.4 μm, 35 ppt). Cultures were fed ad libitum with a combination of ground TetraVeggie algae wafers and powdered Spirulina. Prior to use in any thermal exposure assays, cultures were maintained in the laboratory for at least 1 month (one generation) at 20°C with a 12-h light/dark cycle.

Survivorship of Acute Heat Stress Across Temperatures

Tolerance of a 1-hour heat stress at different temperatures was measured using methods similar to those previously described for *T. californicus* (Willett, 2010; Kelly et al., 2012; Tangwancharoen and Burton, 2014; Pereira et al., 2017; Leong et al., 2018; Willett and Son, 2018). In brief, groups of 10 adult copepods from each population were removed from stock cultures by glass pipette and transferred to separate 15-ml Falcon™ tubes (Thermo Fisher Scientific, Waltham, MA) containing 10-ml of 20°C filtered seawater. After 10 min, the tubes were submerged in a preheated water bath (Julabo USA Inc., Allentown, MA) at one of four temperatures: 34, 35, 36, or 37°C. Following 1 h of heat stress, tubes were

moved to a beaker containing 20°C water for an additional hour to allow the temperature inside the tubes to gradually decrease back to holding conditions. Copepods were then transferred to a fresh 10-cm petri dish containing 20°C filtered seawater. Tolerance of the acute high temperature exposures was assessed after 3 days as the proportion of surviving individuals in each group of 10 (n = 6 per population and temperature).

Knockdown Temperature

Maximum tolerated temperature during a ramping heat stress was assessed by knockdown temperature (i.e., the temperature at which movement and responsiveness cease; e.g., Gilchrist and Huey, 1999; Hoffmann et al., 2003). For each trial, eight adult copepods from each population were individually pipetted from stock cultures into 0.2-ml strip tubes (without caps) and carryover water was replaced with 100 µl of 20°C filtered seawater. After approximately a 10-min recovery, the strip tubes were placed in an Applied Biosystems SimpliAmp™ Thermal Cycler (Thermo Fisher Scientific, Waltham, MA). Locations of individuals from each population were randomized in the thermal cycler for each trial. The heat stress regime utilized the AutoDelta function of the thermal cycler with the following protocol: 20°C for 5 min, +0.1°C every 20 s from 20 to 32°C, and +0.1°C every 60 s from 32 to 45°C. The thermal cycler lid was left open during the temperature ramp and copepods were monitored continuously from above. Once a copepod stopped responding to gentle tapping of their tube, loss of responsiveness was assessed by cycling 40 µl of the water in the tube with a micropipette taking care not to touch the copepod directly. In general, this manipulation results in the observation of active swimming behavior in *T. californicus*; however, at high temperatures, this response is no longer observed and copepods gradually sink to the bottom of the tubes passively. If a copepod actively responded to the water movement, responsiveness tests were paused and monitoring continued. If no active response was observed, the responsiveness test was repeated up to three times (total time for end-point determination for an individual was ~6 s). The first temperature at which a copepod did not respond to three successive tests was recorded as the individual's knockdown temperature (n = 16 per population over two trials). After this end point was determined, individuals were transferred by glass pipette to recovery 10-cm petri dishes containing 20°C filtered seawater (one per population); survivorship 1 day after the assay was >90%.

Developmental Survival and Rate

Gravid females with mature (red) egg sacs were removed from stock cultures by glass pipette and immobilized on filter paper (n = 24 per population). Egg sacs were dissected from the females with a needle and placed in 6-well plates containing 20°C filtered seawater (one egg sac per well). Eggs were allowed to hatch overnight at 20°C, and in the morning, the nauplii (i.e., offspring) from each sac were counted and split between two 6-well plates (one well per plate per egg sac). The two plates were incubated for 21 days at 20 or 25°C (one plate per temperature). Spirulina was added to each well twice per week as a food source, and salinity was adjusted using addition of deionized water to compensate for evaporation weekly. On days 7, 14, and 21, surviving individuals and the number of nauplii that had metamorphosed into copepodids were counted in each well. The number of wells in which adult males were observed was also recorded. The presence of adult males, rather than females, was used, because the final molt to adult male *T. californicus* results in visually conspicuous antennae that are used in mating behaviors (Burton, 1985; Tsuboko-Ishii and Burton, 2017). In contrast, young adult females are visually difficult to distinguish from juvenile females and males until later stages of maturity (Burton, 1985) and thus are suboptimal indicators of developmental stage.

For measurement of developmental rate at 20 and 25°C, mature egg sacs were dissected and split post-hatch as described above (n = 18, 16, and 18 for SD, AB, and SCN, respectively), but in this case split egg sacs were pooled into 10-cm petri dishes (one dish per population and temperature) and developmental stage was monitored daily. The rate of development was tracked by the day of appearance of copepodids in the dish and was scored for each individual (Tangwancharoen and Burton, 2014). Regardless of developmental temperature, the survivorship of offspring for all populations was 78.6–94.0%, and all surviving individuals metamorphosed by 14 days post clutch split.

ATP Synthesis Rate

ATP synthesis assays were conducted using similar methods to those of Ellison and Burton (2006). Mitochondria were isolated from groups of 30 adult copepods per assay (n = 6 per population). Preliminary tests indicated that this number of copepods was sufficient to show linear ATP production over time for at least 1 h across the range of temperatures tested in this study (20 to 40°C). Copepods were rinsed with 200 µl ice cold homogenization buffer (400 mM sucrose, 100 mM KCl, 6 mM EGTA, 3 mM EDTA, 70 mM HEPES, 1% w/v BSA, pH 7.6) (Moyes et al., 1985) and homogenized on ice in 800 µl homogenization buffer with a teflon on glass homogenizer. The homogenate was transferred to 1.5-ml microcentrifuge tubes (Eppendorf, Hamburg, Germany) and centrifuged at 1,000 g for 5 min at 4°C. The supernatant was transferred to new microcentrifuge tubes and was centrifuged at 11,000 g for 10 min at 4°C. The supernatant resulting from this second centrifugation was then removed and the pellet was resuspended in 255 µl assay buffer (560 mM sucrose, 100 mM KCl, 10 mM KH_2PO_4, 70 mM HEPES, pH 7.6; modified from Moyes et al., 1985).

Mitochondrial isolations were split into ten 25-µl aliquots in PCR tubes for ATP synthesis assays at nine incubation temperatures (one tube per temperature: 20, 25, 30, 35, 36, 37, 38, 39, and 40°C, and one tube for measurement of initial ATP concentrations in the assays). The remaining 5 µl of isolate was used for protein content determination. To initiate synthesis assays, 5 µl of a substrate cocktail was added to each tube, and then the tubes were incubated at the desired temperature for 10 min in an Applied Biosystems SimpliAmp™ Thermal

Cycler (Thermo Fisher Scientific, Waltham, MA). The substrate cocktail depended on the electron transport system (ETS) complexes that were used to drive electron transport and subsequent ATP synthesis. In our study, we measured ATP synthesis rate as a result of electron donation to complex I (CI; final substrate concentrations in assay: 5 mM pyruvate, 2 mM malate, and 1 mM ADP), complex II (CII; final substrate concentrations in assay: 10 mM succinate, 0.5 µM rotenone, and 1 mM ADP), and complex I and complex II in combination (CI&II; final substrate concentrations in assay: 5 mM pyruvate, 2 mM malate, 10 mM succinate, and 1 mM ADP). After the incubation period, 25 µl of each assay was added to an equal volume of CellTiter-Glo (Promega, Madison, WI), which both halts ATP synthesis and allows quantification of ATP concentration. Tubes used to measure initial ATP concentrations in the assays also had 5 µl of substrate cocktail, but CellTiter-Glo was added immediately following substrate addition. Therefore, these tubes accounted for any signal that was not a result of ATP synthesis during the assays. After a 10-min incubation at room temperature, the samples and controls were mixed by shaking, read on a luminometer, and compared with a set of ATP standards (5 nM to 10 µM prepared in assay buffer; 25 µl of each standard was mixed with 25 µl of CellTiter-Glo as described above for samples and controls). ATP synthesis rates were calculated after control values were subtracted from sample values, and rates were then normalized for protein content in the corresponding mitochondrial isolation using NanoOrange Protein Quantitation Kit assays (Thermo Fisher Scientific, Waltham, MA) according to the manufacturer's instructions. Note that, while our buffer contained compounds (HEPES, sucrose, and potassium chloride) that have the potential to interfere with this assay at high concentrations (10, 10, and 20 mM, respectively), the final concentrations present after dilution were below these maxima for HEPES and potassium chloride (1.37 and 1.96 mM, respectively), and sucrose concentration was approximately the maximum recommended according to the manufacturer's instructions (10.98 mM).

High-Resolution Respirometry of Cell-Permeabilized Copepods

Respirometry was performed using a Clark-type electrode system (Oxygraph Plus System, Hansatech Instruments Ltd., England). The electrode was calibrated at either 20 or 35°C using air-saturated assay buffer (see "ATP synthesis rate" section above). Groups of 40 adult copepods were crudely homogenized using blue polypropylene pestles (Thomas Scientific, Swedesboro, NJ) in a 1.5-ml microcentrifuge tube to which 500 µl cold (~0°C) BIOPS was added (2.77 mM CaK_2EGTA, 7.23 mM K_2EGTA, 5.77 mM ATP, 6.56 mM $MgCl_2$, 20 mM taurine, 15 mM Phosphocreatine, 20 mM imidazole, 0.5 mM dithiothreitol, 50 mM K-MES, pH 7.1; Lemieux et al., 2011). Homogenized animals were then permeabilized by incubation in BIOPS containing 81.25 µg ml^{-1} saponin (concentration determined from Pichaud et al., 2011, and preliminary trials) for 30 min at 4°C prior to use in respirometry assays. After incubation, BIOPS was removed and 500 µl of assay buffer was added. The permeabilized copepods in assay buffer were then transferred into the respirometry chamber. The ETS was activated with CI substrates (5 mM pyruvate and 5 mM malate) and 2.5 mM ADP, after which state 3 respiration rate was measured (i.e., the maximal respiration rate under phosphorylating conditions; Scheffler, 2008). A 10 µM cytochrome c was then added to assess membrane integrity and in general resulted in no change in respiration rate. Next, 2 µg ml^{-1} oligomycin was added to measure state 4_{ol} respiration rate. State 4 is the rate of respiration in the absence of phosphorylation of ADP, which is the minimum rate required to counter proton leak and maintain proton motive force across the inner mitochondrial membrane; state 4_{ol} achieves this artificially with the addition of oligomycin, which inhibits complex V (Scheffler, 2008). Concentrations of substrates and inhibitors were modified from Pesta and Gnaiger (2012) based on preliminary trials.

Statistical Analyses

All statistical analyses were performed in R v3.4.0 (R Core Team, 2017) using generalized linear models (GLM) and ANOVA followed by post-hoc tests with a threshold for statistical significance of $\alpha = 0.05$. Differences in survival of 1-h acute heat stress were tested with population and exposure temperature as factors in a logistic GLM with a binomial error distribution. Pairwise comparisons among temperatures within populations and among populations within temperatures were conducted by t tests (paired or unpaired as appropriate) with a Bonferroni correction to determine significance. Data for knockdown temperatures and clutch sizes were analyzed by ANOVA with population as a factor followed by Tukey post-hoc tests. The same procedure was utilized to analyze mitochondrial respiration data, but population was added as an additional explanatory factor. Variation in time to metamorphosis (i.e., developmental rate) was assessed among treatments (populations x temperature) by Kruskal-Wallis ANOVA followed by Nemenyi tests. Significance of all pairwise comparisons was determined after a Bonferroni correction of alpha. Differences in developmental survival were calculated for each egg sac (25–20°C; see **Table S1** for group means, metamorphosis and adult proportions) and were analyzed by mixed-effect linear models with fixed effects of population and day and a random effect of egg sac. Post-hoc comparisons were then performed with Tukey tests. Mixed-effect models were also used to assess variation in ATP synthesis rates with population and temperature as fixed effects and mitochondrial isolation as a random effect. Post-hoc pairwise comparisons for ATP synthesis rate were conducted similarly to those for survival of 1-h heat stress but with the use of the Benjamini-Hochberg method to correct for multiple comparisons (Benjamini and Hochberg, 1995). In all cases, interactions between factors were included in the fitted linear models. ANOVA tables for all statistical tests obtained from R are available in the supplementary materials (**Tables S2–S12**).

RESULTS

Thermal Tolerance and Performance

Patterns of variation in tolerance of acute heat stress among populations of *T. californicus* were consistent regardless of the methods used to assess tolerance. Survivorship of 1-h heat stress was affected by a significant interaction between population and exposure temperature ($p = 5.8 \times 10^{-5}$; **Figure 2A**). Post-hoc comparisons detected significant declines in survivorship between 35 and 36°C in all populations ($p \leq 1.4 \times 10^{-5}$). However, the survival proportion of SCN was lower than that of SD at 35°C ($p = 6.9 \times 10^{-4}$) and was lower than the survival proportions of both SD and AB at 36 and 37°C ($p \leq 9.1 \times 10^{-8}$). This pattern of decreased upper thermal tolerance in the northern SCN population was also observed through variation in knockdown temperature among populations ($p = 6.1 \times 10^{-11}$; **Figure 2B**). For both measurements of acute upper thermal tolerance, there were slight trends for lower mean tolerance in AB copepods than in SD copepods, but these trends were not supported statistically after correction for multiple comparisons (1-h heat stress: $p \geq 9.5 \times 10^{-3}$ compared to corrected $\alpha = 1.7 \times 10^{-3}$; knockdown temperature: $p = 0.63$).

We observed significant variation in the number of eggs per clutch among populations ($p = 1.0 \times 10^{-12}$; **Figure 3A**) with smaller egg sacs from AB females than those from either SD or SCN females ($p < 1.0 \times 10^{-4}$). Differences in survival of offspring from split egg clutches over 3 weeks of development and early adulthood at 20 and 25°C were significantly affected by an interaction between population and time ($p = 2.4 \times 10^{-3}$; **Figure 3B**). In general, development at 25°C had either no effect or negative effects on survival compared to development at 20°C in all three populations. There was no variation in the relative effects of development at 25°C on survival with time in either SD or SCN ($p \geq 0.97$), and there were trends for greater negative effects of 25°C on survival in SCN than in SD on all days, but these trends were not significant in post-hoc tests ($p \geq 0.23$). In contrast, the difference in survival between 25 and 20°C in AB became more negative over the 3 weeks with a significant decrease in relative survival at 21 days compared to 7 or 14 days ($p \leq 1.7 \times 10^{-2}$). Additionally, on day 21, the difference in survival between 25 and 20°C was significantly lower in AB than in SD ($p < 1.0 \times 10^{-3}$). Not surprisingly, there were also significant effects of temperature on developmental rate in all three populations with more rapid development at 25°C than at 20°C ($p < 2.8 \times 10^{-11}$ for all populations; **Figure 3C**), although the decrease in median time to metamorphosis varied among populations (7, 8, and 9 days post clutch split at 20°C to 4, 5, and 7 days post clutch split at 25°C for SCN, SD, and AB, respectively). There were also significant effects of population on time to metamorphosis at both temperatures: at 20°C, SCN developed faster than either SD or AB ($p < 8.9 \times 10^{-11}$ for both), and at 25°C, all three populations were significantly different from each other with fastest development in SCN, slowest development in AB, and intermediate developmental rate in SD ($p \leq 5.8 \times 10^{-3}$). Overall, these results suggest modest negative effects of 25°C on development in *T. californicus*, which are generally more pronounced in AB than in the other two populations in our study. Furthermore, AB demonstrates lower performance (i.e., smaller clutch sizes or slower developmental rate) than SD or SCN even at 20°C.

ATP Synthesis Rate and Mitochondrial Respiration

Regardless of the substrates and complexes used (CI, CII, or CI&II) to donate electrons to the ETS and drive ATP synthesis, synthesis rate was affected by significant interactions between population and temperature ($p \leq 5.1 \times 10^{-3}$). If electrons were donated to both CI and CII (**Figure 4A**), ATP synthesis rate increased from 20 to 30°C in all three populations. Synthesis rate then plateaued from 30 to 35°C in SCN and from 30 to 36°C in SD and AB. Above these

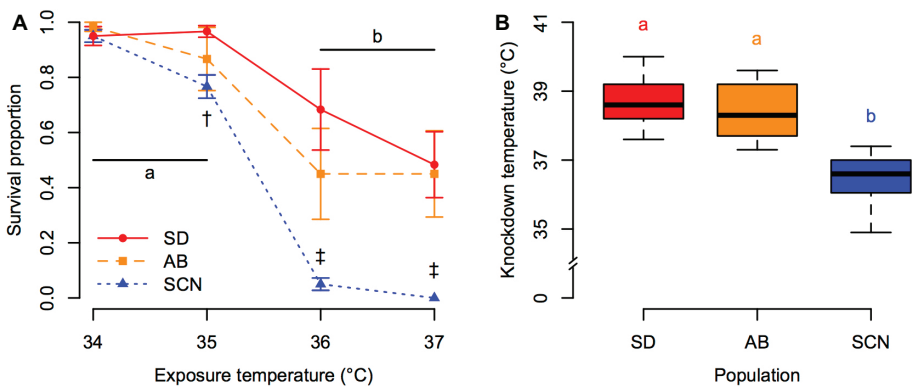

FIGURE 2 | Acute upper thermal tolerance assessed by survivorship of 1-h heat stress **(A)** and knockdown temperature **(B)** in San Diego (SD; red, circles, solid lines), Abalone Cove (AB; orange, squares, dashed lines), and Santa Cruz (SCN; blue, triangles, dotted lines) copepods. **(A)** Data are presented as mean ± SEM; shared letters indicate temperatures that are not significantly different within populations; dagger symbols indicate differences among populations within a temperature († = SCN different from SD, ‡ = SCN different from SD and AB). **(B)** Data are presented as box plots; shared letters indicate populations that do not differ significantly.

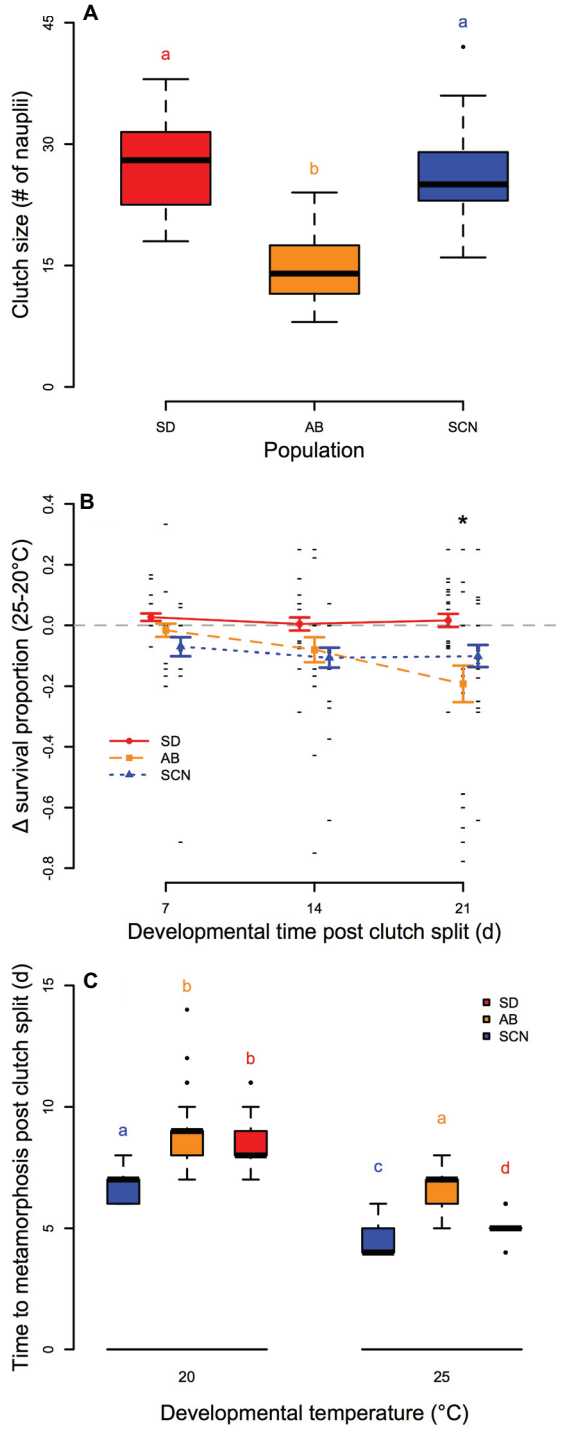

FIGURE 3 | Egg clutch size **(A)**, survival of development at 25°C compared to 20°C **(B)**, and time to metamorphosis at 20 and 25°C **(C)** in San Diego (SD; red, circles, solid lines), Abalone Cove (AB; orange, squares, dashed lines), and Santa Cruz (SCN; blue, triangles, dotted lines) copepods. **(A,C)** Data are presented as box plots; shared letters indicate groups that are not significantly different. **(B)** Data are presented as mean ± SEM; small black dashes display difference for individual clutches; asterisk indicates a significantly lower difference in survival between 25 and 20°C at 21 days than at 7 or 14 days for AB and a significant difference between SD and AB at 21 days.

temperatures, ATP synthesis declined rapidly, and at temperatures greater than 36°C, rates in SCN were either lower than those in AB ($p \leq 8.2 \times 10^{-3}$; 37 and 40°C) or lower than those in AB and SD ($p \leq 2.5 \times 10^{-2}$; 38 and 39°C). SCN ATP synthesis rate was also significantly higher than AB ATP synthesis rate at 25°C ($p = 3.8 \times 10^{-2}$). If only CI substrates were used to drive ATP synthesis (**Figure 4B**), there were increases in synthesis rate with temperature from 20 to 35°C in all populations. At temperatures above 35°C, synthesis rate rapidly declined with temperature in SD and SCN, whereas in AB rates plateaued from 35 to ~37°C before declining at higher temperatures. As a result, there were no significant differences between the populations above 35°C ($p \geq 0.07$). In contrast, CI-driven ATP synthesis was faster in SCN than in AB from 20 to 35°C ($p \leq 3.1 \times 10^{-2}$), and similar trends were observed between SD and AB, although these trends were not detected as significant in post-hoc tests ($0.051 < p < 0.108$ for all). If only CII was used to drive electron transport (**Figure 4C**), patterns of change in ATP synthesis rate with temperature in all populations were similar to those described above for CI&II-fueled ATP synthesis. However, only one population effect on CII-driven synthesis rate was detected by post-hoc tests with a higher rate in AB than in SCN at 40°C ($p = 2.5 \times 10^{-2}$). Taken together, these results suggest that population- or temperature-mediated differences in CI&II ATP synthesis rate in *T. californicus* likely reflect contributions of population and temperature effects on synthesis rate when CI or CII are fueled separately, although under saturating conditions the independent CI and CII rates are not additive when the ETS is provided with both CI and CII substrates in combination. Additionally, our results indicate that AB synthesis rates, particularly when fueled through CI, are compromised relative to at least SCN rates from 20 to ~35°C, and that ATP synthesis capacity suffers high-temperature collapse at lower temperatures in SCN than in either SD or AB.

In general, high-resolution respirometry experiments found that mitochondrial oxygen consumption rates fueled by CI substrates were variable within populations and temperatures in our study, and few differences were resolved statistically. State 3 respiration rate (**Figure 5A**) was not significantly affected by population ($p = 0.47$), temperature ($p = 0.57$), or an interaction between population and temperature ($p = 0.21$), and state 4_{ol} respiration rate (**Figure 5B**) and respiratory control ratio (RCR = state 3/state 4_{ol}; **Figure 5C**) were also unaffected by population ($p \geq 0.19$) or an interaction between population and temperature ($p \geq 0.25$). There were significant main effects of temperature on state IV_{ol} oxygen consumption rate and RCR ($p \leq 3.6 \times 10^{-2}$), but these effects were not resolved by post-hoc tests (within population $p \geq 0.11$). The main effects of temperature that were detected may be a consequence of slight trends for increases in state 4_{ol} respiration rate and decreases in RCR from 20 to 35°C in all populations. Of these trends, the most notable is the decline in mean RCR in SCN at 35°C (post-hoc $p = 0.11$), which may be consistent with the rapid declines in ATP synthesis rate at temperatures above 35°C in SCN described above.

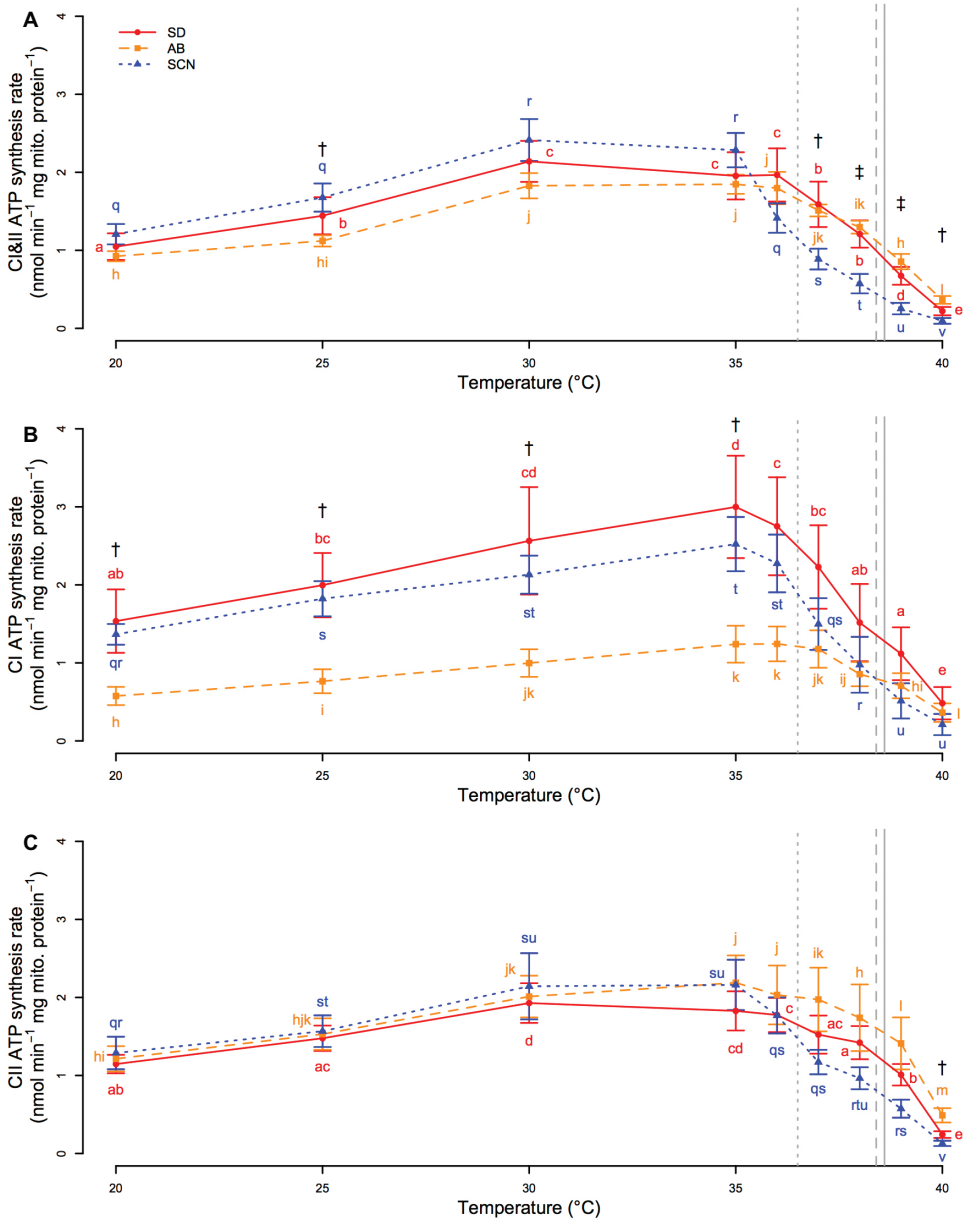

FIGURE 4 | CI&II- **(A)**, CI- **(B)**, and CII-fueled **(C)** ATP synthesis rate from 20 to 40°C in San Diego (SD; red, circles, solid lines), Abalone Cove (AB; orange, squares, dashed lines), and Santa Cruz (SCN; blue, triangles, dotted lines) copepods. Data are presented as mean ± SEM. Letters indicate the results of post-hoc tests within populations. Daggers indicate temperatures at which there is a difference between SCN and AB. Double daggers indicate temperatures at which there is a difference between SCN and both AB and SD. Vertical gray lines display mean knockdown temperatures for each population (SD – solid; AB – dashed; SCN – dotted).

DISCUSSION

The results of the current study demonstrate intraspecific variation in both thermal tolerance and ATP synthesis capacity among allopatric *Tigriopus californicus* populations that are found across a latitudinal thermal gradient. Differences in tolerance of acute high temperatures among populations are generally consistent with variation in habitat temperature, whereas differences in chronic temperature effects among populations are less clearly correlated with environmental temperatures. Populations have temperature-dependent differences in ATP synthesis capacity, as revealed by variation in ATP synthesis rates in isolated mitochondria across temperatures. Furthermore, inter-population differences in loss of synthesis capacity during acute exposure to high temperatures parallel the differences in acute upper thermal tolerance, and variation in ATP synthesis rate among populations at 25°C is potentially consistent with differences in effects of chronic exposure to 25°C on development as well. These results suggest that there are evolved differences in ATP synthesis capacity among populations of *T. californicus* and that these differences

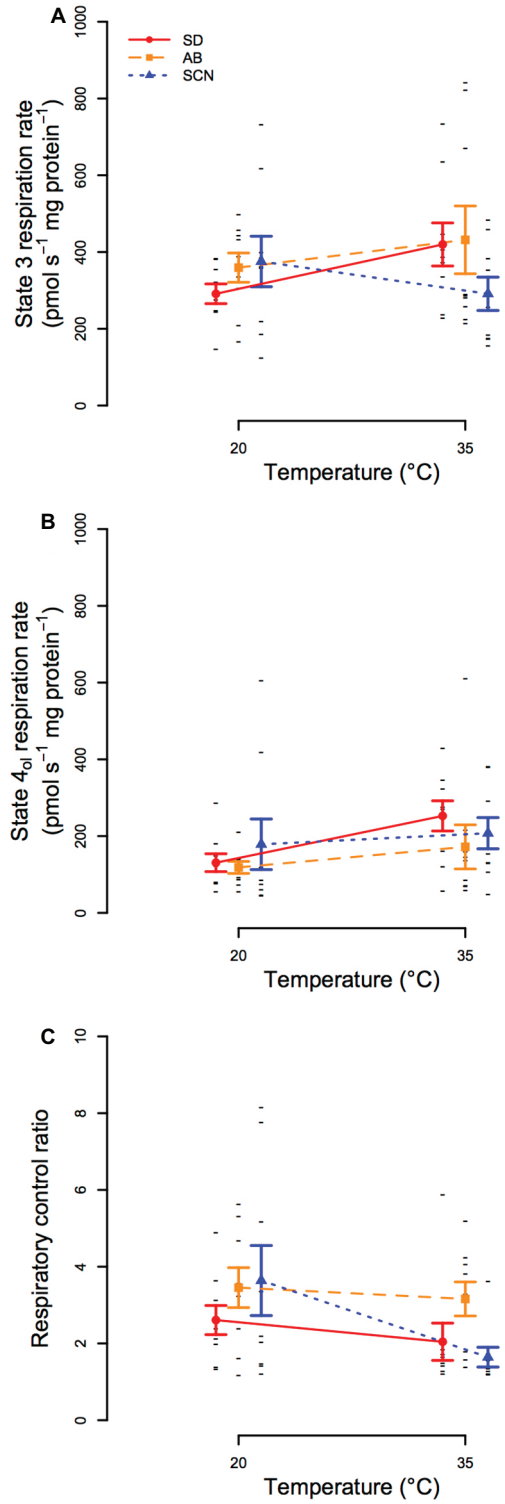

FIGURE 5 | State 3 **(A)** and state 4$_{ol}$ **(B)** mitochondrial respiration and respiratory control ratios (RCRs; **C**) at 20 and 35°C in San Diego (SD; red, circles, solid lines), Abalone Cove (AB; orange, squares, dashed lines), and Santa Cruz (SCN; blue, triangles, dotted lines) copepods. Data are presented as mean ± SEM, and small black dashes display values for each replicate. Significant effects of temperature for state 4$_{ol}$ and RCR were detected by ANOVA, but post-hoc tests did not resolve any statistical differences among groups for all three traits.

are likely involved in local thermal adaptation with latitude in this species, particularly over acute timescales of thermal exposure.

Variation in Thermal Tolerance and Mitochondrial Functions Across Timescales

Several studies have demonstrated intraspecific differences in upper thermal tolerance with latitude in *T. californicus* that are consistent with local thermal adaptation from Mexico to Alaska (Willett, 2010; Kelly et al., 2012; Pereira et al., 2017). These studies employed experimental tests similar to our 1-h heat stress protocol, and our results generally corroborate previous findings for SD, AB, and SCN. Here, we also establish an alternative experimental method to examine variation in acute upper thermal tolerance in *T. californicus* through the use of knockdown temperatures, and we demonstrate that post-hoc tests with data from either of these thermal tolerance methods resolve similar inter-population patterns for variation in upper thermal limits (**Figure 2**). Our knockdown temperature assay is essentially similar to a critical thermal maximum assay (e.g., Beitinger et al., 2000) and provides several advantages such as reducing the number of animals required to measure upper thermal tolerance and allowing repeated tests of variation in upper thermal tolerance among individuals (e.g., Morgan et al., 2018). Therefore, this protocol is likely to facilitate future experiments investigating the genetic basis of variation in upper thermal limits in *T. californicus* and of local thermal adaptation more generally.

There is a growing body of evidence suggesting that collapse of ATP synthesis capacity is mechanistically involved in setting upper thermal limits during acute exposure to high temperature, particularly in fish hearts (Iftikar and Hickey, 2013; Christen et al., 2018; O'Brien et al., 2018). Cardiovascular failure due to arrhythmias is potentially a weak physiological link underlying upper thermal tolerance in fish (e.g., Farrell, 2009), and it is now thought that insufficient energy supply due to decreased mitochondrial ATP synthesis may underlie this heart failure (e.g., Iftikar and Hickey, 2013). Our results suggest that the loss of ATP synthesis capacity may also contribute to setting acute upper thermal limits in *T. californicus* (**Figure 4**), a species that does not rely on a heart to transport oxygen throughout the body. Rapid declines in CI&II-fueled ATP synthesis rate are observed at high temperatures in all three populations in our study, but these declines occur ~1°C lower in SCN than in AB or SD (~36 versus ~37°C; **Figure 4A**). In comparison, mean knockdown temperatures for the three populations are 36.5, 38.4, and 38.6°C for SCN, AB, and SD, respectively. Although the differences between the temperatures that result in high temperature knockdown or initial declines in ATP synthesis capacity vary somewhat among populations, declines in ATP synthesis rate occur at temperatures that are only slightly lower than knockdown temperatures in all cases. Furthermore, if our data are used to estimate CI&II-linked ATP synthesis rate for each population at knockdown temperatures, rates at upper thermal limits are similar regardless of population (0.89, 1.12, and 1.15 nmol min^{-1} mg mito. protein^{-1} for SD, AB, and SCN, respectively).

Here, we also demonstrate inter-population differences in the chronic effects of high temperature on survival and developmental rate in *T. californicus*. In the AB population, development at 25°C resulted in a decrease in survival over time when compared to development at 20°C, and this led to a significant difference in the effects of 25°C on developmental survival in AB compared to SD after 3 weeks (**Figure 3B**). Indeed, there was no evidence for a negative effect of 25°C on survival of development in SD copepods, and similarly, there was no significant effect of 25°C relative to 20°C in SCN. Somewhat contradicting these results for SD and SCN, Edmands and Deimler (2004) found negative effects of 25°C development relative to 15°C development in these populations; but consistent with our study, these authors found no difference between SD and SCN. Regardless, our data suggest that prolonged exposure to 25°C has greater negative effects on AB than on the other two populations in our study.

In all populations, development at 25°C, compared to 20°C, caused an increase in developmental rate (i.e., decrease in time to metamorphosis) that was consistent with temperature coefficients (Q_{10}) of ~2 as would be expected (Hochachka and Somero, 2002); however, the increase in rate was smaller in AB than in either SD or SCN (**Figure 3C**). It is possible that this is simply a consequence of exponential effects of temperature on physiological rates and a lower 20°C rate in AB. Alternatively, there was evidence for reduced ATP synthesis capacity in AB compared to SD or SCN when substrates were provided to both CI and CII (**Figure 4A**) or to CI alone (**Figure 4C**), particularly at 25°C, which could result in trade-offs between development and other physiological costs when AB copepods undergo development at 25°C. Energetic compromises in life history traits in AB are also consistent with smaller egg clutches at 20°C than in the other populations and reduced ATP synthesis rates in AB copepods (at least compared to SCN copepods). The relationship between ATP synthesis rate, particularly under saturating substrate conditions, and energy demand at 20 and 25°C among populations is complex, as both ATP supply and demand are thermally sensitive and demand may vary among populations even at 20°C. However, our results may indicate that intraspecific variation in ATP synthesis capacity is related to thermal effects over prolonged timescales as well as the acute effects discussed above.

Role of Variation in Mitochondrial Functions in Latitudinal Thermal Adaptation

Upper thermal limits in aquatic ectotherms decrease approximately linearly from the equator to the poles (Sunday et al., 2011) closely matching habitat temperatures (Sunday et al., 2012). Because *T. californicus* inhabits splash pools in the extreme upper intertidal, air temperatures are potentially better predictors of habitat temperature than sea surface temperatures for this species (e.g., Pereira et al., 2017), and differences in mean knockdown temperature among our populations (38.6, 38.4, and 36.5°C for SD, AB, and SCN, respectively; **Figure 2**) parallel the differences in mean annual air temperature between the populations (Pereira et al., 2017), although the differences in knockdown temperatures are smaller than those for estimated habitat temperatures. In part due to these similarities, variation in acute upper thermal tolerance is thought to be an important consequence of local thermal adaptation in this species (Willett, 2010; Kelly et al., 2012; Pereira et al., 2017). Thus, by extension, our data suggest that differences in the thermal sensitivity of ATP synthesis capacity (**Figure 4**) likely contribute to local adaptation across this latitudinal gradient. However, it is important to note that our study examined this trait in only three populations of *T. californicus* that are found across a relatively small proportion of the latitudinal range of the species (Mexico to Alaska), and therefore, the extent to which our results can be generalized to larger latitudinal ranges remains unclear and merits future experimental consideration.

The predominant signatures of selection that are typically detected for genes in the mitochondrial genome are those of purifying selection (Stewart et al., 2008; Palozzi et al., 2018), which is perhaps not surprising given the central roles many of these genes play in mitochondrial protein or RNA complexes. However, mitochondrial genes are often involved in adaptive responses (Ballard and Whitlock, 2004), and signatures of directional selection have been detected for some genes encoded in the mitochondrial genome in *T. californicus,* particularly CI genes (*nad3*, *nad5*, and *nad6*; Barreto et al., 2018). Furthermore, nuclear genes encoding products involved in mitochondrial functions have elevated nucleotide substitution rates compared to other nuclear genes in this species (Willett and Burton, 2004; Barreto et al., 2018). Given our results for latitudinal variation in the temperatures that result in the loss of ATP synthesis capacity among populations, it is possible that at least some of this genetic variation contributes to the differences in thermal sensitivity of ATP synthesis rate among populations.

In contrast to variation in upper thermal tolerance at acute timescales of exposure, differences in chronic effects of high temperature on survival or developmental rate were not clearly associated with latitudinal variation in temperature in the current study. Variation in life history traits (i.e., egg clutch size, developmental survival, and developmental rate) and changes in these traits due to elevated temperature were consistent with reduced survival and developmental rate in AB compared to SD and SCN (**Figure 3**). Although our data suggest that variation in ATP synthesis capacity may contribute to these differences (discussed above), these patterns are not obviously related to differences in habitat temperatures among SD, AB, and SCN. Thus, our data for these three populations do not support a role of mitochondria in latitudinal adaptation associated with prolonged thermal exposures (i.e., months or seasons) in *T. californicus*.

Variation in life history traits with latitude, and therefore environmental temperature, is common in ectotherms (e.g., Chung et al., 2018b), and *T. californicus* is not an exception to this trend (Hong and Shurin, 2015). Latitudinal changes in these traits in *T. californicus* are smooth and gradual, such that relatively little variation is expected along the Californian coast in general (Hong and Shurin, 2015), which is consistent with our results in SD and SCN, which span less than half of California's latitudinal range. Therefore, it is possible that comparisons of more geographically distant populations than those used in the current study would reveal variation in

chronic temperature effects on ATP synthesis capacity that parallel differences in habitat temperatures.

Taken together, the data presented in the current study suggest a role for mitochondrial functions, particularly ATP synthesis capacity, in determining the limits of tolerance of both short- and long-term exposures to elevated temperatures. Variation in acute upper thermal tolerance in *T. californicus* is consistent with local thermal adaptation (Willett, 2010; Kelly et al., 2012; Pereira et al., 2017; the current study), and therefore, our results suggest that divergence in ATP synthesis capacity is a component of adaptation across latitudinal thermal gradients as well. Given that the acute effects of temperature in our study more closely paralleled habitat temperatures than chronic effects of temperature, our data also suggest that extreme temperature events impose important selection pressures that likely drive local thermal adaptation, as has been suggested previously (Somero, 2010; Siegle et al., 2018). Determining both the extent to which thermal sensitivity of ATP synthesis capacity influences the effects of these rare events on organisms and the mitochondrial mechanisms that underlie this sensitivity will be critical steps in accurately predicting the impacts of future environmental change on ectotherms.

AUTHOR CONTRIBUTIONS

All authors listed have made a substantial, direct and intellectual contribution to the work, and approved it for publication.

FUNDING

Funding for this study was provided by a National Science Foundation grant to RB (DEB1551466).

ACKNOWLEDGMENTS

The authors thank Rebecca Pak and Antonia Bock for assistance with copepod culturing and thermal tolerance measurements.

SUPPLEMENTARY MATERIAL

The Supplementary Material for this article can be found online at: https://www.frontiersin.org/articles/10.3389/fphys.2019.00213/full#supplementary-material

REFERENCES

Ballard, J. W. O., and Whitlock, M. C. (2004). The incomplete natural history of mitochondria. *Mol. Ecol.* 13, 729–744. doi: 10.1046/j.1365-294X.2003.02063.x

Barreto, F. S., Watson, E. T., Lima, T. G., Willett, C. S., Edmands, S., Li, W., et al. (2018). Genomic signatures of mitonuclear coevolution across populations of *Tigriopus californicus*. *Nat. Ecol. Evol.* 2, 1250–1257. doi: 10.1038/s41559-018-0588-1

Bay, R. A., Rose, N., Barrett, R., Bernatchez, L., Ghalambor, C. K., Lasky, J. R., et al. (2017). Predicting responses to contemporary environmental change using evolutionary response architectures. *Am. Nat.* 189, 463–473. doi: 10.1086/691233

Beitinger, T., Bennett, W., and McCauley, R. (2000). Temperature tolerances of North American freshwater fishes exposed to dynamic changes in temperature. *Environ. Biol. Fish* 58, 237–275. doi: 10.1023/A:1007676325825

Benjamini, Y., and Hochberg, Y. (1995). Controlling the false discovery rate: a practical and powerful approach to multiple testing. *J. R. Stat. Soc. Ser. B* 57, 289–300.

Burton, R. S. (1985). Mating system of the intertidal copepod *Tigriopus californicus*. *Mar. Biol.* 86, 247–252. doi: 10.1007/BF00397511

Burton, R. S. (1998). Intraspecific phylogeography across the point conception biogeographic boundary. *Evolution* 52, 734–745. doi: 10.1111/j.1558-5646.1998.tb03698.x

Christen, F., Desrosiers, V., Dupont-Cyr, B. A., Vandenberg, G. W., Le François, N. R., Tardif, J. C., et al. (2018). Thermal tolerance and thermal sensitivity of heart mitochondria: mitochondrial integrity and ROS production. *Free Radic. Biol. Med.* 116, 11–18. doi: 10.1016/j.freeradbiomed.2017.12.037

Chung, D. J., Bryant, H. J., and Schulte, P. M. (2017a). Thermal acclimation and subspecies-specific effects on heart and brain mitochondrial performance in a eurythermal teleost (*Fundulus heteroclitus*). *J. Exp. Biol.* 220, 1459–1471. doi: 10.1242/jeb.151217

Chung, D. J., Healy, T. M., McKenzie, J. L., Chicco, A. J., Sparagna, G. C., and Schulte, P. M. (2018b). Mitochondria, temperature, and the pace of life. *Integr. Comp. Biol.* 1–13. doi: 10.1093/icb/icy013

Chung, D. J., Morrison, P. R., Bryant, H. J., Jung, E., Brauner, C. J., and Schulte, P. M. (2017b). Intraspecific variation and plasticity in mitochondrial oxygen binding affinity as a response to environmental temperature. *Sci. Rep.* 7, 1–10. doi: 10.1038/s41598-017-16598-6

Chung, D. J., and Schulte, P. M. (2015). Mechanisms and costs of mitochondrial thermal acclimation in a eurythermal killifish *(Fundulus heteroclitus)*. *J. Exp. Biol.* 218, 1621–1631. doi: 10.1242/jeb.120444

Chung, D. J., Sparagna, G. C., Chicco, A. J., and Schulte, P. M. (2018a). Patterns of mitochondrial membrane remodeling parallel functional adaptations to thermal stress. *J. Exp. Biol.* 221:jeb174458. doi:10.1242/jeb.174458

Dahlhoff, E., Brien, J. O., Somero, G. N., and Vetter, R. D. (1991). Temperature effects on mitochondria from hydrothermal vent invertebrates: evidence for adaptation to elevated and variable habitat temperatures. *Physiol. Zool.* 64, 1490–1508. doi: 10.1086/physzool.64.6.30158226

Dahlhoff, E., and Somero, G. N. (1993). Effects of temperature on mitochondria from abalone (genus: *Haliotis*): adaptive plasticity and its limits. *J. Exp. Biol.* 185, 151–168.

Deutsch, C., Ferrel, A., Seibel, B., Pörtner, H.-O., and Huey, R. B. (2015). Climate change tightens a metabolic constraint on marine habitats. *Science* 348, 1132–1136. doi: 10.1126/science.aaa1605

Dhillon, R. S., and Schulte, P. M. (2011). Intraspecific variation in the thermal plasticity of mitochondria in killifish. *J. Exp. Biol.* 214, 3639–3648. doi: 10.1242/jeb.057737

Edmands, S. (2001). Phylogeography of the intertidal copepod *Tigriopus californicus* reveals substantially reduced population differentiation at northern latitudes. *Mol. Ecol.* 10, 1743–1750. doi: 10.1046/j.0962-1083.2001.01306.x

Edmands, S., and Deimler, J. K. (2004). Local adaptation, intrinsic coadaptation and the effects of environmental stress on interpopulation hybrids in the copepod *Tigriopus californicus*. *J. Exp. Mar. Biol. Ecol.* 303, 183–196. doi: 10.1016/j.jembe.2003.11.012

Egginton, S., and Johnston, I. A. (1984). Effects of acclimation temperature on routine metabolism muscle mitochondrial volume density and capillary supply in the elver (*Anguilla anguilla* L.). *J. Therm. Biol.* 9, 165–170. doi: 10.1016/0306-4565(84)90016-0

Ellison, C. K., and Burton, R. S. (2006). Disruption of mitochondrial function in interpopulation hybrids of *Tigriopus californicus*. *Evolution* 60, 1382–1391. doi: 10.1111/j.0014-3820.2006.tb01217.x

Ellison, C. K., and Burton, R. S. (2008). Interpopulation hybrid breakdown maps to the mitochondrial genome. *Evolution* 62, 631–638. doi: 10.1111/j.1558-5646.2007.00305.x

Farrell, A. P. (2009). Environment, antecedents and climate change: lessons from the study of temperature physiology and river migration of salmonids. *J. Exp. Biol.* 212, 3771–3780. doi: 10.1242/jeb.023671

Gilchrist, G. W., and Huey, R. B. (1999). The direct response of *Drosophila melanogaster* to selection on knockdown temperature. *Heredity* 83, 15–29. doi: 10.1038/sj.hdy.6885330

Grim, J. M., Miles, D. R. B., and Crockett, E. L. (2010). Temperature acclimation alters oxidative capacities and composition of membrane lipids without influencing activities of enzymatic antioxidants or susceptibility to lipid peroxidation in fish muscle. *J. Exp. Biol.* 213, 445–452. doi: 10.1242/jeb.036939

Guderley, H. (2004). Metabolic responses to low temperature in fish muscle. *Biol. Rev. Camb. Philos. Soc.* 79, 409–427. doi: 10.1017/S1464793103006328

Hazel, J. R. (1995). Thermal adaptation in biological-membranes is homeoviscous adaptation the explanation. *Annu. Rev. Physiol.* 57, 19–42. doi: 10.1146/Annurev.Ph.57.030195.000315

Healy, T. M., Brennan, R. S., Whitehead, A., and Schulte, P. M. (2018). Tolerance traits related to climate change resilience are independent and polygenic. *Glob. Chang. Biol.* 11, 5348–5360. doi: 10.1111/gcb.14386

Hochachka, P. W., and Somero, G. N. (2002). *Biochemical adaptation: Mechanism and process in physiological evolution*. New York, USA: Oxford University Press.

Hoekstra, L. A., Siddiq, M. A., and Montooth, K. L. (2013). Pleiotropic effects of a mitochondrial-nuclear incompatibility depend upon the accelerating effect of temperature in *Drosophila*. *Genetics* 195, 1129–1139. doi: 10.1534/genetics.113.154914

Hoffmann, A. A., Sørensen, J. G., and Loeschcke, V. (2003). Adaptation of *Drosophila* to temperature extremes: bringing together quantitative and molecular approaches. *J. Therm. Biol.* 28, 175–216. doi: 10.1016/S0306-4565(02)00057-8

Hong, B. C., and Shurin, J. B. (2015). Latitudinal variation in the response of tidepool copepods to mean and daily range in temperature. *Ecology* 96, 2348–2359. doi: 10.1890/14-1695.1

Iftikar, F. I., and Hickey, A. J. R. (2013). Do mitochondria limit hot fish hearts? understanding the role of mitochondrial function with heat stress in *Notolabrus celidotus*. *PLoS One* 8:e64120. doi: 10.1371/journal.pone.0064120

Johnston, I., and Dunn, J. (1987). Temperature acclimation and metabolism in ectotherms with particular reference to teleost fish. *Symp. Soc. Exp. Biol.* 41, 67–93.

Kelly, M. W., Sanford, E., and Grosberg, R. K. (2012). Limited potential for adaptation to climate change in a broadly distributed marine crustacean. *Proc. R. Soc. B Biol. Sci.* 279, 349–356. doi: 10.1098/rspb.2011.0542

Kraffe, E., Marty, Y., and Guderley, H. (2007). Changes in mitochondrial oxidative capacities during thermal acclimation of rainbow trout *Oncorhynchus mykiss:* roles of membrane proteins, phospholipids and their fatty acid compositions. *J. Exp. Biol.* 210, 149–165. doi: 10.1242/jeb.02628

Lemieux, H., Semsroth, S., Antretter, H., Höfer, D., and Gnaiger, E. (2011). Mitochondrial respiratory control and early defects of oxidative phosphorylation in the failing human heart. *Int. J. Biochem. Cell Biol.* 43, 1729–1738. doi: 10.1016/j.biocel.2011.08.008

LeMoine, C. M. R., Genge, C. E., and Moyes, C. D. (2008). Role of the PGC-1 family in the metabolic adaptation of goldfish to diet and temperature. *J. Exp. Biol.* 211, 1448–1455. doi: 10.1242/jeb.014951

Leong, W., Sun, P. Y., and Edmands, S. (2018). Latitudinal clines in temperature and salinity tolerance in tidepool copepods. *J. Hered.* 109, 71–77. doi: 10.1093/jhered/esx061

McClelland, G. B., Craig, P. M., Dhekney, K., and Dipardo, S. (2006). Temperature- and exercise-induced gene expression and metabolic enzyme changes in skeletal muscle of adult zebrafish *(Danio rerio)*. *J. Physiol.* 577, 739–751. doi: 10.1113/jphysiol.2006.119032

Morgan, R., Finnøen, M. H., and Jutfelt, F. (2018). CTmax is repeatable and doesn't reduce growth in zebrafish. *Sci. Rep.* 8, 1–8. doi: 10.1038/s41598-018-25593-4

Moyes, C. D., Moon, T. W., and Ballantyne, J. S. (1985). Glutamate catabolism in mitochondria from *Mya arenaria* mantle: effects of pH on the role of glutamate dehydrogenase. *J. Exp. Zool.* 236, 293–301. doi: 10.1002/jez.1402360306

O'Brien, K. M. (2011). Mitochondrial biogenesis in cold-bodied fishes. *J. Exp. Biol.* 214, 275–285. doi: 10.1242/jeb.046854

O'Brien, K. M., Rix, A. S., Egginton, S., Farrell, A. P., Crockett, E. L., Schlauch, K., et al. (2018). Cardiac mitochondrial metabolism may contribute to differences in thermal tolerance of red- and white-blooded Antarctic notothenioid fishes. *J. Exp. Biol.* 221:jeb.177816. doi:10.1242/jeb.177816

Orczewska, J. I., Hartleben, G., and O'Brien, K. M. (2010). The molecular basis of aerobic metabolic remodeling differs between oxidative muscle and liver of threespine sticklebacks in response to cold acclimation. *AJP Regul. Integr. Comp. Physiol.* 299, R352–R364. doi: 10.1152/ajpregu.00189.2010

Palozzi, J. M., Jeedigunta, S. P., and Hurd, T. R. (2018). Mitochondrial DNA purifying selection in mammals and invertebrates. *J. Mol. Biol.* 430, 4834–4848. doi: 10.1016/j.jmb.2018.10.019

Pereira, R. J., Barreto, F. S., and Burton, R. S. (2014). Ecological novelty by hybridization: experimental evidence for increased thermal tolerance by transgressive segregation in *Tigriopus californicus*. *Evolution* 68, 204–215. doi: 10.1111/evo.12254

Pereira, R. J., Barreto, F. S., Pierce, N. T., Carneiro, M., and Burton, R. S. (2016). Transcriptome-wide patterns of divergence during allopatric evolution. *Mol. Ecol.* 25, 1478–1493. doi: 10.1111/mec.13579

Pereira, R. J., Sasaki, M. C., and Burton, R. S. (2017). Adaptation to a latitudinal thermal gradient within a widespread copepod species: the contributions of genetic divergence and phenotypic plasticity. *Proc. R. Soc. B Biol. Sci.* 284:20170236. doi: 10.1098/rspb.2017.0236

Pesta, D., and Gnaiger, E. (2012). "High-resolution respirometry: OXPHOS protocols for human cells and permeabilized fibers from small biopsies of human muscle" in *Mitochondrial bioenergetics. Methods in molecular biology (methods and protocols)*. eds. C. Palmeira and A. Moreno, vol. 810 (New York, USA: Humana Press).

Peterson, D. L., Kubow, K. B., Connolly, M. J., Kaplan, L. R., Wetkowski, M. M., Leong, W., et al. (2013). Reproductive and phylogenetic divergence of tidepool copepod populations across a narrow geographical boundary in Baja California. *J. Biogeogr.* 40, 1664–1675. doi: 10.1111/jbi.12107

Pichaud, N., Ballard, J. W. O., Tanguay, R. M., and Blier, P. U. (2011). Thermal sensitivity of mitochondrial functions in permeabilized muscle fibers from two populations of *Drosophila simulans* with divergent mitotypes. *Am. J. Physiol. Integr. Comp. Physiol.* 301, R48–R59. doi: 10.1152/ajpregu.00542.2010

Pichaud, N., Ballard, J. W. O., Tanguay, R. M., and Blier, P. U. (2012). Naturally occurring mitochondrial DNA haplotypes exhibit metabolic differences: insight into functional properties of mitochondria. *Evolution* 66, 3189–3197. doi: 10.1111/j.1558-5646.2012.01683.x

Pörtner, H. (2001). Climate change and temperature-dependent biogeography: oxygen limitation of thermal tolerance in animals. *Naturwissenschaften* 88, 137–146. doi: 10.1007/s001140100216

Pörtner, H.-O. (2010). Oxygen- and capacity-limitation of thermal tolerance: a matrix for integrating climate-related stressor effects in marine ecosystems. *J. Exp. Biol.* 213, 881–893. doi: 10.1242/jeb.037523

Pörtner, H. O., Bennett, A. F., Bozinovic, F., Clarke, A., Lardies, M. A., Lucassen, M., et al. (2006). Trade-offs in thermal adaptation: the need for a molecular to ecological integration. *Physiol. Biochem. Zool.* 79, 295–313. doi: 10.1086/499986

Pritchard, J. K., and Di Rienzo, A. (2010). Adaptation - Not by sweeps alone. *Nat. Rev. Genet.* 11, 665–667. doi: 10.1038/nrg2880

Scheffler, I. E. (2008). *Mitochondria*. 2nd Edn. Hoboken, New Jersey: John Wiley & Sons, Inc.

Seebacher, F., Brand, M. D., Else, P. L., Guderley, H., Hulbert, A. J., and Moyes, C. D. (2010). Plasticity of oxidative metabolism in variable climates: molecular mechanisms. *Physiol. Biochem. Zool.* 83, 721–732. doi: 10.1086/649964

Seebacher, F., White, C. R., and Franklin, C. E. (2015). Physiological plasticity increases resilience of ectothermic animals to climate change. *Nat. Clim. Chang.* 5, 61–66. doi: 10.1038/nclimate2457

Siegle, M. R., Taylor, E. B., and O'Connor, M. I. (2018). Prior heat accumulation reduces survival during subsequent experimental heat waves. *J. Exp. Mar. Biol. Ecol.* 501, 109–117. doi: 10.1016/j.jembe.2018.01.012

Somero, G. N. (2010). The physiology of climate change: how potentials for acclimatization and genetic adaptation will determine "winners" and "losers". *J. Exp. Biol.* 213, 912–920. doi: 10.1242/jeb.037473

Stewart, J. B., Freyer, C., Elson, J. L., and Larsson, N. G. (2008). Purifying selection of mtDNA and its implications for understanding evolution and mitochondrial disease. *Nat. Rev. Genet.* 9, 657–662. doi: 10.1038/nrg2396

St-Pierre, J., Charest, P. M., and Guderley, H. (1998). Relative contribution of quantitative and qualitative changes in mitochondria to metabolic compensation during seasonal acclimatisation of rainbow trout *Oncorhynchus mykiss*. *J. Exp. Biol.* 201, 2961–2970.

Sunday, J. M., Bates, A. E., and Dulvy, N. K. (2011). Global analysis of thermal tolerance and latitude in ectotherms. *Proc. R. Soc. B Biol. Sci.* 278, 1823–1830. doi: 10.1098/rspb.2010.1295

Sunday, J. M., Bates, A. E., and Dulvy, N. K. (2012). Thermal tolerance and the global redistribution of animals. *Nat. Clim. Chang.* 2, 686–690. doi: 10.1038/nclimate1539

Tangwancharoen, S., and Burton, R. S. (2014). Early life stages are not always the most sensitive: heat stress responses in the copepod *Tigriopus californicus*. *Mar. Ecol. Prog. Ser.* 517, 75–83. doi: 10.3354/meps11013

Tsuboko-Ishii, S., and Burton, R. S. (2017). Sex-specific rejection in mate-guarding pair formation in the intertidal copepod, *Tigriopus californicus*. *PLoS One* 12, 1–16. doi: 10.1371/journal.pone.0183758

Willett, C. S. (2010). Potential fitness trade-offs for thermal tolerance in the intertidal copepod *Tigriopus californicus*. *Evolution* 64, 2521–2534. doi: 10.1111/j.1558-5646.2010.01008.x

Willett, C. S. (2012). Hybrid breakdown weakens under thermal stress in population crosses of the copepod *Tigriopus californicus*. *J. Hered.* 103, 103–114. doi: 10.1093/jhered/esr109

Willett, C. S., and Burton, R. S. (2004). Evolution of interacting proteins in the mitochondrial electron transport system in a marine copepod. *Mol. Biol. Evol.* 21, 443–453. doi: 10.1093/molbev/msh031

Willett, C. S., and Ladner, J. T. (2009). Investigations of fine-scale phylogeography in *Tigriopus californicus* reveal historical patterns of population divergence. *BMC Evol. Biol.* 9, 1–20. doi: 10.1186/1471-2148-9-139

Willett, C. S., and Son, C. (2018). The evolution of the thermal niche across locally adapted populations of the copepod *Tigriopus californicus*. *Bull. South. Calif. Acad. Sci.* 117, 150–157. doi: 10.3160/3712.1

Conflict of Interest Statement: The authors declare that the research was conducted in the absence of any commercial or financial relationships that could be construed as a potential conflict of interest.

frontiers in Physiology

ORIGINAL RESEARCH
published: 21 May 2019
doi: 10.3389/fphys.2019.00610

Genome-Wide Identification and Expression Profiles of Myosin Genes in the Pacific White Shrimp, *Litopenaeus vannamei*

Xiaoxi Zhang[1,2,3], *Jianbo Yuan*[1,2,4], *Xiaojun Zhang*[1,2,4]*, *Chengzhang Liu*[1,2,4], *Fuhua Li*[1,2,4]* and *Jianhai Xiang*[1,2,4]

[1] Key Laboratory of Experimental Marine Biology, Institute of Oceanology, Chinese Academy of Sciences, Qingdao, China, [2] Laboratory for Marine Biology and Biotechnology, Qingdao National Laboratory for Marine Science and Technology, Qingdao, China, [3] University of Chinese Academy of Sciences, Beijing, China, [4] Center for Ocean Mega-Science, Chinese Academy of Sciences, Qingdao, China

As the main structural protein of muscle fiber, myosin is essential for multiple cellular processes or functions, especially for muscle composition and development. Although the shrimp possess a well-developed muscular system, the knowledge about the myosin family in shrimp is far from understood. In this study, we performed comprehensive analysis on the myosin genes in the genome of the Pacific white shrimp, *Litopenaeus vannamei*. A total of 29 myosin genes were identified, which were classified into 14 subfamilies. Among them, *Myo2* subfamily was significantly expanded in the penaeid shrimp genome. Most of the Myo2 subfamily genes were primarily expressed in abdominal muscle, which suggested that Myo2 subfamily genes might be responsible for the well-developed muscular system of the penaeid shrimp. *In situ* hybridization detection showed that the slow-type muscle myosin gene was mainly localized in pleopod muscle and superficial ventral muscle of the shrimp. This study provides valuable insights into the evolutionary and functional characterization of myosin genes in shrimps, which provides clues for us to understand the well-developed muscular system of shrimp.

Keywords: myosin genes, muscle development, alternative splicing, penaeid shrimp, gene family

OPEN ACCESS

Edited by:
Carlos Rosas, National Autonomous University of Mexico, Mexico

Reviewed by:
Theresa Joan Grove, Valdosta State University, United States
Tiziano Verri, University of Salento, Italy

***Correspondence:**
Xiaojun Zhang
xjzhang@qdio.ac.cn
Fuhua Li
fhli@qdio.ac.cn

Specialty section:
This article was submitted to Aquatic Physiology, a section of the journal Frontiers in Physiology

Received: *23 January 2019*
Accepted: *29 April 2019*
Published: *21 May 2019*

Citation:
Zhang X, Yuan J, Zhang X, Liu C, Li F and Xiang J (2019) Genome-Wide Identification and Expression Profiles of Myosin Genes in the Pacific White Shrimp, Litopenaeus vannamei. Front. Physiol. 10:610. doi: 10.3389/fphys.2019.00610

INTRODUCTION

Nearly all eukaryotic cells possess myosin proteins, which bind to filamentous actin and produce physical forces through ATP hydrolysis (Richards and Cavalier-Smith, 2005; Sebé-Pedrós et al., 2014). Myosin plays key roles in muscle composition and various cellular activities, including cytokinesis, organelle transport, cell polarization, intracellular transport and signal transduction (Hofmann et al., 2009; Bloemink and Geeves, 2011; Hartman et al., 2011; Pette and Staron, 2015). The Myo2 subfamily (Myosin 2), also known as myosin heavy chain (MYH or MHC), are the main component of the contractile muscle. They are considered to be conventional myosins, while the other subfamilies are considered to be unconventional myosins. The Myo2 subfamily genes can be classified into three groups, including fast-type, slow-type and non-muscle type. The Myo2 subfamily proteins can form large bipolar filaments through tail-directed homo-oligomerization, while the tails of the unconventional myosins typically direct binding to membrane and other proteins (Woolner and Bement, 2009).

Myosin consists of three domains, including a conserved motor (or head) domain with actin-binding activities, a short neck that serves as a binding site for myosin light chains, and a variable tail that generally mediates interaction with the motor "cargo" to determine the functional specificity of the motor (Berg et al., 2001; Richards and Cavalier-Smith, 2005). In general, it is very difficult to investigate the myosin gene family systemically due to their extensive alternative splicing events, large sizes and high copy numbers. Although crustaceans are a large, diverse group, limited myosin genes have been reported, except that 17 myosin genes in 13 classes have been characterized in *Daphnia duplex* (Odronitz and Kollmar, 2008). In addition, a few *Myo2* sequences have been cloned from *Marsupenaeus japonicus*, *Penaeus monodon,* and *Litopenaeus vannamei*, respectively (Koyama et al., 2013). Hence, studies on the myosin gene family in crustaceans will enhance our understanding on their structure, function and evolution.

The Pacific white shrimp *L. vannamei* is one of the most economically important marine aquaculture species in the world (FAO, 2014). Based on the whole genome sequences (Zhang et al., 2019) and the transcriptome data, we performed a genome-wide analysis on the myosin gene family of *L. vannamei*. This study provides valuable resources for the shrimp myosin genes, which will increase our understanding on the crustacean muscular system.

MATERIALS AND METHODS

Genome and Transcriptome Data

The genomic data of *L. vannamei* (PRJNA438564), *Lepeophtheirus salmonis* (GCA_001005205.1), *Parhyale hawaiensis* (GCA_001587735.1), *Eulimnadia texana* (GCA_002872375.1), were obtained from NCBI GenBank and Ensemble database. Our previous research conducted RNA-seq on several libraries, (I) five larval stages, including embryo, nauplius, zoea, mysis and post-larvae (Wei et al., 2014); (II) eight molting stages, including the inter-molt (C), pre-molt (D0, D1, D2, D3, D4), and post-molt (P1 and P2) stages (Gao et al., 2015); (III) 16 adult tissues, including antennal gland, brain, hemocyte, epidermis, eyestalk, gill, hepatopancreas, heart, intestine, abdominal muscle, lymphoid organ, ovary, stomach, testis, thoracic ganglion, and abdominal ganglion (Zhang et al., 2018).

Isolation and Annotation of Myosin Genes

The full protein sequences of the *L. vannamei* genome were searched against the myosin head (motor domain) (PF00063) to find all the candidate myosin genes by using HMMER3.0 (Potter et al., 2018). All possible myosin transcripts were collected from the transcriptome data. Then, the redundant sequences were removed using CAP3 program (Huang and Madan, 1999). The candidate sequences were submitted to SMART (Letunic et al., 2014) and InterPro (Finn et al., 2016) databases to determine the integrity of the motor domain. More myosin sequences used in this study were collected from CyMoBase[1] and (Hammesfahr et al., 2010).

Gene Structure and Alternative Splicing

The characteristics of myosin genes, including the location, gene length, open reading frame (ORF), exon number and the number of deduced amino acids were analyzed in detail. To illustrate the structure of myosin genes, all alternative spliced exons were characterized by mapping all variant transcripts to the shrimp genome.

Phylogenetic Analysis

The amino acid sequences of the conserved myosin head domain were aligned by MUSCLE program (version 3.8.31) (Edgar, 2004) with default parameters. A neighbor-joining (NJ) phylogenetic tree with 1000 bootstrap replicates was constructed by MEGA7.0 program (Kumar et al., 2016), and visualized using iTOL (Letunic and Bork, 2007). To investigate the evolution of the myosin gene family of shrimp, a class occurrence tree of 29 arthropods was generated by using the method described by Odronitz et al. (2009).

Transcription Regulatory Element Identification

To investigate whether the expanded muscle-type Myo2 genes are associated with muscle composition or development, transcription regulatory elements of muscle-type Myo2 genes were predicted. In detail, the promoter regions, located at the 2 kb upstream of the transcriptional start site, were first extracted from the shrimp genome. The transcription regulatory elements were then predicted by Signal Scan[2] with TRANSFAC database and the PATCH algorithm integrated in the GeneXplain platform[3]. In order to decrease the false positive rate, we intersected the predicted results of Signal Scan and GeneXplain.

Expression Patterns at Early Development Stages and Different Tissues of Adults

In previous studies, we conducted Digital Gene Expression Profiling (DGE) to sequence 20 larval stages and 16 adult tissues of *L. vannamei*, and the RPKM (reads per kilobases per million reads) values of all transcripts were calculated (Zhang et al., 2018). The RPKM values of myosin genes were extracted and normalized with log2 conversion. Heat maps were created using TBtools software (Chen et al., 2018).

In situ Hybridization

In this study, *LvMYH5* was characterized to be a slow-type muscle Myo2 gene. To further distinguish fiber types and muscle distribution of the abdominal muscle of shrimp, *in situ* hybridization was performed according to the protocol

[1]https://www.cymobase.org/

[2]https://www-bimas.cit.nih.gov/molbio/signal/

[3]http://gene-regulation.com/

TABLE 1 | The 29 myosin genes identified from *L. vannamei* genome.

Myosin name	Genome position	Position (bp)	Exon	No. of aa	Unigenes
LvMyo1A	LVANscaffold_1022	139086: 159076	23	1081	Unigene0007554
LvMyo1B	LVANscaffold_2218	313258: 311201	20	1032	Unigene0049576
	LVANscaffold_3160	506207: 527443			
LvMyo1C	Unavailable	Unavailable	Unavailable	1177	c78174_g1
LvMyo1D	LVANscaffold_2215	1434634: 1447801	21	1177	c83379_g1
LvMYH1	LVANscaffold_3755	173364: 184470	22	1913	AB758443.1
LvMYH2	LVANscaffold_2946	891867: 984674	24	1972	c81769_g2
	LVANscaffold_675	114493: 156039			
LvMYH3	LVANscaffold_2985	675886: 686178	>18	1911	CL120.Contig45_All
LvMYH4	LVANscaffold_904	105970: 114423	11	1124	AB759099.1
LvMYH5	LVANscaffold_1838	9836: 15995	>8	>1198	AB759100.1
LvMYH6	LVANscaffold_2713	277521: 272168	22	1909	AB759104.1
		197752: 212409			
LvMYH7	LVANscaffold_2713	44648: 62854	22	1909	AB758444.1
LvMYH8	LVANscaffold_2713	169683: 186166	21	1909	Unigene7586_All
LvMYH9	LVANscaffold_904	190184: 192834	>21	1911	CL120.Contig24_All
		14479: 24317			
LvMYH10	LVANscaffold_904	26105: 36210	>14	1915	CL120.Contig4_All
LvMYH11	LVANscaffold_904	184800: 190271	19	1913	CL120.Contig83_All
		166283: 179232			
LvMYH12	LVANscaffold_904	236788: 225555	>20	1911	CL120.Contig50_All
LvMYH13	LVANscaffold_660	671473: 678521	>14	1911	CL120.Contig15_All
LvMYH14	LVANscaffold_1774	1247154: 1253260	>18	1929	CL120.Contig53_All
	LVANscaffold_854	418893: 427114			
LvMYH15	LVANscaffold_903	446522: 459841	>18	1909	CL120.Contig13_All
LvMYH16	LVANscaffold_1774	1258456: 1265373	>8	>1321	CL120.Contig78_All
LvMyo5	LVANscaffold_441	69978: 76891	37	1853	c81514_g1
		270006: 345054			
LvMyo6	LVANscaffold_1654	616383: 635879	29	1257	Unigene0049576
	LVANscaffold_1737	4719 : 14556			
LvMyo7A	LVANscaffold_2760	317572: 400940	40	2158	c83722_g3
LvMyo9	LVANscaffold_1465	684100: 748649	33	2057	c80593_g1
LvMyo15	LVANscaffold_2015	255392: 276113	20	1137	c83307_g1
LvMyo18	LVANscaffold_1503	325742: 153935	31	2037	c75923_g3
LvMyo20	LVANscaffold_609	944458: 956786	>18	1010	Unigene0091838
LvMyo21	LVANscaffold_2019	461705: 493440	26	1269	c83155_g1
LvMyo22	LVANscaffold_1625	630095: 647523	>35	1963	c83429_g1

developed in our laboratory (Zhang et al., 2018). Briefly, primers LvMYH5-pF with T7 promoter sequence and LvMYH5-R (**Supplementary Table 1**) were designed to amplify the cDNA fragments as the template of *LvMYH5* to synthesize sense probe. Primers LvMYH5-pR with T7 promoter sequence and LvMYH5-F were designed as the template to synthesize antisense probe. PCR products were purified using MiniBEST DNA Fragment Purification Kit (Takara, Japan). The Digoxigenin (DIG)-labeled sense and antisense RNA probes were transcribed by TranscriptAid T7 High Yield Transcription Kit (Thermo Fisher Scientific, United States) and synthesized using DIG RNA Labeling Mixture (Roche, Germany), respectively, and stored at −80°C.

Transverse sections with 5–7 μm thickness were prepared from polyformaldehyde fixed abdominal muscle of juvenile shrimp (about 2 cm in body length) embedded in paraffin (Sigma, Germany), and hybridization was performed following the general protocol of DIG RNA labeling kit (SP6/T7) (Roche, Germany). The final concentration of both anti-sense and sense RNA probes were 1.5 ng/μl. Subsequently, alkaline phosphatase-conjugated anti-DIG antibody and NBT/BCIP (DIG Nucleic Acid Detection Kit, Roche) were used to detect RNA probes and observed under Nikon Eclipse 80i microscope (Nikon, Japan).

RESULTS

Identification of Myosin Genes

A total of 29 myosin genes were identified in *L. vannamei*, including 15 muscle-type Myo2 genes, one non-muscle type Myo2 gene and 13 unconventional myosin genes (**Table 1**). Among them, five muscle-type myosin genes had been

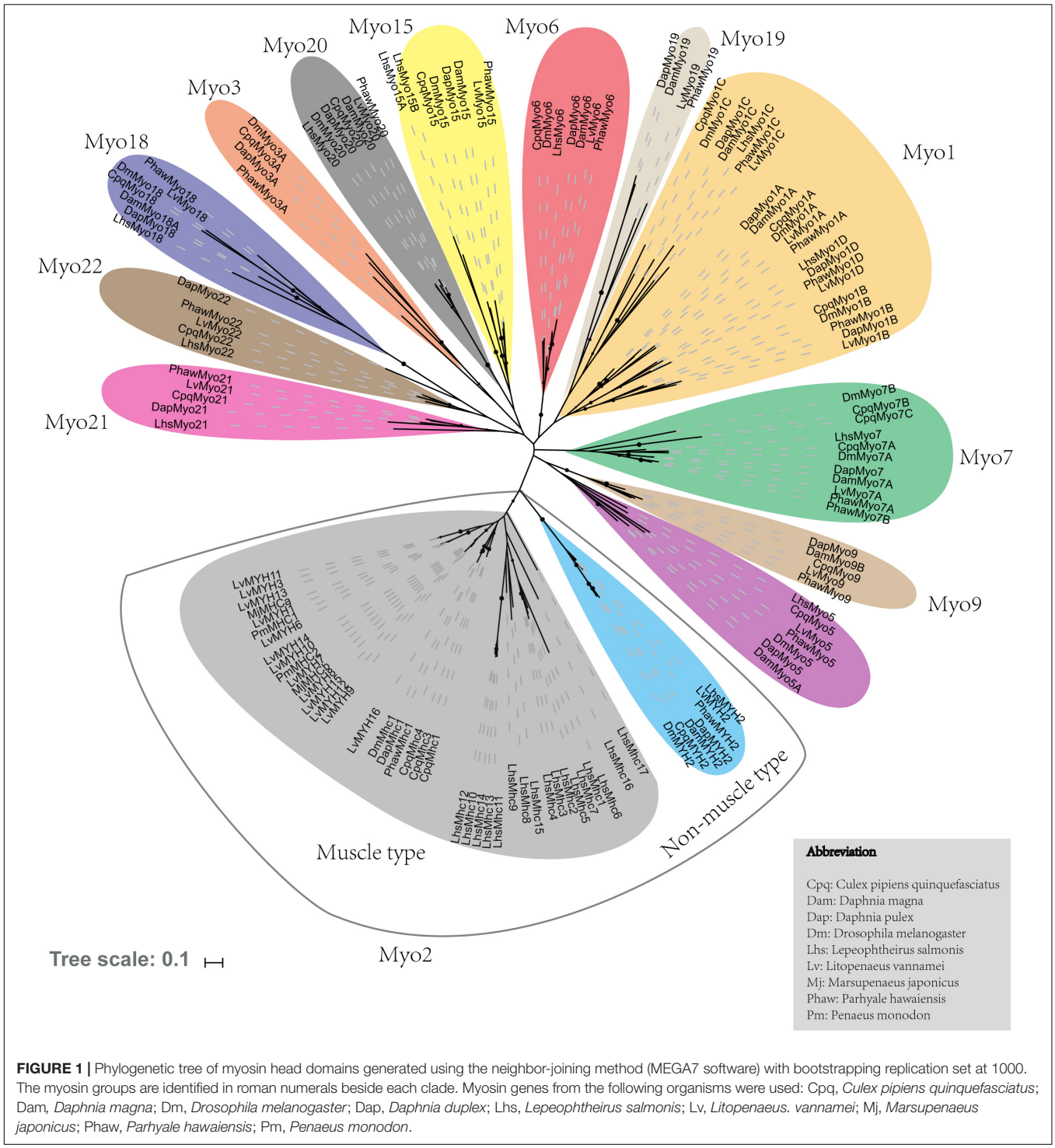

FIGURE 1 | Phylogenetic tree of myosin head domains generated using the neighbor-joining method (MEGA7 software) with bootstrapping replication set at 1000. The myosin groups are identified in roman numerals beside each clade. Myosin genes from the following organisms were used: Cpq, *Culex pipiens quinquefasciatus*; Dam, *Daphnia magna*; Dm, *Drosophila melanogaster*; Dap, *Daphnia duplex*; Lhs, *Lepeophtheirus salmonis*; Lv, *Litopenaeus. vannamei*; Mj, *Marsupenaeus japonicus*; Phaw, *Parhyale hawaiensis*; Pm, *Penaeus monodon*.

reported previously, including *LvMHC1*, *LvMHC2, LvMHC4, LvMHC5,* and *LvMHC6* (Koyama et al., 2012, 2013). They were designated as *LvMYH1*, *LvMYH7, LvMYH4, LvMYH5,* and *LvMYH6,* respectively, in this study to avoid confusion with major histocompatibility complex genes. The gene structure of these 29 myosin genes showed high complexity with the sizes ranging from 6.159 to 171.807 kb that corresponded to encode proteins of 1,010-2,158 aa (**Table 1**). Phylogenetic analysis indicated that these myosin genes were clustered into 14 distinct groups, namely 14 subfamilies, *Myo1, muscle-type Myo2, non-muscle type Myo2, Myo3, Myo5, Myo6, Myo7, Myo9, Myo15, Myo18, Myo19, Myo20, Myo21, and Myo22. Myo1* can be further divided into four subfamilies, *Myo1A*, *Myo1B*, *Myo1C,* and *Myo1D*. These myosin genes within

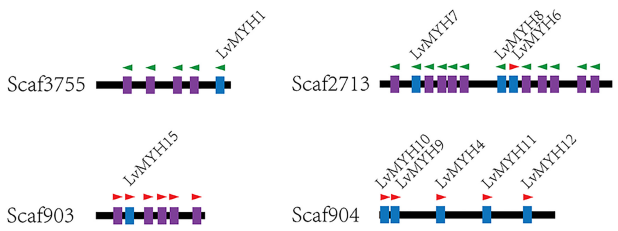

FIGURE 2 | Representation of paralogous muscle-type Myo2 gene clusters arranged on different scaffolds of *L. vannamei*. Blue: the complete muscle-type MYH gene. Purple: fragmental Myo2-like gene sequences or pseudogenes of MYH. The green and red triangles represent transcription orientation.

each subfamily shared similar protein domains. Furthermore, *Myo1* and the muscle-type *Myo2* were the two largest clades including 22 and 40 myosin genes in the phylogenetic tree of this study, respectively. However, the smallest clade *Myo19* only included 4 myosin genes. All the 29 myosin genes identified in this study fell into 14 distinct clades and were closely related to the homologous proteins from other species (**Figure 1**). Of these genes, 15 muscle-type Myo2 genes were monophyletic with 27 muscle-type Myo2 genes from other arthropods.

Fifteen muscle-type Myo2 genes exhibited conspicuous lineage-specific expansion in the shrimp genome. Among them, eight Myo2 genes were tandemly distributed in two clusters (**Figure 2**), *LvMYH9*, *LvMYH10*, *LvMYH4*, *LvMYH11,* and *LvMYH12* were located on the Scaffold 904, *LvMYH7*, *LvMYH8,* and *LvMYH6* were located on the Scaffold 2713. Besides, at least 19 fragmental muscle-type *Myo2*-like sequences or pseudogenes were located on the Scaffold 903, Scaffold 2713 and Scaffold 3755 (**Figure 2**). The others scattered in the shrimp genome (**Table 1**).

Myosin Functional Domain

Generally, homologous myosin genes of different species possess similar domain architecture (Richards and Cavalier-Smith, 2005). All myosin genes identified in this study contained a large ATPase motor domain which hydrolyzes ATP, except for *LvMYH4*, which encodes a headless myosin. In addition, all the myosin genes contained at least one isoleucine-glutamine (IQ) motif except for *LvMyo6* (**Figure 3**). The myosin genes could be classified into different groups with diverse functions based on the remaining domains and variable number of IQ motifs. *LvMyo5* contained six IQ domains and a unique C-terminal DIL domain. *LvMyo19*, *LvMyo20,* and *LvMyo21* had truncated tail regions. Notably, all muscle-type Myo2 proteins contained an N-terminal SH3-like fold, a large ATPase motor domain,

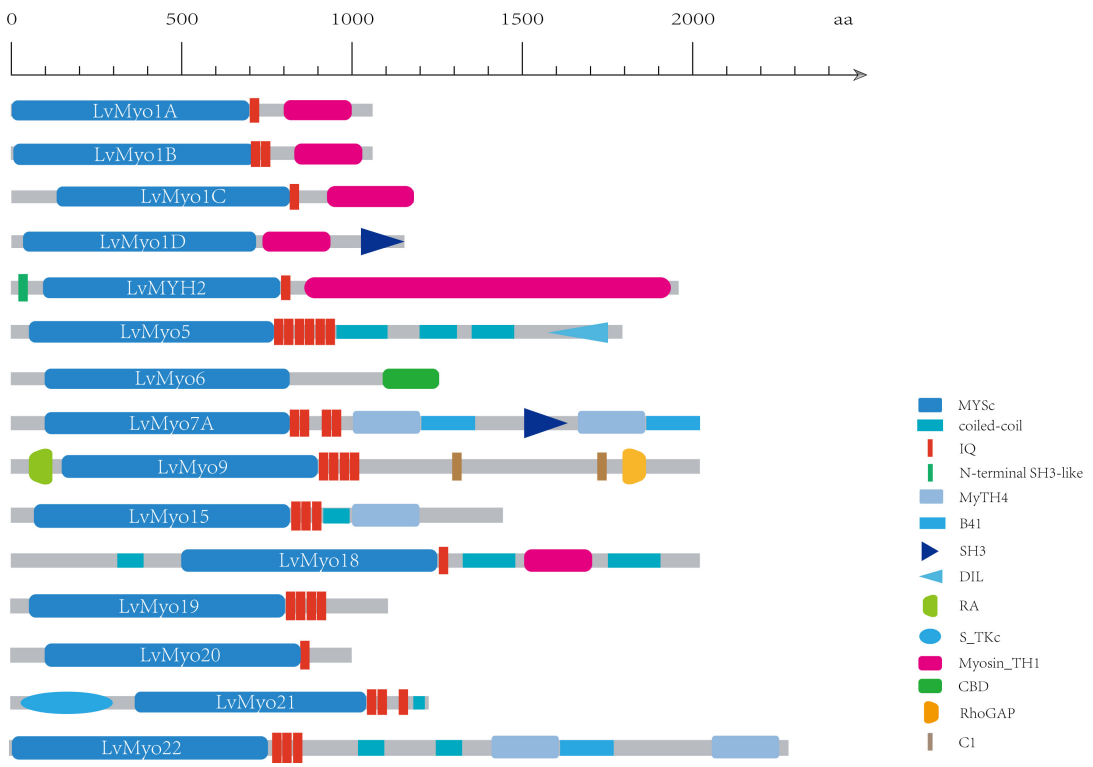

FIGURE 3 | Schematic diagram of shrimp unconventional myosin structures. The putative domains or motifs were identified using the Pfam and SMART databases with the default parameters. MYSc, Myosin head, large ATPase; IQ, isoleucine-glutamine motif; DIL, dilute; CBD, cargo binding domain; MyTH4, myosin tail homology 4; B41, band 4.1, ezrin, radixin, and moesin; SH3, src homology 3; RA, Ras association (RalGDS/AF-6) domain; C1, Protein kinase C conserved region 1; RhoGAP, Rho GTPase-activating protein; S_TKC, Serine/Threonine protein kinases, catalytic domain. Myosin_TH1, myosin tail homology 1.

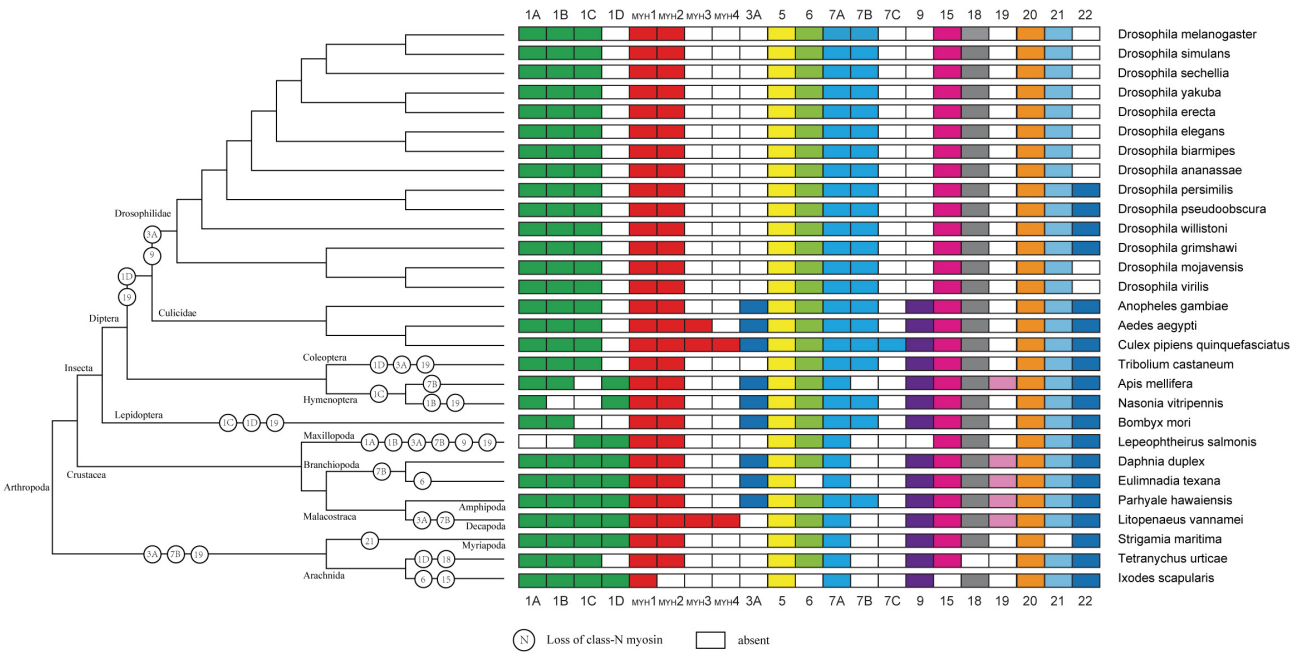

FIGURE 4 | Myosin gain and loss in arthropod species. Tree on the left illustrates the phylogenetic relationships of species used (no scale). Colored boxes indicate the presence of certain myosin subfamily members in each species. Empty boxes mean the potential loss of particular myosin genes.

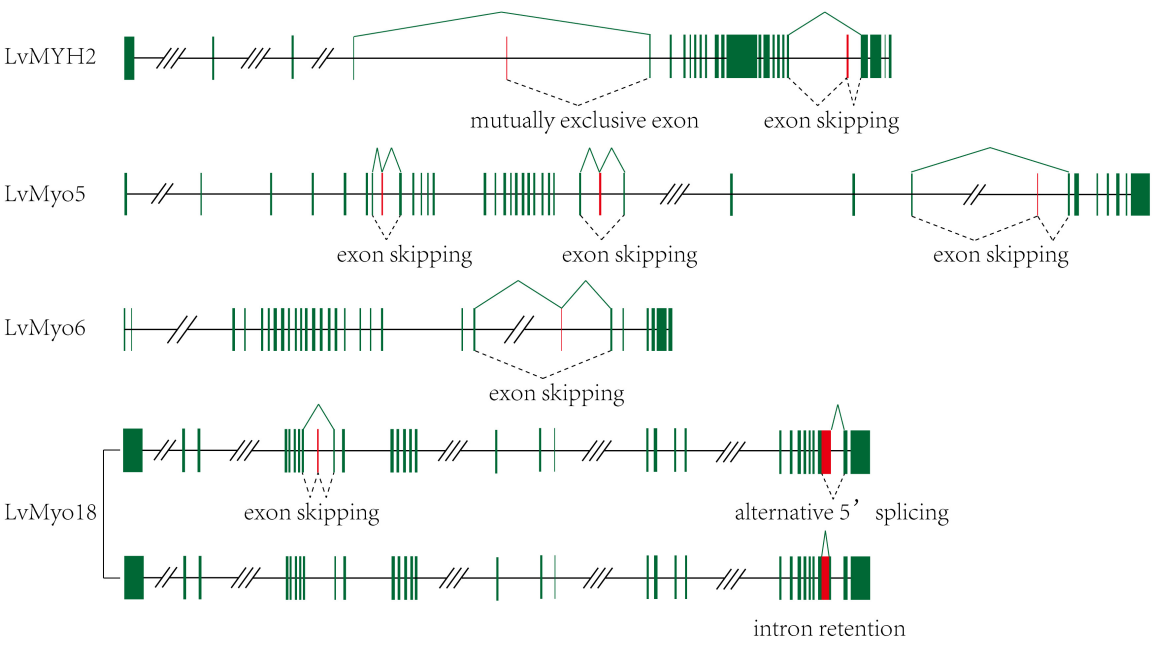

FIGURE 5 | Transcript evidences and splicing patterns for unconventional myosin genes in *L. vannamei*. Green boxes: exons; red boxes: alternative splicing exons; line, introns. Three-slashes represent large intron, and two-slashes represent genomic gap.

an IQ motif, and a large C-terminal myosin tail. However, the N-terminal SH3-like domain was absent in unconventional myosin genes of *L. vannamei*. Compared with *DamMyo18* and *DapMyo18*, the upstream PDZ domain was absent in *PhawMyo18* and *LvMyo18*.

Phylogenetic Analysis

As expected, the crustacea formed a distinct clade from other arthropods, and *L. vannamei* was most closely related to *P. hawaiensis* belonging to Malacostraca clades (**Figure 4**). In addition, arthropods contained 14 classes (groups) of myosin

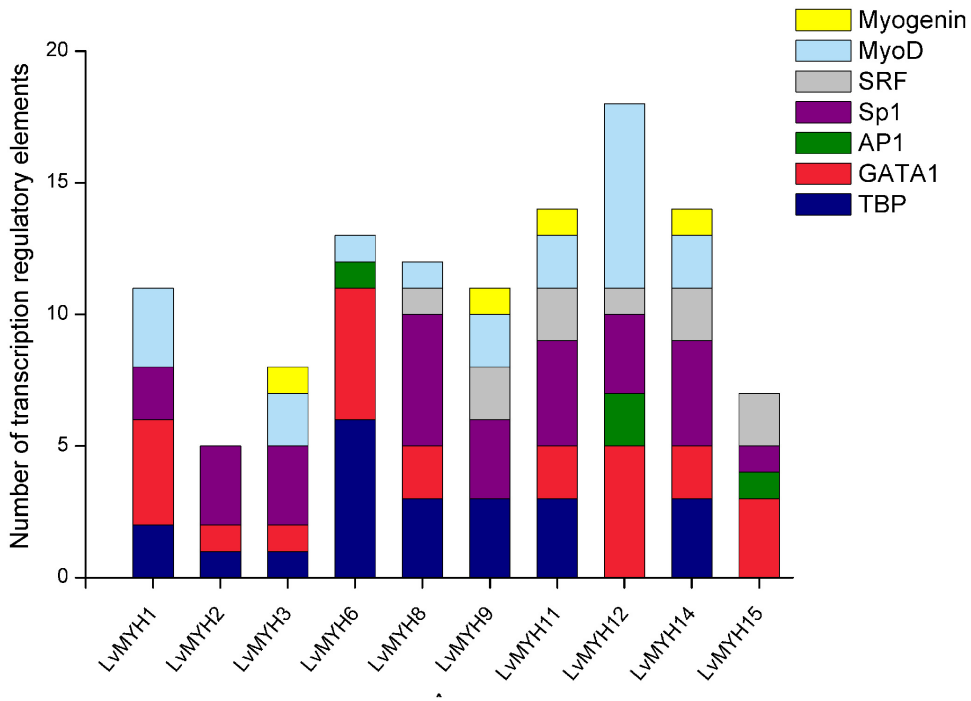

FIGURE 6 | Transcription regulatory elements in the promoters of several muscle-type Myo2 genes that are related to muscle development. SRF, serum response factor; Sp1, specificity protein 1; AP1, activator protein 1; TBP, TATA-binding protein.

genes including muscle-type *Myo2*, non-muscle *Myo2* (*MYH2*), *Myo5*, *Myo6, Myo7A, Myo15, Myo18*, *Myo20,* and *Myo21* with a few exceptions. For example, non-muscle type *Myo2*, *Myo6,* and *Myo15* were absent in *Ixodes scapularis*, and *Myo18* and *Myo21* were not found in *Tetranychus urticae* and *Strigamia maritima*, respectively. Most of these myosin genes were present in crustaceans, so we inferred that the last common crustacean ancestor had already contained these classes of myosin genes.

Alternative Splicing

Among the 29 myosin genes, four genes underwent alternative splicing (**Figure 5** and **Supplementary Table 2**). The unspliced transcript of *LvMYH2* encoded 1,972 aa protein, and the corresponding spliced transcripts encoded 1,982 and 1,970 aa when the exon 20 was retained and exon 4 was mutually excluded, respectively. *LvMyo5* possessed at least three splicing events, the unspliced transcript encoded 1,853 aa and the corresponding spliced transcript encoded 1,833, 1,804 and 1,846 aa with the exon 7, 24 and 28 were skipped, respectively. In the case of *LvMyo6*, an exon skipping event occurred in exon 22, and the corresponding spliced transcript encoded 1,238 aa, whereas the unspliced transcript encoded 1,257 aa. As for *LvMyo18*, the unspliced transcript generated 2,037 aa in length. Exon 8 of *LvMyo18-A1* transcript was retained, and the corresponding spliced transcript encoded 2,061 aa. Alternatively, a novel 660 bp intron between exon 28 and exon 29 of *LvMyo18-A2* transcript was retained. Furthermore, an alternative acceptor site was found in exon 29 of *LvMyo18-A3* transcript, and the corresponding spliced transcript encoded 2,066 aa.

Transcription Regulatory Elements of the Muscle-Type *Myo2* Promoters

A large number of muscle development-related transcription factors binding to the upstream promoter sequences of 10 *LvMYH*s were identified, including TATA-binding protein (TBP), GATA-1, activator protein 1 (AP1), specificity protein 1 (Sp1), serum response factor (SRF), myogenic differentiation 1 (MyoD) and myogenin (**Figure 6**). *LvMYH1*, *LvMYH2*, *LvMYH3*, *LvMYH6*, *LvMYH8*, *LvMYH9*, *LvMYH11*, *LvMYH12*, *LvMYH14,* and *LvMYH15* possessed 11, 5, 8, 13, 12, 11, 14, 18, 14, and 7 binding sites of muscle-related transcription factors, respectively. Among them, *LvMYH12* contained the highest number of binding sites of five muscle-related transcription factors. In addition, all analyzed LvMYH genes possessed at least one binding site of MyoD, except for *LvMYH2* and *LvMYH15*. The *LvMYH3*, *LvMYH9*, *LvMYH11,* and *LvMYH14*, might be activated by myogenin (**Figure 6**).

Temporal and Spatial Expression Patterns of Myosin Genes

We analyzed the temporal and spatial expression patterns of myosin genes based on the transcriptome of tissues or development stages (**Figure 7**). The results revealed that seven Myo2 subfamily genes, *LvMYH3*, *LvMYH6*, *LvMYH8*,

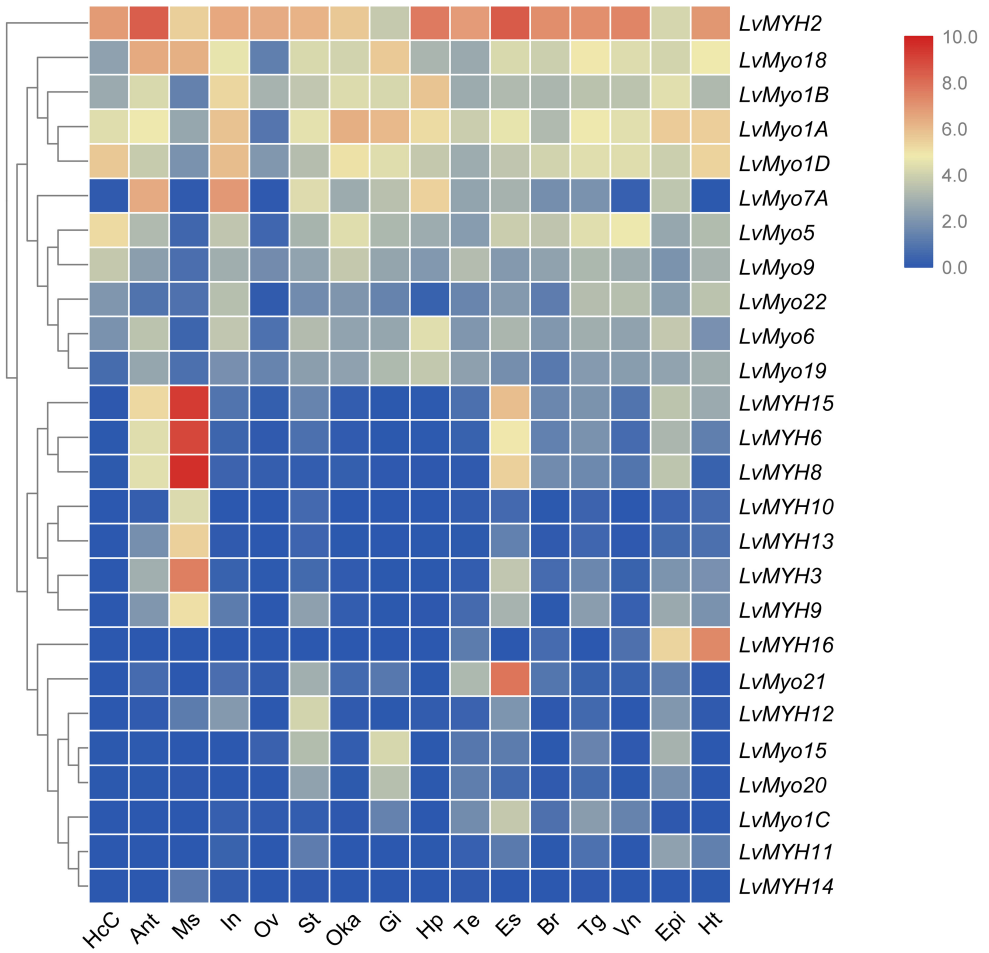

FIGURE 7 | The expression profiles of myosin genes in 16 adult tissues. Log2-transformed expression values were used to create the heat map. The red or blue colors represent the higher or lower relative abundance of each myosin gene, respectively. To the left are myosin genes; the top lists the adult tissues of *L. vannamei*. (HcC, hemocyte cells; Ant, antennary gland; Ms, abdominal muscle; In, intestine; Ov, ovary; St, stomach; Oka, lymphoid organ; Gi, gill; Hp, hepatopancreas; Te, testis; Es, eyestalk; Br, brain; Tg, thoracic ganglion; Vn, ventral nerve; Epi, epidermis; Ht, heart).

LvMYH9, *LvMYH10*, *LvMYH13,* and *LvMYH15,* were specifically highly expressed in the abdominal muscle. *LvMYH12* was exclusively expressed in stomach, and *LvMYH16* was particularly abundant in heart and epidermis. The expression levels of *LvMYH11* and *LvMYH14* were very low in all tissues. Similarly, the unconventional myosin genes also showed tissue-specific expression patterns; for instance, *LvMyo5* was specifically expressed in hemocyte, and *LvMyo21* exhibited high expression level in eyestalk.

All myosin genes were detectable with dynamic expression patterns during the whole developmental stage. Most of muscle-type Myo2 genes were highly expressed between the larvae in membrane (Lim) stage and the post-larva stage (P1) (**Figure 8**). For instance, *LvMYH2*, *LvMYH3,* and *LvMYH10* were expressed from Lim stage to nauplius 6 (N6) stage, and *LvMYH6*, *LvMYH8*, *LvMYH9*, and *LvMYH15* were highly expressed from zoea 1 (Z1) to P1 stage. However, unconventional myosin genes exhibited a distinct pattern, *LvMyo1A*, *LvMyo1B*, *LvMyo1D*, *LvMyo9*, *LvMyo15,* and *LvMyo19* were mainly expressed from zygote to gastrula stage, and *LvMyo7A* and *LvMyo20* were expressed from limb bud embryo 1 (Lbe1) stage to N6 stage.

In situ Hybridization

Shrimp abdominal muscle could be divided into four functional muscle groups, the superficial ventral muscle, the lateral muscle, the dorsal muscle and the main ventral muscle. The morphological organization of the skeletal muscle was displayed by the hematoxylin-eosin (H&E) staining (**Figure 9A**). *In situ* hybridization detection showed that *LvMYH5*, characterized as a marker gene of slow-type skeletal muscle Myo2, was mainly expressed in pleopod muscle and superficial ventral muscle (**Figure 9C**). They were attached between yokes of thin cuticle lying transversely across the posterior portion of each abdominal segment beneath the ventral nerve cord, and presumably function to hold the articular cuticle between the abdominal segments in place. However, no significant signal was observed in flexor and extensor muscle (**Figure 9B**).

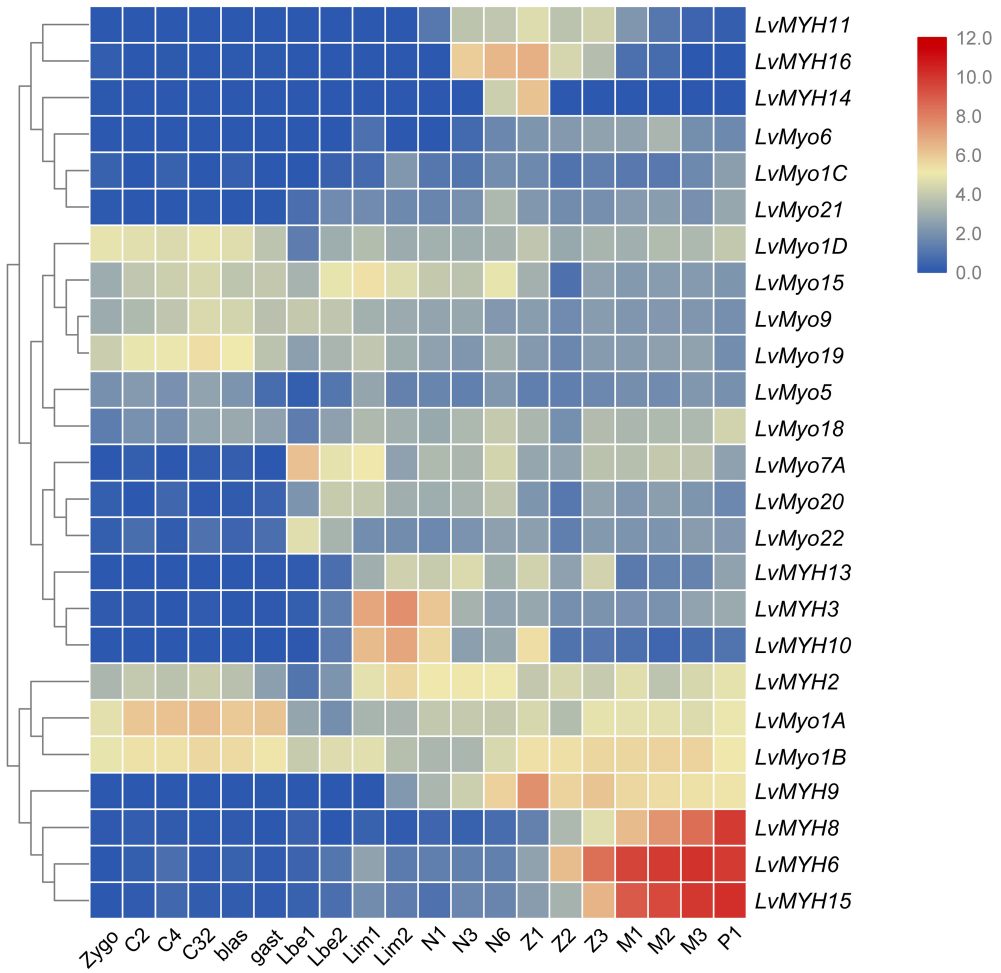

FIGURE 8 | The expression profiles of myosin genes during development of *L. vannamei*. Log2-transformed expression values were used to create the heat map. The red or blue colors represent the higher or lower relative abundance of each myosin gene, repectively. On the right are myosin genes; the bottom lists different larval stages of *L. vannamei*, from left to right: zygote, 2 cells (C2), 4 cells (C4), 32 cells (C32), blastula (blas), gastrula (gast), limb bud embryo 1 (Lbe1), limb bud embryo 2 (Lbe2), larva in membrane 1 (Lim1), larva in membrane 2 (Lim2), Nauplius 1 (N1), Nauplius 2 (N2), Nauplius 3 (N3), Nauplius 6 (N6), Zoea 1 (Z1), Zoea 2 (Z2), Zoea 3 (Z3), Mysis 1 (M1), Mysis 2 (M2), Mysis 3 (M3), and Post-larva 1 (P1).

DISCUSSION

The Evolutionary Relationship of Myosin Genes in Arthropods

The evolutionary relationship of myosin family is limited in crustaceans due to the lack of Crustacea genome and difficulties for myosin gene identification. With the decoding of more and more Crustacea genomes, we are now in a position to validate the evolution of myosin genes proposed previously in arthropods and gain new insights in crustaceans. In accordance with previous study (Odronitz et al., 2009), all myosin subfamilies are shared in arthropods, suggesting that the common ancestor of arthropod has already owned all myosin classes (Odronitz and Kollmar, 2007). Meanwhile, the evolution of arthropods is likely accompanied by taxon- or species-specific losses of certain myosin classes. For example, Myriopoda and Arachnida appeared to have lost *Myo3A* and *Myo19* classes, and Drosophilidae have lost *Myo1D*, *Myo3A*, *Myo9,* and *Myo19* classes. As Crustacea, Maxillopoda may have lost *Myo1A* and *Myo1B* after separating from Branchiopoda and Malacostraca. The potential lack of the *Myo3* class in *L. vannamei* and *L. salmonis* may be specific characteristic of species. In agreement with the results of several comparative genome analyses (Hill, 2005; Colbourne et al., 2011; Chipman et al., 2014; Kao et al., 2016), the Crustacea clade is more closely related to the Hexapoda clade, but the Myriapoda clade is closer relative to the Arachnida.

Gene Expansion of Muscle-Type *Myo2* Subfamilies

Gene family expansion generally results for a strengthened phenotype. In the *L. vannamei* genome, the muscle-type *Myo2* subfamilies showed significant expansion. Eight of 15 muscle-type Myo2 genes are tandemly duplicated. In addition, numerous fragmental muscle-type *Myo2*-like sequences or pseudogenes

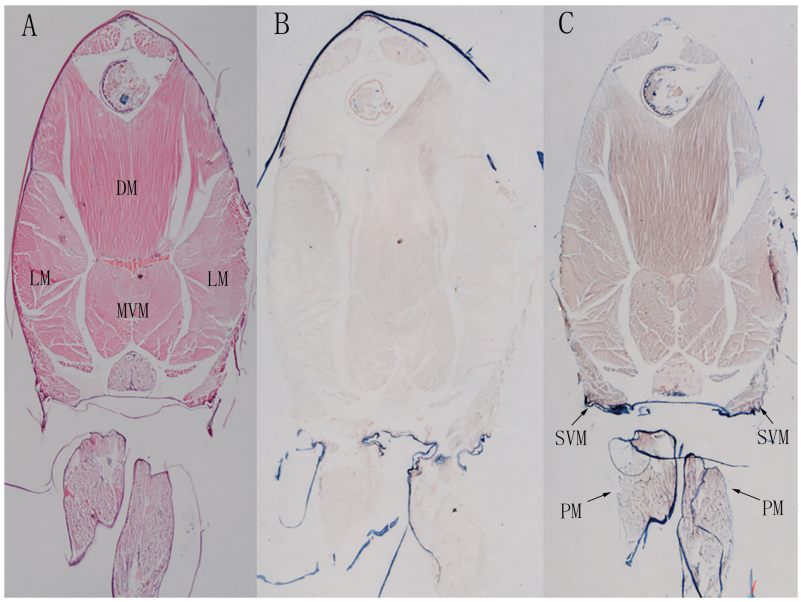

FIGURE 9 | The localization of *LvMYH5* in the abdominal muscle and pleopod muscle of *L. vannamei*. **(A)** Hematoxylin-eosin (H&E) staining and **(B)** a sense probe were used as the control for **(C)** the antisense probe hybridization. LM, the lateral muscle; DM, the dorsal muscle; MVM, the main ventral muscle; PM, the pleopod muscle; SVM, the superficial ventral muscle. The picture of H&E staining was from our previous study (Zhang et al., 2018).

near the LvMYH cluster were also detected. Furthermore, most of the expanded muscle-type Myo2 genes possess binding sites of various myogenesis related transcription factors, such as Sp1 (Biesiada et al., 1999), AP-1 (Andreucci et al., 2002), myogenin (Hasty et al., 1993) and MyoD (Tapscott et al., 1988). It was reported that *LvMYH1* and *LvMYH7* were located in all fibers of abdominal muscles containing extensor and flexor muscles by *in situ* hybridization (Koyama et al., 2012, 2013). These results indicate that these expanded muscle-type Myo2 genes might be associated with muscle composition or development. In accordance with our previous study (Zhang et al., 2018), this study reveals the pleopod muscle and superficial ventral muscle of *L. vannamei* contain slow-type oxidative muscle fibers.

The muscle of shrimp accounts for more than half of the total body weight (Chen and Chen, 2001), but the mechanism of its well-developed muscular system is unknown. Our previous study has also indicated large expansion of actin gene family in *L. vannamei* (Zhang et al., 2018), which encodes structural proteins of muscle fiber together with muscle-type myosin heavy chains. Taken together, we speculate that the well-developed muscular system of *L. vannamei* might be associated with the massive expansion of muscle-type actin genes and muscle-type Myo2 genes.

Alternative Splicing of Shrimp Myosin Genes

In most arthropods, MYH1 with multiple complex alternative splicing patterns was observed to be involved in muscle composition (Bernstein et al., 1986; Rozek and Davidson, 1986; Nyitray et al., 1994; Odronitz and Kollmar, 2008; Kollmar and Hatje, 2014). For example, the *D. duplex MYH1* (*Mhc1*) contains nine sets of mutually exclusive spliced exons (MXEs), and *Drosophila melanogaster MYH1* contains five clusters of MXEs and 480 combinations of alternative splicing patterns are possibly existed (Odronitz and Kollmar, 2008). Consistent with the report that crustacean *L. salmonis* contains 17 Myo2 genes without MXEs (Kollmar and Hatje, 2014), no MXE has been found in the 15 muscle-type Myo2 genes in this study. This implies that the last common ancestor of crustacean might have developed a MXE-less muscle-type Myo2 gene and followed by extensive gene duplications. Multiple, but not alternatively spliced myosin heavy chain genes are therefore a common characteristic of crustacean (Kollmar and Hatje, 2014). This might be caused by the loss of introns in the ancient muscle-type myosin heavy chain gene during arthropods evolution (Odronitz and Kollmar, 2008). However, unconventional myosin genes exhibited higher diversity due to the exon skipping in *L. vannamei*. It indicated that alternative splicing could potentially yield unconventional myosin variants with diverse functions.

Special Expression Patterns of Shrimp Myosin Genes

Most of muscle-type Myo2 genes of *L. vannamei* were primarily expressed during larva in membrane and post-larvae stages. Combined with our previous study on actin gene family (Zhang et al., 2018), the whole early development stage of shrimp can be grouped into three periods. In the beginning of early development period (zygote to gastrula), most muscle-type Myo2 and actin genes are not expressed, then begin to be expressed in the second period (limb embryo and larvae in membrane stage),

and their expression levels reach to the peak and remain at high levels in the third period (zoea to post-larvae stage). According to the report by Hertzler and Freas (2009), major ventral pleonal muscle and dorsal pleonal muscle of *L. vannamei* formed at the zoea stage, while pleopod muscle and major pleonal muscle formed in Mysis stage. Therefore, the high expression of muscle-type Myo2 and actin genes in these stages is compatible with the formation and development of pleonal and pleopod muscle.

The genes regulating muscle development, such as transcription factors, start to be expressed and to activate the co-expression of actin and myosin gene clusters at the nauplius stage. It promotes growth of muscle fibers in the larvae stage. Furthermore, compared with multiple alternative splicing of a single gene, the gene clusters have equivalent effects on improving the expression of transcripts, and strengthening the function of proteins (Talavera et al., 2007). Therefore, it is reasonable to conclude that the gene expansion of muscle-type Myo2 and actin genes may contribute to abundant fast-type muscle fibers and the explosive force of the shrimp abdominal muscles.

CONCLUSION

In summary, we identified 29 myosin genes in the *L. vannamei* genome, and classified them into 14 subfamilies. Their genome localization, gene structure, protein domains, *trans*-acting elements in promoter regions and molecular evolution were comprehensively analyzed. Their temporal and spatial expression profiles provide insights into their important functions in muscle composition and development. Moreover, the expanded muscle-type Myo2 subfamily may explain the well-developed muscular system of *L. vannamei*. Collectively, this study will provide important clues for future research on the function of myosin genes in shrimp.

ETHICS STATEMENT

This study was carried out in accordance with the recommendations of Welfare ethics of experimental animals and safety inspection system of animal experiments, laboratory animal management and ethics Committee of IOCAS. The protocol was approved by the laboratory animal management and ethics Committee of IOCAS.

AUTHOR CONTRIBUTIONS

JX, FL, and XnZ conceived and designed the study. XiZ and CL collected the data. XiZ conducted the bioinformatics analyses, performed all experiments and wrote the manuscript. JY, XnZ, and FL revised the manuscript.

FUNDING

This work was financially supported by the National Key R&D Program of China (2018YFD0900103), the National Natural Science Foundation of China (31830100 and 41876167), and China Agriculture Research System-47 (CARS-47).

ACKNOWLEDGMENTS

We thank Dr. Qing Guo for her help in performing the *in situ* hybridization experiment.

SUPPLEMENTARY MATERIAL

The Supplementary Material for this article can be found online at: https://www.frontiersin.org/articles/10.3389/fphys.2019.00610/full#supplementary-material

REFERENCES

Andreucci, J. J., Grant, D., Cox, D. M., Tomc, L. K., Prywes, R., Goldhamer, D. J., et al. (2002). Composition and function of AP-1 transcription complexes during muscle cell differentiation. *J. Biol. Chem.* 277:16426.

Berg, J. S., Powell, B. C., and Cheney, R. E. (2001). A millennial myosin census. *Mol. Biol. Cell* 12, 780–794.

Bernstein, S. I, Hansen, C. J., Becker, K. D., Roche, E. S., Donady, J. J., and Emerson, C. P. (1986). Alternative RNA splicing generates transcripts encoding a thorax-specific isoform of Drosophila melanogaster myosin heavy chain. *Mol. Cell. Biol.* 6:2511.

Biesiada, E., Hamamori, Y., Kedes, L., and Sartorelli, V. (1999). Myogenic basic helix-loop-helix proteins and sp1 interact as components of a multiprotein transcriptional complex required for activity of the human cardiac α-actin promoter. *Mol. Cell. Biol.* 19, 2577–2584.

Bloemink, M. J., and Geeves, M. A. (2011). Shaking the myosin family tree: biochemical kinetics defines four types of myosin motor. *Semin. Cell Dev. Biol.* 22, 961–967. doi: 10.1016/j.semcdb.2011.09.015

Chen, C., Xia, R., Chen, H., and He, Y. (2018). TBtools, a Toolkit for Biologists integrating various HTS-data handling tools with a user-friendly interface. *bioRxiv*

Chen, Q., and Chen, X.-H. (2001). Effect of different salinity culture on flesh content and nutrients of *Penaeus vannamei*. *Mar. Sci.* 25, 16–28.

Chipman, A. D., Ferrier, D. E. K., Brena, C., Qu, J., Hughes, D. S. T., Schröder, R., et al. (2014). The first myriapod genome sequence reveals conservative arthropod gene content and genome organisation in the centipede *Strigamia maritima*. *PLoS Biol.* 12:e1002005. doi: 10.1371/journal.pbio.1002005

Colbourne, J. K., Pfrender, M. E., Gilbert, D., Thomas, W. K., Tucker, A., Oakley, T. H., et al. (2011). The ecoresponsive genome of *Daphnia pulex*. *Science* 331:555. doi: 10.1126/science.1197761

Edgar, R. C. (2004). MUSCLE: multiple sequence alignment with high accuracy and high throughput. *Nucleic Acids Res.* 32, 1792–1797.

FAO (2014). *Cultured Aquatic Species Information Programme-Litopenaeus vannamei*. Rome: FAO.

Finn, R. D., Attwood, T. K., Babbitt, P. C., Bateman, A., Bork, P., Bridge, A. J., et al. (2016). InterPro in 2017—beyond protein family and domain annotations. *Nucleic Acids Res.* 45, D190–D199. doi: 10.1093/nar/gkw1107

Gao, Y., Zhang, X., Wei, J., Sun, X., Yuan, J., Li, F., et al. (2015). Whole transcriptome analysis provides insights into molecular mechanisms for molting in *Litopenaeus vannamei*. *PLoS One* 10:e0144350. doi: 10.1371/journal.pone.0144350

Hammesfahr, B., Odronitz, F., and Kollmar, M. (2010). Cymobase – the reference database for cytoskeletal and motor proteins. *Biophys. J.* 98. doi: 10.1016/j.bpj.2009.12.3036

Hartman, M. A., Finan, D., Sivaramakrishnan, S., and Spudich, J. A. (2011). Principles of unconventional myosin function and targeting. *Ann. Rev. Cell Dev. Biol.* 27:133. doi: 10.1146/annurev-cellbio-100809-151502

Hasty, P., Bradley, A., Morris, J. H., Edmondson, D. G., Venuti, J. M., Olson, E. N., et al. (1993). Muscle deficiency and neonatal death in mice with a targeted mutation in the myogenin gene. *Nature* 364:501.

Hertzler, P. L., and Freas, W. R. (2009). Pleonal muscle development in the shrimp Penaeus (Litopenaeus) vannamei (Crustacea: Malacostraca: Decapoda: Dendrobranchiata). *Arth. Struct. Dev.* 38, 235–246. doi: 10.1016/j.asd.2008.12.003

Hill, C. A. (2005). The *Ixodes scapularis* genome project: an opportunity for advancing tick research. *Trends Parasitol.* 21:151.

Hofmann, W. A., Richards, T. A., and De, L. P. (2009). Ancient animal ancestry for nuclear myosin. *J. Cell Sci.* 122, 636–643. doi: 10.1242/jcs.030205

Huang, X., and Madan, A. (1999). CAP3: A DNA sequence assembly program. *Genome Res.* 9, 868–877.

Kao, D., Lai, A. G., Stamataki, E., Rosic, S., Konstantinides, N., Jarvis, E., et al. (2016). The genome of the crustacean Parhyale hawaiensis, a model for animal development, regeneration, immunity and lignocellulose digestion. *eLife* 5:e20062. doi: 10.7554/eLife.20062

Kollmar, M., and Hatje, K. (2014). Shared gene structures and clusters of mutually exclusive spliced exons within the metazoan muscle myosin heavy chain genes. *PLoS One* 9:e88111. doi: 10.1371/journal.pone.0088111

Koyama, H., Akolkar, D. B., Piyapattanakorn, S., and Watabe, S. (2012). Cloning, expression, and localization of two types of fast skeletal myosin heavy chain genes from black tiger and Pacific white shrimps. *J. Exp. Zool. Part A Ecol. Genet. Physiol.* 317, 608–621. doi: 10.1002/jez.1752

Koyama, H., Piyapattanakorn, S., and Watabe, S. (2013). Cloning of skeletal myosin heavy chain gene family from adult pleopod muscle and whole larvae of shrimps. *J. Exp. Zool. Part A Ecol. Genet. Physiol.* 319, 268–276. doi: 10.1002/jez.1791

Kumar, S., Stecher, G., and Tamura, K. (2016). MEGA7: molecular evolutionary genetics analysis version 7.0 for bigger datasets. *Mol. Biol. Evol.* 33:1870. doi: 10.1093/molbev/msw054

Letunic, I., and Bork, P. (2007). *Interactive Tree Of Life (ITOL): an Online Tool for Phylogenetic Tree Display and Annotation*. Oxford: Oxford University Press.

Letunic, I., Doerks, T., and Bork, P. (2014). SMART: recent updates, new developments and status in 2015. *Nucleic Acids Res.* 43, D257–D260. doi: 10.1093/nar/gku949

Nyitray, L., Jancsó, A., Ochiai, Y., Gráf, L., and Szentgyörgyi, A. G. (1994). Scallop striated and smooth muscle myosin heavy-chain isoforms are produced by alternative RNA splicing from a single gene. *Proc. Natl. Acad. Sci. U.S.A.* 91:12686.

Odronitz, F., Becker, S., and Kollmar, M. (2009). Reconstructing the phylogeny of 21 completely sequenced arthropod species based on their motor proteins. *BMC Genomics* 10:173. doi: 10.1186/1471-2164-10-173

Odronitz, F., and Kollmar, M. (2007). Drawing the tree of eukaryotic life based on the analysis of 2,269 manually annotated myosins from 328 species. *Genome Biol.* 8, 1–23.

Odronitz, F., and Kollmar, M. (2008). Comparative genomic analysis of the arthropod muscle myosin heavy chain genes allows ancestral gene reconstruction and reveals a new type of 'partially' processed pseudogene. *BMC Mol. Biol.* 9:21. doi: 10.1186/1471-2199-9-21

Pette, D., and Staron, R. S. (2015). Myosin isoforms, muscle fiber types, and transitions. *Microsc. Res. Tech.* 50, 500–509.

Potter, S. C., Luciani, A., Eddy, S. R., Park, Y., Lopez, R., and Finn, R. D. (2018). HMMER web server: 2018 update. *Nucleic Acids Res.* 46, W200–W204. doi: 10.1093/nar/gky448

Richards, T. A., and Cavalier-Smith, T. (2005). Myosin domain evolution and the primary divergence of eukaryotes. *Nature* 436, 1113–1118.

Rozek, C. E., and Davidson, N. (1986). Differential processing of RNA transcribed from the single-copy Drosophila myosin heavy chain gene produces four mRNAs that encode two polypeptides. *Proc. Natl. Acad. Sci. U.S.A.* 83, 2128–2132.

Sebé-Pedrós, A., Grau-Bové, X., Richards, T. A., and Ruiz-Trillo, I. (2014). Evolution and classification of myosins, a paneukaryotic whole-genome approach. *Genome Biol. Evol.* 6, 290–305. doi: 10.1093/gbe/evu013

Talavera, D., Vogel, C., Orozco, M., Teichmann, S. A., and Cruz, X. D. L. (2007). The independence of alternative splicing and gene duplication. *PLoS Comput. Biol.* 3:e33.

Tapscott, S. J., Davis, R. L., Thayer, M. J., Cheng, P. F., Weintraub, H., and Lassar, A. B. (1988). MyoD1: a nuclear phosphoprotein requiring a Myc homology region to convert fibroblasts to myoblasts. *Science* 242, 405–411.

Wei, J., Zhang, X., Yu, Y., Huang, H., Li, F., and Xiang, J. (2014). comparative transcriptomic characterization of the early development in Pacific White Shrimp *Litopenaeus vannamei*. *PLoS One* 9:e106201. doi: 10.1371/journal.pone.0106201

Woolner, S., and Bement, W. M. (2009). Unconventional myosins acting unconventionally. *Trends Cell Biol.* 19, 245–252. doi: 10.1016/j.tcb.2009.03.003

Zhang, X., Yuan, J., Sun, Y., Li, S., Gao, Y., Yu, Y., et al. (2019). Penaeid shrimp genome provides insights into benthic adaptation and frequent molting. *Nat. Commun.* 10:356. doi: 10.1038/s41467-018-08197-4

Zhang, X., Zhang, X., Yuan, J., Du, J., Li, F., and Xiang, J. (2018). Actin genes and their expression in pacific white shrimp, Litopenaeus vannamei. *Mol. Genet. Genomics* 293, 479–493.

Conflict of Interest Statement: The authors declare that the research was conducted in the absence of any commercial or financial relationships that could be construed as a potential conflict of interest.

frontiers in Physiology

ORIGINAL RESEARCH
published: 25 June 2019
doi: 10.3389/fphys.2019.00739

Sea Surface Temperature Modulates Physiological and Immunological Condition of *Octopus maya*

Cristina Pascual[1,2], Maite Mascaro[1,2], Rossanna Rodríguez-Canul[3], Pedro Gallardo[1], Ariadna Arteaga Sánchez[1,2], Carlos Rosas[1,2] and Honorio Cruz-López[4]*

[1] Unidad Multidisciplinaria de Docencia e Investigación, Facultad de Ciencias, Universidad Nacional Autónoma de México, Sisal, Mexico, [2] Laboratorio Nacional de Resiliencia Costera, Consejo Nacional de Ciencia y Tecnología, Sisal, Mexico, [3] Laboratorio de Inmunología y Biología Molecular, Centro de Investigación y de Estudios Avanzados del Instituto Politécnico Nacional, Unidad Mérida, Merida, Mexico, [4] Posgrado en Ecología Molecular y Biotecnología, Universidad Autónoma de Baja California, Ensenada, Mexico

Octopus maya is a valuable endemic species of the Yucatán Peninsula (YP). This area can be divided into distinct regions depending on the presence of cold waters associated to upwelling events during spring and summer. This study was designed to determine if the physiological and immunological condition of *O. maya* show a relationship with variation of the sea surface temperature associated with the seasonal upwelling. A total of 117 organisms were collected from February to July in three fishing zones: Ría Lagartos located in the upwelling zone; Seybaplaya corresponding to the non-upwelling zone, and Sisal, the transitional zone. The organisms were examined in terms of physiological (total weight, the weight of the gonad and digestive gland, osmotic pressure, hemocyanin, protein, glucose, and cholesterol concentrations in plasma), and immunological variables (total hemocyte count, hemagglutination, phenoloxidase system activity, total phenoloxidase plasma activity, and lysozyme activity). Multivariate one-way ANOVA showed overall significant differences between groups of octopus by month/zone of capture, indicating that the physiological-immunological condition of *O. maya* is related to a temperature gradient. Wild octopuses captured at the upwelling zone and the transitional zone (Ría Lagartos and Sisal) in February, March, and April -with temperatures lower than 27°C- were in better conditions: larger size, high concentrations of hemocyanin, and low activity of the phenoloxidase system. Octopuses captured in the warmer waters (28–30°C) of the non-upwelling and transitional zones (Seybaplaya and Sisal) during June and July, could be reflecting the metabolic stress through immunological compensation mechanisms with higher activity of the phenoloxidase system, despite having a lower concentration of hemocytes, hemocyanin, and proteins. Although the movement of individual *O. maya* along the YP throughout their life cycle has not yet been determined, direct development and benthic behavior could limit the mobility of the organisms in such a way that their physiological and immunological condition might reflect adaptation to the regional environment. This information could help understand the performance of octopuses in their distribution area, which sustains an important fishery.

Keywords: *Octopus maya*, hemolymph, eco-immunology, physiology, immunological indicators

OPEN ACCESS

Edited by:
Pierre Blier, Université du Québec à Rimouski, Canada

Reviewed by:
Ione Hunt Von Herbing, University of North Texas, United States
Alexssandro Geferson Becker, Universidade Federal do Paraná, Setor Palotina, Brazil

****Correspondence:***
Cristina Pascual
pascual.cristina@ciencias.unam.mx

Specialty section:
This article was submitted to Aquatic Physiology, a section of the journal Frontiers in Physiology

Received: *02 November 2018*
Accepted: *28 May 2019*
Published: *25 June 2019*

Citation:
Pascual C, Mascaro M, Rodríguez-Canul R, Gallardo P, Sánchez AA, Rosas C and Cruz-López H (2019) Sea Surface Temperature Modulates Physiological and Immunological Condition of Octopus maya. Front. Physiol. 10:739. doi: 10.3389/fphys.2019.00739

INTRODUCTION

Octopus maya (Voss and Solís-Ramírez, 1966) is an endemic species of the Yucatán Peninsula (YP), Mexico. This species alone sustains the main *Octopus* fishery in the American continent with annual production ranging from 8,000 to 20,000 tons (Markaida et al., 2017). The geographical distribution of *O. maya* is the smallest in size among all the cephalopod's species, and it coincides with the area of influence of summer upwelling of sub-superficial subtropical waters from de Caribbean to the YP shelf characterized by temperatures between 16 and 22°C (Enriquez et al., 2013). This upwelling affects only the eastern portion of the YP continental shelf, resulting in a summer eastern-to-western thermal gradient with low-to-high temperatures, offering different and unique environments to aquatic species of the zone (Zavala-Hidalgo et al., 2006). The life cycle of *O. maya* occurs in the YP and is of around 8–12 months (Hanlon and Forsythe, 1985). Females of the species may lay from 1,500 to 2,000 eggs with average size of 17 mm in length and produce large benthic hatchlings measuring around 6–7 mm mantle length (Roper et al., 1984; Caamal-Monsreal et al., 2015; Tercero et al., 2015).

Octopus maya is an ectothermic organism, and recently relevant knowledge has been gained to understand its thermal tolerance in experimental studies. When octopus are exposed to high temperatures (>28°C) adverse effects are observed on growth (Noyola et al., 2013a,b), reproductive efficiency (Caamal-Monsreal et al., 2016; López-Galindo et al., 2018), and embryonic development (Juárez et al., 2015). However, little is known about the effect of changes on temperature on the physiology and immune response of *O. maya*. In the face of the climatic change scenario, there is relevant information showing a greater susceptibility to opportunistic infections at the population level (Paillard et al., 2004; Mydlarz et al., 2006). The main results of ocean warming are the decrease of oxygen levels and acidification in the coastal waters to mention some. Hypoxia can directly affect the immunocompetence of marine invertebrates, but the mechanical links between temperature and immune response are still unsolved (Mydlarz et al., 2006). In this sense, the biochemical and immune metabolites measured in the hemolymph can provide information to assess the health status and physiology of a given organism (Fazio, 2019). This approach has been widely used for clinical diagnosis in veterinary settings.

The immune system is involved in the preservation of the biological integrity of living organisms as it allows the recognition and neutralization of non-self-molecules either from the environment or produced by metabolic processes. The defense mechanisms of invertebrates are considered simple since they lack processes that are present in vertebrates, such as immunoglobulin-mediated immune memory. Nevertheless, modern cephalopods appeared at the same time as bony fish, more than 200 million years ago (Hochner et al., 2006), indicating they have developed similarly diverse, successful strategies to cope with infections and other harmful elements of the environment.

So far, in cephalopods, the main line of defense from foreign substance rely on peripheral cells or hemocytes which have phagocytic, encapsulation and neutralization capabilities and are also involved in inflammatory and injury healing processes (Beuerlein et al., 2002). In invertebrates the amplification of defense mechanisms is associated to the prophenoloxidase (proPO) system found within hemocytes granules (Söderhäll and Smith, 1983; Söderhäll and Häll, 1984). The proPO system is directly released when hemocytes are stimulated by fungal or bacterial beta-glucans (βG) or lipopolysaccharides (LPS) (Söderhäll and Häll, 1984); signals associated with the wound and cellular damage (DAMPs) (Dubovskiy et al., 2016), or by recognition serum proteins which warn hemocytes (Vargas-Albores et al., 1996, 1997). Once activated, the proPO system produces several factors that stimulate hemocytes to eliminate the foreign material by phagocytosis, nodule formation and/or encapsulation (Söderhäll and Smith, 1983; Sung et al., 1998). Phagocytosis is one of the most important mechanisms of hemocytes immune response. During this process, phagolysosomes are formed, and highly reactive lytic substances such as peroxide, superoxide, and nitric oxide derivatives are released (Muñoz et al., 2000; Campa-Córdova et al., 2002). The process is known as a respiratory burst and has an essential role in hemocytes microbicide activity (Song and Hsieh, 1994).

Among components of the immune system are lectins, a very diverse group of proteins capable of recognizing carbohydrates. Several studies have pointed out the capacity of *O. vulgaris* plasma to agglutinate bacteria and erythrocytes (Rögener et al., 1987). Fisher and DiNuzzo (1991) conducted a comprehensive study that demonstrated hemagglutination activity against isolated bacteria and seven types of erythrocytes of octopus *O. maya*, Japanese squid, *Sepioteuthis lessoniana*; and common cuttlefish, *Sepia officinalis*. These results demonstrated the diverse recognition abilities and the existence of molecules that participate in the hemagglutination processes. Lysozymes — a group of proteases capable of hydrolyzing components of microorganism's surface —, are also found among the humoral effectors of the immune response. These enzymes are found in hemocytes vacuoles and are secreted to the hemolymph by these and other cells (Locatello et al., 2013).

Cephalopods have a closed circulatory system which transports hemolymph through blood vessels and capillaries. Plasma metabolites concentrations reflect metabolic adjustments associated to the type of food ingested, energy demands and physiological adaptations that take place when organisms are exposed to different environmental conditions (Pascual et al., 2003, 2004). The main evaluation criteria used to determine the physiological condition of cephalopods at population level include biochemical characterization of the digestive gland, gonads, and muscle tissues (Rosas et al., 2002; Sieiro et al., 2006; Gallardo et al., 2017). The mobilization of reserves has been associated with the weight of the digestive gland, one of the main catabolism organs. In previous studies, we determined that the plasmatic metabolites of *O. maya* (total proteins, acylglycerols, cholesterol, and glucose), are related to the quality of the dietary intake as well as their nutritional condition (Aguila et al., 2007; Moguel et al., 2010; Martínez et al., 2014; Linares et al., 2015). In marine invertebrates the metabolites variation has been related to the general physiological condition that helps to understand

what kind of metabolic route is used under a given condition; acclimation temperature (Sánchez et al., 2001); size-based selection program on blood metabolites and immune response (Pascual et al., 2004); and immune response against a specific viral infection (Pascual-Jiménez et al., 2012).

This study was developed to evaluate if the variations on the sea surface temperature related to the seasonal upwelling of the Yucatán Peninsula, Mexico, had a relationship with the health status of the octopuses. Based on the information on the thermal tolerance of the species, we hypothesized that the octopuses captured in the localities and months with sea surface temperatures >28°C will present a less optimal physio-immunological condition than the organisms captured in localities and months with lower surface temperature (23–26°C). This information would help to understand the physiological–immunological performance of octopuses in its distribution area that sustains an important fishery activity.

MATERIALS AND METHODS

Sampling Locations

The Campeche Bank is located on the continental shelf of the YP adjacent to the states of Yucatán and Campeche in southwestern Gulf of Mexico. Oceanographic conditions on the shelf, and the presence of local upwelling allows differentiation of three environmental zones with contrasting temperature regimes (Enriquez et al., 2013). Samples of octopus *O. maya* were collected at three locations from February to July, 2010: Ría Lagartos (21°38′N, 88°10′W) located in the upwelling zone (Z1); Seybaplaya (19°38′N, 90°41′W) corresponding to a zone with no influence of upwelling (Z3); and Sisal (21°09′N, 90°01′O), a zone of transition located between the two former locations (Z2). The main upwelling event occurs from July to September in Z1, is less prominent in Z2, and is absent in Z3 (Merino, 1997).

Octopus Sampling

A total of 117 organisms were analyzed: 24 from Ría Lagartos, 66 from Sisal, and 27 from Seybaplaya. The total weight of the captured organisms ranged from 100.67 to 1,934.2 g Immediately after capture, octopuses were placed in a closed tank with seawater that was kept circulating using a submersible water pump. The boat headed to the dock where they were transferred to a collecting tank connected to a 250 L tank used for transportation to laboratory facilities at UMDI-Sisal, Yucatán, Mexico. Total transportation from the dock to the laboratory lasted around 2–7 h, and the temperature of the water during transportation fluctuated between 25 and 28°C. Each transportation tank was provided with several 4-inch PVC tubes that were placed inside as individual shelters to reduce interaction stress among the organisms. Once in the laboratory, organisms were placed individually in 80 L tanks with seawater at 27–28°C with constant flow and aeration. Water passed through 5 μm filters with replacement rate equivalent to 300% per day. In such conditions, it was possible to maintain ammoniacal nitrogen and nitrite levels below 0.1 mg ml^{-1}, nitrate below 50 mg ml^{-1}, and pH between 7.7 and 8.2, values recommended as appropriate to keep different species of octopus in captivity, including *O. maya* (Hanlon and Forsythe, 1985).

Hemolymph Sampling

Before hemolymph sampling, octopuses were anesthetized by hypothermia at 10°C for several minutes (Cruz-López, 2010; Linares et al., 2015; Roumbedakis et al., 2017). This was observed physically by reduction of the breathing rate (indicated by contractions of the mantle), and reduction of locomotor activity. After that, each animal was removed from the cold water and hemolymph was drawn from the cephalic aorta using a pre-chilled catheter connected to a 5 ml Falcon tube and immediately kept refrigerated (2–8°C) to be used few hours later (Cruz-López, 2010). Hemolymph was centrifuged at 800 × *g* for 5 min at 4°C to separate the plasma, which was used to evaluate plasmatic metabolites, phenoloxidase (PO) and hemagglutination activity. The cellular pellet from each sample was washed twice with isotonic solution (IS: 0.45 M NaCl, 10 mM KCl, 10 mM HEPES, 7.3 pH, and 10 mM EDTA–Na_2) and centrifuged as described above. The cellular pellet was then re-suspended several times with cacodylate buffer (10 mM cacodylic acid, 10 mM CaCl, pH 7.0) in an equal volume of hemolymph and centrifuged at 13,000 × *g* for 5 min at 4°C. The supernatant was used to evaluate the PO activity from degranulated hemocytes.

Physiological Variables

Soon after hemolymph collection, octopuses were euthanized by brain puncture (Boyle, 1976; Fiorito et al., 2015). Thereafter, animals were weighed (total weight), and the gonad and the digestive gland were removed and weighed separately. Glucose, cholesterol, and acylglycerides concentrations in plasma were determined in triplicate in 96-well flat bottom plates using specific commercial chromogenic kits (Sera Pack Plus Bayer®), adding 10 μl of plasma to 200 μl of the appropriate enzyme reagent for each sample. Protein concentrations were also determined in triplicate in 96-well flat bottom plates. The plasma was previously diluted in sterile water (400×) and then 10 μl of this solution was mixed with 200 μl of commercial solution (Biorad Protein assay 500-0006) according to the Bradford (1976) method. Bovine serum albumin was used as a standard. Absorbance values of all metabolites were recorded in a microplate reader (Benchmark Plus BioRad). A standard curve was developed for each metabolite and linearity was confirmed. The concentration (mg ml^{-1}) of samples were calculated using the standard curves.

Hemocyanin concentration was measured by placing 10 μl of hemolymph diluted in 990 μl of Tris 0.1M, pH 8.0, in a 10-mm cuvette. The absorbance was measured at 335 nm (Genesys 10 UV-Vis, Thermo Scientific). Hemocyanin concentration was calculated using an extinction coefficient of 17.26 calculated on the basis of the functional subunit of 74 kDa (Chen and Cheng, 1993a,b). To measure the osmotic pressure, we placed 20 μl of hemolymph in a micro-osmometer (3MO Plus, Advanced Micro-osmometer). Results were expressed as mOsm kg^{-1} (Lignot et al., 2000).

Immunological Variables

Hemagglutination activity was measured using human blood (type O+) obtained from a local blood bank. Samples of 50 μl of octopus plasma were added to a U-shaped 96-well microliter plate, and twofold serial dilution were prepared using 0.9% saline solution as the diluent. Prior to use, erythrocytes were washed three times with 0.9% saline solution, centrifuged at 380 × *g* at 25°C for 5 min, and then adjusted to a final volume of 2%. An equal volume of the erythrocyte solution was added to each well and incubated for 3 h at room temperature. In controls, plasma was replaced by 0.9% saline solution. Plasma hemagglutination titer was expressed as the reciprocal of the highest dilution showing a positive visible pattern of agglutination (Pascual-Jiménez et al., 2012).

Phenoloxidase system activity was measured by spectrophotometry in triplicate in 96-well flat bottom plates (Hernández-López et al., 1996). The technique was adjusted for *O. maya* (Roumbedakis et al., 2017). The plasma and degranulated hemocytes plasma of 50 μl samples were incubated for 10 min at 37°C to transform proPO into phenoloxidase (PO) without using exogenous trypsin. To evaluate total phenoloxidase activity, plasma was incubated with 50 μl of trypsin (bovine pancreatic 0.1 mg ml^{-1}; Sigma T8003). Then, 180 μl of L-3,4-dihydroxyphenylalanine (L-DOPA, 3 mg ml^{-1}; Sigma D9628) were added to each well and the microplate incubated for more than 10 min at 37°C. Absorbance was measured at 490 nm in a microplate reader (Benchmark Plus BioRad). Results were expressed as the increment of 0.001 in optical density.

Total hemocytes were counted in a Neubauer chamber from a hemolymph aliquot fixed with 4% formaldehyde in Alsever solution (115 mM $C_6H_{12}O_6$, 30 mM $Na_3C_6H_5O_7$, 338 mM NaCl, 10 mM EDTA.Na_2, pH 7.0) with a 1:3 dilution (Roumbedakis et al., 2017). Samples were kept at 2–8°C, for a maximum period of 10 days before analysis. Counting was performed in duplicate covering a minimum area count of 0.04 mm^{-3} and expressed as cells mm^{-3}.

Lysozyme activity was quantified according to the turbidimetric method of Parry et al. (1965) with slight modification. *Micrococcus* were suspended in 0.05 M sodium phosphate buffer (pH 7.3), transferred to a cuvette and read at UV-vis spectrophotometer at 530 nm. Hemolymph (100 μl) was transferred to the cuvette, and the reduction in absorbance was recorded. The result was expressed as U ml^{-1}.

To avoid immune system activation by endotoxins, all glassware was washed with Etoxa-clean prior to use and solutions were prepared using pyrogen-free water and filtered through a 0.2 μm Acrodisc.

Statistical Analysis

Multivariate analyses are useful to determine whether individuals can be characterized by a set of attributes (i.e., physiological and immunological variables). With a principal coordinate analysis (PCoA, Legendre and Legendre, 1998), we used a set of 13 physiological and immunological variables to order the organisms. Localities analyzed are close to the limits of the geographic distribution of *O. maya* (west, east, and intermediate zones), and reflect, in turn, the influence of seasonal upwelling and the pattern of sea surface temperature on the coast of the Yucatán Peninsula.

Physiological descriptors were total weight (Wtot g), digestive gland (Wdgl g) and gonad weight (Wgon g), glucose (Glucose mg ml^{-1}), cholesterol (Cholest mg ml^{-1}), plasmatic proteins (Protein mg ml^{-1}), osmotic pressure (OP mOml kg^{-1}) and hemocyanin concentration (Hemocy mM). Immunological descriptors were total hemocyte count (THC cells mm^{-3}), hemagglutination activity (Hemag titer), lysozyme activity (Lyzoz U ml^{-1}), phenoloxidase system activity (PO Sys OD 490 nm) and total phenoloxidase activity in plasma (PO Plas OD 490 nm). Samples (n = 117) were analyzed using Gower's dissimilarity index (Legendre and Legendre, 1998). Weight data was previously square root transformed. A permutational MANOVA was used to examine variations in these descriptors amongst octopus combining month and zones of collection (Anderson, 2001) (see the section "Sampling Locations"). The underlying experimental design was a one-way model with six levels (February, March, and June from the transitional zone at Sisal; March and June from the upwelling zone at Ría Lagartos; and July from the non-upwelling zone: Seybaplaya). Because the number of samples differed among levels, a Type III sum of squares was used for the partitioning of total variation. A maximum of 9,999 unrestricted permutations of raw data were used to obtain the empirical distribution of *pseudo-F* values (Anderson, 2001; McArdle and Anderson, 2001). Multivariate paired comparisons between all six centroids were obtained following a similar procedure to calculate empirical *pseudo-t* values. In addition, two tables with values of physiological and immunological descriptors was make by locality.

RESULTS

Ordination by PCoA of the physiological and immunological descriptors of *O. maya* showed that 59.2% of total variation was explained with the first two principal coordinates (**Figure 1A**) and increased to 71% when a third coordinate was considered (**Table 1** and **Figure 1B**). The PCoA configuration showed how samples representing octopus were effectively ordered in the first and second axes in a way that corresponded to a temperature gradient related to the month – zone in which they were captured (**Figure 2**). The activity of the phenoloxidase system and total phenoloxidase activity in plasma were strongly correlated with PCoA 1, largely contributing to the separation of samples in the horizontal axis (**Table 2**). Hemocyanin was also strongly but inversely correlated with the PO system and activity, and to a lesser degree, with the weight of the digestive gland, gonad and total weight. The concentration of glucose and proteins were inversely correlated with cholesterol and lysozyme activity on the vertical axis, so that samples with high glucose and protein concentration were low in cholesterol concentration and lysozyme activity (**Table 3**). While the third principal coordinate only explained 11.8% of total variation in the data, separation of samples in a third dimension (depth) was mainly given by the digestive gland, gonad, and total weight.

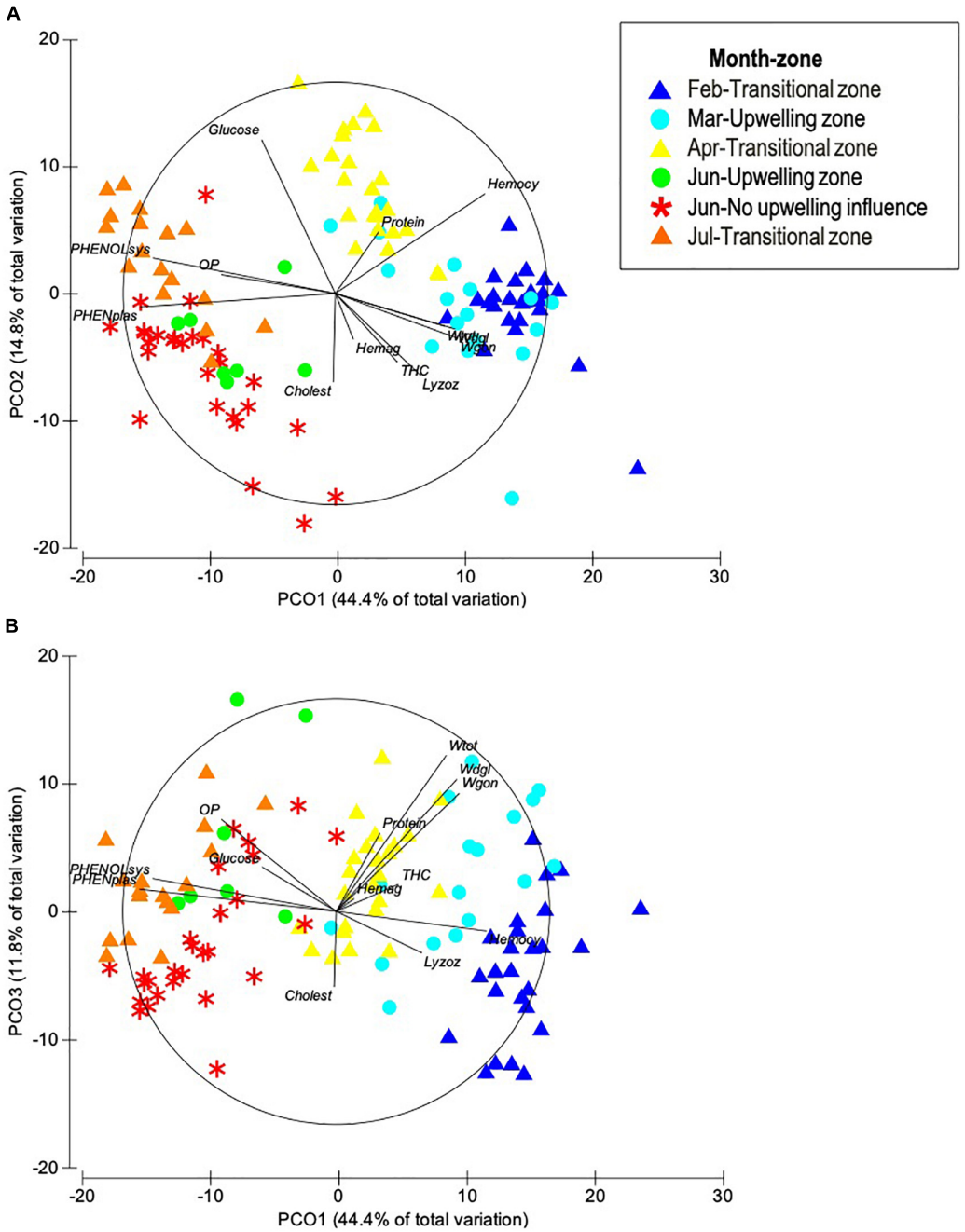

FIGURE 1 | Principal coordinates **(A)** PC1 vs. PC2, and **(B)** PC1 vs. PC3 of eight physiological and five immunological multivariate descriptors measured in adult *O. maya* captured at three locations in the coast of Yucatán on five different months: February, March, and June at Sisal; March and June at Ría Lagartos; and July at Seybaplaya; $n = 117$.

The multivariate one-way ANOVA showed overall significant differences amongst groups of octopus classified by month – zone of capture (**Table 4**); paired multivariate *t*-tests showed all six groups were statistically distinguishable from each other (**Table 5**). Ordination in these axes showed that octopus from February and March collected at the transitional and upwelling zones were among the largest, closely followed by those obtained in April at the transitional zone, and a few of the largest individuals obtained in June at the upwelling zone. Most octopus collected during June and July at the non-upwelling zone and at the transitional zone had intermediate weights. However, some of the individuals in these months and locations were among the smallest collected.

TABLE 1 | Results of PCoA on eight physiological and five immunological multivariate descriptors measured in adult *O. maya* captured at three locations in the coast of Yucatán on five different months: February, April, and July at transitional zone (Sisal); March and June at the upwelling zone (Ría Lagartos); and June at the non-upwelling zone (Seybaplaya).

	PCoA 1	PCoA 2	PCoA 3
Variation (%)	44.4%	14.8%	11.8%
Total weight	0.515	0.155	**−0.734**
Digestive gland weight	0.565	0.169	**−0.622**
Gonad weight	0.577	0.213	**−0.555**
Proteins	0.205	**−0.292**	−0.368
Cholesterol	−0.010	**0.420**	0.355
Glucose	−0.347	**−0.728**	−0.208
Osmotic pressure	**−0.538**	−0.089	−0.432
Total hemocyte count	0.293	0.325	−0.127
Hemocyanin	**0.705**	**−0.472**	0.092
Hemagglutination	0.085	0.217	−0.060
Phenoloxidase system	**−0.860**	−0.168	−0.155
Phenoloxidase plasma	**−0.922**	0.064	−0.105
Lysozyme	0.402	**0.388**	0.195

The amount of variation (%) explained by the first three principal coordinates, as well as Spearman correlation coefficients between descriptors and coordinates, are shown. Descriptors contributing the most to the ordination of samples in each principal coordinate are in bold.

TABLE 2 | Immunological variables of *Octopus maya* in three zones of Yucatán Peninsula: Seybaplaya, Sisal, and Ría Lagartos.

Immunological variables	*N*	Average	*SD*
Total hemocytes count, cel mm^{-3}	**117**	**15,411**	**7,871**
Seybaplaya	27	14,433	8,964
Sisal	66	13,445	5,453
Ría Lagartos	24	21,916	9,013
Hemagglutination, titer	**117**	**4.73**	**0.85**
Seybaplaya	27	4.85	0.53
Sisal	66	4.60	0.94
Ría Lagartos	24	4.96	0.81
Total phenoloxidase plasma OD 490 nm	**117**	**0.129**	**0.092**
Seybaplaya	27	0.209	0.022
Sisal	66	0.111	0.093
Ría Lagartos	24	0.085	0.086
Phenoloxidase activity system, OD 490 nm	**117**	**0.358**	**0.198**
Seybaplaya	27	0.480	0.120
Sisal	66	0.332	0.229
Ría Lagartos	24	0.295	0.099
Lysozyme, U ml^{-1}	**117**	**8727**	**3951**
Seybaplaya	27	7216	2315
Sisal	66	9091	4632
Ría Lagartos	24	9429	2910

Number of organisms by locality, average value, standard deviation.

DISCUSSION

The physiological and immunological parameters of *O. maya* were studied considering the influence of the seasonal upwelling throughout its geographical distribution in the Yucatán Peninsula, Mexico. Multivariate analyses indicated that the health of the organisms correlated with a temperature gradient, which was in turn linked to the zone and month where the octopuses were captured. The temperature in the studied zones

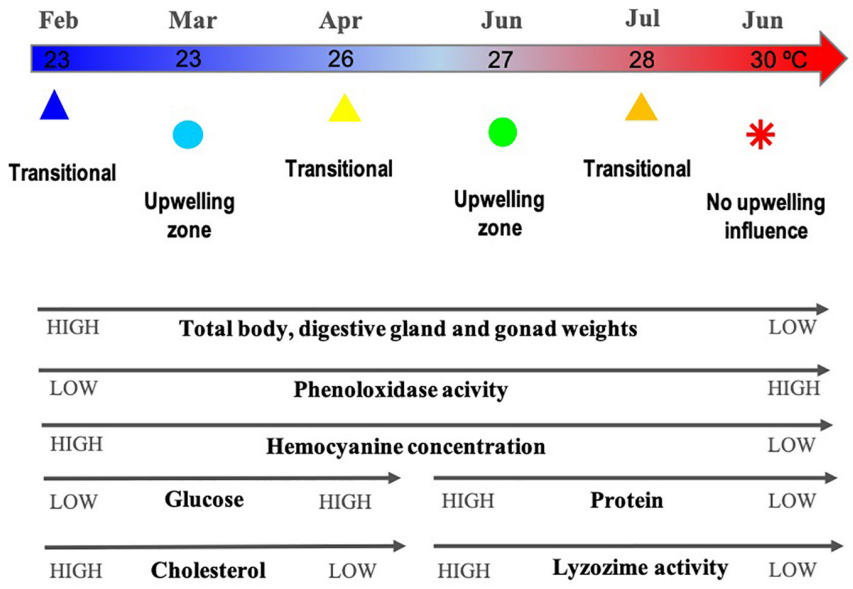

FIGURE 2 | Diagram of variation of the physiological and immunological indicators associated with the thermal gradient related to months/zones where *O. maya* were captured: February, March, and July at the transitional zone (Sisal); March and June at the upwelling zone (Ría Lagartos); and June at the non-upwelling zone (Seybaplaya); *n* = 117. Monthly mean sea surface temperature around the Yucatán Peninsula from National Geophysical Data Center (period 2006–2015) (National Oceanic and Atmospheric Administration [NOAA], 2017).

TABLE 3 | Physiological variables of *Octopus maya* of three zones of Yucatán Peninsula: Seybaplaya, Sisal, and Ría Lagartos.

Physiological variables	*N*	Average	*SD*
Total weight, g	**117**	**576.13**	**260.72**
Seybaplaya	27	462.49	246.29
Sisal	66	561.43	169.74
Ría Lagartos	24	743.01	384.75
Digestive gland weight, g	**117**	**16.14**	**9.45**
Seybaplaya	27	12.28	7.87
Sisal	66	15.53	5.77
Ría Lagartos	24	22.15	15.16
Hemocyanin, mmol/l	**117**	**1.45**	**0.62**
Seybaplaya	27	0.88	0.22
Sisal	66	1.72	0.60
Ría Lagartos	24	1.36	0.53
Osmotic pressure, mOsm kg^{-1}	**117**	**1150**	**27**
Seybaplaya	27	1150	18
Sisal	66	1145	22
Ría Lagartos	24	1164	42
Proteins, mg ml^{-1}	**117**	**108.73**	**27.39**
Seybaplaya	27	98.01	14.14
Sisal	66	106.48	30.46
Ría Lagartos	24	127.01	20.94
Cholesterol, mg ml^{-1}	**117**	**0.078**	**0.026**
Seybaplaya	27	0.119	0.011
Sisal	66	0.067	0.012
Ría Lagartos	24	0.062	0.017
Glucose, mg ml^{-1}	**117**	**0.143**	**0.074**
Seybaplaya	27	0.103	0.026
Sisal	66	0.163	0.084
Ría Lagartos	24	0.129	0.061

Number of organisms by locality, average value, and standard deviation.

TABLE 4 | Results of one-way permutational multiple MANOVA's applied on eight physiological and five immunological multivariate descriptors measured in adult *O. maya* captured at three locations in the coast of Yucatán on five different months: February, April, and July at the transitional zone (Sisal); March and June at the upwelling zone (Ría Lagartos); and June at the non-upwelling zone (Seybaplaya).

Source of variation	df	SS	MS	*pseudo-F*	*P*	Unique permutations
Month-location	5	21542	4308	38.5	<0.001	9909
Residuals	111	12432	112			
Total	116	33974				

The degrees of freedom (df), the multivariate sum of squares (SS), mean square (MS), pseudo-F and p-values, and the number of unique permutations for each test are shown.

TABLE 5 | Results of permutational paired *t*-tests that compared centroids representing data of eight physiological and five immunological multivariate descriptors measured in adult *O. maya* captured at three locations in the coast of Yucatán on five different months: February, April, and July at the transitional zone (Sisal); March and June at the upwelling zone (Ría Lagartos); and June at the non-upwelling zone (Seybaplaya).

	Feb-Sisal	Mar-Ría	Apr-Sisal	Jun-Seyba	Jun-Ría
Mar-Ría	3.50				
Apr-Sisal	6.33	4.24			
Jun-Seyba	8.97	6.37	6.96		
Jun-Ría	6.11	4.02	4.99	3.93	
Jul-Sisal	9.67	6.88	6.69	4.72	3.59

Pseudo-t values and permutational p-values were all <0.001; between 9803 and 9958 unique permutations were used in tests.

ranged from 22 to 30°C based on sea-surface and from 100 m depth temperatures data from the National Geophysical Data Center (National Oceanic and Atmospheric Administration [NOAA], 2017) and upwelling studies (Zavala-Hidalgo et al., 2006; Enriquez et al., 2013).

It has been demonstrated that high temperatures (28–31°C) affect *O. maya* reproductive capability by inhibiting the spawning of females (Juárez et al., 2015), compromising the maturation of males (López-Galindo et al., 2018), and affecting the viability of eggs and progeny growth (Sanchez-García et al., 2017). In the present study, individuals collected in warmer waters at the non-upwelling zone and in the transitional zone on June and July (28–30°C), both showed high phenoloxidase activity and low hemocyanin concentration. Conversely, individuals captured in the cold months (February, March, and April) in the upwelling and transition zones (Ría Lagartos and Sisal) had low values of both of the aforementioned indicators. The benthic temperature in these two zones was lower (22–27°C) than that of the non-upwelling zone (23–30°C). This data is relevant because to our knowledge this is the first study that evaluate, through immunological and physiological variables, the effect of temperature on health status of wild organisms of *O. maya*.

Immunological adaptation to unfavorable conditions could allow organisms to maintain immunity to avoid infectious diseases caused by opportunistic pathogens. If the exposure to thermal stress is prolonged and/or it happens in combination with a secondary stressor (for example, hypoxia or acidification), this could deteriorate the physiological condition of the individuals, compromising immunity and facilitating disease outbreaks in marine animals (Parisi et al., 2017). Octopuses captured in the warmer waters could be reflecting the metabolic stress associated with temperatures above 27°C, along with immunological compensation mechanisms with higher activity of the phenoloxidase system, despite having a lower concentration of hemocytes, hemocyanin, and proteins than those observed in octopuses captured in upwelling or transition zones (Seybaplaya, Campeche and Sisal, Yucatán), where water temperature is below 26°C, from April to June. To better understand the complex multimeric system that amplifies the immune response and cellular communication in octopuses, the phenoloxidase system was evaluated by the reaction between the humoral components and the elements of degranulated hemocytes in hemolymph, and total phenoloxidase activity in plasma. Low activity of lysozymes in the same organisms could indicate that the higher activity of the phenoloxidase system was not associated with the presence of bacteria in the hemolymph and could be associated to cellular stress, such as oxidative stress. Sanchez-García et al. (2017) investigated the thermal sensitivity of *O. maya* embryos

based on growth, respiratory metabolism, and antioxidant mechanisms to define thermal limits. They found that above 27°C embryos experienced negative changes in enzymes involved in antioxidative mechanisms (acetylcholinesterase activity, catalase activities, and total glutathione). Although our work did not include antioxidant metabolism biomarkers, the immunological components analyzed support the hypothesis that immunological compensation occurs when the temperature is above 27°C. However, further experimental work is needed to address such hypothesis.

The fact that octopuses present significant variation in their immunological and physiological condition associated with sea surface temperature opens the possibility of using these organism as bioindicators. Previous monitoring studies have demonstrated that many of the parameters of bivalves can vary significantly among sites and seasons, suggesting that environmental and endogenous factors may affect the immune system and the susceptibility to opportunistic pathogens (Carballal et al., 1998; Duchemin et al., 2007). Hemogram characteristics in a population of cultured mussels revealed that the concentration of circulating *Mytilus galloprovincialis* hemocytes fluctuated following a seasonal pattern (Carballal et al., 1998). Another study of hemocytes from native and invasive Mytilus congeners (*Mytilus californianus* and *Mytilus galloprovincialis*, respectively) found that DNA damage, cellular stress response and apoptosis were induced by acute temperature stress (Yao and Somero, 2012). Paillard et al. (2004) investigated the effect of temperature on the immune response and its relationship with the development of Brown Ring Disease (BRD). Clams kept at different temperatures (8, 14, and 21°C) were experimentally challenged with the pathogen *Vibrio tapetis*, the etiologic agent of BRD. Results demonstrated significant effects of temperature on disease development and on hemolymph immune parameters, including total and viable hemocyte count and, lysozyme activity.

Invertebrate immune reactions are often accompanied by the melanization cascade or proPO activation, which is intimately associated with the onset of factors that stimulate cellular defense by aiding phagocytosis and encapsulation reactions (Sritunyalucksana and Söderhall, 2000). During activation of phenoloxidase system and melanization, some ROS and reactive nitrogen species (RNS) are generated, including superoxide anion (Whitten and Ratcliffe, 1999), nitric oxide (Nappi et al., 2000) and hydrogen peroxide (Dubovskii et al., 2010). These reactive molecules can enhance immunocompetence but uncontrolled can also damage tissues. ROS interaction with the components of the phenoloxidase system could represent an advantage in terms of containment during the melanization process because it takes place at a specific site and for limited time, regulated by antioxidant enzymes such as glutathione which accompany node or capsule formation (see the review, encapsulation and nodulation in insect: Dubovskiy et al., 2016).

Based on the results of the present study, the distribution area of *O. maya* can be divided into two well-differentiated thermal zones: an eastern zone influenced by upwelling pulses and a western zone with no upwelling influence. Studies of reproductive conditions suggest that variations in population parameters could be linked to these thermal zones (Angeles-González et al., 2017). In accordance, a genetic analysis using multilocus microsatellite markers of wild *O. maya* showed that this population is structured in two clusters that match the different thermal zones (Juárez et al., 2018). Whilst the movement of individual *O. maya* throughout the YP during its life cycle has not been determined, direct development and benthic behavior could limit the mobility of the organisms in such a way that health conditions of octopuses might reflect physiological adaptation to regional environmental conditions.

Temperature is one of the main environmental factors that govern the metabolism of marine ectotherms, but the way in which these organisms respond to stress will depend on the thermal tolerance of the species (result of evolutionary processes), and its life history, i.e., the nutritional condition and immunological adaptation could also be crucial to their ability to absorb the effects of thermal stress. For example, Parisi et al. (2017), studied the combined effects of changes in temperature and food availability plus increased hypoxia in the marine mussel *Mytilus galloprovincialis*. They found that an increase in temperature affected the functionality of esterase and alkaline phosphatase enzymes. However, under normoxic conditions, food had a buffering effect that counteracted the negative effects of high temperature. At extreme temperatures, energy demands of metabolism might not be satisfied because organisms are unable to supply enough oxygen at the cell level (Pörtner and Farrel, 2008). This hypothesis further states that the aerobic scope, growth, activity, maintenance, reproduction, and storage are linked to the physiological responses which depend on ATP produced by aerobic metabolism (Sokolova et al., 2012). Hence, physiological and immunological markers can be useful to understand the health condition of organisms by reflecting the metabolic adjustments linked to energy demands and defense mechanisms in extreme conditions.

Stress is a general adaptive reaction crucial for survival and basically positive involving the neuroendocrine and the immune systems. Studies on biological and evolutionary implications of stress response indicate that in all bilaterian metazoans, the molecular mediators of the stress response, i.e., corticotrophin-releasing hormone, corticotrophin, catecholamines, and glucocorticoids, have been preserved during evolution (Ottaviani and Malagoli, 2009; Heather et al., 2015). The neuroendocrine and immune response shows a combinatorial strategy where the repetitive use of a set of signaling molecules is shared by the immune and neuroendocrine systems for different functions (Di Cosmo and Polese, 2016). A clear example of this intricate correlation is observed during the eggs-caring period: female octopuses spawn once in their life and eat less or stop feeding when caring for the eggs (Wodinsky, 1977). Research on the health status of *O. maya* females on different days after spawning reflected consumption of reserves coinciding with an increased immune process characterized by hemagglutination and phenoloxidase activity (Roumbedakis et al., 2017). These results show that despite the long starvation period, females sustain an adequate state of health to care for their spawn by resorting to immune compensation, in the opposite direction to the energy metabolism of the organisms.

Most information on the immune system and physiological condition of cephalopods comes from research carried out under laboratory conditions (Hanlon and Messenger, 1996; Gestal and Castellanos-Martínez, 2015; Roumbedakis et al., 2017). Although field observations are difficult to perform and involve the interaction of diverse environmental factors that affect the physio-immunological condition of the organisms, they can contribute with valuable information to better understand the connection between environment and organismal immunity. This information could be relevant to make predictions about the effects of climate change and environment on immunocompetence and disease outbreaks.

CONCLUSION

In conclusion, temperature is a key factor that modulates *O. maya's* reproduction, early development, metabolism, and immune system. Results obtained from wild octopuses show that organisms from natural temperatures lower than 27°C (upwelling zone and transitional zone in March and April) are in better conditions indicated by larger size, high concentrations of hemocyanin and low activity of the phenoloxidase system. Our work complements the studies carried out on the species' thermal tolerance, reinforcing the idea that *O. maya* sensitivity to temperature may be relevant in monitoring programs to detect environmental changes associated with global warming.

ETHICS STATEMENT

The Mexican official norm (NOM-062-ZOO-1999) on the technical specifications for the production, use and care of laboratory animals does not include fish or invertebrates, and regulations on the matter are scarce. We followed the Guide for the Care and Use of Experimental Animals in Research and Teaching of the Faculty of Superior Studies-Cuautitlán (http://www.cuautitlan.unam.mx/) at Universidad Nacional Autónoma de México.

AUTHOR CONTRIBUTIONS

CP, CR, HC-L, AS, and RR-C designed and ran laboratory analysis. MM and CP analyzed and interpreted the data. CP, RR-C, MM, AS, HC-L, and PG contributed to writing the manuscript. All authors reviewed, edited and approved the final manuscript.

FUNDING

This study was part of the Project FOMIX-CONACYT 108675. We appreciate the financial support from the Dirección General de Asuntos del Personal Académico (DGAPA) of the Universidad Nacional Autónoma de México with the projects IN223416, IN229819, and IT20111.

ACKNOWLEDGMENTS

We give special thanks to Claudia Caamal, Karla Escalante, Richard Mena and our colleagues from Universidad Nacional Autónoma de México (UNAM) for their collaboration in many different aspects of this work.

REFERENCES

Aguila, J., Cuzon, G., Pascual, C., Domingues, P. M., Gaxiola, G., Sánchez, A., et al. (2007). The effects of fish hydrolysate (CPSP) level on *Octopus maya* (Voss and Solis) diet: digestive enzyme activity, blood metabolites, and energy balance. *Aquaculture* 273, 641–655. doi: 10.1016/j.aquaculture.2007.07.010

Anderson, M. J. (2001). A new method for non-parametric multivariate analysis of variance. *Austral Ecol.* 26, 32–46. doi: 10.1111/j.1442-9993.2001.01070.pp.x

Angeles-González, L. E., Calva, R., Santos -Valenzia, J., Avila- Poveda, O., Olivares, A., Diaz, F., et al. (2017). Temperature modulates spatio-temporal variability of the functional reproductive maturation of *Octopus maya* (Cephalopoda) on the shelf of the yucatan peninsula, Mexico. *J. Molluscan Stud.* 83, 280–288. doi: 10.1093/mollus/eyx013

Beuerlein, K., Löhr, S., Westermann, B., Ruth, P., and Schipp, R. (2002). Components of the cellular defense and detoxification system of the common cuttlefish *Sepia officinalis* (Mollusca, Cephalopoda). *Tissue Cell* 34, 390–396. doi: 10.1016/S0040816602000708

Boyle, P. R. (1976). Receptor units responding to movement in the octopus mantle. *J. Exp. Biol.* 65, 1–9.

Bradford, M. M. (1976). A rapid and sensitive method for the quantitation of microgram quantities of protein utilizing the principle of protein-dye binding. *Anal. Biochem.* 72, 248–254. doi: 10.1016/0003-2697(76)90527-3

Caamal-Monsreal, C., Mascaró, M., Gallardo, P., Rodríguez, S., Noreña-Barroso, E., Domingues, P., et al. (2015). Effects of maternal diet on reproductive performance of *O. maya* and its consequences on biochemical characteristics of the yolk, morphology of embryos and hatchling quality. *Aquaculture* 441, 84–94. doi: 10.1016/J.AQUACULTURE.2015.01.020

Caamal-Monsreal, C., Uriarte, I., Farias, A., Díaz, F., Sánchez, A., Re, D., et al. (2016). Effects of temperature on embryo development and metabolism of *O. maya*. *Aquaculture* 451, 156–162. doi: 10.1016/J.AQUACULTURE.2015.09.011

Campa-Córdova, A. I., Hernández-Saavedra, N. Y., De Philippis, R., and Ascencio, F. (2002). Generation of superoxide anion and SOD activity in haemocytes and muscle of American white shrimp (*Litopenaeus vannamei*) as a response to β-glucan and sulphated polysaccharide. *Fish Shellfish Immunol.* 12, 353–366. doi: 10.1006/FSIM.2001.0377

Carballal, M. J., Lopez, C., Azevedo, C., and Villalba, A. (1998). Hemolympe cell types of mussel *Mytilus galloprovincialis*. *Dis. Aquat. Organ.* 29, 127–135. doi: 10.3354/dao029127

Chen, C., and Cheng, S. Y. (1993a). Hemolymph PCO2, hemocyanin, protein level and urea excretions of *Penaeus monodon* exposed to ambient ammonia. *Aquat. Toxicol.* 27, 281–292.

Chen, C., and Cheng, S. Y. (1993b). Studies on hemocyanin and hemolymph protein levels of *Penaeus japonicus* based on sex, size, and moulting cycle. *Comp. Biochem. Physiol. B* 106, 293–296.

Cruz-López, H. (2010). *Caracterización Estacional de la Condición Fisiológica de la Población Silvestre del Pulpo Rojo Octopus Maya (Voss y Solís-Ramírez, 1966) en la Localidad de Sisal, Yucatán, México*. Guadalajara: UAG.

Di Cosmo, A., and Polese, G. (2016). Neuroendocrine-immune systems response to environmental stressors in the cephalopod *Octopus vulgaris*. *Front. Physiol.* 7:434. doi: 10.3389/fphys.2016.00434

Dubovskii, I., Grizanova, E., Chertkova, E., Slepneva, I., Komarov, D., Vorontsova, Y., et al. (2010). Generation of reactive oxygen species and activity of antioxidants in hemolymph of the moth larvae *Galleria mellonella* (L.) (Lepidoptera: Piralidae) at development of the process of encapsulation. *J. Evol. Biochem. Physiol.* 46, 35–43.

Dubovskiy, I., Kryukova, N., Glupov, V., and Ratcliffe, N. (2016). Encapsulation and nodulation in insect. *Invertebrate Surviv. J.* 13, 229–246.

Duchemin, M., Wessel, N., Fournier, M., and Auffret, M. (2007). Flow cytometric measurement of the clearance rate in the blue mussel *Mytilus edulis* and the development of a new individual exposure system for aquatic immunotoxicological studies. *Environ. Pollut.* 153, 492–496.

Enriquez, C., Mariño-Tapia, I., Jeronimo, G., and Capurro-Filograsso, L. (2013). Thermohaline processes in a tropical coastal zone. *Cont. Shelf Res.* 69, 101–109. doi: 10.1016/j.csr.2013.08.018

Fazio, F. (2019). Fish hematology analysis as an important tool of aquaculture: a review. *Aquaculture* 500, 237–242.

Fiorito, G., Affuso, A., Basil, J., Cole, A., Girolamo, P., D'Angelo, L., et al. (2015). guidelines for the care and welfare of cephalopods in research – a consensus based on an initiative by CephRes, FELASA and the boyd group. *Lab. Anim.* 49, 1–90. doi: 10.1177/0023677215580006

Fisher, W. S., and DiNuzzo, A. R. (1991). Agglutination of bacteria and erythrocytes by serum from six species of marine molluscs. *J. Invertebr. Pathol.* 57, 380–394. doi: 10.1016/0022-2011(91)90142-D

Gallardo, P., Olivares, A., Martínez-Yáñez, R., Caamal-Monsreal, C., Domingues, P. M., Mascaró, M., et al. (2017). Digestive Physiology of *Octopus maya* and *O. mimus*: temporality of Digestion and Assimilation Processes. *Front. Physiol.* 8:355. doi: 10.3389/fphys.2017.00355

Gestal, C., and Castellanos-Martínez, S. (2015). Understanding the cephalopod immune system based on functional and molecular evidence. *Fish Shellfish Immunol.* 46, 120–130. doi: 10.1016/j.fsi.2015.05.005

Hanlon, R. T., and Forsythe, J. W. (1985). Advances in the laboratory culture of octopuses for biomedical research. *Lab. Anim. Sci.* 35, 33–40.

Hanlon, R. T., and Messenger, J. B. (1996). *Cephalopod Behaviour*. Cambridge: Cambridge University Press.

Heather, D., Taewoo, R., Donelson, J., Van Herwerden, L., Seridi, L., and Ghosheh, Y. (2015). Molecular processes of transgenerational acclimation to a warming ocean. *Nat. Clim. Chang.* 5, 1074–1078.

Hernández-López, J., Gollas-Galván, T., and Vargas-Albores, F. (1996). Activation of the prophenoloxidase system of the brown shrimp (*Penaeus californiensis* Holmes). *Comp. Biochem. Physiol. C Pharmacol. Toxicol. Endocrinol.* 113, 61–66. doi: 10.1016/0742-8413(95)02033-0

Hochner, B., Shomrat, T., and Fiorito, G. (2006). The octopus: a model for a comparative analysis of the evolution of learning and memory mechanisms. *Biol. Bull.* 10, 308–317. doi: 10.2307/4134567

Juárez, O. E., Enríquez, L., Camarena-Rosales, F., Arena, L., Galindo-Sánchez, C. E., Lafarga-De la Cruz, F., et al. (2018). Genetic monitoring of the mexican four-eyed octopus *Octopus maya* population: new insights and perspectives for the fishery management. *Fish. Res.* 206, 109–114. doi: 10.1016/J.FISHRES.2018.05.002

Juárez, O. E., Galindo-Sánchez, C. E., Díaz, F., Re, D., Sánchez-García, A. M., Camaal-Monsreal, C., et al. (2015). Is temperature conditioning *Octopus maya* fitness? *J. Exp. Mar. Bio. Ecol.* 467, 71–76. doi: 10.1016/j.jembe.2015.02.020

Legendre, P., and Legendre, L. (1998). *Numerical Ecology*. 2nd Edn. Amsterdam: Elsevier, 853.

Lignot, J.-H., Spanings-Pierrot, C., and Charmantier, G. (2000). Osmoregulatory capacity as a tool in monitoring the physiological condition and the effect of stress in crustaceans. *Aquaculture* 191, 209–245. doi: 10.1016/S0044-8486(00)00429-4

Linares, M., Caamal-Monsreal, C., Olivares, A., Sánchez, A., Rodríguez, S., Zúñiga, O., et al. (2015). Timing of digestion, absorption and assimilation in octopus species from tropical (*Octopus maya*) and subtropical-temperate (*O. mimus*) ecosystems. *Aquat. Biol.* 24, 127–140. doi: 10.3354/ab00642

Locatello, L., Fiorito, G., Finos, L., and Rasotto, M. B. (2013). Behavioural and immunological responses to an immune challenge in *Octopus vulgaris*. *Physiol. Behav.* 122, 93–99. doi: 10.1016/J.PHYSBEH.2013.08.029

López-Galindo, L., Galindo-Sánchez, C., Olivares, A., Avila-Poveda, O. H., Díaz, F., Juárez, O. E., et al. (2018). Reproductive performance of *Octopus maya* males conditioned by thermal stress. *Ecol. Indic.* 96, 437–447. doi: 10.1016/J.ECOLIND.2018.09.036

Markaida, U., Méndez-Loeza, I., and Rosales-Raya, M. L. (2017).). Seasonal and spatial trends of mayan octopus, *Octopus maya*, population dynamics from campeche, Mexico. *J. Mar. Biol. Assoc. U.K.* 97, 1663–1673. doi: 10.1017/S0025315416001132

Martínez, R., Gallardo, P., Pascual, C., Navarro, J. C., Sánchez, A., Caamal-Monsreal, C., et al. (2014). Growth, survival and physiological condition of *Octopus maya* when fed a successful formulated diet. *Aquaculture* 42, 310–317.

McArdle, B. H., and Anderson, M. J. (2001). Fitting multivariate models to community data: a comment on distance-based redundancy analysis. *Ecology* 82, 290–297.

Merino, M. (1997). Upwelling on the yucatan shelf: hydrographic evidence. *J. Mar. Syst.* 13, 101–121. doi: 10.1016/S0924-7963(96)00123-6

Moguel, C., Mascaró, M., Avila-Poveda, O., Caamal-Monsreal, C., Sánchez, A., Pascual, C., et al. (2010). Morphological, physiological, and behavioural changes during post-hatching development of *Octopus maya* (Mollusca: Cephalopoda) with special focus on digestive system. *Aquat. Biol.* 9, 35–48.

Muñoz, M., Cedeño, R., Rodríguez, J., Van Der Knaap, W. P. W., Mialhe, E., and Bachère, E. (2000). Measurement of reactive oxygen intermediate production in haemocytes of the penaeid shrimp, *Penaeus vannamei*. *Aquaculture* 191, 89–107. doi: 10.1016/S0044-8486(00)00420-8

Mydlarz, L. D., Jones, L. E., and Harvell, C. D. (2006). Innate immunity, environmental drivers, and disease ecology of marine and freshwater invertebrates. *Annu. Rev. Ecol. Evol. Syst.* 37, 251–288. doi: 10.1146/annurev.ecolsys.37.091305.110103

Nappi, A. J., Vass, E., Frey, F., and Carton, Y. (2000). Nitric oxide involvement in *Drosophila* immunity. *Nitric Oxide* 4, 423–430.

National Oceanic and Atmospheric Administration [NOAA] (2017). *State of the Climate: Global Climate Report for Annual 2016*. Available at: https://www.ncdc.noaa.gov/sotc/global/201613

Noyola, J., Caamal-Monsreal, C., Díaz, F., Re, D., Sánchez, A., and Rosas, C. (2013a). Thermopreference, tolerance and metabolic rate of early stages juvenile *Octopus maya* acclimated to different temperatures. *J. Therm. Biol.* 38, 14–19. doi: 10.1016/J.JTHERBIO.2012.09.001

Noyola, J., Mascaró, M., Caamal-Monsreal, C., Noreña-Barroso, E., Díaz, F., Re, D., et al. (2013b). Effect of temperature on energetic balance and fatty acid composition of early juveniles of *Octopus maya*. *J. Exp. Mar. Bio. Ecol.* 445, 156–165. doi: 10.1016/J.JEMBE.2013.04.008

Ottaviani, E., and Malagoli, D. (2009). Around the word stress: its biological and evolutive implications. *Invertebrate Surviv. J.* 6, 1–6.

Paillard, C., Le Roux, F., and Borrego, J. J. (2004). Bacterial disease in marine bivalves, a review of recent studies: trends and evolution. *Aquat. Living Resour.* 17, 477–498. doi: 10.1051/alr:2004054

Parisi, M., Mauro, M., Sara, G., and Cammarata, M. (2017). Temperature increases, hypoxia, and changes in food availability affect immunological biomarkers in the marine mussel *Mytilus galloprovincialis*. *J. Comp. Physiol. B* 187, 1117–1126. doi: 10.1007/s00360-017-1089-2

Parry, R. M., Chandan, R. C., and Shahani, K. M. (1965). A rapid and sensitive assay of muramidase. *Exp. Biol. Med.* 119, 384–386. doi: 10.3181/00379727-119-30188

Pascual, C., Arena, L., Cuzon, G., Gaxiola, G., Taboada, G., Valenzuela, M., et al. (2004). Effect of a size-based selection program on blood metabolites and immune response of *Litopenaeus vannamei* juveniles fed different dietary carbohydrate levels. *Aquaculture* 230, 405–416. doi: 10.1016/S0044-8486(03)00438-1

Pascual, C., Sánchez, A., Sánchez, A., Vargas-Albores, F., LeMoullac, G., and Rosas, C. (2003). Haemolymph metabolic variables and immune response in *Litopenaeus setiferus* adult males: the effect of an extreme temperature. *Aquaculture* 218, 637–650. doi: 10.1016/S0044-8486(02)00300-9

Pascual-Jiménez, C., Huchin-Mian, J. P., Simões, N., Briones-Fourzán, P., Lozano-Álvarez, E., Sánchez-Arteaga, A., et al. (2012). Physiological and immunological characterization of Caribbean spiny lobsters *Panulirus argus* naturally infected with *Panulirus argus* virus 1 (PaV1). *Dis. Aquat. Organ.* 100, 113–124. doi: 10.3354/dao02497

Pörtner, H. O., and Farrel, A. (2008). Physiology and climate change. *Science* 322, 690–692. doi: 10.1126/science.1163156

Rögener, W., Renwrantz, L., and Uhlenbruck, G. (1987). Analysis of *Octopus vulgaris* hemolymph containing a glycoprotein with blood group A-like properties. *Comp. Biochem. Physiol. B Biochem.* 86, 347–351. doi: 10.1016/0305-0491(87)90304-X

Roper, C. F. E., Sweeney, M. J., and Nauen, C. E. (1984). Cephalopods of the world: an annotated and illustrated catalogue of species of interest to fisheries. *FAO Fish. Synop.* 125, 1–277.

Rosas, C., Cuzon, G., Gaxiola, G., Pascual, C., Taboada, G., Arena, L., et al. (2002). An energetic and conceptual model of the physiological role of dietary carbohydrates and salinity on *Litopenaeus vannamei* juveniles. *J. Exp. Mar. Biol. Ecol.* 268, 47–67.

Roumbedakis, K., Mascaró, M., Martins, M. L., Gallardo, P., Rosas, C., and Pascual, C. (2017). Health status of post-spawning *Octopus maya* (Cephalopoda: Octopodidae) females from Yucatan Peninsula, Mexico. *Hydrobiologia* 808, 23–34. doi: 10.1007/s10750-017-3340-y

Sánchez, A., Pascual, C., Saìnchez, A., Vargas-Albores, F., Le Moullac, G., and Rosas, C. (2001). Hemolymph metabolic variables y immune response in *Litopenaeus setiferus* adult males: the effect of acclimation. *Aquaculture* 198, 13–28.

Sanchez-García, A., Rodríguez-Fuentes, G., Díaz, F., Galindo-Sánchez, C. E., Ortega, K., Mascaró, M., et al. (2017). Thermal sensitivity of *Octopus maya* embryos as a tool for monitoring the effects of environmental warming in the Southern of Gulf of Mexico. *Ecol. Indic.* 72, 574–585. doi: 10.1016/J.ECOLIND.2016.08.043

Sieiro, M. P., Aubourg, S. P., and Rocha, F. (2006). Seasonal study of the lipid composition in different tissues of the common octopus (*Octopus vulgaris*). *Eur. J. Lipid Sci. Technol.* 108, 479–487. doi: 10.1002/ejlt.200500322

Söderhäll, K., and Häll, L. (1984). Lipopolysaccharide-induced activation of prophenoloxidase activating system in crayfish haemocyte lysate. *BBA Gen. Subj.* 797, 99–104. doi: 10.1016/0304-4165(84)90387-8

Söderhäll, K., and Smith, V. J. (1983). Separation of the haemocyte populations of Carcinus maenas and other marine decapods, and prophenoloxidase distribution. *Dev. Comp. Immunol.* 7, 229–239. doi: 10.1016/0145-305X(83)90004-6

Sokolova, I. M., Frederich, M., Bagwe, R., Lannig, G., and Sukhotin, A. A. (2012). Energy homeostasis as an integrative tool for assesing limits of environmental stress tolerance in aquatic invertebrates. *Mar. Environ. Res.* 79, 1–15. doi: 10.1016/j.marenvres.2012.04.003

Song, Y. L., and Hsieh, Y. T. (1994). Immunostimulation of tiger shrimp (*Penaeus monodon)* hemocytes for generation of microbicidal substances: analysis of reactive oxygen species. *Dev. Comp. Immunol.* 18, 201–209.

Sritunyalucksana, K., and Söderhall, K. (2000). The proPO and clotting system in crustaceans. *Aquaculture* 191, 53–69.

Sung, H. H., Chang, H. J., Her, C. H., Chang, J. C., and Song, Y. L. (1998). Phenoloxidase Activity of Hemocytes Derived from *Penaeus monodonand* and *Macrobrachium rosenbergii*. *J. Invertebr. Pathol.* 71, 26–33. doi: 10.1006/jipa.1997.4703

Tercero, J. F., Rosas, C., Mascaro, M., Poot, G., Domingues, P., Noreña, E., et al. (2015). Effects of parental diets supplemented with different lipid sources on *Octopus maya* embryo and hatching quality. *Aquaculture* 448, 234–242. doi: 10.1016/J.AQUACULTURE.2015.05.023

Vargas-Albores, F., Jiménez-Vega, F., and Söderhäll, K. (1996). A plasma protein isolated from brown shrimp (*Penaeus californiensis*) which enhances the activation of prophenoloxidase system by β-1,3-glucan. *Dev. Comp. Immunol.* 20, 299–306. doi: 10.1016/S0145-305X(96)00007-9

Vargas-Albores, F., Jiménez-Vega, F., and Yepiz-Plascencia, G. M. (1997). Purification and comparison of beta-1,3-glucan binding protein from white shrimp (*Penaeus vannamei*). *Comp. Biochem. Physiol. B. Biochem. Mol. Biol.* 116, 453–458.

Voss, G. L., and Solís-Ramírez, M. J. (1966). *Octopus maya*, a new species from the bay of campeche. *Bull. Mar. Sci.* 16, 615–625.

Whitten, M. M. A., and Ratcliffe, N. A. (1999). In vitro superoxide activity in the haemolymph of the West Indian leaf cockroach, *Blaberus discoidalis*. *J. Insect Physiol.* 45, 667–675.

Wodinsky, J. (1977). Hormonal inhibition of feeding and death in octopus-control by optic gland secretion. *Science* 198, 948–951.

Yao, C. L., and Somero, G. N. (2012). The impact of acute temperature stress on hemocytes of invasive and native mussels (*Mytilus galloprovincialis* and *Mytilus californianus*): DNA damage, membrane integrity, apoptosis and signaling pathways. *J. Exp. Biol.* 215(Pt 24), 4267–4277. doi: 10.1242/jeb.073577

Zavala-Hidalgo, J., Gallegos-García, A., Martínez-López, B., Morey, S. L., and O'Brien, J. J. (2006). Seasonal upwelling on the western and southern shelves of the gulf of Mexico. *Ocean Dyn.* 56:333. doi: 10.1007/s10236-006-0072-3

Conflict of Interest Statement: The authors declare that the research was conducted in the absence of any commercial or financial relationships that could be construed as a potential conflict of interest.

frontiers in Physiology

ORIGINAL RESEARCH
published: 04 October 2019
doi: 10.3389/fphys.2019.01220

From Africa to Antarctica: Exploring the Metabolism of Fish Heart Mitochondria Across a Wide Thermal Range

*Florence Hunter-Manseau[1], Véronique Desrosiers[1], Nathalie R. Le François[2], France Dufresne[1], H. William Detrich III[3], Christian Nozais[1] and Pierre U. Blier[1]**

[1] *Département de Biologie, Université du Québec à Rimouski, Rimouski, QC, Canada,* [2] *Biodôme de Montréal, Montréal, QC, Canada,* [3] *Department of Marine and Environmental Sciences, Northeastern University Marine Science Center, Nahant, MA, United States*

OPEN ACCESS

Edited by:
Jose Pablo Vazquez-Medina, University of California, Berkeley, United States

Reviewed by:
Joanna Joyner-Matos, Eastern Washington University, United States
Caroline Williams, University of California, Berkeley, United States

***Correspondence:**
Pierre U. Blier
pierre_blier@uqar.ca

Specialty section:
This article was submitted to Aquatic Physiology, a section of the journal Frontiers in Physiology

Received: *29 January 2019*
Accepted: *06 September 2019*
Published: *04 October 2019*

Citation:
Hunter-Manseau F, Desrosiers V, Le François NR, Dufresne F, Detrich HW III, Nozais C and Blier PU (2019) From Africa to Antarctica: Exploring the Metabolism of Fish Heart Mitochondria Across a Wide Thermal Range. Front. Physiol. 10:1220. doi: 10.3389/fphys.2019.01220

The thermal sensitivity of ectotherms is largely dictated by the impact of temperature on cellular bioenergetics, particularly on mitochondrial functions. As the thermal sensitivity of bioenergetic pathways depends on the structural and kinetic properties of its component enzymes, optimization of their *collective* function to different thermal niches is expected to have occurred through selection. In the present study, we sought to characterize mitochondrial phenotypic adjustments to thermal niches in eight ray-finned fish species occupying a wide range of thermal habitats by comparing the activities of key mitochondrial enzymes in their hearts. We measured the activity of four enzymes that control substrate entrance into the tricarboxylic acid (TCA) cycle: pyruvate kinase (PK), pyruvate dehydrogenase complex (PDHc), carnitine palmitoyltransferase (CPT), and hydroxyacyl-CoA dehydrogenase (HOAD). We also assayed enzymes of the electron transport system (ETS): complexes I, II, I + III, and IV. Enzymes were assayed at five temperatures (5, 10, 15, 20, and 25°C). Our results showed that the activity of CPT, a gatekeeper of the fatty acid pathway, was higher in the cold-water fish than in the warmer-adapted fish relative to the ETS (complexes I and III) when measured close to the species optimal temperatures. The activity of HOAD showed a similar pattern relative to CI + III and thermal environment. By contrast, PDHc and PK did not show the similar patterns with respect to CI + III and temperature. Cold-adapted species had high CIV activities compared to those of upstream complexes (I, II, I + III) whereas the converse was true for warm-adapted species. Our findings reveal a significant variability of heart mitochondrial organization among species that can be linked to temperature adaptation. Cold-adapted fish do not appear to compensate for PDHc activity but likely adjust fatty acids oxidation through higher activities of CPT and HOAD relative to complexes I + III.

Keywords: temperature, adaptation, pyruvate dehydrogenase complex, carnitine palmitoyl transferase, hydroxyacyl-CoA dehydrogenase, electron transport system, energy metabolism, fatty acid metabolism

INTRODUCTION

Mitochondrial ATP production depends on the interactions of various metabolic pathways. These pathways contain a variety of enzymes which are differentially affected by temperature. Thus any changes in temperature will induce a shift in the relative control strength of key steps of aerobic pathways (Blier et al., 2014). Lasting changes in environmental temperature will subject mitochondrial energy production to selective pressure to compensate for the adverse thermal impacts on the limiting or controlling steps of respiration.

In fish, the cardiovascular system is strongly affected by temperature and part of this sensitivity appears to be dictated by mitochondrial functions (Iftikar and Hickey, 2013). The thermal sensitivity of state 3 mitochondrial respiration in the heart of the Atlantic wolffish (*Anarhichas lupus*) has been shown to be similar to that of the pyruvate dehydrogenase complex (PDHc) but to differ from the sensitivity of other mitochondrial enzymes (Lemieux et al., 2010a,b). This has led authors to suggest that state 3 may be limited at low temperature in part by the activity of PDHc when mitochondria are fed with pyruvate. Moreover, at low temperature, PDHc activity was much higher in the heart mitochondria of wolffish, a cold-temperate adapted ectotherm than in the rat, consistent with a compensatory adjustment of this enzyme (Lemieux et al., 2010a,b). Further work on *Drosophila simulans* revealed an excess of complex IV (CIV) capacity at low temperature, indicating upstream limitation in the electron transport system (ETS) with PDHc as the likely cause of this limitation (Pichaud et al., 2010, 2011). These authors further noted that *Drosophila* CIV controlled mitochondrial metabolism at high temperature but not at low temperature. Takeuchi et al. (2009) showed that *D. simulans* mutants with a deficiency causing elevation of intracellular calcium concentration also had higher PDHc activity in colder environments compared to congeners without the mutation. Since calcium is a PDHc activator, the authors proposed that induction of this enzyme led to tolerance of colder temperatures by the mutants. Together, these results support the hypothesis that an excess of CIV activity at low temperature occurs due to a rate-limiting step upstream in ectotherms (Blier et al., 2014).

Another significant pathway for fish bioenergetics is the lipid metabolism. Lipids are important catabolic substrates for fish heart as they have the greatest energy density of the different fuels of metabolism, which makes them perfectly suited for energy-expensive activities (Magnoni and Weber, 2007; Weber, 2011). Circulating triacylglycerol (TAG) levels in resting rainbow trout (*Oncorhynchus mykiss*) have been shown to be sufficient to sustain exercise, which probably explains why TAG levels do not increase with long-term activity (Magnoni et al., 2008). A predominance of lipid oxidation over protein and carbohydrate in rainbow trout swimming at different speeds (Lauff and Wood, 1996) further portrays the importance of lipid oxidation in fish energetics.

Despite the importance of lipid metabolism, relatively few studies have evaluated the impact of temperature on mitochondrial fatty acid oxidation. Fatty acid molecules require a transporter, carnitine palmitoyltransferase (CPT), to translocate them through the mitochondrial membrane. CPT is embedded in the mitochondrial membrane, which tends to become more rigid as temperature declines (Weber, 2011) and therefore impair lipid transport. Conversely, elevation of the activities of enzymes of the β-oxidation pathway [in particular β-hydroxyacyl-CoA dehydrogenase (HOAD)], by enhancing the concentration gradient of lipids across the inner membrane (Weber, 2011), may offset reduced CPT activity at low temperature. In a comparison of mitochondrial metabolism between two ecotypically similar fishes, one Antarctic (*Trematomus newnesi*) and one temperate (*Tautoga onitis*), Crockett and Sidell (1990) found significantly higher activities of CPT (1.9-fold increase) and HOAD (27.2-fold) in the polar species. Two demersal fish species, the Antarctic *Gobionotothen gibberifrons* and the temperate *Myoxocephalus octodecimspinosus*, gave similar, but less pronounced, trends: the polar fish showed a 1.3-fold higher activity of CPT and a 6.8-fold higher activity of HOAD. Based on these results, Crockett and Sidell (1990) suggested that fatty acids are an important fuel source for metabolism in polar fish.

Determination of the temperature dependence of mitochondrial function and the activities of key enzymes should help us identify components that are able to acclimatize or adapt to thermal variation. Based on previous studies (summarized in Blier et al., 2014), we hypothesize that the activities of enzymes responsible for providing substrates to the tricarboxylic acid (TCA) cycle (PDHc, CPT, and HOAD), have been increased relative to those of ETS enzymes (complexes I, II, III, and IV), in cold-living species compared to temperate or warm adapted species. If this hypothesis is correct, then our results will provide a new framework for monitoring evolutionary compensation of mitochondrial metabolism in fish taxa across a wide range of thermal habitats. Any divergence in the relative proportion of key enzymes activities, when measured at or close to optimal temperature, will show the evolutionary plasticity of heart mitochondrial phenotypes and point out characters that could be under selective pressure to adapt to changing environmental conditions.

MATERIALS AND METHODS

Experimental Animals

Eight species with different thermal requirements were used to conduct the experiment. Two cold-water notothenioid species, the marbled notothen (*Notothenia rossii*, Richardson, 1844; T_{opt} = −1.9 to 2°C, Strobel et al., 2012) and the humphead notothen (*Gobionotothen gibberifrons*, Lönnberg, 1905; T_{opt} = −1.9 to 2°C, Bilyk and DeVries, 2011), were collected by bottom trawling from the ARSV *Laurence M. Gould* near Palmer Station, Antarctica. Two North Atlantic cold-temperate species acclimated to 10°C, the spotted wolfish (*Anarhichas minor*, Olafsen, 1772; T_{opt} = 10.3°C, Hansen and Falk-Petersen, 2002) and the Atlantic cod (*Gadus morhua*, Linnaeus, 1758; T_{opt} = 9 to 12°C, Pederson and Jobling, 1989), were provided

by the Maurice Lamontagne Institute (Department of Fisheries and Oceans of Canada, Mont-Joli, QC, Canada). Two temperate water species acclimated to either 13 or 15°C, the Arctic char (*Salvelinus alpinus*, Linnaeus, 1758, T_{opt} = 12 to 15°C, Jobling et al., 1992) and the striped bass (*Morone saxatilis*, Walbaum, 1792, T_{opt} = 18°C, Cox and Coutant, 1981) were also used. Arctic char were provided by a fish farm (Pisciculture des Monts de Bellechasse Inc., Saint-Damien-de-Buckland, QC, Canada) and bass by the Ministère des Forêts, de la Faune et des Parcs du Québec (Fish hatchery of Baldwin-Coaticook, QC, Canada). Two warm-water species, acclimated to 23–25°C, Nile tilapia (*Oreochromis niloticus*, Linnaeus, 1758; T_{opt} = 30.1°C, Xie et al., 2011) and common carp (*Cyprinus carpio*, Linnaeus, 1758; T_{opt} = 25°C, Watanabe et al., 1996), were provided by the Biodôme of Montreal (Montreal, QC, Canada). Some Nile tilapia were supplied by Urban Food Ecosystems (Montreal, QC, Canada). All manipulations were performed in agreement with ethical regulation of animals use for research in Canada [permit #CPA-65-16-174 from the animal ethics committee of the Université du Québec à Rimouski (Rimouski, QC, Canada)].

Four of the species belong to the more basal orders of the clupeocephala taxa (*G. morhua*, Gadiformes; *S. alpinus*, Salmoniformes; *C. carpio*, Cypriniformes, and *O. niloticus*, Cichliformes) which cover a range of optimal temperatures from 9 to 30°C. The four other species belong to the more derived order of Perciformes and cover a range of optimal temperatures from approximately 0–18°C. In the group of non-perciformes, the species more closely related to perciformes is *O. niloticus* with the highest optimal temperature of 30°C. We chose species in these two groups to ensure overlap in optimal temperature range that would be independent of phylogeny. Furthermore, there is no clear association of optimal temperature with phylogenic relationship. For example, *O. niloticus* (T_{opt} = 30.1°C) is more distant from *A minor* (T_{opt} = 10.3°C) than from both notothenoid species (T_{opt} close to 0°C) and the most distant species from *O. niloticus* is *C carpio*, with the most similar optimal temperature (25°C) (see the phylogeny of ray-finned fishes by Hughes et al., 2018). This allowed to avoid bias in the relation of metabolic characters with optimal temperature that would be associated to phylogenetic inertia.

Tissue/Sample Preparation

After recording mass and length (total and standard), fish were euthanized with tricaine methanesulfonate (MS-222 0.25 g/L). Hearts were dissected, weighed, flash frozen (in liquid nitrogen) and stored at −80°C until analyses. For each species and analysis, an average of five hearts were pooled to provide sufficient material. The pools were made randomly to amount to comparable weight between the pool of the same species. The majority of the pools contain mature and immature fish. Using this method, three pools (n = 3) were made for *N. rossii*, *G. Morhua*, *O. niloticus*, and *C. carpio*, four pools (n = 4) were made for *S. Alpinus*, *G. gibberifrons*, and *A. minor* and five pools (n = 5) were made for *M. saxatilis*. Hearts were thawed on ice in a cold room (+4°C) and then homogenized on ice in 50 mM potassium phosphate buffer pH 8.0 (with 1 mM EDTA) using a Polytron (PT 2500E, Kinematica AG, Bohemia, NY, United States) for three periods of 10-s each. Homogenates were flash frozen, then stored at −80°C until use.

Enzymatic Assays

The enzymatic activities were determined at 5, 10, 15, 20, and 25°C for four species (wolfish, cod and the two notothens); at 10, 15, 20, and 25°C for tilapia, Arctic char and bass; and at only 15 and 25°C for the carp (due to limited quantity of tissue).

Assays at 25°C were performed with a UV/Vis spectrophotometer (Ultrospec 3100pro UV/visible spectrophotometer, GE Healthcare, Mississauga, ON, Canada) equipped with a temperature-controlled cuvette holder connected to a 25°C water circuit or with a microplate reader with temperature control (EnVision Multilabel Plate Reader 2104-0010A, PerkinElmer, Waltham, MA, United States). Activities at 15 and 20°C were performed with a second microplate reader (Power Wave XS2, BioTek, Winooski, VT, United States), whereas activities at 5 and 10°C were measured in a cold room with a UV/Vis spectrophotometer (Ultrospec 2100pro UV/visible spectrophotometer, GE Healthcare, Mississauga, ON, Canada).

Protocols used for enzymatic assays were adapted as follows: PK from Pelletier et al. (1994); CII from Lemieux et al. (2010a); ETS from Madon et al. (1998); CI from Janssen et al. (2007); and PDHc, CPT, HOAD, CS, and CIV from Thibault et al. (1997). All measurements were obtained at least in duplicates.

Pyruvate kinase (PK, EC 2.7.1.40) activity was measured for four min at 340 nm to follow the disappearance of NADH (extinction coefficient ε_{340} = 6.22 ml cm^{-1} μmol^{-1}) in a reaction medium containing 50 mM imidazole-HCl, 10 mM $MgCl_2$, 100 mM KCl, 5 mM ADP, 0.15 mM NADH, 5 mM phosphoenolpyruvate and 0.6 U ml^{-1} lactate dehydrogenase, pH 7.4.

Pyruvate dehydrogenase complex (EC 1.2.4.1) activity was measured at 500 nm to follow the reduction of *p*-iodonitrotetrazolium violet (INT, extinction coefficient ε_{500} = 15.4 ml cm^{-1} μmol^{-1}) in a reaction medium containing 50 mM Tris–HCl, 0.05% (v/v) Tween 20, 1 mM $MgCl_2$, 2.5 mM NAD, 0.5 mM EDTA, 0.1 mM coenzyme A, 0.3 mM oxalate, 0.6 mM INT, 6 U ml^{-1} lipoamide dehydrogenase, 0.2 mM thiamine pyrophosphate and 5 mM pyruvate (omitted for the control), pH 8.0. Samples were incubated on ice with 80 mM $MgCl_2$, centrifuged at 10,000 *g* (4°C) and the pellet was discarded prior to the analysis.

Carnitine palmitoyltransferase (EC 2.3.1.2) activity was measured at 412 nm to follow the reduction of 5,5′-dithiobis-2-nitrobenzoic acid (DTNB, extinction coefficient ε_{412} = 14.15 ml cm^{-1} μmol^{-1}) in a reaction medium containing 75 mM Tris–HCl, 1.5 mM EDTA, 0.25 mM DTNB, 0.035 mM palmitoyl-CoA and 2 mM L-carnitine (omitted for the control), pH 8.0. Samples were centrifuged at 3000 *g* (4°C) and the pellet was discarded prior to the analysis.

β-hydroxyacyl dehydrogenase (HOAD, EC 1.1.1.35) activity was measured at 340 nm to follow the disappearance of NADH (extinction coefficient ε_{340} = 6.22 ml cm^{-1} μmol^{-1}) in a reaction medium containing 100 mM triethanolamine-HC1, 5 mM EDTA,

1 mM KCN, 0.115 mM NADH, and 0.05 mM acetoacetyl-CoA (omitted for the control), pH 7.0. Samples were centrifuged at 3000 *g* (4°C) and the pellet was discarded prior to the analysis.

Citrate synthase (CS, EC 2.3.3.1) activity was measured at 412 nm to follow the reduction of 5,5′-dithiobis-2-nitrobenzoic acid (DTNB, extinction coefficient ε_{412} = 14.15 ml cm^{-1} μmol^{-1}) using a reaction medium containing 100 mM imidazole-HCl, 0.1 mM DTNB, 0.1 mM acetyl-CoA and 0.15 mM oxaloacetic acid (omitted for the control), pH 8.0.

NADH:ubiquinone reductase (CI, EC 1.6.5.3) activity was measured at 600 nm to follow the reduction of 2,6-dichloroindophenol (DCIP, extinction coefficient ε_{600} = 19.1 ml cm^{-1} μmol^{-1}). Homogenates were centrifuged at 3000 *g* (4°C) prior to the analysis. The supernatants were incubated for 10 min at the proper assay temperature in a reaction medium containing 100 mM imidazole, 2.5 mg ml^{-1} BSA, 5 mM $MgCl_2$, 4 μM antimycin A, 10 mM sodium azide, 50 μM DCIP, 65 μM ubiquinone (coenzyme Q1) and 5 μM rotenone (only for the control), pH 8.0. The reaction was initiated by addition of 0.14 mM NADH.

Succinate dehydrogenase (CII, EC 1.3.5.1) activity was measured at 600 nm to follow the reduction of 2,6-dichloroindophenol (DCIP, extinction coefficient ε_{600} = 19.1 ml cm^{-1} μmol^{-1}). Homogenates were incubated for 5 min at the desired assay temperature in a reaction medium containing 100 mM imidazole, 20 mM succinate, 4 μM antimycin A, 5 μM rotenone and 10 mM sodium azide, pH 7.2. The reaction was started by addition of 50 μM DCIP and 65 μM ubiquinone (omitted for the control).

CI + CIII activity was measured at 490 nm to follow the reduction of *p*-iodonitrotetrazolium violet (INT, extinction coefficient ε_{490} = 15.91 ml cm^{-1} μmol^{-1}) in a reaction medium containing 100 mM potassium phosphate, 0.85 mM NADH, 2 mM INT and 0.2% (v/v) Triton X-100, pH 8.5.

Cytochrome c oxidase (CIV, EC 1.9.3.1) activity was measured at 550 nm to follow the oxidation of reduced cytochrome c (extinction coefficient ε_{550} = 29.5 ml cm^{-1} μmol^{-1}) in a reaction medium containing 100 mM potassium phosphate, 0.05% (v/v) Tween 20 and 100 μM equine heart cytochrome c, pH 8.0. Just before analysis, cytochrome c was reduced with the addition of sodium dithionite without excess (4.5 mM final concentration). Samples were centrifuged at 3000 *g* (4°C) and the pellet was discarded prior to the analysis.

Chemicals

Most chemicals were provided by Sigma Aldrich (Oakville, ON, Canada). EDTA, KCl, K_2HPO_4, and KH_2PO_4 were obtained from VWR (Ville Mont-Royal, QC, Canada), cytochrome c from equine heart was provided by Alfa Aesar (Tewksbury, MA, United States), and the protein standard was from Bio-Rad (Mississauga, ON, Canada).

Calculations

Enzyme activities were normalized per protein unit. The bicinchoninic acid (BCA) method (Smith et al., 1985) was used to determine protein concentration. To compare the activity of enzymes from upstream of the ETS to the ETS, we used these enzyme ratios: PDHc/CI + CIII, PDHc/CIV, CPT/CI + CIII, CPT/CIV, HOAD/CI + CIII, HOAD/CIV, CPT/PDHc, HOAD/PDHc, PK/CI + CIII, PK/CIV, CI/CIV, CII/CIV, CI/CI + CIII, CI + CIII/CIV, CS/CI + CIII, and CS/CIV at the essay temperature closest to the species' optimal temperature (5°C for the two species of notothen, 10°C for wolfish and cod, 15°C for Arctic char, 20°C for bass, and 25°C for tilapia and the carp). We expressed activities as ratios to characterize the organization of mitochondria instead of documenting only the content of each enzyme in different species. We also ran Pearson correlation analyses on enzyme activities (correlation between enzymes) and on the different ratios (ratios measured at close to optimal temperature correlated to the estimated optimal temperature). The objective was to have a picture of mitochondrial organization at different thermal conditions for the different fish species to test our hypothesis that fish adapted to cold environment have to compensate for the limitation at steps upstream of the ETS and therefore should express higher ratio of activities of enzymes responsible for entrance of electrons over the enzymes controlling the oxidative process.

Statistics

All statistics were performed using the R platform (R Core Team, 2017). Significant differences between the activity ratios of the eight species were tested using one-way ANOVA. Tukey HSD tests were used to determine significant differences between groups. Normality and homogeneity of variances were analyzed using Shapiro-Wilk and Levene's tests, respectively. When needed, a $\log_{10}$ transformation was used to respect the assumptions of the ANOVA. A statistical significance level of $\alpha = 0.05$ was used for all tests. In all graphs, results are presented without transformations. We also performed a regression analysis to complement ANOVAs. The different ratios of activities measured close to optimal temperature were correlated with estimated optimal temperatures. Strong correlation would support the prediction of adjustments of the metabolic trait, expressed by a ratio, to environmental temperature.

RESULTS

The capacity to feed the TCA cycle through PDHc or PK, when measured at a temperature close to the optimum of each species and compared to the activity of the ETS enzymes (CI + CIII or CIV), varied little among most of the species examined (**Figures 1A–C**), although the cold-temperate wolfish (*A. minor*) and the warm-adapted carp (*C. carpio*) showed higher relative levels of PDHc activity. Ratios of activities of PK over Complex IV, the last enzyme of glycolysis which feed mitochondria with pyruvate, were higher for species adapted to warmer temperature with the exception of *G. morhua* (**Figure 1D**). The correlation of PK/CIV with optimal temperature was high and significant (**Supplementary Figure S2B**, $R^2 = 0.56$, $p < 0.001$).

The capacity to feed TCA by fatty acid oxidation, appears higher in cold-adapted fish since the activities of CPT, relative to CI + CIII are greater for the three species with lowest

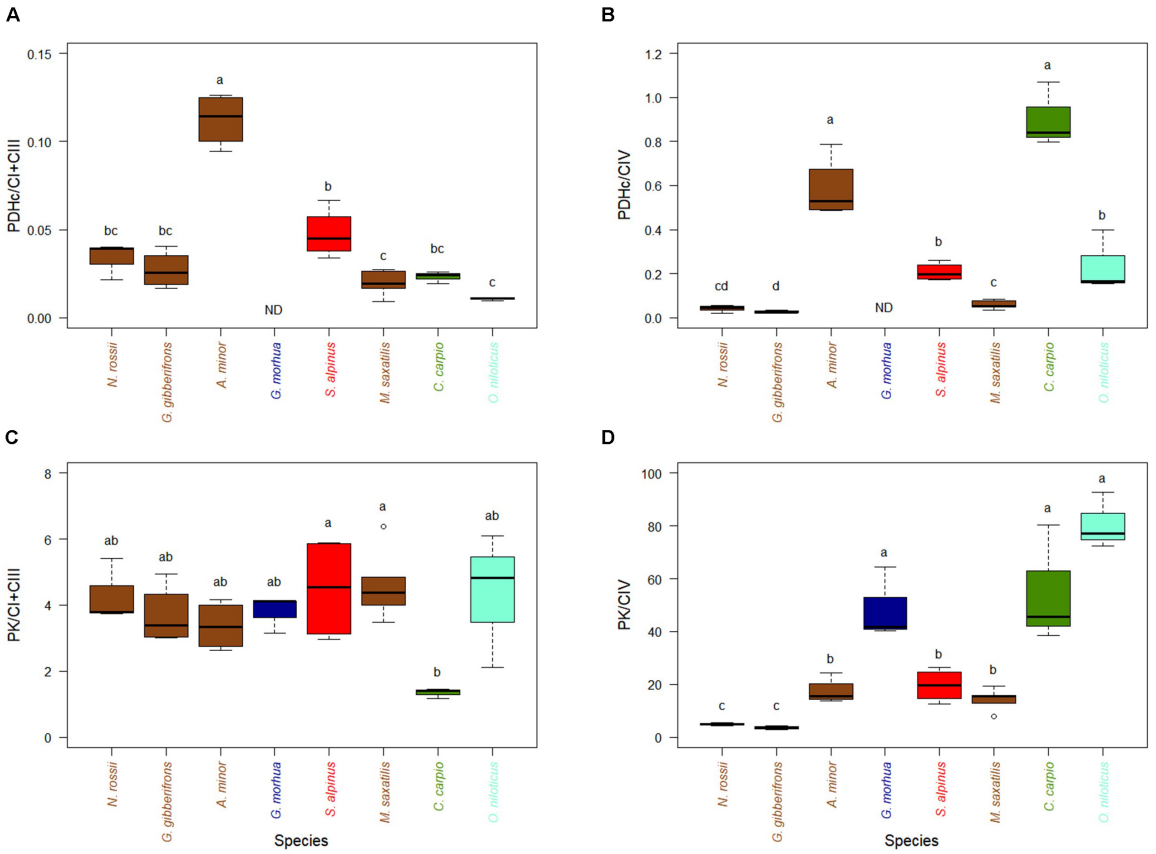

FIGURE 1 | Activity of mitochondrial substrate entrance enzymes of pyruvate pathway (PDHc and PK) in hearts of cold-adapted fish (left), cold-temperate adapted fish, and warm-adapted fish (right). Activities were measured at temperature near their thermal optimum. **(A)** Pyruvate dehydrogenase complex (PDHc) expressed relative to CI + CIII activity. **(B)** PDHc expressed relative to CIV activity. **(C)** PK activity expressed relative to CI + CIII. **(D)** PK activity expressed relative to CIV. Values are represented as mean ± sem. Statistical differences are represented with letters ($p < 0.05$). ND: no data. *Notothenia rossii* ($n = 3$). *Gobionotothen gibberifrons* ($n = 4$). *Anarhichas minor* ($n = 4$). *Gadus morhua* ($n = 3$). *Salvelinus alpinus* ($n = 4$). *Morone saxatilis* ($n = 5$). *Cyprinus carpio* ($n = 3$). *Oreochromis niloticus* ($n = 3$). Brown boxes represent Perciformes, dark blue Gadiforme, red Salmoniforme, green Cypriniformes, and light blue is Cichliformes.

optimal temperatures when compared to four of the five species adapted to higher temperatures (**Figure 2A**). This difference was lost when CPT was normalized to CIV activity (**Figure 2B**). Two cold-temperate species, *A. minor* and *G. morhua*, had the highest relative CPT/CIV activities. The activity of HOAD, a key enzyme of the β-oxidation pathway, relative to CI + CIII, partly mimicked the differences observed for CPT (**Figure 2C**). However, this trend disappeared again when HOAD was normalized to CIV activity, with two warm-adapted species (*C. carpio* and *O. niloticus*) expressing higher relative activities (**Figure 2D**). Interestingly, the relative activities of either CPT or HOAD over PDHc did not show any specific trend with temperature (**Figures 2E,F**). Capacities to oxidize fatty acids, compared to pyruvate oxidation, were, however, greater in two cold-adapted species (*N. rossii* and *G. gobionotothens*) and a temperate species (*M. saxatilis*). The correlations of key enzymes of metabolites entrance in oxidative phosphorylation, with CI + CIII or CIV (**Supplementary Figure S5**) show the same relations. They reveal a strong correlation of HOAD activity with CI + CIII (**Supplementary Figure S5D**).

With respect to the ETS, activities of CI relative to CIV were higher for the two warm-adapted species and lower for the cold-adapted species, and this trend was repeated for CII (**Figures 3B,C**), for example *C. carpio* showed higher activity than *O. niloticus*. When normalized to CI + CIII, activities of CI did not display any trend with thermal optimum of the different species (**Figure 3A**). Relative activities of CI + CIII normalized to CIV were greater for warm-adapted species (*C. carpio* and *O. niloticus*) than for the other species at their optimal temperatures (**Figure 3D**). Interestingly, when normalizing activities with either CI + CIII or CIV, very different and often opposite trends with estimated optimal temperatures were observed. CPT, HOAD, and CS all decreased with increases in optimal temperature when normalized per CI + CIII while HOAD, PK, CS as well as CI and CII increased when normalized per CIV (see **Supplementary Figures S1–S4**).

Activities of CS, a TCA cycle enzyme, tended to decrease with optimal species temperature when compared to activities of CI + CIII (**Figure 3E**). This is also observed when

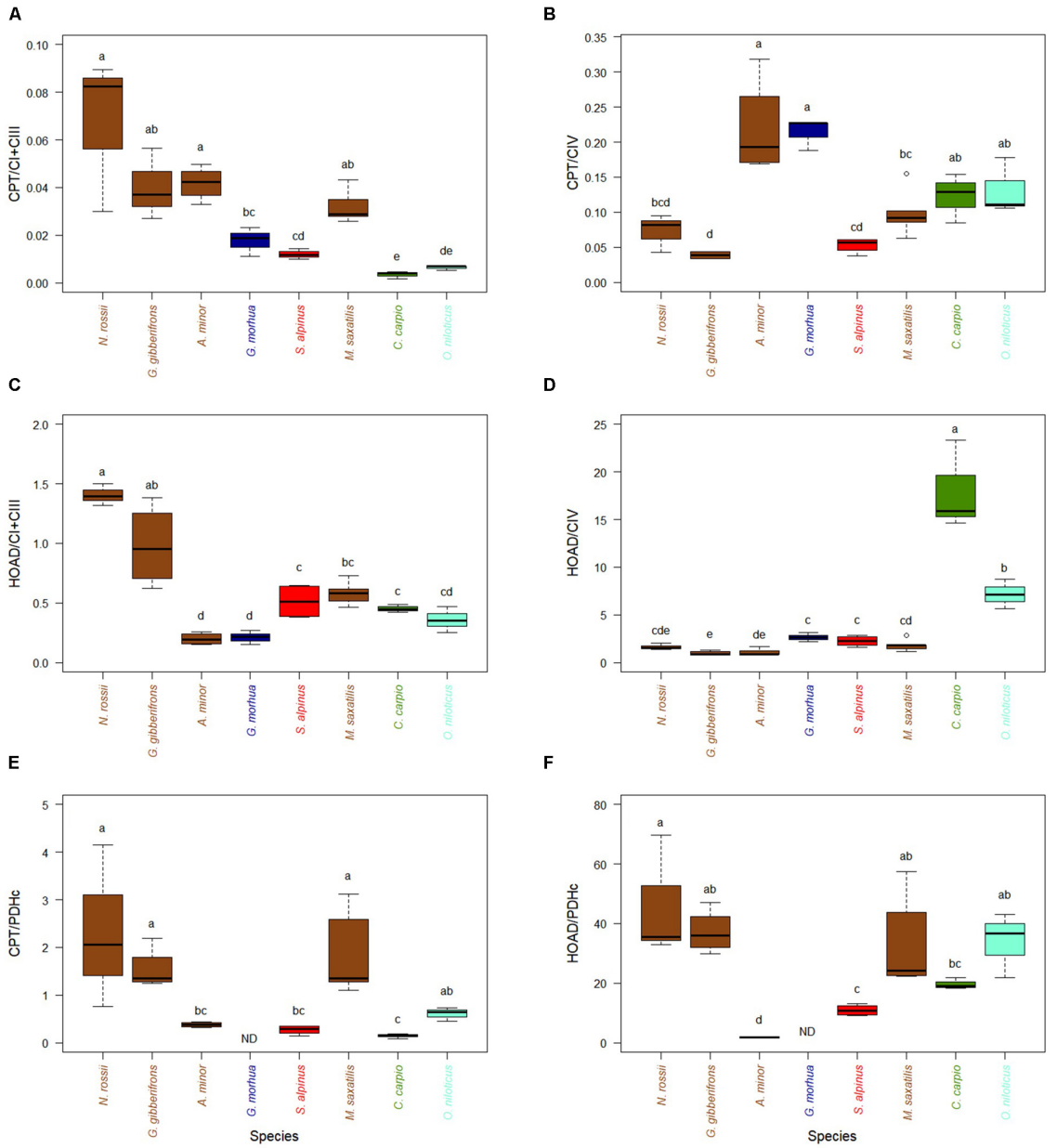

FIGURE 2 | Activity of mitochondrial substrate entrance enzymes of pyruvate pathway (normalized with ETS enzyme activities (CI + CIII and CIV) or PDHc, in hearts of cold-adapted fish (left), cold-temperate adapted fish, and fish species adapted to warmer habitats (right). Enzyme activities were measured at temperature near their thermal optimum. **(A)** Carnitine palmitoyltransferase (CPT) expressed relative to CI + CIII. **(B)** CPT expressed relative to CIV. **(C)** 3-Hydroxyacyl-CoA dehydrogenase (HOAD) expressed relative to CI + CIII. **(D)** 3-HOAD expressed relative to CIV. **(E)** CPT expressed relative to pyruvate dehydrogenase complex (PDHc). **(F)** 3-HOAD expressed relative to PDHc. Values are represented as mean ± SEM. Statistical differences are represented with letters ($p < 0.05$). *Notothenia rossii* ($n = 3$). *Gobionotothen gibberifrons* ($n = 4$). *Anarhichas minor* ($n = 4$). *Gadus morhua* ($n = 3$). *Salvelinus alpinus* ($n = 4$). *Morone saxatilis* ($n = 5$). *Cyprinus carpio* ($n = 3$). *Oreochromis niloticus* ($n = 3$). Brown boxes represent Perciformes, dark blue Gadiforme, red Salmoniforme, green Cypriniformes, and light blue is Cichliformes.

CS/CI + CIII ratios are correlated with optimal temperature (**Supplementary Figure S4B**, $R^2 = 0.48$, $p < 0.001$). For CS/CIV ratio (**Figure 3F**) the correlation with optimal temperature was significantly reversed but the relationship was not as strong (**Supplementary Figure S4A**, $R^2 = 0.26$, $p < 0.003$). When correlating the different enzymes measured at optimal temperatures to identify those for which activities co-vary (**Supplementary Figures S5, S6**), the only correlation we identified was HOAD with CI + CIII (**Supplementary Figure S5D**, $R^2 = 0.82$; $p < 0.001$) and CII with CIV (**Supplementary Figure S6C**, $R^2 = 0.62$; $p < 0.001$). Enzyme activities (expressed per mg of proteins) for each species and measured at different temperatures are presented in **Supplementary Figures S7–S10**.

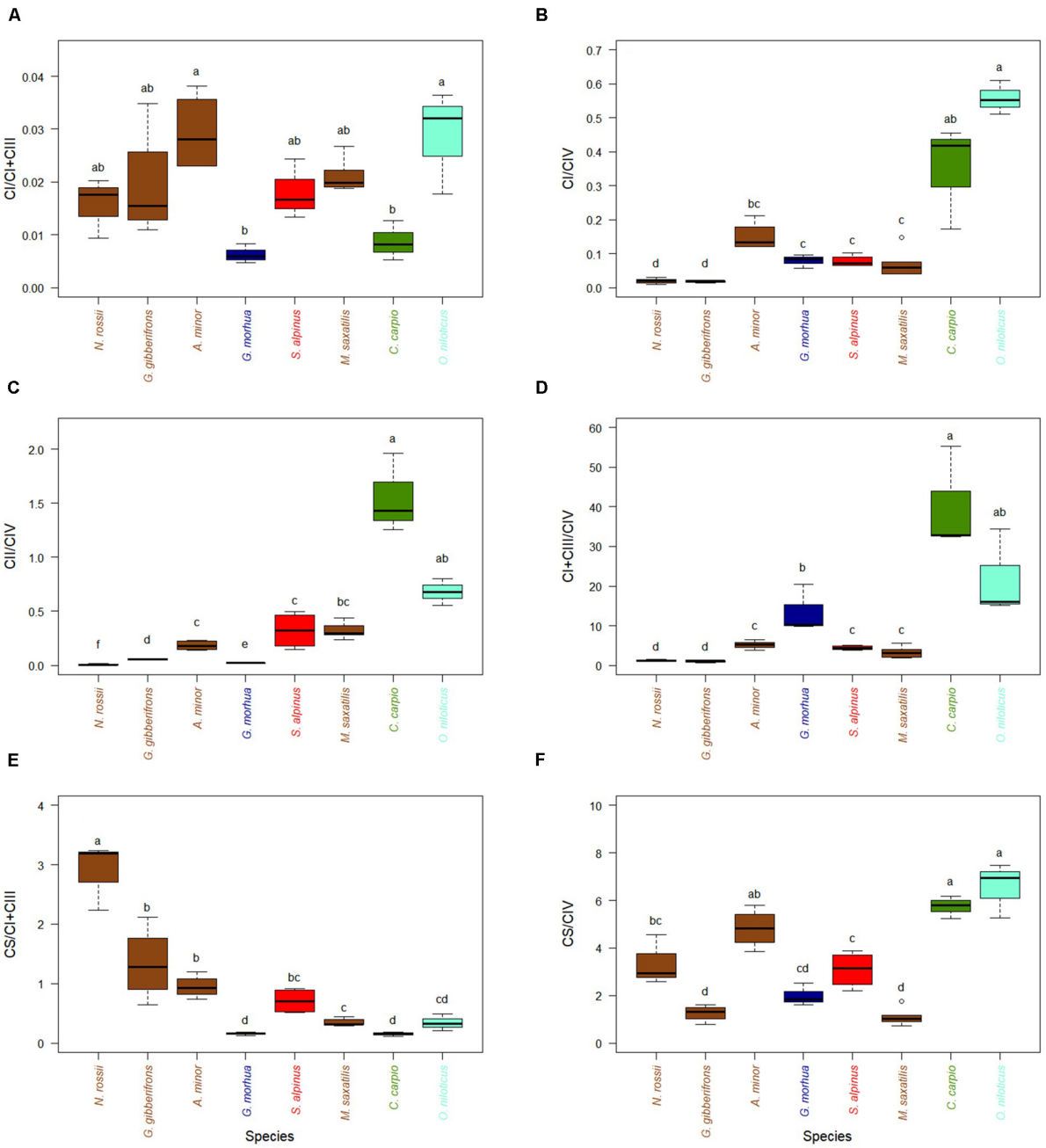

FIGURE 3 | Activity ratios of CS and ETS enzymes in hearts of cold-adapted fish (left), cold-temperate adapted fish and fish species adapted to warmer habitats (right). Enzymes activities were measured at temperature near their thermal optimum. **(A)** CI activity expressed relative to CI + CIII. **(B)** CI activity expressed relative to CIV. **(C)** CII activity expressed relative to CIV. **(D)** CI + CIII activity expressed relative to CIV. **(E)** CS activity expressed relative to CI + CIII. **(F)** CS activity expressed relative to CIV. Values are represented as mean ± SEM. Statistical differences are represented with letters ($p < 0.05$). *Notothenia rossii* ($n = 3$). *Gobionotothen gibberifrons* ($n = 4$). *Anarhichas minor* ($n = 4$). *Gadus morhua* ($n = 3$). *Salvelinus alpinus* ($n = 4$). *Morone saxatilis* ($n = 5$). *Cyprinus carpio* ($n = 3$). *Oreochromis niloticus* ($n = 3$). Brown boxes represent Perciformes, dark blue Gadiforme, red Salmoniforme, green Cypriniformes, and light blue is Cichliformes.

DISCUSSION

In this report, we characterize the cardiac mitochondrial pathways of eight ray-finned fish species that inhabit thermal niches spanning most of the range occupied by the Actinopterygii. Our goal was to identify potential evolutionary adjustments of mitochondrial metabolism in fish taxa across a wide range of thermal habitats. Knowing key characters of mitochondria associated to specific thermal niche should help to point out steps needed to adapt to changes in habitat

temperatures and therefore refine further studies on adaptability of ectotherms to temperature.

Prior work on the thermal sensitivity of mitochondrial metabolism in fish have often focused on enzymes of OXPHOS, the PDHc and some enzymes of TCA cycle such as CS, but have largely neglected fatty acid oxidation pathways (Takeuchi et al., 2009; Lemieux et al., 2010a,b; Blier et al., 2014; but see Ekström et al., 2017). Here, we have investigated enzymes that control substrate entrance, including lipids and carbohydrates, into the TCA cycle, as well as enzyme complexes of the electron transport chain. PDHc, the gatekeeper of the glucose oxidation pathway, showed no evidence of compensation, relative to ETS enzyme activities, in cold-adapted fish species, compared to temperate or warm adapted species, refuting our prediction based on prior work (Takeuchi et al., 2009; Lemieux et al., 2010a,b). Rather, the activity of CPT, a gatekeeper of the fatty acid oxidation pathway, when normalized with respect to the ETS (CI + III), revealed a strong compensation of fatty acid oxidation in heart mitochondria of cold-water fish species. Two of the three species adapted to the coldest environment showed ratios more than two times higher than those of four of the five species adapted to higher temperature. This is even more evident when the ratios are correlated to the estimated optimal temperatures. Similarly, HOAD activity appeared to be adjusted, with some variation, to maintain fatty acid oxidation capacity at low temperature. The correlation of HOAD with CI + CIII activities among species might suggest a coevolution in the regulation of the expression of these enzymes leading to coordination of fatty acid oxidation capacity with ETS. The ratio obtained for either CPT or HOAD over CI + III were, however, calculated with activities measured at 5°C in both cold-adapted notothenioid fish due to the technical difficulties to measure at 0°C even though these fish are adapted to temperature close to or below 0°C. A temperature of 5°C is significantly higher than "optimal" temperature and these ratios may represent heat shock conditions. To examine this possibility as well as the physiological significance of the ratios obtained from assays at 5°C, we estimated the activities of enzymes at 0°C by extrapolating from regression of activities at 5, 10, and 15°C. From these extrapolations the CPT/CI + III ratio is lower at 0°C in *N. rossii* than at 5°C (0.03 instead of 0.06) with no significant difference between both temperatures. In *G. gibberifrons*, the ratio from extrapolated activities at 0°C is, however, almost three times higher than at 5°C (0.11 instead of 0.04, with 0.11 being outside the range of standard deviation of the ratio at 5°C). Ratios calculated for 0°C are still higher than the ratios of four of the five fish species adapted at higher temperatures. For the ratios of HOAD over CI + III., extrapolations at 0°C show a higher ratio only for *G. gibberifrons* (1.3 instead of 0.9 but within the range of standard deviation of the ratio at 5°C). These observations suggest that temperature sensitivity of lipid oxidation, which provides a high proportion of the energy requirements of fish heart, could be compensated at key steps (CPT and HOAD) likely to maintain mitochondrial capacity at low temperature. All the fish were collected or acclimated at temperatures close to the estimated optimal temperatures. We suspect that these ratios approximate mitochondrial characters allowing optimal capacity to oxidize fatty acids in the range of temperature encountered during their life cycle. Comparison of the activity of PK, the final glycolytic enzyme, to complexes I + III suggests that the relative capacity to provide pyruvate to mitochondria is conserved among the eight species at their respective optimal temperatures. However, warm-living fish have PK/CIV ratios that are much larger than those of cold-adapted species.

The relationship of the ratios of gatekeeper enzymes over ETS enzymes with temperature is, however, dependent on the complex used to normalize the activity (denominator of the ratio). As mentioned CPT, HOAD, and CS decrease with increases in optimal temperature when normalized per CI + CIII while HOAD, PK, CS as well as CI and CII increase when normalized per CIV. This is partly explained by the relation of CI + CIII with CIV at different temperatures of adaptation. The ratio of CI + CIII over CIV increases with increases in optimal temperatures (**Supplementary Figure S6B**). This clearly shows that the organization of the ETS in fish heart mitochondria is variable and appears to be associated to environmental temperature. The predicted pattern of organization (higher gatekeeper enzymes over oxidative capacity) is revealed only when their activities are normalized by CI + CIII.

In mouse heart, Lemieux et al. (2017) measured a weak control of oxidative phosphorylation by Cytochrome c Oxidase at physiological temperature while they showed Lemieux et al. (2008) that the thermal sensitivity of cytochrome c oxidase cannot drive the thermal sensitivity of mitochondrial respiration, ruling out significant control of oxidative phosphorylation at this level. An excess of cytochrome c oxidase capacity relative to OXPHOS of at least 1.5-fold has been reported for the heart mitochondria of three fish species (*Bellapiscis medius*, *Forsterygion varium*, and *F. malcolmi*) at three temperatures [15, 25, and 30°C; Hilton et al. (2010)]. Much higher activities of Cytochrome c oxidase than the whole Electron Transfer System have also been reported in the heart of three species of wrasses (*Notolabrus celidotus*, *Notolabrus fucicola*, and *Thalassoma lunare*), Iftikar et al., 2014. This excess of Cytochrome c Oxidase may suggest low control by CIV over maximal respiration (but see Blier and Lemieux, 2001). If CIV insures low level of control over the maxima catalytic capacity of mitochondria, the ratios expressed per CI + III activity might be more physiologically significant and the trend observed among species could reveal a higher increased capacity to provide electrons to CI and CII through fatty acid oxidation. The increase in the ratio of CI + III/CIV at higher temperatures is, however, intriguing. One hypothesis is that ETS over CIV ratio could evolve to insure proper reduction state and associated catalytic capacity and regulatory properties.

Compensation of mitochondrial energy production in cold-living fish can occur at the organellar level via increases in mitochondrial volume density (Strobel et al., 2013), greater inner membrane surface density (St.-Pierre et al., 1998), and modifications in membrane composition (Kraffe et al., 2007; Grim et al., 2010). Mitochondrial content is often evaluated using CS activity, and cristae surface area can be estimated from CIV activity (Larsen et al., 2012). The trend observed in our CS/CI + CIII ratio data suggest higher volume/surface ratio for cold-adapted species, consistent with

higher mitochondrial content, and an increase in mitochondria surface density in warm-adapted species. However, based on the CS/CIV ratios, the species studied are likely to have similar mitochondrial volume/surface ratios, with the exception of the two warm-adapted species. We suggest that thermal adaptation of mitochondrial metabolism in fish most likely results from compensation at the level of enzymatic properties, quantities and metabolic organization rather than organellar quantity or volume.

Homeoviscous adaptation through changes in the lipid composition of mitochondrial membranes can play an important role in acclimation and adaptation of energy metabolism to cold and warm temperatures (Guderley and St-Pierre, 2002; Kraffe et al., 2007; Pörtner et al., 2007; Grim et al., 2010; Hofmann and Todgham, 2010). Such remodeling can have big impacts on the activities of enzymes that are embedded in the mitochondrial membranes, including CPT and the four respiratory complexes. However, our data cannot address whether the activities of these enzymes from the species that we have examined are modulated through temperature-dependent adjustments of membrane composition and properties.

In this study, we have characterized heart mitochondrial phenotypes from eight fish species adapted to different thermal habitats by comparing the activities of enzymes from different steps of mitochondrial respiration and electron transport. We suggest that natural selection driven by habitat temperature has shaped mitochondrial function and regulation (Blier et al., 2014; Lemieux et al., 2017) such that distinct mitochondrial pathways allow cold- and warm-living fish to optimize aerobic capacity and regulation. Our results demonstrate important variability of organization in the heart mitochondrial pathway among fish species of various thermal habitats. Among the characters, two appear related to optimal temperature; ratios of CPT/CI + CIII and ratios of HOAD/CI + CIII. These increases in activities of fatty acid oxidation enzymes in cold adapted fish are complemented by increase in a key enzyme of TCA (CS). It is unlikely that these relationships are induced by phylogenetic relationship since fish from four basal orders (Gadiformes, Salmoniformes, Cyprinoformes, and Cichliformes) cover an optimal temperature range from 9 to 30°C while the four other species are all from the Perciforme order and cover a temperature range from 0 to 18°C, with the Cichliformes (*O. niloticus*; 30°C) being closer to Perciformes than to others. Furthermore, the optimal temperatures in the perciformes fish from the present study are independent of the phylogenetic distance (see the phylogeny of Hughes et al., 2018). The strong correlation observed between CPT/CI + CIII or HOAD/CI + CIII and optimal temperature could therefore likely be associated to adaptation to the temperature regime. These results are in line with the demonstration of higher ability to oxidize fatty acids in the muscle of two temperate fish species (*M. saxatilis* and *O. mykiss*) following acclimation to low temperature (Rodnick and Sidell, 1994; St.-Pierre et al., 1998). Before concluding that these ratios represent clear improvement of the ability to oxidize fatty acids in cold-adapted species through increments of gatekeeper steps, we need to know which character sets the oxidative capacity of mitochondria (CI + CIII or CIV). One way to address this question would be to estimate the control strength of different steps of mitochondrial pathways and to compare the ability to oxidize fatty acids at different temperatures in different species from a wide range of thermal habitats.

The changing thermal environments that will result from climate change might therefore affect mitochondrial functions differently according to the thermal niche of the species. For example, a fish species adapted to cold environment may therefore be more affected by the thermal sensitivity of gate keepers of fatty acid oxidation (CPT) while warm adapted species could be more impaired by the impact of temperature on CIV. A corollary of this is that following rapid temperature changes, populations might face an excess of these key enzymes potentially resulting in an increase in reduction status of ETS and thus a burst of ROS production (see Christen et al., 2018). This study clearly reveals the urgency of further studies scrutinizing the extent to which selection could remodel mitochondrial organization rather than only accommodating mitochondrial content.

ETHICS STATEMENT

This study was carried out in accordance with the principles of the Basel Declaration and recommendations of Canadian Council of Animal Care. The protocol was approved by the Comité de Protection des Animaux de l'UQAR.

AUTHOR CONTRIBUTIONS

FH-M carried out the experiments and statistical analyses, and drafted the manuscript. PB designed the study, obtained the funding, supervised the analysis, and revised the manuscript. VD supervised FH-M during biochemical analysis. NL and HD conducted the field research program that obtained the Antarctic fish samples and revised the manuscript. NL sampled Arctic fish and provided the tilapia. FD and CN participated in the analysis and revised the manuscript. HD helped to get access to the biological material and revised the manuscript.

FUNDING

This work was funded by the Natural Sciences and Engineering Research Council of Canada (NSERC) through a grant from the discovery program to PB (RGPIN 155926). FH-M obtained graduate scholarships from the Fonds de Recherche du Québec – Nature et Technologies (FRQNT) and the Natural Sciences and Engineering Research Council of Canada (NSERC). HD and NL were supported by the U.S. National Science Foundation grant PLR-1444167 from the Office/Division of Polar Programs.

ACKNOWLEDGMENTS

We are grateful for the assistance of the staff of the Biodôme of Montreal, the Maurice-Lamontagne Institute (especially to Denis Chabot), and the fish hatchery of Baldwin-Coaticook (notably

to Mario Lessard) while working at these locations and for the fish provided for this project. We were thankful to our colleagues at the Université du Québec à Rimouski for their assistance in every aspect of the project. We gratefully acknowledge the logistic support provided by the staff of the Division of Polar Programs of the U.S. National Science Foundation, by the personnel of the Antarctic Support Contract group, and by the captains and crews of the Antarctic Research and Supply Vessel *Laurence M. Gould*. This is contribution #398 from the Marine Science Center at Northeastern University.

SUPPLEMENTARY MATERIAL

The Supplementary Material for this article can be found online at: https://www.frontiersin.org/articles/10.3389/fphys.2019.01220/full#supplementary-material

REFERENCES

Bilyk, K. T., and DeVries, A. L. (2011). Heat tolerance and its plasticity in Antarctic fishes. *Comp. Biochem. Physiol. A Mol. Integr. Physiol.* 158, 382–390. doi: 10.1016/j.cbpa.2010.12.010

Blier, P. U., and Lemieux, H. (2001). The impact of the thermal sensitivity of cytochrome c oxidase on the respiration rate of Arctic char red muscle mitochondria. *J. Comp. Physiol. B Biochem. Syst. Environ. Physiol.* 171, 247–253. doi: 10.1007/s003600000169

Blier, P. U., Lemieux, H., and Pichaud, N. (2014). Holding our breath in our modern world: will mitochondria keep the pace with climate changes? *Can. J. Zool.* 92, 591–601. doi: 10.1139/cjz-2013-83

Christen, F., Desrosiers, V., Dupont-Cyr, B. A., Vandenberg, G. W., Le François, N. R., Tardif, J.-C., et al. (2018). Thermal tolerance and thermal sensitivity of heart mitochondria: mitochondrial integrity and ROS production free radic. *Biol. Med.* 116, 11–18. doi: 10.1016/j.freeradbiomed.2017.12.037

Cox, D. K., and Coutant, C. C. (1981). Growth dynamics of juvenile striped bass as functions of temperature and ration. *Trans. Am. Fish. Soc.* 110, 226–238. doi: 10.1577/1548-8659(1981)110<226:gdojsb>2.0.co;2

Crockett, E. L., and Sidell, B. D. (1990). Some pathways of energy metabolism are cold adapted in Antarctic fishes. *Physiol. Zool.* 63, 472–488. doi: 10.1086/physzool.63.3.30156223

Ekström, A., Sandblom, E., Blier, P. U., Cyr, B.-D., Brijs, J., and Pichaud, N. (2017). Thermal sensitivity and phenotypic plasticity of cardiac mitochondrial metabolism in european perch, perca fluviatilis. *J. Exp. Biol.* 220, 386–396. doi: 10.1242/jeb.150698

Grim, J. M., Miles, D. R. B., and Crockett, E. L. (2010). Temperature acclimation alters oxidative capacities and composition of membrane lipids without influencing activities of enzymatic antioxidants or susceptibility to lipid peroxidation in fish muscle. *J. Exp. Biol.* 213, 445–452. doi: 10.1242/jeb.036939

Guderley, H., and St-Pierre, J. (2002). Going with the flow or life in the fast lane: contrasting mitochondrial responses to thermal change. *J. Exp. Biol.* 205, 2237–2249.

Hansen, T. K., and Falk-Petersen, I. B. (2002). Growth and survival of first-feeding spotted wolffish (Anarhichas minor, Olafsen) at various temperature regimes. *Aquacul. Res.* 33, 1119–1127. doi: 10.1046/j.1365-2109.2002.00756.x

Hilton, Z., Clements, K. D., and Hickey, A. J. (2010). Temperature sensitivity of cardiac mitochondria in intertidal and subtidal triplefin fishes. *J. Comp. Physiol. B* 180, 979–990. doi: 10.1007/s00360-010-0477-7

Hofmann, G. E., and Todgham, A. E. (2010). Living in the now: physiological mechanisms to tolerate a rapidly changing environment. *Annu. Rev. Physiol.* 72, 127–145. doi: 10.1146/annurev-physiol-021909-135900

Hughes, L. C., Ortí, G., Huang, Y., Sun, Y., Baldwin, C. C., Thompson, A. W., et al. (2018). Comprehensive phylogeny of ray-finned fishes (Actinopterygii) based on transcriptomic and genomic data. *PNAS* 115, 6249–6254. doi: 10.1073/pnas.1719358115

Iftikar, F. I., and Hickey, A. J. (2013). Do mitochondria limit hot fish hearts? Understanding the role of mitochondrial function with heat stress in *Notolabrus celidotus*. *PLoS One* 8:e64120. doi: 10.1371/journal.pone.0064120

Iftikar, F. I., MacDonald, J. R., Baker, D. W., Renshaw, G. M. C., and Hickey, A. J. R. (2014). Could thermal sensitivity of mitochondria determine species distribution in a changing climate? *J. Exp. Biol.* 217, 2348–2357. doi: 10.1242/jeb.098798

Janssen, A. J. M., Trijbels, F. J. M., Sengers, R. C. A., Smeitink, J. A. M., Van Den Heivel, L. P., Wintjes, L. T. M., et al. (2007). Spectrophotometric assay for complex I of the respiratory chain in tissue samples and cultured fibroblasts. *Clin. Chem.* 53, 729–734. doi: 10.1373/clinchem.2006.078873

Jobling, M., Jørgensen, E. H., Christiansen, J. S., Arnesen, A. M., and Palsson, J. Ø. (1992). Investigation of growth requirements and aquaculture potential of Arctic char (*Salvelinus alpinus*). *Icel. Agric. Sci.* 6, 47–62.

Kraffe, E., Marty, Y., and Guderley, H. (2007). Changes in mitochondrial oxidative capacities during thermal acclimation of rainbow trout Oncorhynchus mykiss: roles of membrane proteins, phospholipids and their fatty acid compositions. *J. Exp. Biol.* 210, 149–165. doi: 10.1242/jeb.02628

Larsen, S., Nielsen, J., Hansen, C. N., Nielsen, L. B., Wibrand, F., Stride, N., et al. (2012). Biomarkers of mitochondrial content in skeletal muscle of healthy young human subjects. *J. Physiol.* 590, 3349–3360. doi: 10.1113/jphysiol.2012.230185

Lauff, R. F., and Wood, C. H. (1996). Respiratory gas exchange, nitrogenous waste excretion, and fuel usage during aerobic swimming in juvenile rainbow trout. *J. Comp. Physiol. B* 166, 501–509. doi: 10.1007/s003600050038

Lemieux, H., Blier, P. U., and Gnaiger, E. (2017). Remodeling pathway control of mitochondrial respiratory capacity by temperature in mouse heart: electron flow through the Q-junction in permeabilized fibers. *Sci. Rep.* 7:2840. doi: 10.1038/s41598-017-02789-8

Lemieux, H., Blier, P. U., and Tardif, J. C. (2008). Does membrane fatty acid composition modulate mitochondrial functions and their thermal sensitivities?. *Comp. Biochem. Physiol. Part A Mol. Integr. Physiol.* 149, 20–29. doi: 10.1016/j.cbpa.2007.09.015

Lemieux, H., Tardif, J. C., Dutil, J. D., and Blier, P. U. (2010a). Thermal sensitivity of cardiac mitochondrial metabolism in an ectothermic species from a cold environment, Atlantic wolffish (*Anarhichas lupus*). *J. Exp. Mar. Biol. Ecol.* 384, 113–118. doi: 10.1016/j.jembe.2009.12.007

Lemieux, H., Tardif, J. C., and Blier, P. U. (2010b). Thermal sensitivity of oxidative phosphorylation in rat heart mitochondria: does pyruvate dehydrogenase dictate the response to temperature? *J. Therm. Biol.* 35, 105–111. doi: 10.1016/j.jtherbio.2009.12.003

Madon, S. P., Schneider, D. W., and Stoeckel, J. A. (1998). In-situ estimation of zebra mussel metabolic rates using the electron transport system (ETS) assay. *J. Shellfish Res.* 17, 195–204.

Magnoni, L., Vaillancourt, E., and Weber, J. M. (2008). High resting triacylglycerol turnover of rainbow trout exceeds the energy requirements of endurance swimming. *Am. J. Physiol. Regul. Integr. Comp. Physiol.* 295, R309–R315. doi: 10.1152/ajpregu.00882.2007

Magnoni, L., and Weber, J. M. (2007). Endurance swimming activates trout lipoprotein lipase: plasma lipids as a fuel for muscle. *J. Exp. Biol.* 210, 4016–4023. doi: 10.1242/jeb.007708

Pederson, T., and Jobling, M. (1989). Growth rates of large, sexually mature cod, *Gadus morhua*, in relation to condition and temperature during an annual cycle. *Aquaculture* 81, 161–168. doi: 10.1016/0044-8486(89)90242-1

Pelletier, D., Dutil, J.-D., Blier, P., and Guderley, H. (1994). Relation between growth rate and metabolic organization of white muscle, liver and digestive tract in cod, *Gadus morhua*. *J. Comp. Physiol. B* 164, 179–190. doi: 10.1007/BF00354078

Pichaud, N., Ballard, J. W., Tanguay, R. M., and Blier, P. U. (2011). Thermal sensitivity of mitochondrial functions in permeabilized muscle fibers from two populations of Drosophila simulans with divergent mitotypes. *Am. J. Physiol. Regul. Integr. Comp. Physiol.* 301, R48–R59. doi: 10.1152/ajpregu.00542.2010

Pichaud, N., Chatelain, E. H., Ballard, J. W., Tanguay, R., Morrow, G., and Blier, P. U. (2010). Thermal sensitivity of mitochondrial metabolism in two distinct

mitotypes of *Drosophila simulans*: evaluation of mitochondrial plasticity. *J. Exp. Biol.* 213, 1665–1675. doi: 10.1242/jeb.040261

Pörtner, H. O., Peck, L., and Somero, G. (2007). Thermal limits and adaptation in marine Antarctic ectotherms: an integrative view. *Phil. Trans. R. Soc. B* 362, 2233–2258. doi: 10.1098/rstb.2006.1947

R Core Team (2017). *R: A Language and Environment for Statistical Computing*. Vienna: R Foundation for Statistical Computing.

Rodnick, K. J., and Sidell, B. D. (1994). Cold acclimation increases carnitine palmitoyltransferase I activity in oxidative muscle of striped bass. *Am. J. Physiol.* 266 (2 Pt 2), R405–R412.

Smith, P. K., Krohn, R. I., Hermanson, G. T., Mallia, A. K., Gartner, F. H., Provenzano, M. D., et al. (1985). Measurement of protein using bicinchoninic acid. *Anal. Biochem.* 150, 76–85. doi: 10.1016/0003-2697(85)90442-7

St.-Pierre, J., Charest, P.-M., and Guderley, H. (1998). Relative contribution of quantitative and qualitative changes in mitochondria to metabolic compensation during seasonal acclimatisation of rainbow trout *Oncorhynchus mykiss*. *J. Exp. Biol.* 201, 2961–2970.

Strobel, A., Bennecke, S., Leo, E., Mintenbeck, K., Pörtner, H. O., and Mark, F. C. (2012). Metabolic shifts in the Antarctic fish *Notothenia rossii* in response to rising temperature and PCO2. *Front. Zool.* 9:28. doi: 10.1186/1742-9994-9-28

Strobel, A., Leo, E., Pörtner, H. O., and Mark, F. C. (2013). Elevated temperature and PCO2 shift metabolic pathways in differentially oxidative tissues of *Notothenia rossii*. *Comp. Biochem. Physiol. B Biochem Mol Biol.* 166, 48–57. doi: 10.1016/j.cbpb.2013.06.006

Takeuchi, K.-I., Nakano, Y., Kato, U., Kaneda, M., Aizu, M., Awano, W., et al. (2009). Changes in temperature preferences and energy homeostasis in dystroglycan mutants. *Science* 323, 1740–1743. doi: 10.1126/science.1165712

Thibault, M., Blier, P. U., and Guderley, H. (1997). Seasonal variation of muscle metabolic organization in rainbow trout (*Oncorhynchus mykiss*). *Fish Physiol. Biochem.* 16, 139–155. doi: 10.1007/BF00004671

Watanabe, T., Takeuchi, T., Satoh, S., and Kiron, V. (1996). Digestible crude protein contents in various feedstuffs determined with four freshwater fish species. *Fish. Sci.* 62, 278–282. doi: 10.2331/fishsci.62.278

Weber, J. M. (2011). Metabolic fuels: regulating fluxes to select mix. *J. Exp. Biol.* 214(Pt 2), 286–294. doi: 10.1242/jeb.047050

Xie, S., Zheng, K., Chen, J., Zhang, Z., Zhu, X., and Yang, Y. (2011). Effect of water temperature on energy budget of Nile tilapia, Oreochromis niloticus. *Aquac. Nutr.* 17, e683–e690. doi: 10.1111/j.1365-2095.2010.00827.x

Conflict of Interest: The authors declare that the research was conducted in the absence of any commercial or financial relationships that could be construed as a potential conflict of interest.

frontiers in Physiology

ORIGINAL RESEARCH
published: 24 March 2020
doi: 10.3389/fphys.2020.00248

Hypoxia Tolerance of 10 Euphausiid Species in Relation to Vertical Temperature and Oxygen Gradients

Nelly Tremblay[1], Kim Hünerlage[2] and Thorsten Werner[3]*

[1] Shelf Sea System Ecology, Alfred-Wegener-Institut Helmholtz-Zentrum für Polar- und Meeresforschung, Helgoland, Germany, [2] Institute for Sea Fisheries, Thünen Institute, Bremerhaven, Germany, [3] Nature and Biodiversity Conservation Union, Berlin, Germany

Oxygen Minimum Zones prevail in most of the world's oceans and are particularly extensive in Eastern Boundary Upwelling Ecosystems such as the Humboldt and the Benguela upwelling systems. In these regions, euphausiids are an important trophic link between primary producers and higher trophic levels. The species are known as pronounced diel vertical migrators, thus facing different levels of oxygen and temperature within a 24 h cycle. Declining oxygen levels may lead to vertically constrained habitats in euphausiids, which consequently will affect several trophic levels in the food web of the respective ecosystem. By using the regulation index (RI), the present study aimed at investigating the hypoxia tolerances of different euphausiid species from Atlantic, Pacific as well as from Polar regions. RI was calculated from 141 data sets and used to differentiate between respiration strategies using median and quartile (Q) values: low degree of oxyregulation ($0.25 < \text{RI median} < 0.5$); high degree of oxyregulation ($0.5 < \text{RI median} < 1$; $Q1 > 0.25$ or $Q3 > 0.75$); and metabolic suppression (RI median, Q1 and Q3 < 0). RI values of the polar (*Euphausia superba*, *Thysanoessa inermis*) and sub-tropical (*Euphausia hanseni*, *Nyctiphanes capensis*, and *Nematoscelis megalops*) species indicate a high degree of oxyregulation, whereas almost perfect oxyconformity (RI median ≈ 0; $Q1 < 0$ and $Q3 > 0$) was identified for the neritic temperate species *Thysanoessa spinifera* and the tropical species *Euphausia lamelligera.* RI values of *Euphausia distinguenda* and the Humboldt species *Euphausia mucronata* qualified these as metabolic suppressors. RI showed a significant impact of temperature on the respiration strategy of *E. hanseni* from oxyregulation to metabolic suppression. The species' estimated hypoxia tolerances and the degree of oxyconformity vs. oxyregulation were linked to diel vertical migration behavior and the temperature experienced during migration. The results highlight that the euphausiid species investigated have evolved various strategies to deal with different levels of oxygen, ranging from species showing a high degree of oxyconformity to strong oxyregulation. Neritic species may be more affected by hypoxia, as these are often short-distance-migrators and only adapted to a narrow range of environmental conditions.

Keywords: oxygen minimum zones, diel vertical migration, krill, respiration rate, regulation index

OPEN ACCESS

Edited by:
Silvia Franzellitti, University of Bologna, Italy

Reviewed by:
Folco Giomi, University of Padova, Italy
Santiago Hernández-León, University of Las Palmas de Gran Canaria, Spain

****Correspondence:***
Nelly Tremblay
Nelly.tremblay@awi.de

Specialty section:
This article was submitted to Aquatic Physiology, a section of the journal Frontiers in Physiology

Received: *28 June 2019*
Accepted: *04 March 2020*
Published: *24 March 2020*

Citation:
Tremblay N, Hünerlage K and Werner T (2020) Hypoxia Tolerance of 10 Euphausiid Species in Relation to Vertical Temperature and Oxygen Gradients. Front. Physiol. 11:248. doi: 10.3389/fphys.2020.00248

INTRODUCTION

Oxygen concentration and water temperature are two important abiotic factors influencing several physiological processes, such as metabolic rate, energy expenditure, as well as the horizontal and vertical distribution of animals living in the world's oceans (Torres and Childress, 1983; Claireaux and Lagardère, 1999; Ekau et al., 2010). However, both factors are not evenly distributed and temperature and oxygen levels at the surface area are usually higher, compared to deeper water layers. Water temperature is influenced by solar radiation, i.e., latitude and water turbulence. In contrast, oxygen concentration is affected by physical replenishment (mixing), bacterial decomposition and animal respiration. Temperature and oxygen profiles of the water column show a more or less steady decline from upper to deeper water layers (weak thermo- and oxycline) or a more saltatory pattern (strong thermo- and oxycline). In the oceans, the depth and strength of the thermocline vary between season and year. It is semi-permanent in the tropics, variable in temperate regions, and shallow to non-existent in Polar regions. High oxygen concentrations are found at high latitudes, whereas at mid-latitudes, in particular off the western coasts of the continents, oxygen-deficient zones, so-called Oxygen Minimum Zones (OMZs), prevail. Consequently, the ecosystems in the world's oceans are characterized by distinct oxygen and temperature regimes shaping the different species' behavior, distribution and physiological processes.

In the anticipated future, anthropogenic induced changes, such as rising nutrient loads coupled with climate change, will cause regional declines in oceanic dissolved oxygen, mainly due to increased stratification and reduced mixing, and an increase in water temperature (Diaz and Rosenberg, 2008; Keeling et al., 2010). Increasing temperature is known to negatively impact the hypoxia tolerance of animals and at the same time raise their energy expenditures. Furthermore, as water temperature rises, oxygen solubility decreases. Thus, decreasing oxygen levels accompanied by increasing temperatures may affect key processes and trophic interactions including community composition, energy flows, migration patterns, and consequently biogeochemical processes (Ekau et al., 2018) and will exert significant pressure on pelagic communities. This applies particularly to planktonic species, such as euphausiids, which cannot, or only to a very limited degree, escape unfavorable environmental conditions (Verheye and Ekau, 2005). As a consequence, it is expected that some areas may experience a shift from an abundant and diverse regime to one that is lean and dominated by vertical migrators (Wishner et al., 2013; Elder and Seibel, 2015).

Evaluation of time series already revealed vertical expansion of OMZs during the last decades (Stramma et al., 2008). It is assumed that these OMZs will further expand, which can happen horizontally into areas previously not experiencing hypoxic conditions, or consist of vertical expansion of an existing OMZ, while coastal hypoxia will increase in extent and severity (Levin, 2018). Compared to other hypoxic habitats, the particular nature of such an OMZ is that it is characterized by moderate to severe hypoxia (<2 mg O_2 L^{-1}) over very large areas (∼8% of total oceanic area; Paulmier and Ruiz-Pino, 2009) and over long time periods. They differ from the "dead zones" phenomena caused by anthropogenic coastal eutrophication found, e.g., in the Gulf of Mexico (Rabalais et al., 2002; Diaz and Rosenberg, 2008). OMZs are permanent midwater features occurring at intermediate depth (300–2,500 m) in most of the oceans (Emelyanov, 2005). The largest and most pronounced OMZs are located in the Northern Indian Ocean, the Eastern Atlantic off northwest Africa, and the Eastern Tropical Pacific (ETP) (Wyrtki, 1962; Kamykowski and Zentara, 1990; Olson et al., 1993). Notably, the OMZ of the ETP and the Eastern Atlantic off northwest Africa have expanded to higher latitudes during the past 50 years (Stramma et al., 2008), suggesting changes in zoogeographic distribution patterns, compression of habitats, and restricted zones of biomass production (Prince and Goodyear, 2006; Koslow et al., 2011; Stramma et al., 2011; Gilly et al., 2013). The shallow and severe OMZ in the ETP is due to the poor lateral ventilation of surface waters (Reid, 1965; Luyten et al., 1983) and the formation of a strong thermocline, which limits O_2 diffusion into the deeper layers of the ocean (Lavín et al., 2006). Very high temperatures at the surface result in strong stratification, at which the zooplankton aggregate and locally increase the oxygen consumption (Bianchi et al., 2013). At this depth, oxygen is consumed faster than it is replaced by the horizontal mixing of the water mass (Wyrtki, 1962; Fiedler and Talley, 2006; Karstensen et al., 2008), creating the shallow OMZ. The oxygen utilization is particularly enhanced during El Niño-Southern Oscillation and inter-annual changes in upwelling conditions, thus partly explaining the vertical OMZ expansion of the ETP since the 1980s (Ito and Deutsch, 2013).

Compared to Eastern Boundary Upwelling Systems (EBUEs), such as the California, Humboldt, and Benguela Current ecosystems with their pronounced OMZs, the oxygen levels of Polar regions are higher and water temperatures are much lower. No real OMZs exist in these areas and species living there may not be forced to develop adaptations to cope with low oxygen levels. However, mild-hypoxia (50% air saturation) was reported in the Indian sector of the Southern Ocean at depth greater than 500 m (Dehairs et al., 1990) and deoxygenation in the Southern Ocean is currently taking place at 200–400 m depth between 50 and 60° of latitude (Matear et al., 2000; Aoki, 2005). In the Artic, the potential effects of global warming and changes in deep-sea circulation on the oxygenation of the deep ocean is monitored continuously in Fram Strait, West Spitsbergen, the only deep connection between the central Arctic Ocean and the Nordic Seas (Friedrich et al., 2014). The Arctic ecosystem is far from being classified as hypoxic, but strong increase in the annual mean net heat transport within the waters of the West Spitsbergen Current could potentially affect oxygen levels to less than 80% air saturation.

Euphausiids, or krill, are distributed ubiquitously across the globe and often dominate zooplankton communities in terms of abundance and biomass throughout the world's oceans. Euphausiids form a pivotal component of many food webs and are known as pronounced diel vertical migrators, thereby contributing to the vertical flux of carbon and facing

different levels of oxygen and temperature within a 12 h period. During diel vertical migration (DVM), many euphausiid species cross pronounced gradients of temperature, salinity, and oxygen indicating that these species must be of a broad ecophysiological plasticity. In this regard, euphausiids are ideal model organisms for studying the interactions between organismal and environmental variability (Mangel and Nicol, 2000). Euphausiids and other taxa living in areas with pronounced OMZs have to physiologically and/or behaviorally adapt to low oxygen levels or will be excluded from these areas or at least their vertical distribution ranges will be limited. A typical euphausiid DVM pattern consists of an upward migration at dusk to feed in the upper, productive layers of the oceans, and a downward movement at dawn to avoid visual predators (Zaret and Suffern, 1976; Ohman, 1984), decreasing at the same time their metabolic rates due to the lower water temperature and O_2 concentrations (McLaren, 1963; Enright, 1977). Euphausiids channel energy from lower (phytoplankton, small zooplankton) to higher (fish, birds, and even whales) trophic levels. Accordingly, as varying oxygen and temperature levels will likely alter these species' vertical and horizontal distribution ranges, this may impact a larger part of the whole food web, and even impinge on fisheries yield.

Adaptations of animals to low dissolved oxygen concentrations are driven by strong selective pressures to maintain aerobic metabolism (Seibel, 2011). Most animals facing low oxygen concentrations respond either by decreasing their oxygen consumption rates, known as oxyconformity, or by maintaining a constant oxygen uptake irrespective of the ambient oxygen levels, known as oxyregulation. However, as analyzed mathematically by Cobbs and Alexander (2018) using/applying seven different functions and as discussed by Wood (2018), animals seldom show perfect oxyconformity or oxyregulation. Accordingly, species' metabolic responses to declining oxygen levels lay somewhere between the two ends of this continuum (Mueller and Seymour, 2011). Furthermore, at a certain species-specific oxygen pressure, animals are unable to maintain their normoxic metabolic rate and have to goose anaerobic metabolism. This point is called 'critical oxygen partial pressure' (P_{crit}) and can be determined by analyzing the response of the metabolic rate (respiration) to declining oxygen concentrations. Oxyconformers do not regulate their oxygen demand as, physiologically, these species do not need to enhance the transport of oxygen to the metabolizing tissues when oxygen is decreasing. Thus, the capability of an animal to either regulate its oxygen uptake in combination with the P_{crit} value or reduce its respiration rate when ambient oxygen levels decrease provides meaningful information about their ability to survive hypoxic events and represent an important ecological tipping point to understand the resilience of populations to declining levels of oxygen (Mueller and Seymour, 2011). A third strategy called metabolic suppression entails the suppression of total energy consumption by shutting down intensive energy demanding processes (Seibel, 2011; Seibel et al., 2016). This strategy has been observed in euphausiid species inhabiting regions where oxygen decline was faster than euphausiid oxygen demands (Seibel et al., 2016).

In this paper, we aim to characterize the hypoxia tolerance of 10 dominant euphausiid species from the Atlantic and the Pacific Ocean, including three prominent EBUEs (Benguela, California, and the Humboldt Current system), and both Polar regions at *in situ* temperatures by analyzing the regulation index (RI) to explain the DVM behavior in their habitat.

MATERIALS AND METHODS

Ten euphausiid species were collected between 2010 and 2013 during several small- or large-scale expeditions to the Benguela, California, and Humboldt Current systems (BCS, CCS, and HCS), the Eastern Tropical Pacific (ETP), the Arctic and the Antarctic (details compiled in **Table 1**). Polar (Antarctic and Arctic: between −0.5°C and 5.5°C), temperate (NCCS and HCS: between 6.5°C and 15.1°C), sub-tropical (BCS: between 8.0°C and 21°C), and tropical (ETP: between 14.6°C and 30.2°C) temperature gradients as well as different hypoxic conditions (severe and shallow: ETP and HCS; severe and deep: BCS; moderate: NCCS; and non-existent: Antarctica and Arctic) are thus covered by the habitat of the species studied (**Figure 1**).

All samplings were executed during night time, when euphausiids are more abundant at the surface, to avoid overstressing the experimental animals by reducing catch time. Live adult euphausiids, in healthy condition (showing a lot of movement and with no visible damage), were manually sorted into bins filled with filtered seawater at *in situ* temperature and acclimated for at least 6 (CCS, HCS, ETP, and Antarctica) or 12 h (BCS and Arctic) prior to starting respirometry procedures to make sure that all animals are in a post-absorptive state.

Respirometry

The measurements were conducted in the dark to mimic the conditions of the time of the day when euphausiids should be in deeper water and hypoxic conditions when hypoxia applied to the area. The same closed configuration system, chamber volume (20 mL; except for Antarctica where chamber volume was 250 mL to account for the larger size of *Euphausia superba*) and measurement method were used in all areas. The oxygen level within the chamber decreased as the effect of respiration. Measurements were carried out at *in situ* temperature for the 10 species, and at four different temperatures for *Thysanoessa inermis* (Arctic; 2, 4, 8, and 10°C) and *Euphausia hanseni* (BCS; 5, 10, 15, and 20°C) to assess how temperature modulates intraspecific hypoxia tolerance (**Table 1**). Both species were acclimated at a rate of 1°C h^{-1} to colder and warmer temperatures for at least 12 h after completion of the 12 h post-capture acclimation. The thermal ramp steepness and amplitude took into consideration the vertical migration temperature gradient that *E. hanseni* experience during DVM (Werner and Buchholz, 2013) and the Arrhenius breakpoint temperature (12°C) of *T. inermis* (Huenerlage and Buchholz, 2015; Huenerlage et al., 2016).

OXY-4 or -10 channel PreSens Oxygen Measurement system (Regensburg, Germany) was used with dipping probes DP-PSt3 or planar oxygen-sensitive foils PSt3 integrated in the chambers.

TABLE 1 | From North to South: Sampling areas (latitude/longitude), species names, number of individuals analyzed (*n*), specimens mean weight (±standard deviation; W, wet weight; D, dry weight) and respiration measurement information in the Benguela, Northern California, and Humboldt Current systems (BCS, CCS, and HCS), in the Eastern Tropical Pacific (ETP), in the Arctic (Kongsfjord, Spitsbergen) and in Antarctica (South Georgia).

Area	Date	Latitude/longitude	Cruise/boat	Sampling gear	Species	Measurement			
						n	Weight (mg)	Temperature (°C)	Mean duration (h)
Arctic	Aug 2012	78.95° N/12.33°E	MS Teisten	1-m^2 Tucker trawl,	*Thysanoessa inermis*	6	90 ± 33(W)	2	27.8
	Apr 2013			1,000 μm mesh size, soft		4	84 ± 2 (W)	6	9.2
	Aug 2013			cod-end, speed of two knots		8	66 ± 14 (W)	8	6.0
						4	124 ± 25 (W)	10	4.3
NCCS	Sep 2011	44.7°N/124.7°W	RV Elahka	Bongo, 0.6 m diameter,	*Euphausia pacifica*	17	9 ± 6 (D)	10	3.8
	Apr 2012			333 μm black mesh, non-filtering cod-end, obliquely to ∼25 m	*Thysanoessa spinifera*	6	37 ± 21 (D)	10	3.5
ETP	Feb 2012	19.2°N/104.7°W	Fiberglass boat (6 m)	1 m diameter, 3 m long, 300 μm mesh, non-filtering cod-end, obliquely	*Euphausia distinguenda*	10	3.0 ± 0.5 (D)	20	3.6
				∼30 m,speed of 4 km h^{-1}, 10 min	*Euphausia lamelligera*	3	0.7 ± 0.3 (D)	20	3.2
BCS	Sep 2010	23°S/13°W	RSS Discovery	1-m^2 Multiple Opening and Closing	*Euphausia hanseni*	4	122 ± 21 (W)	5	3.6
	Feb 2011		RV Maria	Net and Environmental Sensor		22	96 ± 25 (W)	10	4.3
			S. Merian	System, 2,000 μm mesh size, soft		4	115 ± 11 (W)	15	3.3
	Sep 2013		RV Meteor	cloth cod-end, speed of two knots	*Nematoscelis megalops*	11	53 ± 9 (W)	20	3.3
						2	110 ± 13 (W)	10	0.7
					Nyctiphanes capensis	13	31 ± 8 (W)	10	13.1
HCS	Aug 2011	36.5°S/73.1°W	RV Kay-Kay II	1 m diameter, 5 m long, 300 μm black mesh, non-filtering cod end	*Euphausia mucronata*	5	6 ± 4 (D)	8	11.8
Antarctica	Jan 2012	53–55°S/37–41°W	RRS James Clark Ross	Rectangular midwater trawl of 8 m^2 mouth area	*Euphausia superba*	21	296 ± 64 (D)	4	12.7

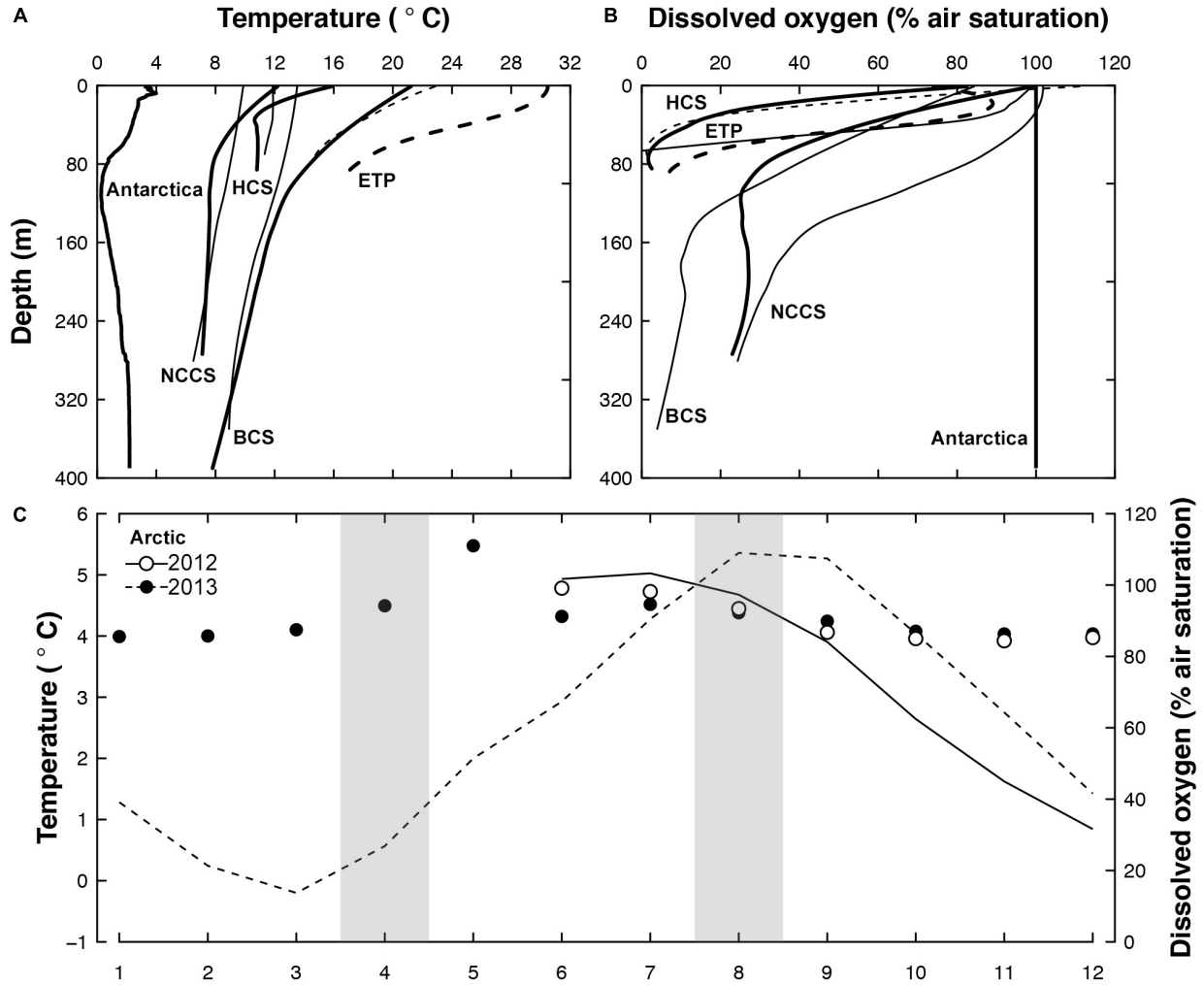

FIGURE 1 | Temperature and oxygen during sampling periods. Depth profiles of **(A)** mean water temperature and **(B)** dissolved oxygen in Antarctica, the Humboldt current system [HCS], the Eastern Tropical Pacific [ETP], the Benguela Current System [BCS], and the Northern California Current System [NCCS]. Bold lines represent summer conditions and dashed lines the ETP area. **(C)** Monthly mean temperature (line) and dissolved oxygen (dots) in the Arctic with sampling periods shaded in gray. Data were compiled from the AWIPEV underwater observatory located at 12 m water depth (Fischer et al., 2018a,b).

Probes and foils were calibrated at *in situ* temperature prior to measurements at 0% air saturation with sodium sulfite (Na_2SO_3; 1 g in 100 mL water) and at 100% air saturation with air-saturated water (10 min after air injection in stirred water for 20 min). The system was equipped with four (OXY-4) or ten (OXY-10) chambers including respectively one or two blanks (for seawater bacterial oxygen demand). All chambers were filled with filtered local seawater at 100% air saturation and the oxygen concentration in each chamber was measured every 15 or 30 s. The first 30 min of each measurement were discarded to allow acclimation to chamber. Movements of the pleopods and/or heartbeats of the animals were visually monitored to make sure that they were alive during the entire duration of the measurement. Wet or dry (48 h at 50°C) weight of the preserved animal was measured after completion of the respiration measurement (information provided in **Table 1**). All respiration rates were reported as mL O_2 h^{-1} g wet $weight^{-1}$. For some species, only the dry weight was available and it was converted to wet weight using the euphausiids conversion equation of Kiørboe (2013) to allow comparison among the 10 species. The programming environment for data analyses and graphics R (R Core Team[1]) was used to calculate the RI [see section "Regulation Index (RI)"] [script provided as **Supplementary Material** (see **Supplementary Data Sheet 1**)].

Regulation Index (RI)

Mueller and Seymour (2011) were the first to propose the use of the RI to assess regulation ability of aquatic organisms that do not present a clear critical oxygen partial pressure (P_{crit}) in their respiration pattern. The authors advised to fit a curve (straight line, quadratic or one-phase association) with the highest r^2 to the respiration rate data for each individual plotted against the whole

[1]www.r-project.org

oxygen concentration range measured within the respiration chamber (ideally from 100 to 0% air saturation). RI corresponded to the proportion of the area bounded by a linear regression that represented how respiration rates would decline if the animals showed complete oxyconformity (perfect oxyconformity; RI = 0) and a horizontal line at maximum oxygen consumption (perfect regulation; RI = 1). The perfect oxyconformity linear regression assumes zero respiration rate at 0% air saturation (**Figure 2A**).

The present work used 141 respiration data sets [available in **Supplementary Material** (see **Supplementary Data Sheet 1**)], in which the experimental oxygen concentration dropped to ≤50% of the respective experiments' start concentration. In order to reduce user interpretation in calculating RI by mean of the best fitted curve, no parametric model was fitted to the original data sets. The area under curve was computed using R package "MESS" (Ekstrøm, 2018) with the natural spline interpolation (loess) for dissolved oxygen concentration as *x*-values and respiration rates as *y*-values. The same procedure was conducted with the linear regression that represents perfect oxyconformity and perfect oxyregulation. When the natural spline interpolation of the data was below the linear regression of perfect oxyconformity, RI became negative and was calculated from the area bounded by the horizontal line at $y = 0$ and the linear regression that represented perfect oxyconformity (**Figure 2B**). A negative RI value can thus be interpreted as hypoxia-sensitivity (Alexander and McMahon, 2004), but could be an indication of metabolic suppression, as respiration rates are significantly reduced. Respiration strategies using median and quartile values were defined as: low degree of oxyregulation ($0.25 <$ RI median < 0.5); high degree of oxyregulation ($0.5 <$ RI median < 1; Q1 > 0.25 or Q3 > 0.75); oxyconformity (RI median≈ 0; Q1 < 0 and Q3 > 0) and metabolic suppression (RI median, Q1 and Q3 < 0).

Statistical Analysis

All statistics and figures were done with R (R Core Team, 2020). For interspecific (*in situ* temperature) and intraspecific (among temperature for *E. hanseni* and *T. inermis*) hypoxia tolerance comparison, the non-parametric Kruskal–Wallis test was conducted (normality and variance homogeneity were not met). Significant level of all comparisons was fixed at 95% ($p < 0.05$). For *post hoc* comparison a multiple comparison test from the package "pgirmess" (Giraudoux, 2018) was applied.

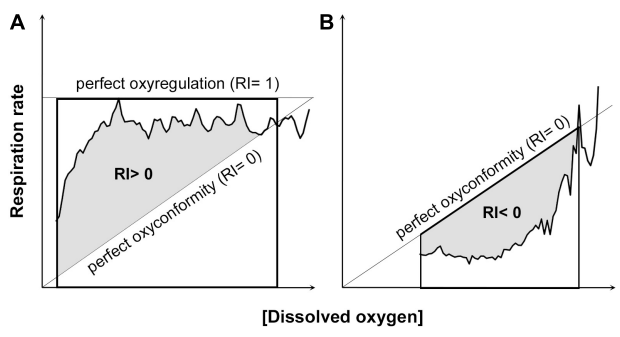

FIGURE 2 | Examples of regulation index (RI) calculations. As shown by Mueller and Seymour (2011), the area under the curve and above the linear regression of perfect oxyconformity was used to calculate a positive RI **(A)**. In contrast, a negative RI was calculated as the area bounded by the area above the curve and the linear regression of perfect oxyconformity **(B)**.

RESULTS

The overall view of the euphausiids' respiration rates over decreasing dissolved oxygen concentration at *in situ* temperature shows different magnitude and patterns (**Figure 3**). Comparing this magnitude by area, the highest respiration rates were observed in *Euphausia pacifica* (NCCS), *Euphausia lamelligera* (ETP), and *Nematoscelis megalops* (BCS). Different magnitude and patterns were also seen intraspecifically when *T. inermis* and *E. hanseni* were acclimated at lower or higher temperatures (**Figures 4**, **5**). The respiration rates of *T. inermis* increased at 8 and 10°C (**Figures 4C,D**) in comparison to 2 and 6°C (**Figures 4A,B**) during the whole oxygen range measured. For *E. hanseni*, respiration rates were similar at all temperatures in the high-oxygen levels between 80 and 100% air saturation (**Figure 5**).

The RI of *Euphausia superba* (Antarctica), *Thysanoessa inermis* (Arctic), *Euphausia hanseni* (BCS), and *Nyctiphanes capensis* (BCS) were significantly higher than the RI of the tropical and temperate species *Euphausia distinguenda* (ETP) and *Euphausia mucronata* (HCS), respectively (**Figure 6A**, $\chi^2 = 56.05$, $p < 0.000$, **Table 2**). Median RI values ≥0.5 of the polar (*E. superba*, *T. inermis*), temperate (*E. pacifica*), and sub-tropical (*E. hanseni*, *N. megalops*, and *N. capensis*) species indicated a high degree of oxyregulation, whereas the neritic temperate (*T. spinifera*) and tropical (*E. lamelligera*) species showed a low regulation ability as RI values fluctuated between −0.25 and 0.25 (**Figure 6A** and **Table 2**). Quartiles values below and above 0 of *T. spinifer*a and *E. lamelligera* indicate almost perfect oxyconformity of these species. The oceanic tropical species *E. distinguenda* and the Humboldt endemic species *E. mucronata* were qualified as metabolic suppressors with RI median and quartile values well below 0 (**Figure 6A** and **Table 2**).

Regulation index did not change significantly with temperature for *T. inermis* (**Figure 6B**), but it did in *E. hanseni* from high oxyregulation to metabolic suppression, when acclimation temperature was decreased to 5°C (compared to 20°C; $\chi^2 = 14.53$, $p = 0.002$; **Figure 6C**).

DISCUSSION

Euphausiids and other zooplankton taxa perform DVM to feed on the phytoplankton-rich upper water layers during night time and to reduce mortality from visual predation during the day. These benefits are counteracted by higher energy demands due to increased swimming speeds and higher water temperatures in upper water layers and reduced

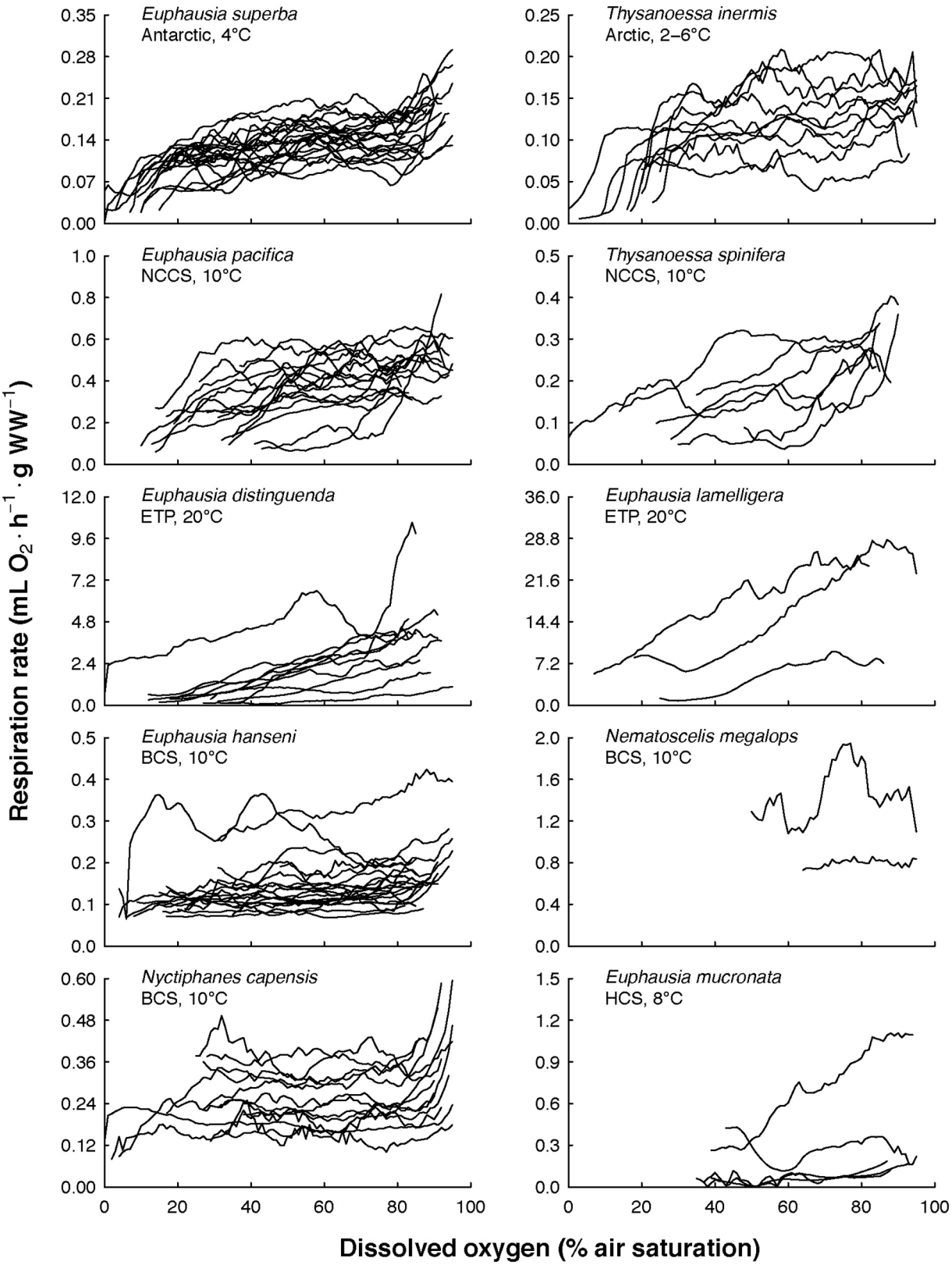

FIGURE 3 | Euphausiids' respiration rates over decreasing dissolved oxygen concentration at *in situ* temperature. The 10 euphausiids species were from both Polar regions, three major Eastern Boundary Upwelling Systems (NCCS, Northern California Current System; BCS, Benguela Current System; HCS, Humboldt Current System), and one tropical region (ETP, Eastern Tropical Pacific).

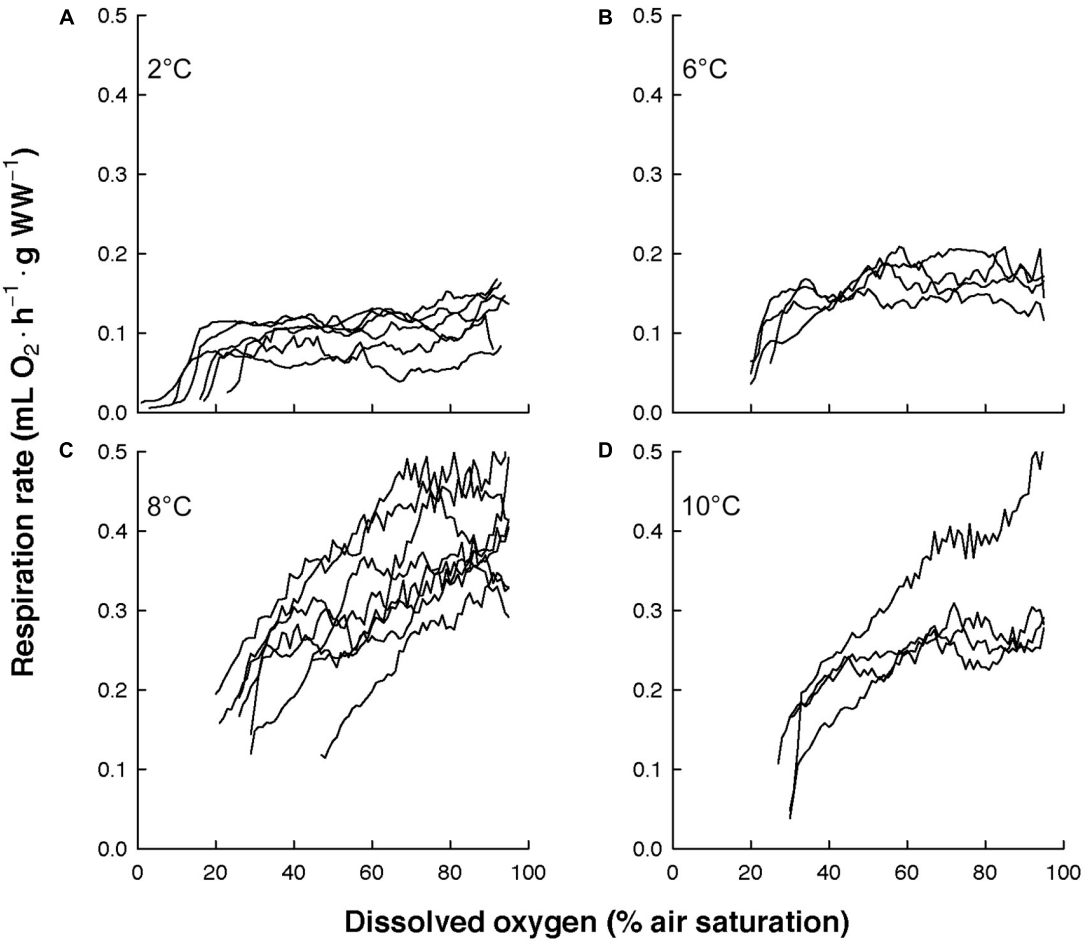

FIGURE 4 | Respiration rates of *Thysanoessa inermis* over decreasing dissolved oxygen concentration at four temperatures. **(A)** at 2°C (n = 6), **(B)** at 6°C (n = 4), **(C)** at 8°C (n = 8), and **(D)** at 10°C (n = 4).

growth and reproduction rates in deeper, cold water layers. Thus, animals performing DVM have to compensate with increased energy expenditures. Furthermore, they must have evolved physiological and behavioral adaptations to the strong gradients of oxygen and temperature in the water column. As some species suppress their metabolism (Seibel et al., 2016), determination of metabolic rates of diel vertical migrators is crucial to assess the role and quantify the contribution of these animals to the downward transport of carbon and thus carbon fluxes in the oceans. The environmental conditions prevailing in the different ecosystems in terms of oxygen availability and vertical temperature profiles seem to have caused specific physiological adaptations in euphausiids – mostly irrespective of the actual oxygen and temperature level and the time spent in the OMZs. Species which come across the shallowest severe hypoxia levels during their DVM show metabolic suppression [in the Humboldt Current System (HCS) and ETP]. In contrast, the three species from the Benguela Current System (BCS), characterized by a deeper OMZ, maintain constant oxygen uptakes irrespective of the ambient oxygen levels. These differences may indicate that a steep decline in oxygen levels constitutes a physiological threshold at which euphausiids must significantly shut down their metabolic functions (Seibel et al., 2016).

Shallow OMZs

The hypoxia tolerance of the euphausiid species adapted to the OMZs of the HCS and the ETP was assessed using the RI. In the literature, typical low P_{crit} between 0.6 and 1.7 kPa at 13°C and 23°C (corresponding to 3% and 8% air saturation) were obtained by Teal and Carey (1967) and Kiko et al. (2016), who were working on *Euphausia mucronata* from the HCS. This euphausiid species performs extensive DVM down to 250 m into the OMZ in all seasons (Escribano et al., 2000; Antezana, 2002b). However, highest abundances of this species occur in areas where the upper boundary of the OMZ is deeper (Escribano et al., 2000). During the warm season at 12°C and 13°C, *E. mucronata* maintains the same rate regardless of whether exposed to surface pO_2 (70% air saturation or 17 kPa), or to pO_2 typical for OMZ layers (20% air saturation or 4 kPa; Antezana, 2002a; Donoso and Escribano, 2014). The temperature used by the authors cited above represents the

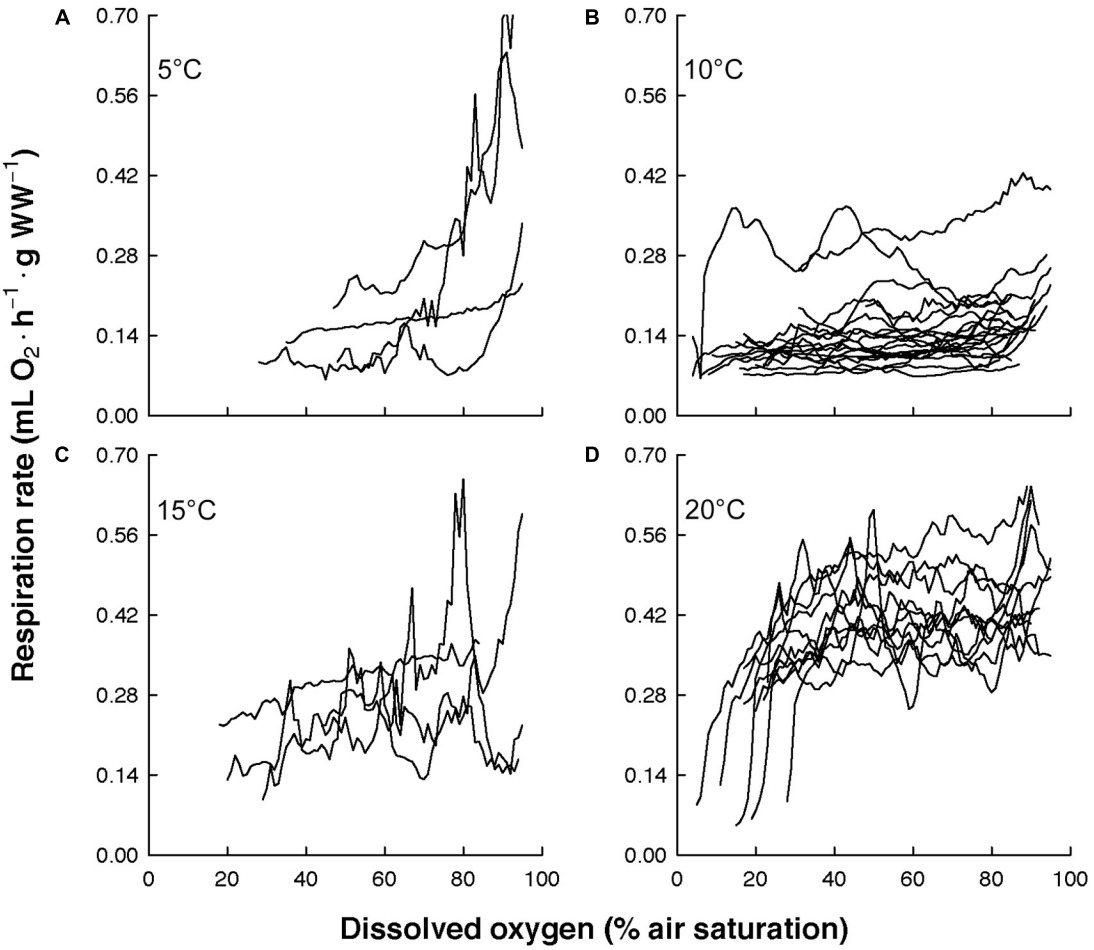

FIGURE 5 | Respiration rates of *Euphausia hanseni* over decreasing dissolved oxygen concentration at four temperatures. **(A)** at 5°C (n = 4), **(B)** at 10°C (n = 22), **(C)** at 15°C (n = 4), and **(D)** at 20°C (n = 11).

warmer range in subsurface water of the area (50–200 m), while the present study was simulating the coldest temperature that can be encountered in the same water depth or at surface during "normal" or cold (La Niña) years between 40°S and 17°S off Chile (Strub et al., 1998). As seen from the changes in RI following the decreasing temperature in *Euphausia hanseni* from the BCS, the OMZ-adapted species of the genus *Euphausia* may regulate their metabolic rates when exposed to warmer surface temperature and tend to conform or suppress their metabolism when exposed to the colder thermal limit of their deeper habitat. This may explain why no oxyregulation pattern at all was observed at 8°C in *E. mucronata*, despite the long duration of the measurement.

The tendency to conform or suppress the metabolism at colder temperature may be also true for *Euphausia distinguenda* from the ETP (corresponding to sub-surface temperature) as shown here with our measurement at 20°C. From field samples collected at different depths above and into the OMZ of the ETP off Mexico, Herrera et al. (2019) observed the highest specific Electron Transfer System (ETS) activity between 3.20 and 3.93 mL O_2 L^{-1} (48 to 58% air saturation) at 25°C, meaning that the species was still relying on aerobic processes half-way within the oxycline. This ETP species is also reported in the OMZ of the HCS (Antezana, 2009). Both *E. distinguenda* and *E. mucronata* possess larger gills relative to their body size (Antezana, 2002a), increasing contact surface for O_2 diffusion from the hypoxic environment. Antezana (2009) also observed that both were among the last OMZ species to begin their ascent to the surface at dusk in the HCS, thus extending the deep hypoxic residence time to a maximum. Habitat segregation was suggested to explain this behavior, which consists in avoiding spatial and temporal co-occurrence with other species within the same area. This finding was based on body and gills size analysis, feeding appendages, and HCS food resources. *Euphausia lamelligera*, the other ETP species also endemic to the OMZ, dominates the neritic zone while *E. distinguenda* distributes more in oceanic waters (Brinton, 1962, 1979; Färber-Lorda et al., 1994, 2004, 2010). Because of its neritic preference, *E. lamelligera* does not migrate as much as *E. distinguenda*, explaining probably why this species is almost a perfect oxyconformer rather than a metabolic

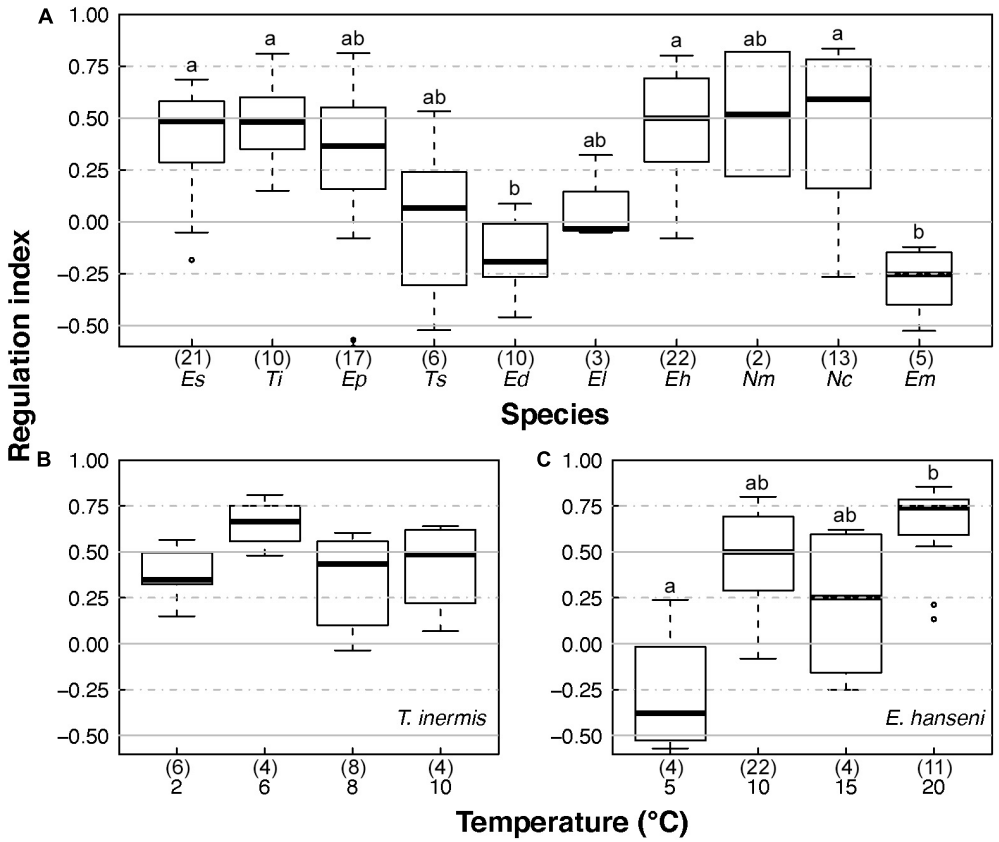

FIGURE 6 | Euphausiids' regulation indices at *in situ* temperature and after temperature acclimation. **(A)** Regulation indices of the 10 euphausiid species investigated at *in situ* temperature, **(B)** regulation indices of *T. inermis* acclimated at 2, 6, 8, and 10°C, and **(C)** regulation indices of *E. hanseni* acclimated at 5, 10, 15, and 20°C. *Es*, *E. superba*; *Ti*, *T. inermis*; *Ep*, *E. pacifica*; *Ts*, *T. spinifera*; *Ed*, *E. distinguenda*; *El*, *E. lamelligera*; *Eh*, *E. hanseni*; *Nm*, *N. megalops*; *Nc*, *N. capensis*; *Em*, *E. mucronata*. Numbers in parentheses give the numbers of samples analyzed. Horizontal bars in the box plots indicate the median. The upper and lower edges of the rectangles show the first and third quartiles, respectively. Vertical error bars extend to the lowest and highest values in a 1.5-fold inter-quartile range (R Core Team, 2020). Lower case letters indicate significant differences.

suppressor. Both species are thus highly hypoxia tolerant, reflected mainly by their low RI. As high temperature pushes physiological limits, a small sub-mesoscale oxygen variability in the ETP of ≤1% could affect their vertical and horizontal distribution (Wishner et al., 2018). Accordingly, even small changes in oxygen availability may exert strong pressure on these animals, leading to unexpected changes in ecosystem structure and functioning in the near future. Species of the ETP are adapted to low oxygen and high temperature, but as they live at the edge of their maximum thermal limit, further warming could have negative impact on the fitness of both species as their higher brood size depends on the coastal upwelling dynamics between January and June (Ambriz-Arreola et al., 2015, 2018). A negative RI was initially not proposed by Mueller and Seymour (2011) when developing the RI as a new method to assess hypoxia tolerance of aquatic ectotherms. However, as shown for weak oxyregulating (or perfect oxyconformers) and metabolic suppressing species presented in this study, a negative RI is relevant and thus presents a further development for the use of this index. The corroboration of the presence of metabolism suppression associated with a negative RI remains to be shown looking at physiological metabolic markers (e.g., enzymatic activity, ATP production, anaerobic end-products). This pattern was previously described as hypoxia-sensitivity by Alexander and McMahon (2004).

Deep OMZ

In the BCS, *E. hanseni* and *Nematoscelis megalops* dominate the shelf break surroundings, i.e., partly sharing one habitat in this upwelling region (Barange and Stuart, 1991; Barange et al., 1991). The species *E. hanseni* performs extensive DVM from 0 to 200 and even 1,000 m water depth (Barange, 1990; Barange and Stuart, 1991; Barange and Pillar, 1992; Werner and Buchholz, 2013), while *N. megalops* is characterized as a weak migrator (Werner and Buchholz, 2013). In contrast to *E. hanseni*, *N. megalops* has a broader distribution and can be found at both sides of the equator: in the mid-latitude zones of the subtropical-temperate North Atlantic (10–60°N), in the warm-temperate belts of the South Atlantic, the Indian Ocean and the South Pacific (35–50°S), in the Mediterranean Sea (e.g., Gopalakrishnan, 1974), in subarctic regions (Zhukova et al., 2009), even up to 79°N in the high

TABLE 2 | Regulation index (RI) for 10 euphausiid species investigated.

Species	Temperature (°C)	RI			Strategy
		Median	Quartile 1	Quartile 3	
Euphausia superba	4	0.48	0.29	0.58	High oxyregulation
Thysanoessa inermis	2	0.34	0.32	0.46	Low oxyregulation
	2–6	0.48	0.35	0.60	High oxyregulation
	6	0.66	0.60	0.72	High oxyregulation
	8	0.43	0.17	0.54	Low oxyregulation
	10	0.49	0.30	0.60	High oxyregulation
Euphausia pacifica	10	0.36	0.16	0.55	Low oxyregulation
Thysanoessa spinifera	10	0.07	−0.31	0.24	Conformity
Euphausia distinguenda	20	−0.19	−0.26	−0.03	Metabolic suppression
Euphausia lamelligera	20	−0.03	−0.04	0.14	Conformity
Euphausia hanseni	5	−0.38	−0.50	−0.15	Metabolic suppression
	10	0.50	0.29	0.69	High oxyregulation
	15	0.25	−0.11	0.58	Conformity/regulation
	20	0.74	0.59	0.79	High oxyregulation
Nematoscelis megalops	10	0.52	0.37	0.67	High oxyregulation
Nyctiphanes capensis	10	0.59	0.16	0.78	High oxyregulation
Euphausia mucronata	8	−0.26	−0.40	−0.15	Metabolic suppression

RI was calculated from 141 data sets and used to differentiate between respiration strategies using median and quartile values: low degree of oxyregulation (0.25 < RI median < 0.5); high degree of oxyregulation (0.5 < RI median < 1; Q1 > 0.25 or Q3 > 0.75); oxyconformity (RI median≈0; Q1 < 0 and Q3 > 0), and metabolic suppression (RI median, Q1 and Q3 < 0).

Arctic Kongsfjord (Buchholz et al., 2009; Huenerlage and Buchholz, 2015). Morphologically and ecologically, *N. megalops* is very similar to *Nematoscelis difficilis* from the ETP and California Current System (Karedin, 1971; Gopalakrishnan, 1974, 1975). Those species are observed within the OMZ, but in its upper boundary (Tremblay et al., 2010; Werner and Buchholz, 2013), probably taking advantage of the accumulation of organisms to actively feed. The third species *Nyctiphanes capensis* shows extraordinarily high abundances over the Namibian shelf in water <200 m depth (Barange and Stuart, 1991; Barange and Pillar, 1992).

E. hanseni and *N. capensis* have one of the highest RI values of all species analyzed meaning that they cover their energy requirements at low oxygen levels in the coldest temperature experienced in their habitat. RI values were enhanced in *E. hanseni* acclimated at 20°C compared to 10°C, which is similar to results of Teal and Carey (1967) and Kiko et al. (2016) at sub-surface temperature conditions with the species *E. mucronata* from the HCS. However, the respiration rate of *N. megalops* investigated here was 10-fold higher than of *E. hanseni* and *N. capensis*, which is not consistent with what was reported before by Werner et al. (2012). The number of individuals here reported is small, and the specimens were probably stressed as the duration of the measurement was short (less than 1 h) compared to other nine species analyzed. Despite this fast decrease in oxygen, it is possible to say that *N. megalops* was regulating its respiration rate. This ability may explain its persistence in the OMZ 24 h a day. Consequently, *N. megalops* must have evolved efficient adaptations to deal with low oxygen levels, such as, e.g., a high respiratory surface (gills) and/or a general low oxygen demand due to its smaller vertical migration movement. Thus, the ability of an animal to either maintain a constant oxygen uptake irrespective of the ambient oxygen levels or decrease its oxygen consumption rates when ambient oxygen levels decrease seems not to be influenced by its DVM behavior in the first place.

Seasonal OMZ

Off Oregon (United States), in the Northern California Current System (NCCS), two euphausiid species dominate the macrozooplankton community: the oceanic *Euphausia pacifica* (Brinton, 1962) with DVM between the surface and depths of at least 250 m (Brinton, 1967) and the neritic cold upwelling-associated *Thysanoessa spinifera* (Brinton, 1962; Smith and Adams, 1988; Lavaniegos and Ambriz-Arreola, 2012). Because of its neritic lifestyle, *T. spinifera* does not migrate as deep as *E. pacifica*, but, instead, remain within the upper 100 m during day and night and swarm in summer at surface for reproduction (Brinton, 1962; Smith and Adams, 1988). This species is also known for its narrow plasticity when facing changes in the physical oceanographic conditions (Brinton, 1979). Indeed, *T. spinifera* is strongly influenced by the North Pacific Gyre Oscillation (Di Lorenzo et al., 2008; Sydeman et al., 2013). This oscillation is connected with the winds and upwelling responses (Chenillat et al., 2012) and corroborates the upwelling preference of this species. Important changes in both species' distribution occurred during the El Niño event of 1992–1993, after which biomass of *T. spinifera* fell by more than 70% off Oregon and British-Columbia (Tanasichuk, 1999). In the southern part of the CCS (at approximately 30°N; Off Baja California), *E. pacifica* took some time to recover after the El Niño event of 1997–1998, but was abundant again during summers of

2000, 2002, and 2005. These high abundances were linked to La Niña in 2000, a sub-Arctic water intrusion in 2002 and to high upwelling conditions in 2005 (Lavaniegos and Ambriz-Arreola, 2012). It is clear that El Niño brings low upwelling conditions (low food availability) and warmer deoxygenated water, which are not optimal for the temperate species of the NCCS.

A different pattern within the respiratory response to declining pO_2 was observed between *T. spinifera* and *E. pacifica*. The neritic lifestyle, short vertical migration distance, and strong association with upwelling areas (high nutrients, cold temperature, and lower oxygen concentration) match the comparatively low metabolic rate of *T. spinifera* compared to oceanic *E. pacifica*. The strong association of *T. spinifera* with upwelling conditions likely signifies an oxyconformity strategy to tolerate the typical low oxygen concentration of upwelled water. So far, no acoustic or direct observations of hypoxia and warming effects on *T. spinifera* have been reported. However, massive stranding events in several bays on the US West Coast over an area of approximately 400 km between Oregon and California were observed in summer of 2013 and related to the strongly hypoxic conditions prevailing regionally (Leising et al., 2014). This hypoxic zone was extending into the upper 50–100 m of the water column. A similar situation was observed in the Gulf of California (Mexico) with the subtropical species *N. difficilis* (López-Cortés et al., 2006), the counterpart in the Pacific of *N. megalops*. The authors proposed that high unusual upwelling conditions promoted a phytoplankton bloom, which indirectly depleted the oxygen concentration with the sinking of organic matter. This would have forced the mesopelagic *N. difficilis* to migrate upward toward more oxygenated waters and then to be washed out by the surface currents. *N. difficilis* was shown to be relatively tolerant to hypoxic conditions, but less than the tropical species *Euphausia eximia* (Tremblay et al., 2010; Seibel et al., 2016) and *Nemastocelis gracilis* (Seibel et al., 2016).

High tolerance to hypoxia was assumed in the past for *E. pacifica* because of its low critical oxygen partial pressure (P_{crit} = 18 mm Hg, 2 kPa or 11% air saturation at 10°C), lower than what the species experiences *in situ* at 350 m depth in its habitat (off South California; Childress, 1975). In fjords and bays their downward migration is often reduced (Bollens et al., 1992), sometimes limited by seasonal hypoxic or anoxic conditions in bottom water layers (Kunze et al., 2006). In these environments, P_{crit} values of *E. pacifica* were higher (P_{crit} = 4 kPa or 20% air saturation at 10°C), showing less hypoxia tolerance (Ikeda, 1977). The RI of *E. pacifica* indicated that this species is not an outstanding oxyregulator as BCS and polar species. The high standard deviation of RI may speak for a lack of a consistent strategy when dissolved oxygen concentration decrease at *in situ* temperature.

Alternation between El Niño and La Niña events maintains the abundance of krill across time in the NCCS, but it is clear that if strong El Niño event like the one of 1997–1998 last longer or occurs more often, both *T. spinifera* and *E. pacifica* stocks would probably disappear from the NCCS and continue their life cycle at higher latitudes in the Gulf of Alaska, where they are not so affected by the El Niño event. This would have strong consequences for the higher trophic levels of the NCCS.

Cold Regions and OMZ-Free

The polar species *Euphausia superba* and *Thysanoessa inermis* exhibit also one of the highest RI among the 10 species assessed. The Antarctic krill *E. superba* is a central constituent of Antarctic food webs and forms large biomasses in the Southern Ocean (Atkinson et al., 2004; Murphy et al., 2007). Cumulative impacts of sea ice decline and ocean warming have negatively modified the abundance, distribution and life cycle of this species (Flores et al., 2012). The species *T. inermis* is restricted to the North Atlantic, North Pacific and the shelf region around Spitsbergen, continuously advected to the Arctic by the ocean currents from the Barents Sea where they have their major spawning ground. Both polar species are known as pronounced vertical migrators with some flexibility depending on food availability and predation risk (Kaartvedt et al., 1996; Cresswell et al., 2009).

As oxygen levels in Polar regions are relatively high, it appears that there is no compelling need to evolve adaptations to low oxygen levels. However, both species are well known for their dense swarming behavior and may experience reduced oxygen levels in these dense aggregations (Brierley and Cox, 2010). According to Brierley and Cox (2010), the oxygen concentration in a median packed *E. superba* swarm (40 m diameter, 111 ind. m^{-3}) can fall from 6.8 to 5.8 mL O_2 L^{-1} (76 to 65% air saturation or 16 to 14 kPa in South Georgia) after approximately 3 min spent in the middle. Swarm density can reach 25,000 ind m^{-3} (Hamner and Hamner, 2000) or spread over hundreds km^{-2} (Nowacek et al., 2011), so it can be easily envisaged that the reduction in oxygen availability in the middle of these biological features may be dramatically higher. This is probably the reason why *E. superba* and *T. inermis* deploy unexpected high hypoxia tolerance at *in situ* temperatures. As temperature generates higher energy demands in *T. inermis* (>three-fold), temperature rise in the North-Arctic of 3°C above the current summer conditions could lead to increased competition with other warmer adapted species, like *Meganyctiphanes norvegica* and *N. megalops* (Huenerlage and Buchholz, 2015). So far, this Arcto-boreal species seems to benefit from the current higher water temperatures in the Arctic as it seems to reproduce successfully in the Kongsfjorden (Buchholz et al., 2012).

RI or Others?

Even though temperature increases the metabolic activity, hence the energy demands of an animal, the present study suggests that the ability to cope with low oxygen levels is not always worse at higher temperatures for hypoxia-adapted species. A possible explanation could be that despite higher energy expenditure other processes such as diffusion rates are also enhanced, providing sufficient oxygen for an animal. As a consequence, we suggest that it is of crucial importance to measure respiration rates at *in situ* temperatures when comparing the hypoxia tolerances of various species within and between ecosystems.

Furthermore, the RI value, as a proxy for the capability of an animal to withstand low oxygen levels, seems to be indicative for the oxygen tolerance for its own. Low RI values were possible to determine for species such as *E. mucronata*, *E. distinguenda*, and *E. lamelligera* as they were showing oxyconformity or metabolic

suppression patterns. In contrast, *E. hanseni* and *N. capensis* occurring in the BCS show high RI values. However, all species are known to withstand comparably low oxygen levels. This highlights the need to analyze the RI, additionally to P_{crit}, to get a wider understanding of the species-specific adaptation strategies. Standardization to calculate RI is important as its determination depend on the model used (Cobbs and Alexander, 2018). In the present work, in order to reduce user interpretation in calculating RI by mean of the best fitted curve, we used the area under curve of the original data sets.

The analysis of the ETS activity and the contribution of the alternative oxidase (AOX) pathway are parameters that could be implemented to understand other metabolic adaptations related to vertical oxygen and temperature gradients. High specific ETS activities were observed in zooplankton collected in the Equatorial-Subtropical Atlantic mesopelagic zone (Hernández-León et al., 2019), also coinciding with a previous observation in the Eastern Equatorial Pacific (Herrera et al., 2019). The authors discussed this observation as an adaptation of migrant zooplankton to endure the adverse conditions of low temperature and low oxygen in deep waters. The AOX pathway is also a promising avenue to explore in response to temperature and oxygen vertical gradients as it has been identified and expressed in the copepod *Tigriopus californicus* in response to cold and heat stress compared to normal rearing temperature (Tward et al., 2019). This pathway could be an important player to support partial electron transport in order to stabilize mitochondrial membrane potential during metabolic suppression of OMZ-adapted species when residing for some hours in hypoxic conditions, as seen in the gills of freshwater bivalves adapted to hypoxia (Yusseppone et al., 2018).

It is known that species or populations of species confined to one hemisphere or a particular part of the ocean (neritic vs. oceanic) become often specialists (Jones and Cheung, 2017). They are in most cases neither widely distributed nor physiologically versatile, and can be predicted to especially suffer from the effects of ocean warming and OMZs' expansion. This may be also true for euphausiid species, but this study clearly illustrates that most euphausiids, using different strategies, cope with a range of different oxygen and temperature levels – showing high physiological plasticity – and hence, explaining why this successful taxon is predominate in all the world's oceans. However, species from the NCCS, ETP and the Arctic may be more vulnerable to future environmental conditions with increased water temperatures and decreased oxygen levels.

DATA AVAILABILITY STATEMENT

All datasets generated for this study are included in the article/**Supplementary Material**.

AUTHOR CONTRIBUTIONS

All authors participated in the concept of the study. NT conducted the experiments, analyzed the results, draw the figures, wrote, and revised the manuscript. KH conducted the experiments and contributed to data analysis, writing and revision of the manuscript. TW conducted the experiments, analyzed the results, and contributed to writing and revision of the manuscript.

FUNDING

This study was funded by the GENUS project, Bundesministerium für Bildung und Forschung (BMBF, 03F0497F, Germany) and supported by the Alfred-Wegner-Institute for Polar and Marine Research (PACES, WP2T2) as well as the French-German AWIPEV project KOP 124, RIS ID 3451. We acknowledge support by the Open Access Publication Funds of Alfred-Wegener-Institut Helmholtz-Zentrum für Polar- und Meeresforschung.

ACKNOWLEDGMENTS

We thank the Captains and crew of the RV Meteor, the RV Maria S. Merian, RV Kay-Kay II, RV Elahka, RRS James Clark Ross (JR260, supported by the Ecosystems programme at the British Antarctic Survey, funded by the Natural Environment Research Council), and the RSS Discovery for excellent support on-board. We are further grateful for the professional support by the AWIPEV station leaders, (logistic) engineers, and the captains of the Kings Bay AS workboat MS Teisten, Ny-Alesund, Spitsbergen. We thank the scientists Carmen Franco-Gordo, Israel Ambriz-Arreola, and Eva Kozak from the Centro de Ecología Costera de la Universidad de Guadalajara (San Patricio de Melaque, Mexico), Rubén Escribano, Pamela Hidalgo, Ramiro Riquelme-Bugueño from the Pelagic and Mesozooplankton Laboratory of the Centro de Investigación Oceanográfica del Pacífico Sur-Oriental de la Universidad de Concepción (Concepción, Chile), C. Tracy Shaw, William T. Peterson (deceased 08/2017), Jay Peterson from the Hatfield Marine Science Center of Oregon State University (Newport, United States) and Sophie Fielding and Geraint A. Tarling from the British Antarctic Survey (Cambridge, United Kingdom) for the record of environmental information, and their support in collecting zooplankton samples. We thank the reviewers for their critical comments that improved the quality of the article. This work was presented as "Krill worldwide: A comparison of hypoxia tolerances of euphausiid species from Atlantic, Pacific and Polar regions" in the Third International Symposium on Effects of Climate Change on the World's Oceans held in Santos City (Brazil) on March 23–27th, 2015 (Werner et al., 2015). Finally, we are deeply grateful to our Ph.D. supervisors, Doris Abele and Friedrich Buchholz, for providing us the opportunity to work in these projects. The idea was developed and partly presented in the doctoral thesis of NT and TW.

SUPPLEMENTARY MATERIAL

The Supplementary Material for this article can be found online at: https://www.frontiersin.org/articles/10.3389/fphys.2020.00248/full#supplementary-material

REFERENCES

Alexander, J. E. Jr., and McMahon, R. F. (2004). Respiratory response to temperature and hypoxia in the zebra mussel *Dreissena polymorpha*. *Comp. Biochem.Physiol. A* 137, 425–434. doi: 10.1016/j.cbpb.2003.11.003

Ambriz-Arreola, I., Gómez-Gutiérrez, J., Franco-Gordo, M. C., and Kozak, E. R. (2015). Reproductive biology, embryo and early larval morphology, and development rates of krill (*Euphausia lamelligera* and *Euphausia distinguenda*), endemic to the Eastern Tropical Pacific. *Sex. Early Dev. Aquat. Org.* 1, 143–161. doi: 10.3354/sedao00014

Ambriz-Arreola, I., Gómez-Gutiérrez, J., Franco-Gordo, M. C., Plascencia-Palomera, V., Gasca, R., Kozak, E. R., et al. (2018). Seasonal succession of tropical community structure, abundance, and biomass of five zooplankton taxa in the central Mexican Pacific. *Cont. Shelf Res.* 168, 54–67. doi: 10.1016/j.csr.2018.08.007

Antezana, T. (2002a). "Adaptive behaviour of *Euphausia mucronata* in relation to the oxygen minimum layer of the Humboldt Current," in *Oceanography of the eastern Pacific II*, ed. J. F. ärber-Lorda (Mexico: Editorial CICESE), 29–40.

Antezana, T. (2002b). "Vertical distribution and diel migration of *Euphausia mucronata* in the oxygen minimum layer of the Humboldt Current," in *Oceanography of the eastern Pacific II*, ed. J. F. ärber-Lorda (Mexico: Editorial CICESE), 29–40.

Antezana, T. (2009). Species-specific patterns of diel migration into the oxygen minimum zone by euphausiids in the humboldt current ecosystem. *Progr. Oceanogr.* 83, 228–236. doi: 10.1016/j.pocean.2009.07.039

Aoki, S. (2005). Interdecadal water mass changes in the Southern Ocean between 30°E and 160°E. *Geophys. Res. Lett.* 32:L07607.

Atkinson, A., Siegel, V., Pakhomov, E., and Rothery, P. (2004). Long-term decline in krill stock and increase in salps within the Southern Ocean. *Nature* 432, 100–103. doi: 10.1038/nature02996

Barange, M. (1990). Vertical migration and habitat partitioning of six euphausiid species in the northern Benguela upwelling system. *J. Plank. Res.* 12, 1223–1237. doi: 10.1093/plankt/12.6.1223

Barange, M., Gibbons, M. J., and Carola, M. (1991). Diet and feeding of *Euphausia hanseni* and *Nematoscelis megalops* (Euphausiacea) in the northern Benguela Current: ecological significance of vertical space partitioning. *Mar. Ecol. Progr. Ser.* 73, 173–181. doi: 10.3354/meps073173

Barange, M., and Pillar, S. C. (1992). Cross-Shelf Circulation, zonation and maintenance mechanisms of *Nyctiphanes capensis* and *Euphausia hanseni* (Euphausiacea) in the Northern Benguela Upwelling System. *Cont. Shelf Res.* 12, 1027–1042. doi: 10.1016/0278-4343(92)90014-b

Barange, M., and Stuart, V. (1991). Distribution patterns, abundance and population dynamics of the euphausiids *Nyctiphanes capensis* and *Euphausia hanseni* in the Northern Benguela Upwelling System. *Mar. Biol.* 109, 93–101. doi: 10.1007/bf01320235

Bianchi, D., Galbraith, E. D., Carozza, D. A., Mislan, K. A. S., and Stock, C. A. (2013). Intensification of open-ocean oxygen depletion by vertically migrating animals. *Nat. Geosci.* 6, 545–548. doi: 10.1038/ngeo1837

Bollens, S. M., Frost, B. W., and Lin, T. S. (1992). Recruitment, growth, and diel vertical migration of *Euphausia pacifica* in a temperate fjord. *Mar. Biol.* 114, 219–228. doi: 10.1007/bf00349522

Brierley, A. S., and Cox, M. J. (2010). Shapes of krill swarms and fish schools emerge as aggregation members avoid predators and access oxygen. *Curr. Biol.* 20, 1758–1762. doi: 10.1016/j.cub.2010.08.041

Brinton, E. (1962). The distribution of Pacific euphausiids. *Bull. Scripps Inst. Oceanogr.* 8, 51–269.

Brinton, E. (1967). Vertical migration and avoidance capability of euphausiids in the California Current. *Limnol. Oceanogr.* 12, 451–483. doi: 10.4319/lo.1967.12.3.0451

Brinton, E. (1979). Parameters relating to the distributions of planktonic organisms, especially euphausiids in the eastern tropical Pacific. *Progr. Oceanogr.* 8, 125–168.

Buchholz, F., Buchholz, C., and Weslawski, J. M. (2009). Ten years after: krill as indicator of changes in the macro-zooplankton communities of two Arctic fjords. *Polar Biol.* 33, 101–113. doi: 10.1007/s00300-009-0688-0

Buchholz, F., Werner, T., and Buchholz, C. (2012). First observation of krill spawning in the high Arctic Kongsfjorden, west Spitsbergen. *Polar Biol.* 35, 1273–1279. doi: 10.1007/s00300-012-1186-3

Chenillat, F., Rivière, P., Capet, X., Di Lorenzo, E., and Blanke, B. (2012). North Pacific Gyre Oscillation modulates seasonal timing and ecosystem functioning in the California Current upwelling system. *Geophys. Res. Lett.* 39:L01606.

Childress, J. (1975). The respiratory rates of midwater crustaceans as a function of depth of occurrence and relation to the oxygen minimum layer off southern California. *Comp. Biochem. Physiol. A* 50, 787–799. doi: 10.1016/0300-9629(75)90146-2

Claireaux, G., and Lagardère, J. P. (1999). Influence of temperature, oxygen and salinity on the metabolism of the European sea bass. *J. Sea Res.* 42, 157–168. doi: 10.1016/s1385-1101(99)00019-2

Cobbs, G. A., and Alexander, J. E. (2018). Assessment of oxygen consumption in response to progressive hypoxia. *PLoS ONE* 13:e208836–e208820.

Cresswell, K. A., Tarling, G. A., Thorpe, S. E., Burrows, M. T., Wiedenmann, J., et al. (2009). Diel vertical migration of Antarctic krill (*Euphausia superba*) is flexible during advection across the Scotia Sea. *J. Plank. Res.* 31, 1265–1281. doi: 10.1093/plankt/fbp062

Dehairs, F., Goeyens, L., Stroobants, N., Bernard, P., Goyet, C., Poisson, A., et al. (1990). On suspended barite and the oxygen minimum in the Southern Ocean. *Global Biogeochem. Cycles* 4, 85–102. doi: 10.1029/gb004i001p00085

Di Lorenzo, E., Schneider, N., Cobb, K. M., Franks, P. J. S., Chhak, K., Miller, A. J., et al. (2008). North pacific gyre oscillation links ocean climate and ecosystem change. *Geophys. Res. Lett.* 35:L08607.

Diaz, R. J., and Rosenberg, R. (2008). Spreading dead zones and consequences for marine ecosystems. *Science* 321, 926–929. doi: 10.1126/science.1156401

Donoso, K., and Escribano, R. (2014). Mass-specific respiration of mesozooplankton and its role in the maintenance of an oxygen-deficient ecological barrier (BEDOX) in the upwelling zone off Chile upon presence of a shallow oxygen minimum zone. *J. Mar. Syst.* 129, 166–177. doi: 10.1016/j.jmarsys.2013.05.011

Ekau, W., Auel, H., Hagen, W., Koppelmann, R., Wasmund, N., Bohata, K., et al. (2018). Pelagic key species and mechanisms driving energy flows in the northern Benguela upwelling ecosystem and their feedback into biogeochemical cycles. *J. Mar. Syst.* 188, 49–62. doi: 10.1016/j.jmarsys.2018.03.001

Ekau, W., Auel, H., Pörtner, H.-O., and Gilbert, D. (2010). Impacts of hypoxia on the structure and processes in pelagic communities (zooplankton, macro-invertebrates and fish). *Biogeoscience* 7, 1669–1699. doi: 10.5194/bg-7-1669-2010

Ekstrøm, C. T. (2018). *MESS: Miscellaneous Esoteric Statistical Scripts. R Package Version* 0.5.2. Available online at: https://CRAN.R-project.org/package=MESS (accessed February 19, 2020).

Elder, L. E., and Seibel, B. A. (2015). The thermal stress response to diel vertical migration in the hyperiid amphipod *Phronima sedentaria*. *Comp. Biochem. Physiol. A* 187, 20–26. doi: 10.1016/j.cbpa.2015.04.008

Emelyanov, E. (2005). *The Barrier Zones in the Ocean*. Berlin: Springer.

Enright, J. T. (1977). Diurnal vertical migration: adaptive significance and timing. *Part* 1. Selective advantage: a metabolic model. *Limnol. Oceanogr* 22, 856–872. doi: 10.4319/lo.1977.22.5.0856

Escribano, R., Marín, V., and Irribarren, C. (2000). Distribution of *Euphausia mucronata* at the upwelling area of Peninsula Mejillones, northern Chile: the influence of the oxygen minimum layer. *Sci. Mar.* 64, 69–77. doi: 10.3989/scimar.2000.64n169

Färber-Lorda, J., Lavín, M. F., and Guerrero-Ruiz, M. A. (2004). Effects of wind forcing on the trophic conditions, zooplankton biomass and krill biochemical composition in the Gulf of Tehuantepec. *Deep Sea Res. Pt. II* 51, 601–614. doi: 10.1016/j.dsr2.2004.05.022

Färber-Lorda, J., Lavín, M. F., Zapatero, M. A., and Robles, J. M. (1994). Distribution and abundance of euphausiids in the Gulf of Tehuantepec during wind forcing. *Deep-Sea Res. Pt. I* 41, 359–367. doi: 10.1016/0967-0637(94)90008-6

Färber-Lorda, J., Trasviña, A., and Cortés-Verdín, P. (2010). Summer distribution of euphausiids in the entrance of the Sea of Cortés in relation to hydrography. *Deep-Sea Res. Pt. II* 57, 631–641. doi: 10.1016/j.dsr2.2009.10.012

Fiedler, P., and Talley, L. (2006). Hydrography of the eastern tropical Pacific: a review. *Progr. Oceanogr.* 69, 143–180. doi: 10.1016/j.pocean.2006.03.008

Fischer, P., Schwanitz, M., Brand, M., Posner, U., Brix, H., and Baschek, B. (2018a). *Hydrographical Time Series Data of the Littoral Zone of Kongsfjorden, Svalbard 2012*. Helgoland: Alfred Wegener Institute - Biological Institute Helgoland, PANGAEA. doi: 10.1594/PANGAEA.896828

Fischer, P., Schwanitz, M., Brand, M., Posner, U., Brix, H., and Baschek, B. (2018b). *Hydrographical Time Series Data of the Littoral Zone of Kongsfjorden, Svalbard 2013*. Helgoland: Alfred Wegener Institute - Biological Institute Helgoland, PANGAEA doi: 10.1594/PANGAEA.896822

Flores, H., Atkinson, A., Kawaguchi, S., Krafft, B. A., Milinevsky, G., Nicol, S., et al. (2012). Impact of climate change on Antarctic krill. *Mar. Ecol. Progr. Ser.* 458, 1–19.

Friedrich, J., Janssen, F., Aleynik, D., Bange, H. W., Boltacheva, N., Çagatay, M. N., et al. (2014). Investigating hypoxia in aquatic environments: diverse approaches to addressing a complex phenomenon. *Biogeoscience* 11, 1215–1259. doi: 10.5194/bg-11-1215-2014

Gilly, W. F., Beman, J. M., Litvin, S. Y., and Robison, B. H. (2013). Oceanographic and biological effects of shoaling of the oxygen minimum zone. *Ann. Rev. Mar. Sci.* 5, 393–420. doi: 10.1146/annurev-marine-120710-100849

Giraudoux, P. (2018). *Pgirmess: Spatial analysis and Data Mining for Field Ecologists. R Package Version* 1.6.9. Available online at: https://CRAN.R-project.org/package=pgirmess (accessed February 19, 2020).

Gopalakrishnan, K. (1974). Zoogeography of the genus *Nematoscelis* (Crustacea: Euphausiacea). *Fish. Bull.* 72, 1039–1074.

Gopalakrishnan, K. (1975). Biology and taxonomy of the genus *Nematoscelis* (Crustacea: Euphausiacea). *Fish. Bull.* 73, 797–814.

Hamner, W., and Hamner, P. (2000). Behavior of Antarctic krill (*Euphausia superba*): schooling, foraging, and antipredatory behavior. *Can. J. Fish. Aqua. Sci.* 57, 192–202. doi: 10.1139/f00-195

Hernández-León, S., Calles, S., Fernández, and de Puelles, M. L. (2019). The estimation of metabolism in the mesopelagic zone: disentangling deep-sea zooplankton respiration. *Progr. Oceanogr.* 178:102163. doi: 10.1016/j.pocean.2019.102163

Herrera, I., Yebra, L., Antezana, T., Giraldo, A., Färber-Lorda, J., and Hernández-León, S. (2019). Vertical variability of *Euphausia distinguenda* metabolic rates during diel migration into the oxygen minimum zone of the Eastern Tropical Pacific off Mexico. *J. Plank. Res.* 41, 165–176. doi: 10.1093/plankt/fbz004

Huenerlage, K., and Buchholz, F. (2015). Thermal limits of krill species from the high-Arctic Kongsfjord (Spitsbergen). *Mar. Ecol. Progr. Ser.* 535, 89–98. doi: 10.3354/meps11408

Huenerlage, K., Cascella, K., Corre, E., Toomey, L., Lee, C.-Y., Buchholz, F., et al. (2016). Responses of the arcto-boreal krill species Thysanoessa inermis to variations in water temperature: coupling Hsp70 isoform expressions with metabolism. *Cell Stress Chaperon.* 6, 969–981. doi: 10.1007/s12192-016-0720-6

Ikeda, T. (1977). The effect of laboratory conditions on the extrapolation of experimental measurements to the ecology of marine zooplankton II. Effect of oxygen saturation on the respiration rate. *Bull. Plank. Soc. Jap.* 24, 19–28.

Ito, T., and Deutsch, C. (2013). Variability of the oxygen minimum zone in the tropical North Pacific during the late twentieth century. *Global Biogeochem. Cycles* 27, 1119–1128. doi: 10.1002/2013gb004567

Jones, M. C., and Cheung, W. W. L. (2017). Using fuzzy logic to determine the vulnerability of marine species to climate change. *Glob. Change Biol.* 24, e719–e731. doi: 10.1111/gcb.13869

Kaartvedt, S., Melle, W., Knutsen, T., and Skjoldal, H. R. (1996). Vertical distribution of fish and krill beneath water of varying optical properties. *Mar. Ecol. Progr. Ser.* 136, 51–58. doi: 10.3354/meps136051

Kamykowski, D., and Zentara, S. J. (1990). Hypoxia in the world ocean as recorded in the historical data set. *Deep Sea Res. Pt I* 37, 1861–1874. doi: 10.1016/0198-0149(90)90082-7

Karedin, E. P. (1971). About identity between *Nematoscelis megalops* G.O. *Sars,* 1885, *N. difficilis* Hansen 1911 (Euphausiacea, Crustacea) and validity of distinguishing *N. difficilis* Hansen. *Izv. tikhookean. nauchnoissled. Inst. ryb. Khoz. Okeanogr.* 75, 121–129.

Karstensen, J., Stramma, L., and Visbeck, M. (2008). Oxygen minimum zones in the eastern tropical Atlantic and Pacific oceans. *Progr. Oceanogr.* 77, 331–350. doi: 10.1016/j.pocean.2007.05.009

Keeling, R., Körtzinger, A., and Gruber, N. (2010). Ocean deoxygenation in a warming world. *Annu. Rev. Mar. Sci.* 2, 199–229. doi: 10.1146/annurev.marine.010908.163855

Kiko, R., Hauss, H., Buchholz, F., and Melzner, F. (2016). Ammonium excretion and oxygen respiration of tropical copepods and euphausiids exposed to oxygen minimum zone conditions. *Biogeoscience* 13, 2241–2255. doi: 10.5194/bg-13-2241-2016

Kiørboe, T. (2013). Zooplankton body composition. *Limnol. Oceanogr.* 58, 1843–1850. doi: 10.4319/lo.2013.58.5.1843

Koslow, J. A., Goericke, R., Lara-Lopez, A., and Watson, W. (2011). Impact of declining intermediate-water oxygen on deepwater fishes in the California current. *Mar. Ecol. Progr. Ser.* 436, 207–218. doi: 10.3354/meps09270

Kunze, E., Dower, J. F., Beveridge, I., Dewey, R., and Bartlett, K. P. (2006). Observations of biologically generated turbulence in a coastal inlet. *Science* 313, 1768–1770. doi: 10.1126/science.1129378

Lavaniegos, B. E., and Ambriz-Arreola, I. (2012). Interannual variability in krill off Baja California in the period 1997–2005. *Progr. Oceanogr.* 97, 164–173. doi: 10.1016/j.pocean.2011.11.008

Lavín, M. F., Fiedler, P. C., Amador, J. A., Ballance, L. T., Farber-Lorda, J., and Mestas-Nuñez, A. M. (2006). A review of eastern tropical Pacific oceanography: summary. *Progr. Oceanogr.* 69, 391–398. doi: 10.1016/j.pocean.2006.03.005

Leising, A. W., Schroeder, I. D., Bograd, S. J., Bjorkstedt, E. P., Field, J., Sakuma, K., et al. (2014). State of the California Current 2013–2014: El Nino looming. *California. Coop. Ocean. Fish. Investig. Rep.* 55, 51–87.

Levin, L. A. (2018). Manifestation, drivers, and emergence of open ocean deoxygenation. *Annu. Rev. Mar. Sci.* 10, 229–260. doi: 10.1146/annurev-marine-121916-063359

López-Cortés, D., Bustillos-Guzmán, J., and Gárate-Lizárraga, I. (2006). Unusual mortality of krill (Crustacea: Euphausiacea) in Bahía de La Paz, Gulf of California. *Pac. Sci.* 60, 235–242. doi: 10.1353/psc.2006.0010

Luyten, J. R., Pedlosky, J., and Stommel, H. (1983). The ventilated thermocline. *J. Phys. Oceanogr.* 13, 292–309.

Mangel, M., and Nicol, S. (2000). Krill and the unity of biology. *Can. J. Fish. Aquat. Sci.* 57, 1–5. doi: 10.1139/f00-203

Matear, R., Hirst, A., and McNeil, B. (2000). Changes in dissolved oxygen in the Southern Ocean with climate change. *Geochem. Geophys. Geosyst.* 1:1050.

McLaren, I. A. (1963). Effects of temperature on growth of zooplankton, and the adaptive value of vertical migration. *J. Fish. Board Canada* 20, 685–727. doi: 10.1139/f63-046

Mueller, C. A., and Seymour, R. S. (2011). The regulation index: a new method for assessing the relationship between oxygen consumption and environmental oxygen. *Physiol. Biochem. Zool.* 84, 522–532. doi: 10.1086/661953

Murphy, E. J., Watkins, J. L., Trathan, P. N., Reid, K., Meredith, M. P., Thorpe, S. E., et al. (2007). Spatial and temporal operation of the Scotia Sea ecosystem: a review of large-scale links in a krill centred food web. *Philos. Trans. R. Soc. B* 362, 113–148. doi: 10.1098/rstb.2006.1957

Nowacek, D. P., Friedlaender, A. S., Halpin, P. N., Hazen, E. L., Johnston, D. W., Read, A. J., et al. (2011). Super-aggregations of krill and humpback whales in Wilhelmina Bay, Antarctic Peninsula. *PLoS ONE* 6:e19173. doi: 10.1371/journal.pone.0019173

Ohman, M. D. (1984). Omnivory by *Euphausia pacifica*: the role of copepod prey. *Mar. Ecol. Progr. Ser.* 19, 125–131. doi: 10.3354/meps019125

Olson, D. B., Hitchcock, G. L., Fine, R. A., and Warren, B. A. (1993). Maintenance of the low-oxygen layer in the central Arabian Sea. *Deep-Sea Res. Pt II* 40, 673–685. doi: 10.1016/0967-0645(93)90051-n

Paulmier, A., and Ruiz-Pino, D. (2009). Oxygen minimum zones (OMZs) in the modern ocean. *Prog.Oceanogr.* 80, 113–128. doi: 10.1016/j.pocean.2008.08.001

Prince, E. D., and Goodyear, C. P. (2006). Hypoxia-based habitat compression of tropical pelagic fishes. *Fish. Oceanogr.* 15, 451–464. doi: 10.1111/j.1365-2419.2005.00393.x

R Core Team (2020). *R: A Language and Environment for Statistical Computing*. Vienna: R Core Team. Available online at: https://www.R-project.org/ (accessed February 19, 2020).

Rabalais, N. N., Turner, R. E., and Wiseman, W. J. (2002). Gulf of Mexico hypoxia, A.K.A. *"The dead zone"*. *Ann. Rev. Ecol. Syst.* 33, 235–263. doi: 10.1146/annurev.ecolsys.33.010802.150513

Reid, J. L. (1965). Intermediate waters of the Pacific Ocean. *Johns Hopkins Oceanogr. Study* 2, 1–85.

Seibel, B. A. (2011). Critical oxygen levels and metabolic suppression in oceanic oxygen minimum zones. *J. Exp. Biol.* 214, 326–336. doi: 10.1242/jeb.049171

Seibel, B. A., Schneider, J. L., Kaartvedt, S., Wishner, K. F., and Daly, K. L. (2016). Hypoxia tolerance and metabolic suppression in oxygen minimum zone euphausiids: implications for ocean deoxygenation and biogeochemical cycles. *Integr. Comp. Biol.* 56, 510–523. doi: 10.1093/icb/icw091

Smith, S. E., and Adams, P. B. (1988). Daytime surface swarms of *Thysanoessa spinifera* (Euphausiacea) in the Gulf of the Farallones, California. *Bull. Mar. Sci.* 42, 76–84.

Stramma, L., Johnson, G. C., Sprintall, J., and Mohrholz, V. (2008). Expanding oxygen-minimum zones in the tropical oceans. *Science* 320, 655–658. doi: 10.1126/science.1153847

Stramma, L., Prince, E. D., Schmidtko, S., Luo, J., Hoolihan, J. P., Visbeck, M., et al. (2011). Expansion of oxygen minimum zones may reduce available habitat for tropical pelagic fishes. *Nat. Clim. Change* 2, 33–37. doi: 10.1038/nclimate1304

Strub, P. T., Mesías, J. M., Montecino, V., Rutllant, J., and Salinas, S. (1998). Coastal ocean circulation off western South America. *Sea* 11, 273–313.

Sydeman, W. J., Santora, J. A., Thompson, S. A., Marinovic, B., and Lorenzo, E. D. (2013). Increasing variance in North Pacific climate relates to unprecedented ecosystem variability off California. *Glob. Change Biol.* 19, 1662–1675. doi: 10.1111/gcb.12165

Tanasichuk, R. W. (1999). Interannual variation in the availability and utilization of euphausiids as prey for Pacific hake (*Merluccius productus*) along the south-west coast of Vancouver Island. *Fish. Oceanogr.* 8, 150–156. doi: 10.1046/j.1365-2419.1999.00100.x

Teal, J. M., and Carey, F. G. (1967). Respiration of a euphausiid from the oxygen minimum layer. *Limnol. Oceanogr.* 12, 548–550. doi: 10.4319/lo.1967.12.3.0548

Torres, J. J., and Childress, J. J. (1983). Relationship of oxygen consumption to swimming speed in *Euphausia pacifica*. *Mar. Biol.* 74, 79–86. doi: 10.1007/bf00394278

Tremblay, N., Gómez-Gutiérrez, J., Zenteno-Savín, T., Robinson, C. J., and Sánchez-Velasco, L. (2010). Role of oxidative stress in seasonal and daily vertical migration of three krill species in the Gulf of California. *Limnol. Oceanogr.* 55, 2570–2584. doi: 10.4319/lo.2010.55.6.2570

Tward, C. E., Singh, J., Cygelfarb, W., and McDonald, A. E. (2019). Identification of the alternative oxidase gene and its expression in the copepod *Tigriopus californicus*. *Comp. Biochem.Physiol. B* 228, 41–50. doi: 10.1016/j.cbpb.2018.11.003

Verheye, H. M., and Ekau, W. (2005). Maintenance mechanisms of plankton populations in frontal zones in the Benguela and Angola Current systems: a preface. *Afr. J. Mar.e Sci.* 27, 611–615. doi: 10.2989/18142320509504121

Werner, T., and Buchholz, F. (2013). Diel vertical migration behaviour in Euphausiids of the northern Benguela current: seasonal adaptations to food availability and strong gradients of temperature and oxygen. *J. Plank. Res.* 35, 792–812. doi: 10.1093/plankt/fbt030

Werner, T., Hünerlage, K., Verheye, H., and Buchholz, F. (2012). Thermal constraints on the respiration and excretion rates of krill, *Euphausia hanseni* and *Nematoscelis megalops*, in the northern Benguela upwelling system off Namibia. *Afr. J. Mar. Sci.* 34, 391–399. doi: 10.2989/1814232x.2012.689620

Werner, T., Tremblay, N., Hünerlage, K., and Buchholz, F. (2015). "Krill worldwide: A comparison of hypoxia tolerances of euphausiid species from Atlantic, Pacific and Polar Regions," in *Proceedings of the Third International Symposium on Effects of Climate Change on the World's Oceans*, Santos City. Available online at: https://epic.awi.de/id/eprint/37766/ (accessed February 19, 2020).

Wishner, K. F., Outram, D. M., Seibel, B. A., Daly, K. L., and Williams, R. L. (2013). Zooplankton in the eastern tropical north pacific: boundary effects of oxygen minimum zone expansion. *Deep-Sea Res. Pt. I* 79, 122–140. doi: 10.1016/j.dsr.2013.05.012

Wishner, K. F., Seibel, B. A., Roman, C., Deutsch, C., Outram, D., Shaw, C. T., et al. (2018). Ocean deoxygenation and zooplankton: Very small oxygen differences matter. *Sci. Adv.* 4:eaau5180. doi: 10.1126/sciadv.aau5180

Wood, C. M. (2018). The fallacy of the Pcrit– are there more useful alternatives? *J. Exp. Biol.* 221, jeb163717–jeb163719.

Wyrtki, K. (1962). The oxygen minima in relation to ocean circulation. *Deep Sea Res. Oceanogr. Abst.* 9, 11–23.doi: 10.1016/0011-7471(62)90243-7

Yusseppone, M. S., Rocchetta, I., Sabatini, S. E., Luquet, C. M., Ríos, de Molina, M. D. C., et al. (2018). Inducing the alternative oxidase forms part of the molecular strategy of anoxic survival in freshwater bivalves. *Front. Physiol.* 9:100.

Zaret, T. M., and Suffern, J. S. (1976). Vertical migration in zooplankton as a predator avoidance mechanism. *Limnol. Oceanogr.* 21, 804–813. doi: 10.4319/lo.1976.21.6.0804

Zhukova, N. G., Nesterova, V. N., Prokopchuk, I. P., and Rudneva, G. B. (2009). Winter distribution of euphausiids (Euphausiacea) in the Barents Sea (2000–2005). *Deep-Sea Res. Pt. II* 56, 1959–1967. doi: 10.1016/j.dsr2.2008.11.007

Conflict of Interest: The authors declare that the research was conducted in the absence of any commercial or financial relationships that could be construed as a potential conflict of interest.

Advantages of publishing in Frontiers

OPEN ACCESS
Articles are free to read for greatest visibility and readership

FAST PUBLICATION
Around 90 days from submission to decision

HIGH QUALITY PEER-REVIEW
Rigorous, collaborative, and constructive peer-review

TRANSPARENT PEER-REVIEW
Editors and reviewers acknowledged by name on published articles

Frontiers
Avenue du Tribunal-Fédéral 34
1005 Lausanne | Switzerland

Visit us: www.frontiersin.org
Contact us: info@frontiersin.org | +41 21 510 17 00

REPRODUCIBILITY OF RESEARCH
Support open data and methods to enhance research reproducibility

DIGITAL PUBLISHING
Articles designed for optimal readership across devices

FOLLOW US
@frontiersin

IMPACT METRICS
Advanced article metrics track visibility across digital media

EXTENSIVE PROMOTION
Marketing and promotion of impactful research

LOOP RESEARCH NETWORK
Our network increases your article's readership